For Reference

NOT TO BE TAKEN FROM THIS ROOM

Ex libris
universitatis
albertaensis

QUAECUMQUE VERA

THE UNIVERSITY OF ALBERTA

RELEASE FORM

NAME OF AUTHOR LUBOMIR WOJTIW..............................

TITLE OF THESIS ESTIMATION OF PROBABLE MAXIMUM FLOOD FOR ALBERTA RIVER BASINS.................

....

DEGREE FOR WHICH THESIS WAS PRESENTED DOCTOR OF PHILOSOPHY

YEAR THIS DEGREE GRANTED .....1983........................

Permission is hereby granted to THE UNIVERSITY OF ALBERTA LIBRARY to reproduce single copies of this thesis and to lend or sell such copies for private, scholarly or scientific research purposes only.

The author reserves other publication rights, and neither the thesis nor extensive extracts from it may be printed or otherwise reproduced without the author's written permission.

THE UNIVERSITY OF ALBERTA

ESTIMATION OF PROBABLE MAXIMUM FLOOD FOR ALBERTA RIVER BASINS

by

© LUBOMIR WOJTIW

A THESIS
SUBMITTED TO THE FACULTY OF GRADUATE STUDIES AND RESEARCH
IN PARTIAL FULFILMENT OF THE REQUIREMENTS FOR THE DEGREE
OF DOCTOR OF PHILOSOPHY IN WATER RESOURCES

DEPARTMENT OF CIVIL ENGINEERING

EDMONTON, ALBERTA
SPRING, 1983

Digitized by the Internet Archive
in 2019 with funding from
University of Alberta Libraries

https://archive.org/details/Wojtiw1983

83-63D

THE UNIVERSITY OF ALBERTA
FACULTY OF GRADUATE STUDIES AND RESEARCH

The undersigned certify that they have read, and recommend to the Faculty of Graduate Studies and Research, for acceptance, a thesis entitled ..Estimation of Probable Maximum Flood for Alberta River Basins....................

....

submitted by ....LUBOMIR WOJTIW...........................

in partial fulfilment of the requirements for the degree of DOCTOR OF PHILOSOPHY IN WATER RESOURCES

ABSTRACT

Estimates of probable maximum precipitation (PMP) and probable maximum flood (PMF) are necessary considerations in the design and operation of multipurpose structures in which failure can have catastrophic consequences. Climatological and meteorological studies can be used to gain an understanding of the hydrological phenomena that result in major rainstorms causing extreme flooding.

Meteorological and statistical techniques were used to obtain estimates of PMP for the six major river basins in Alberta. Using three different hydrological models, PMP estimates were employed to obtain estimates of PMF. Using the statistical technique developed by Hershfield, it was found that point estimates of PMP were well correlated within a river basin and were dependent on the position and elevation of the location for which an estimate is required. The resulting relationship provides an easy method of computing point estimates of PMP for locations lacking meteorological data.

The rain-on-snow event had the best potential for producing the maximum water loading. As a result, the contribution of snowmelt to PMF was described, and an equation was developed to estimate maximum snowmelt for Alberta river basins.

To examine the effect of basin shape on PMF the author

devised the Time-Area Probable Maximum Flood Model. This numerical model uses simulation techniques with minimum data requirements and computational efficiency. Its main features allow subdivision of the drainage area, accomodation of the shape of a watershed, consideration of flood travel time, and production of flood hydrographs for a watershed.

Two well-known models were also examined for PMF estimates, parameterization and sensitivity in the Red Deer River Basin: the Streamflow Synthesis and Reservoir Regulation Model and the HYMO Model. The normalized PMF discharges from the three models were compared to the maximum recorded discharges.

The spatial distribution and Q-A relationships for PMF estimates are also presented for the major river basins in Alberta. Combining the results from all the river basins in Alberta, a Q-A relationship with exponent equal to 0.29 seems to best represent the data, while, for individual river basins a square-root (exponent equal to 0.50) describes best the relationship for the enveloping curve of PMF. For many river basins in Alberta the coefficient of the Q-A relationship with a square-root exponent was found to vary logarithmically with slope and intensity.

ACKNOWLEDGEMENTS

The author acknowledges with gratitude his indebtedness to Dr. J. P. Verschuren for suggesting the topic explored in this dissertation and for his advice and criticism throughout the period during which this extensive research was carried out.

Thanks are also due to the Hydrology Branch of Alberta Environment for their financial support, hydrological and meteorological data, the usage of the SSARR Model, and for publishing the report "Estimate of the Maximum Probable Precipitation for Alberta River Basins". My sincere thanks are also extended to the Atmospheric Environment Service (both Edmonton and Toronto offices); Hydrology Branch, Alberta Environment; Department of Civil Engineering, University of Alberta; and Department of Geography, University of Alberta, for advice and use of their data. Thanks are due to the Sanitary Engineering Department, City of Edmonton for the HYMO Model and appropriate information.

I wish to express my thanks to Ms. J. Samoil for reading the final draft and providing editorial comments, to Dr. D.M. Hershfield for acting as the external examiner, and to Drs. L. Gerard, I. Smith, and I. Joliffe for serving on the examining committee.

TABLE OF CONTENTS

CHAPTER PAGE

ABSTRACT iv

ACKNOWLEDGEMENTS vi

TABLE OF CONTENTS vii

LIST OF FIGURES xi

I. INTRODUCTION 1

1.1.0 Background 1

1.1.1 Objectives of Study 3

1.2.0 Literature Review 5

1.2.1 Climatological Studies 5

1.2.2 Synoptic Studies 10

1.2.3 PMP Studies 14

1.2.4 Historical Flood Studies in Alberta 24

1.2.5 Snowmelt Studies 30

1.2.6 Flood Estimates and PMF 34

1.2.7 Computer Simulation Modelling of PMF 44

1.3.0 Sources of Data and Models 51

II. CHARACTERISTICS OF PMP 53

2.1.0 Estimation of PMP by the Physical Method 53

2.1.1 Estimation of Atmospheric Moisture 54

2.1.2 Moisture Maximization 60

2.1.3 Storm Transposition 61

2.2.0 Estimation of PMP by the Statistical Method 63

2.2.1 Statistical Procedure 64

2.2.2 Adjustment of $\overline{X}_n$ and S_n for Maximum Observed Event 65

2.2.3 Adjustment of $\overline{X}_n$ and S_n for Sample Size 68

2.2.4 Adjustment for Fixed Observational Time Intervals 68

2.2.5 Area-Reduction Curves 71

2.2.6 Statistical Estimates for Alberta River Basins 71

2.2.7 Spatial Characteristics of PMPs 72

III. SNOWMELT WITH PMP LOADING 77

3.1.0 Introduction 77

3.2.0 Rain-on-Snow Events 78

3.2.1 Radiation Melt 79

3.2.2 Condensation and Convection Melt 86

3.2.3 Melt from Rainfall 88

3.2.4 Ground Conduction 90

3.3.0 Relationship of Meteorological Parameters 93

3.3.1 Relationship of the Air Temperature 95

3.3.2 Relationship of the Wind Speed 97

3.3.3 Relationship of the Precipitation 99

3.4.0 Maximum Water Loading 101

IV. THE TIME-AREA PROBABLE MAXIMUM FLOOD MODEL 104

4.1.0 Introduction 104

4.2.0 The TAPMF Model 104

4.2.1 Determination of the Inflow Hydrograph 107

4.2.2 Design Storm Hyetograph 108

4.2.3 Separation of Watershed into Isochrones 112

4.2.4 Time-area Histogram 116

4.2.5 Flow Separation 117

4.2.6 Routing Method 118

4.2.7 Operations and Data Requirements 122

V. THE SSARR and HYMO MODELS 124

5.1.0 Introduction 124

5.2.0 SSARR Watershed Model 125

5.2.1 Rainfall-Runoff Ralationships for PMF Estimates 127

5.2.2 Flow Separation 131

5.2.3 Routing of Surface Flow 132

5.2.4 Runoff from Snowmelt 134

5.2.5 Channel Routing 135

5.2.6 PMF Estimates from the SSARR Model 139

5.2.7 Sensitivity of SSARR Model 144

5.3.0 HYMO Model 152

5.3.1 PMF Estimates from the HYMO Model 160

5.3.2 Sensitivity of the HYMO Model 161

VI. COMPARISON OF MODELS 169

6.1.0 Recorded Maximum Discharges 169

6.2.0 Muzik's PMF Estimate 171

6.3.0 PMF Estimates from TAPMF, SSARR, and HYMO Models 172

6.4.0 Ratio of PMF to Maximum Recorded DIscharge 174

VII. PMF EMPIRICAL RELATIONSHIPS FOR ALBERTA RIVER BASINS 178

7.1.0 Introduction 178

7.2.0 PMF Relationship (m = 0.5) 180

7.2.1 Relationship of Coefficient c_1 with Slope 181

7.2.2 Relationship of Coefficient c_1 with Intensity .181

7.3.0 PMF Relationship (m = 1.0) 185

7.4.0 PMF Estimates for Alberta River Basins 187

7.4.1 Spatial Distribution of the Normailzed Discharge 190

7.4.2 Spatial Distribution of the Coefficients 192

7.4.3 Topic of Future Research 192

VIII. DISCUSSION AND CONCLUSIONS 196

8.1.0 Discussion 198

8.2.0 Conclusions 200

8.2.1 Climatology and Meteorology 200

8.2.2 PMP and PMF Estimates 201

BIBLIOGRAPHY 204

APPENDIX A.1 223

APPENDIX A.2 225

APPENDIX A.3 230

APPENDIX A.4 234

LIST OF FIGURES

Figure Page

1.1 Yearly Frequency of Rainstorms with Maximum Depth 50 mm (2 in.) and more in Alberta. 7

1.2 Isopleths of the Number of Storms with Depths 50 mm (2 in.) and more in 100 years. 8

1.3 Isopleths of the Number of Storms with Depths 150 mm (6 in.) and more in 100 years. 9

1.4 The 500 mb Analysis of a Typical Cold Low Over Alberta. 12

1.5 The 1000 mb Analysis of a Typical Cold Low Over Alberta. 13

1.6 Maximum Observed Rainfall as a Function of Area for Chaudiere and St. Francois Watersheds in Quebec. 21

1.7 Maximum Possible Rainfall as a Function of Area for Chaudiere and St. Francois Watersheds in Quebec. 22

1.8 Snowmelt and Precipitation Computed for Various Combinations of Snowmelt. 23

1.9 DAD Curves for 24-,48-,and 72-hour Durations for the Pembina Basin, Alberta. 25

1.10 Enveloping Curves of Known Floods in the United States up to a Given Time Period. 38

1.11 Comparison of Some of the Flood Formulas in General Use. 40

1.12 Envelope Curves of Extreme Floods on Prairies. 44

1.13 Mean Daily Peak Flow Versus Drainage Area for Probable Maximum Floods. 45

1.14 Comparison of Mathematical Formulations in Models. 49

1.15 Probable Maximum Flood Hydrograph at Raven on the Red Deer River. 51

2.1 Pseudoadiabetic Diagram for Dew Point Reduction to

1000 mb at Height Zero. 56

2.2 Maximum Recorded 12-hour Persisting Dew Point Temperatures at 1000 mb for the City of Red Deer. 58

2.3 Isopleths of Maximum 12-hour Persisting Dew Point Temperatures for June. 59

2.4 Depth-Area Curves of Maximized 24-hour PMP for the Red Deer River Basin. 62

2.5 Enveloping Depth-Area-Duration Curves of PMP for the Red Deer River Basin. 64

2.6 Adjustment of Mean of Annual Series for Maximum Observed Rainfall. 66

2.7 Adjustment of Standard Deviation of Annual Series for Maximum Observed Rainfall. 67

2.8 Adjustment of Mean and Standard Deviation of Annual Series for Length of Record. 69

2.9 Average Adjustment of Fixed Interval Precipitation Amounts for Number of Observational Units within the Interval. 70

2.10 Depth-Area, or Area-Reduction, Curves. 72

2.11 24-hour Enveloping Depth-Area Curves for Red Deer River Basin. 73

2.12 Spatial Variation (mm) of the Maximized 24-hour PMP. 74

2.13 Coefficients of Variation of Annual 24-hour Precipitation Extremes. 76

3.1 Variation in Snow Surface Albedo with Time. 81

3.2 Date of Last Snowcover of 25 mm (1 in.) or more for Alberta. 82

3.3 Average Cloudless Day Insolation in Langleys for May 15 and June 15 for Canada. 84

3.4 Temperature Variation for the Red Deer River Basin. 96

3.5 Variation of the Wind Speed for Red Deer River Basin. 99

3.6 24-hour Spatial PMP Variation in the Red Deer River Basin. 102

4.1 The TAPMF Model. 105

4.2 Map of the Watersheds of the Red Deer River Basin. 107

4.3 Maximum Mass Distribution at the Recorded Maximum Depth for Various Durations. 110

4.4 Intensity-Frequency Duration Curves for Edmonton Municipal Airport. 113

4.5 Effect of Shape on the Outflow Hydrograph. 114

4.6 Discharge-Velocity Distributions for a Number of Streams in the Red Deer River System. 115

4.7 Discharge-Velocity Distribution at a Number of Locations on the Red Deer River. 116

5.1 SSARR Watershed Model Flow Chart. 126

5.2 Three Variable Soil Moisture Index Relationships Developed for Bird Creek Basin. 129

5.3 Three Variable Soil Moisture Index Relationships Used for the Little Red Deer River and Design Curve for PMP Loading. 130

5.4 Surface-Subsurface Separation Curve. 132

5.5 Watershed Multiple Phase Storage Routing Available in SSARR. 134

5.6 Split Watershed Option of the Snow Cover Depletion Method Available in the SSARR Model. 136

5.7 A Watershed Configuration Used in SSARR Model for the Red Deer River Basin. 139

5.8 PMF Hydrograph at Sundre and the Largest Recorded Hydrograph at Red Deer. 141

5.9 Variation of the Discharge-Drainage Area Ratio with Area. 143

5.10 Effect on Streamflow of Varying the Surface-Subsurface Separation Relationships. 147

5.11 Effect on Streamflow of Varying the Number of Surface Routing Phases. 149

5.12 Effects of Surface Time of Storage on Streamflow. 151

5.13 Dimensionless Unit Hydrograph Used in the HYMO

Model. 154

5.14 Relationship Between Dimensionless Shape Parameter n and Recession Constant/Time to Peak. 156

5.15 Graphical Solution of Rainfall-runoff Equation. 157

5.16 Variation of the Time Period. 162

5.17 Effect on the Resultant Hydrograph by Variation of the Curve Number in HYMO Model. 164

5.18 Effect of Average Slope of the Watershed on the Resultant Hydrograph. 166

5.19 Area Versus Peak Discharge Relationship for PMF Estimates in the HYMO Model. 168

6.1 Comparison of Recorded Maximum Discharge and PMF Estimates for the Red Deer River Basin. 170

6.2 Ratio of the PMF to Recorded Discharge for Watersheds in the Red Deer River Basin. 175

6.3 Frequency Analysis of the Annual Maxima Discharges of the Red Deer River at Red Deer. 177

7.1 Relationship Between Slope and Coefficient c_1. 182

7.2 Variation of the PMF Discharge with Change in Intensity of the Water Loading. 184

7.3 Relationship of the Water Loading Intensity with Coefficient c_1. 186

7.4 Variation of the Runoff Coefficient c_1 with Average Slope for the Red Deer River Basin. 188

7.5 Relationship Between Normalized Discharge and Drainage Area for Alberta River Basins. 189

7.6 Spatial Variation of Normalized Discharge for Alberta River Basins. 191

7.7 Spatial Distribution of the Coefficient c_1 for Alberta River Basins. 194

7.8 Spatial Distribution of the Runoff Coefficient C for Alberta River Basins. 195

7.9 Relationship between Peak Discharge, Average Slope, and Drainage Area for Alberta River Basins. 197

CHAPTER 1

INTRODUCTION

1.1.0 Background

For many years scientists have recognized the importance of meteorological and climatological phenomena to hydrological problems. Major floods due to severe rainstorms, for example, usually are a result of meteorological conditions and hence require an understanding of the climatology of a given region. Rainfall studies frequently are directed toward estimation of the physical upper limits of storm rainfall in a basin, termed the Probable Maximum Precipitation (PMP). The American Meteorological Society (Huschke, 1970) defines the PMP as "the theoretical greatest depth of precipitation for a given duration that is physically possible over a particular drainage area at a certain time of year. In practice this is derived over flat terrain by storm transposition and moisture adjustment to observed storm patterns". Another more operational definition emphasizing application (Huschke, 1970) states that "PMP is that magnitude of rainfall over a particular basin which will yield the flood flow of which there is virtually no risk of being exceeded."

PMP estimate can be converted into flows by empirical methods or simulation models to produce a theoretical flood that is known as the Probable Maximum Flood (PMF). Estimates

of this flood incorporate meteorological and hydrological parameters in an attempt to describe the physical upper limits to the flooding that could occur over a certain basin during a specified time interval.

For hydrological applications, estimates of PMP and PMF should be considered in the design and operation of multipurpose structures. In some cases, the lack of these estimates has caused underestimation of the necessary design and has resulted in disastrous consequences when a rainfall or flood occurred that exceeded the one used in the design.

Although a number of studies of PMP have been conducted during the past 40 years in the United States, only a few have addressed PMF, and these were only for specific basins. In Canada the number of studies on this topic is even smaller. Only after the disastrous hurricane storm of 14-15 October 1954 (called Hazel) crossed into Ontario from the United States and caused extensive property damage did hydrologists in Canada initiate the much-needed program of PMP studies for Canadian river basins. Research advances have been slow in the last 20 years, with only a few studies published for specific basins. In Alberta, there are very few publications on PMP and PMF, and these are for basins where specific projects were needed. One of the main reasons for limited research on this topic is that these estimates require extensive, time-consuming studies that the user may not have the resources to undertake. Secondly, the required climatological and meteorological data are time consuming

and expensive for the potential user or researcher to obtain. Thirdly, the user often is not familiar with existing hydrological models, especially the more sophisticated ones. The user must know what models are available and where to obtain them, as well as how to use these models and recognize their limitations. These limitations are of key importance, for some models have been misused even though they were designed for specific purposes and regions. A final reason for the minimal effort on this topic has been the lack of a simplified approach for estimating PMP and PMF. It was this deficiency, namely, the lack of a simplified approach for estimating PMF, together with an interest in hydrological research into severe storms that led the author to investigate this topic.

1.1.1 Objectives of Study

The objectives of this study can be divided into two main categories: (a) those dealing with PMP estimates, and (b) those dealing with PMF estimates.

The objectives associated with PMP estimates are:

(1) to obtain a better understanding of the spatial and temporal distribution of PMP in Alberta, including climatological and meteorological analyses of rainstorms and estimates of PMP,

(2) to obtain PMP estimates for the six main river basins in Alberta using the two most common approaches: (a)

the meteorological or traditional approach, and (b) the statistical technique, and

(3) to derive a model for the determination of PMP for any location in Alberta.

The objectives associated with PMF estimates are:

(1) to examine the rain-on-snow event and to define the relevant parameters and processes associated with snowmelt necessary for PMF estimates,

(2) to develop a conceptual model for estimating PMF in Alberta (in this thesis termed the TAPMF Model [1]) and to compare the results of this model with estimates obtained from two generally used hydrological models (SSARR [2] and HYMO [3]) [4] in an Alberta watershed, and

(3) to examine the spatial distribution of PMF estimates in Alberta and to obtain a relationship with which to estimate PMF for ungauged watersheds.

The PMP objectives of this work have been researched previously and were presented in two publications by the author: (1) Verschuren and Wojtiw (1980) and (2) Wojtiw and Verschuren (1981). A summary of the published results is

---

[1] TAPMF Model:Time Area Probable Maximum Flood Model.

[2] SSARR Model:Streamflow Synthesis and Reservoir Regulation Model (U.S. Army Corps of Engineers, 1972).

[3] HYMO:Hydrological Model Computer Language (Williams and Hann, 1973).

[4] The SSARR and HYMO models are poplular models used by government agencies and consultants in Alberta.

presented in Chapter 2 of this thesis. The PMF objectives are examined in Chapters 3 to 7.

Before the results of the research work are presented, a review of the available literature is given. The review has been divided into a number of parts to give the reader a better understanding of the history and techniques involved in PMP and PMF studies: (1) climatological studies; (2) synoptic studies; (3) PMP studies; (4) historical flood studies in Alberta; (5) snowmelt studies; (6) flood estimates and PMF studies; and (7) computer simulation modelling of PMF.

1.2.0 Literature Review

A large number of precipitation studies have been conducted in Alberta. Some of these have examined the climatology of surface rainfall, while others attempted to relate the synoptic weather conditions to precipitation on the surface.

1.2.1 Climatological Studies

In most studies of the climatology of surface precipitation, point measurements are examined in terms of the regional and temporal variations of rainfall. The results of the point measurement analyses indicate variations in the point measurements of precipitation and not variations in the rainstorms, which are areal in dimension. Comparisons are usually made of the heaviest

precipitation between one point and another, which usually are produced by two independent (in time) events. A good example of such a study is the work by Storr (1963, 1967), who examined the precipitation data for the heaviest 1-, 2-, and 3-day rainfalls from 81 stations for each month (May to August) from 1921 to 1960. The results were expressed as maps of heaviest rainfall for the 5-, 10-, and 25-year return period. These maps provide the spatial distribution of the heaviest rainfall, with each point representing the maximum observed value recorded in most cases from independent events.

The first study to examine the climatology of rainstorms in Alberta was the work of Verschuren and Wojtiw (1980) in which the authors identified and analyzed 611 rainstorms (between 1921 and 1978) that produced a minimum depth of 50 mm (2 in.) precipitation. In addition to presenting the yearly frequency of rainstorms (Figure 1.1), the authors showed that an average of about 11 storms ooccurred each year with depths greater than 50 mm (2 in.) and that the number of rainstorms decreased logarithmically with increased depth. Over 50% of the rainstorms in Alberta occurred in June (23.6%) and July (26.7%), with only small percentages occurring in April (5.6%) and September (10.1%). The authors found that the greatest frequency was in the Waterton Lakes National Park area, 2:1 year event for depths 50 mm (2 in.) and more (Figure 1.2); approximately a 1:3 year event for depths 100 mm (4 in.) or more; and

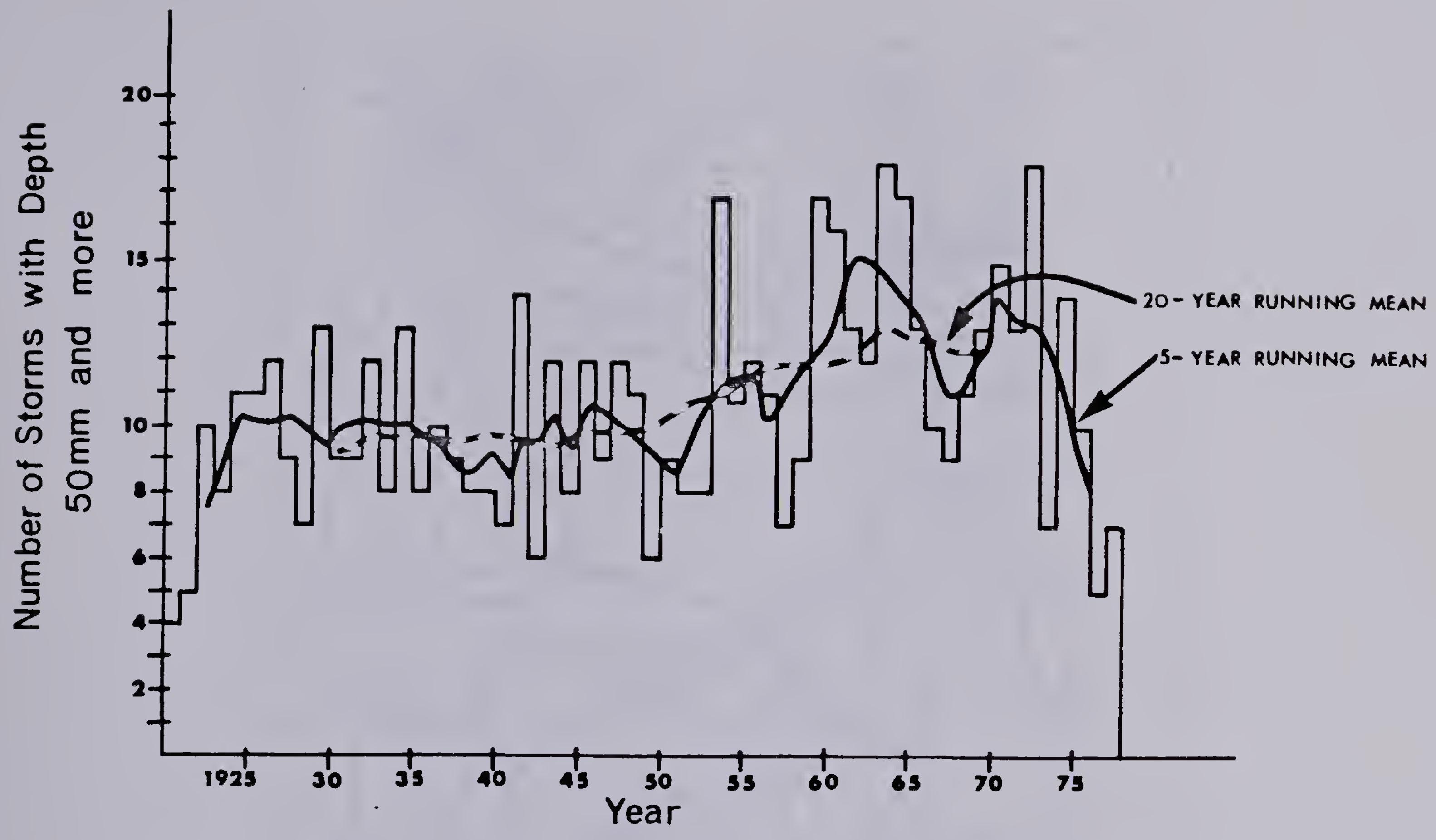

FIGURE 1.1. Yearly Frequency of Rainstorms with Maximum Depth 50 mm (2 in.) and more in Alberta (Verschuren and Wojtiw, 1980).

approximately a 1:10 year event for depths 150 mm (6 in.) or more (Figure 1.3). The frequency decreased along the Continental Divide, with a number of pockets of maxima in central Alberta. Severe storms [5] occur in four main regions (or belts) of the province: the first extends through southern Alberta just south of Calgary; the second is in central Alberta from south of Edson to the Edmonton region; the third is from Lesser Slave Lake to the Fort McMurray

---

[5] Storms that produce depths 150 mm (6 in.) and more.

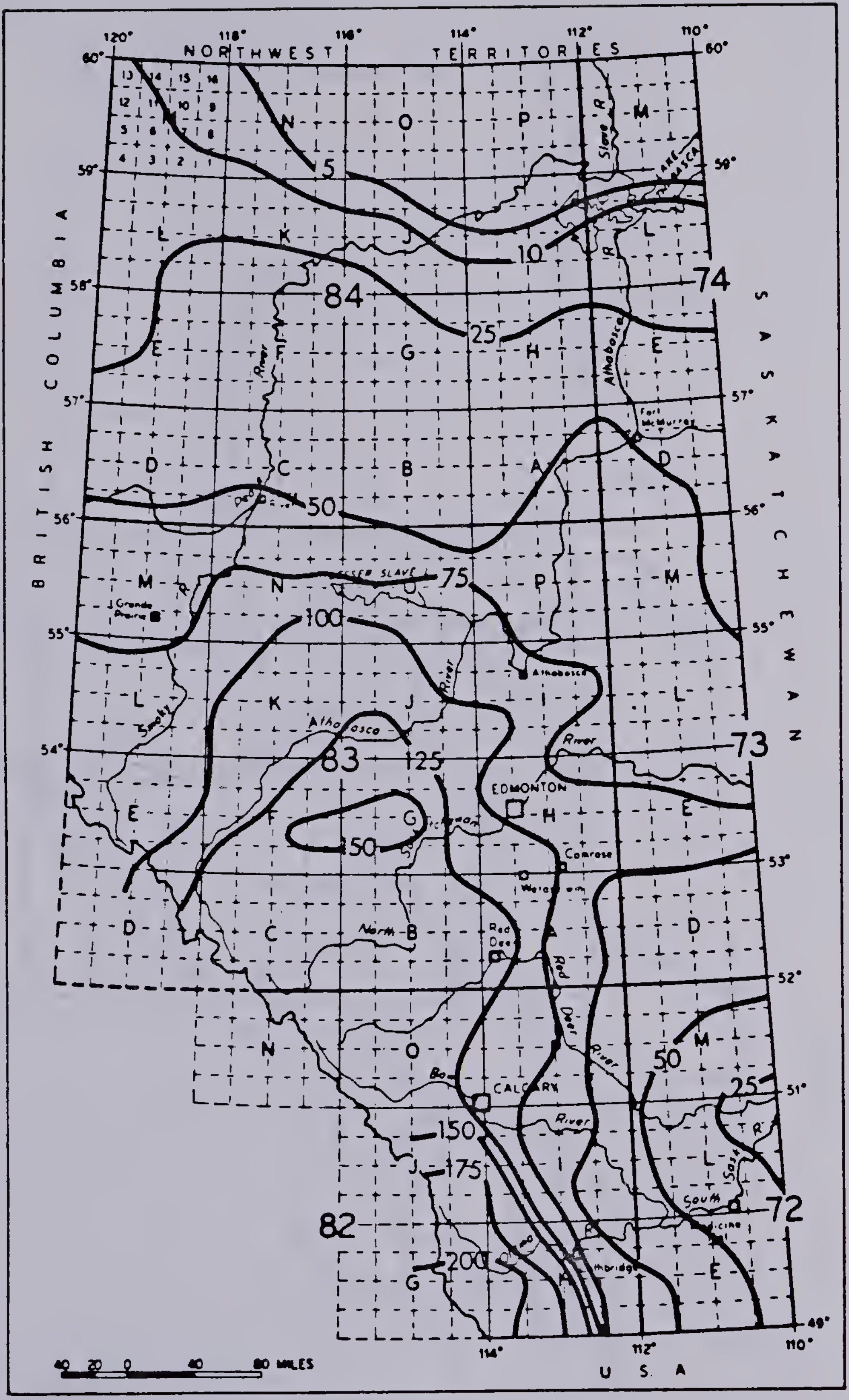

FIGURE 1.2. Isopleths of the Number of Storms with Depths 50 mm (2 in.) and more in 100 years (Verschuren and Wojtiw, 1980).

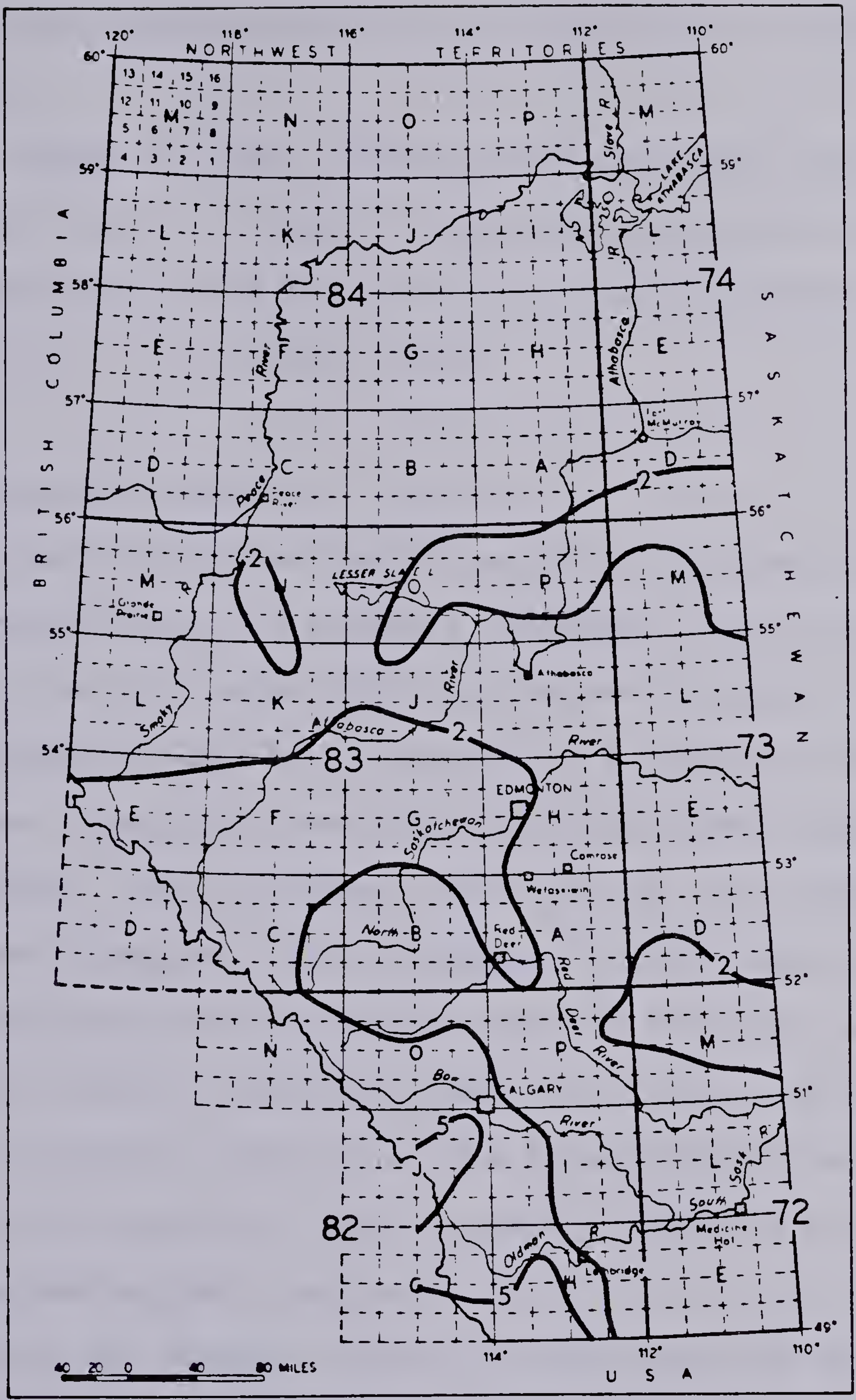

FIGURE 1.3. Isopleths of the Number of Storms with Depths 150 mm (6 in.) and more in 100 years (Verschuren and Wojtiw, 1980).

area; and the fourth is around the Fort Vermilion area. Storms with depths greater than 150 mm (6 in.) usually cause flooding.

A number of other studies have also been published, and although they are listed in the bibliography they are not discussed here since they are not directly relevant to the objectives in this dissertation.

1.2.2 Synoptic Studies

In western Canada the 500 millibar (mb) cold low has been recognized by forecasters (Thompson, 1950) as a synoptic feature responsible for extensive precipitation on the surface in Alberta. Studies of the synoptic conditions of severe rainstorms have also been published (Mokosch, 1961; McKay, 1965b; Burrows, 1966; Warner and Thompson, 1974; and Thompson, 1976). Thompson's 1976 report summarizes the characteristics of storm events of different synoptic scale to identify the storm types most likely to produce extreme rainfall events over the Saskatchewan Basin. In Alberta two categories seem to emerge based on the events' duration and synoptic scale.

The first category contains short-duration and small-scale intense rainfall events; these are produced by thunderstorms. The typical life cycle of a thunderstorm is 3 to 8 hours, and the area exposed to rainfall is approximately several hundred square kilometres. Most of these storms result from daytime heating of the earth's

surface so that although land-use patterns, type of vegetation, and aspect may play roles in determining the point of storm formation, topography cannot otherwise be related to the rainfall intensity. Many of the 1-day extreme annual rainfalls at stations in Alberta are of this type. As a rule, these usually do not result in extensive flooding in Alberta.

The second category contains medium-scale events; these are associated with low-pressure and frontal systems. Most of the 3-day annual extreme rainfalls and probably also several of the 1-day annual extreme rainfalls in the Eastern Slopes and plains are from storms of this scale. Extreme wet periods longer than about 3 days would, in most instances, be due to disturbances on a planetary scale that cause a breakdown in the normal eastward movement of the large-scale pressure configurations. Under such conditions the low-pressure generation areas and the upper-level winds that steer the storm systems remain stationary and cause successive medium-scale storms to track over the same general area for an extended period. Such a situation has been called a cold low and is classed as a medium-scale storm. The 500 mb map (roughly at 5.5 km or 18 000 ft.) and the surface weather map are used to identify such phenomena; examples of these maps are shown in Figures 1.4 and 1.5, respectively.

In Figure 1.4, pressure isopleths of a 500 mb low are shown over south-central Alberta, there is cold air over

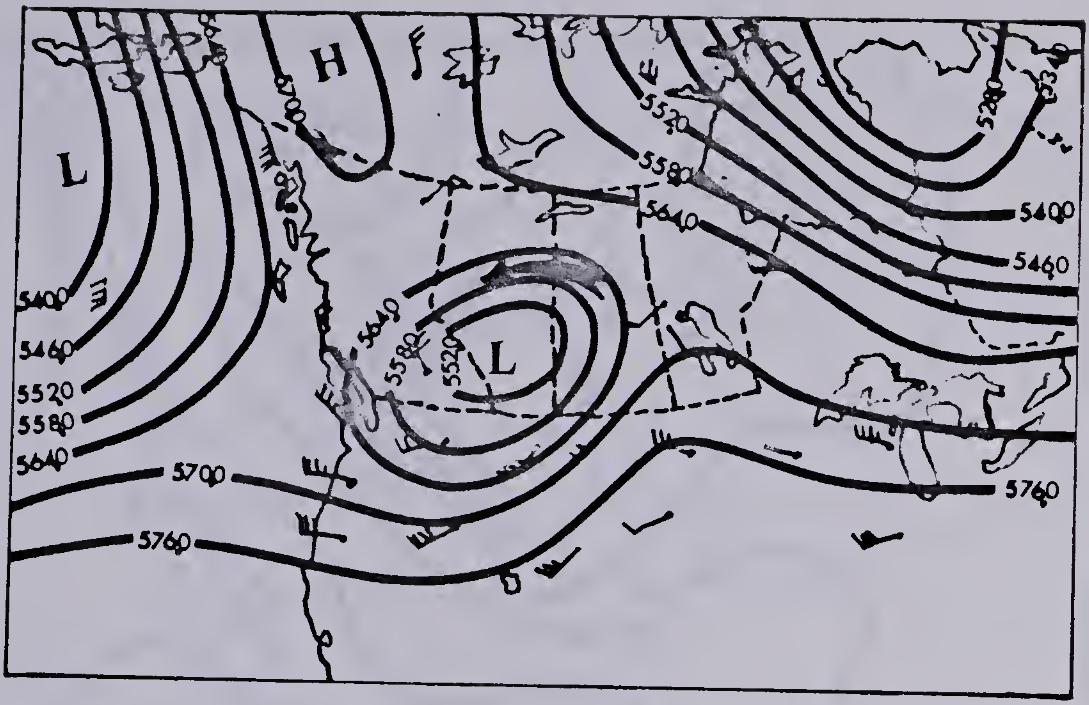

FIGURE 1.4. The 500 mb Analysis of a Typical Cold Low Over Alberta (After Thompson, 1976).

southern Alberta and British Columbia, and warm air is spiralling around the east, north, and northwest sides of the low. In Figure 1.5, pressure isopleths of about 1000 mb are depicted in the figure, and a surface low shown southwest of Edmonton is causing a northeasterly upslope flow of warm moist air over the foothills of the Peace River Basin. The band of warm air on the east, north, and northwest sides of the upper low is often the region of heaviest precipitation in a cold low system, even in the absence of an upslope condition. The existence of the appropriate combination of topography and low-level winds provides additional lift to the already ascending air to further increase the intensity of the precipitation. Thompson (1976) found that the cold low was the most

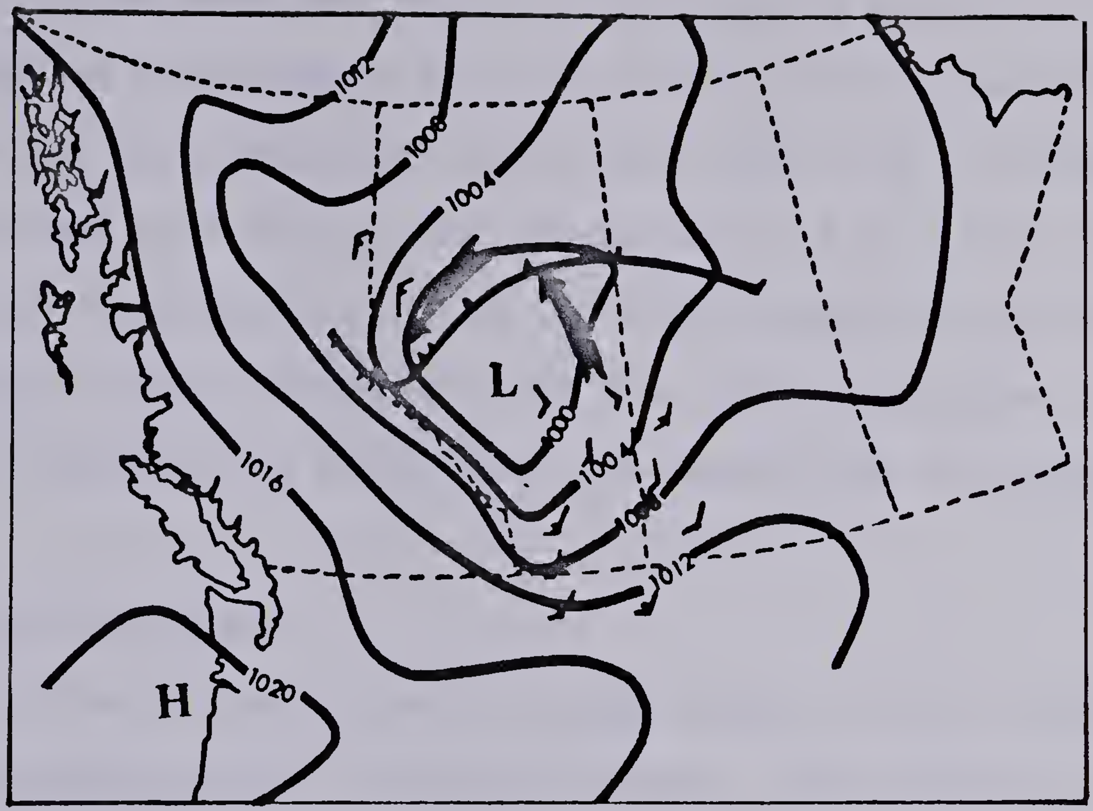

FIGURE 1.5. The 1000 mb Analysis of a Typical Cold Low Over Alberta (After Thompson, 1976).

frequent producer of rainfalls of sufficient intensity to pose a flood threat in the South Saskatchewan River Basin and that this type of storm occurs most frequently during May or June.

Burrows (1966) examined daily precipitation data for 16 years (1950 to 1965) for the Edmonton region and classified the data into two basic types of storms: cold low and cold trough storms. In meteorology a cold trough is an elongated area of relatively low atmospheric pressure (the opposite of a ridge). Of the 60 storms analyzed (with rainfall 19 mm (0.75 in.) or greater), 42 storms were identified as cold low, while 18 were classified as cold trough. In their

study, Verschuren and Wojtiw (1980) found that all 34 severe rainstorms producing 150 mm (6 in.) or more in precipitation at the surface could be classified according to Burrows' scheme and that 85% of the storms were of the cold low type, with the remainder being of the cold trough type. The authors further concluded that the cold low system is usually associated with heavy precipitation in Alberta.

1.2.3 PMP Studies

In the United States a large number of PMP studies have been conducted over the past 40 years. The disastrous floods during the late 1930s directed investigations by a number of researchers (Bailey and Schneider, 1939; Craeger, 1939; and Hathaway, 1939) into the subject of PMF and its relationship to spillway capacity in considering the design of dams. With these studies the concept of PMP gained favor and a number of comprehensive research programs were initiated. By 1939, through advanced studies and a greater accumulation of data, the probability method had been proven to be entirely inadequate. Because of these circumstances, the importance of meteorological studies in the design of flood control structures was realized (Creager, 1939). During this period the idea of mass rainfall curves was developed and used for storm analysis (Bailey and Schneider, 1939; Hathaway, 1939). The next important development was the use of dew points as a measure of the precipitable water in the moist air. Showalter and Solot (1942) concluded that the maximum amount

of rain that can occur over a given basin can be determined from the amount of moist air that can flow over the basin and the maximum amount of moisture that can be precipitated from that moist air.

It was not until 1953 (Paulhus and Gilman, 1953) that Probable Maximum Precipitation was defined and a distinction drawn between it and Probable Maximum Storm. Until then, the terms were used liberally and interchangeably in the literature. The distinction is, that the PMP for a specific area is usually determined by several types of storms, whereas the Probable Maximum Storm is determined by one specific storm. Paulhus and Gilman outlined a maximizing procedure used in the derivation of PMP that consists chiefly of moisture adjustment and, when justifiable, transposition of the observed storms. This procedure serves today as the basis for calculating estimates of PMP and is found in the literature under various names: traditional, meteorological, or physical.

Moisture adjustment of a storm involves estimation of the increased precipitation that could be expected if maximum atmospheric moisture were available. The surface dew point is used as an index of the moisture in the storm and of the maximum moisture in the basin. Paulhus and Gilman further mentioned that their tests indicated that the lowest dew point in the 12-hour period corresponding most nearly to the 12-hour period of greatest rainfall was most representative of the average moisture in the storm center.

This dew point was labelled the representative 12-hour persisting dew point. The maximum 12-hour persisting dew point to which the storm values are adjusted is the highest value below which the dew point did not drop during any 12-hour recorded period. All dew points were reduced pseudoadiabatically to the 1000 mb level to make the dew points for stations at different elevations comparable and to permit the use of tables and charts of moisture in atmospheric columns with base at 1000 mb. Maps of maximum dew points and tables of moisture content, expressed in terms of precipitable water, have been published by the U.S. Department of Commerce (1948, 1951).

For many years this traditional approach continued to be popular and gained general acceptance. In 1961 a different way of calculating PMP was introduced by Hershfield (1961), who proposed a statistical method for the systematic analysis of precipitation data in estimating PMP; this method was modified several years later (Hershfield, 1965). He proposed that the PMP at an observable precipitation point could be estimated from generalized frequency equation (Chow, 1951) of the form

$$X_R = \overline{X} + K\,S_n \qquad (1.1)$$

where X_R is the return period rainfall, $\overline{X}$ and S_n are the mean and standard deviation of a series of n annual maxima for a specific duration, and K is the frequency factor

dependent upon the frequency distribution chosen to fit the data. In the original works by Hershfield (1961, 1965) the frequency factor was found to vary from about 1.2 to 14.5 and was postulated to have a maximum value of 15. This value of 15 has been used by many researchers to estimate PMP without verification or question of applicability. In 1977, Hershfield (1977) published results showing that the PMP at any point was also a function of duration and the mean annual extreme rainfall; for a duration of i hours this can be expressed as follows:

$$K_i = 19\ (10)^{-b\ \overline{X}_i} \qquad (1.2)$$

where K_i is the frequency factor, $\overline{X}_i$ is the mean annual extreme rainfall (inches) for the i hour duration, and b is a constant which varies with duration. For durations of 6 and 24 hours, Equation 1.2 can be expressed as:

(a) for 6-hour duration

$$K_6 = 19\ (10)^{-0.00213\ \overline{X}_6} \qquad (1.3)$$

(b) for 24-hour duration

$$K_{24} = 19\ (10)^{-0.000965\ \overline{X}_{24}} \qquad (1.4)$$

By plotting the constant part of the empirical power coefficients against duration on a log-log graph, a straight line results, thus allowing the interpolation or extrapolation to other durations.

This method is now known as the statistical method of

estimating the PMP. Similar to other schemes dependent on empirical coefficients, the equation proposed by Hershfield is a concise and convenient way of achieving an approximate answer when little is known about the estimated quantity. Its main advantage is that it can be used in remote areas where little meteorological data are available and where it is virtually impossible to make a reasonable estimate using the physical approach.

The PMP obtained by the physical or statistical method is an enveloping value. Even if an excellent theoretical model were available, the analyst would still have to maximize the input. At the present time, the maximization of the parameters is imperfectly understood.

Comparisons of the physical and statistical methods have been made in a number of studies. Most studies in Canada which have used both methods, found that the two methods produced similar results. During the late 1950s and throughout the 1960s a number of studies were conducted to estimate PMP for various Canadian river basins. One of the preliminary studies using PMP estimates for severe storms was researched by Bruce (1957), who performed an analysis of the rainfall for the most severe storm on record in Ontario i.e., hurricane Hazel (14-15 October 1954). At that time, the only Depth-Area-Duration (DAD) analyses available for Canadian storms were for storms that crossed the border from the United States and were documented in "Storm Rainfall in the U.S.". Employing the storm maximization and

transposition methods of Paulhus and Gilman (1953), Bruce obtained preliminary estimates for available DAD analyses for southern Ontario. With this study a need for DAD analyses became apparent, and the Department of Transport's Meteorological Branch (now Atmospheric Environment Service) initiated a program that resulted in the production of the "Storm Rainfall in Canada" series (Atmospheric Environment Service, 1961-). This is a continuing series with a number of rainstorm analyses being added each year from throughout Canada. Although the series mainly emphasizes rainstorms in eastern Canada, slightly over 60 such analyses are for Alberta storms.

Canadian research advanced in the 1960s when a number of studies were conducted to examine the critical meteorological conditions for maximum floods for specific river basins. One such study was done by Bruce and Sporns (1963) for the St.John River Basin, New Brunswick, to provide design engineers with the basic information needed to estimate maximum flood flows. This included data on the physical upper limits to storm rainfall, winter snow accumulation, snowmelt rates, and optimum combinations of snowmelt and rain. DAD analyses of 63 storms were carried out and were used to estimate PMP by the physical approach. The results from this method showed very good agreement with results obtained using the Hershfield method with K equal to 15 in the frequency equation.

A second study was done by Bruce, Richards, and Sporns

(1965) for the Portage Mountain Reservoir on the Peace River in British Columbia. As in the previous study, maximization of the major recorded rainstorms was carried out using the physical approach. When Hershfield's method was used to corroborate the estimates of PMP, it was found that the statistical method gave only slightly lower values than those obtained by the physical analysis.

Another study was performed for the St. Francois and Chaudiere river basins, Quebec, by Gagnon, Pollock, and Sparrow (1970). Similar to the previous two studies, this work considered only the meteorological aspects of rainstorms, snow accumulations, and snowmelt. The physical approach was also used in examining PMP for the two basins. A total of 77 large rainstorms (storms with point rainfalls of more than 50 mm (2 in.) in 24 hours) occurring between 1912 and 1964 were analyzed. Two families of curves or isochrones were obtained. Figure 1.6 shows the maximum observed rainfall, and, Figure 1.7 shows the maximum physically possible rainfall as functions of area. The five largest storms were used to obtain the maximum observed curves. Figure 1.7 gives the maximum possible rainfall for areas of 130 to 12 950 km^2 (50 to 5 000 sq. mi.) and for durations of 6 to 108 hours.

In Alberta, most of the work on estimating PMP has been conducted by McKay (1962, 1964, 1965b, 1966, and 1968); his efforts have concentrated on the statistical approach. In one of the first of these studies (McKay,1965b), the author

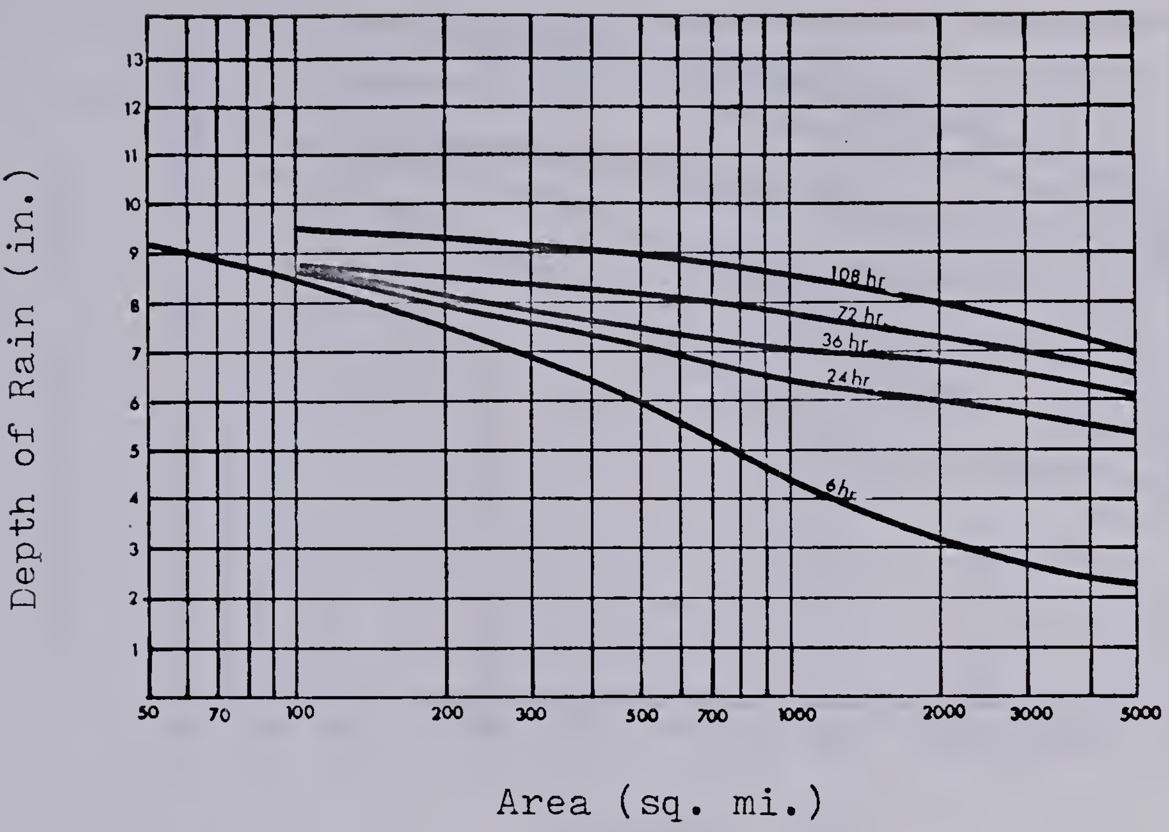

FIGURE 1.6. Maximum Observed Rainfall as a Function of Area for the Chaudiere and St. Francois Watersheds in Quebec (After Gagnon et al., 1970).

obtained estimates of PMP for the prairie provinces by examining 24-hour extreme precipitation values for 191 weather stations with long-term rainfall records from 1916 to 1960. The characteristics of the frequency factor K were presented along with maps of the coefficient of variation and the mean. The author also provided graphs of point for conversion of 24-hour extreme rainfall to other rainfall durations (i.e., 1, 6, and 12 hours). The author concluded that during the late spring and throughout the summer the foothills of southwestern Alberta have the greatest storm potential within Alberta.

In another study, McKay (1968) examined the

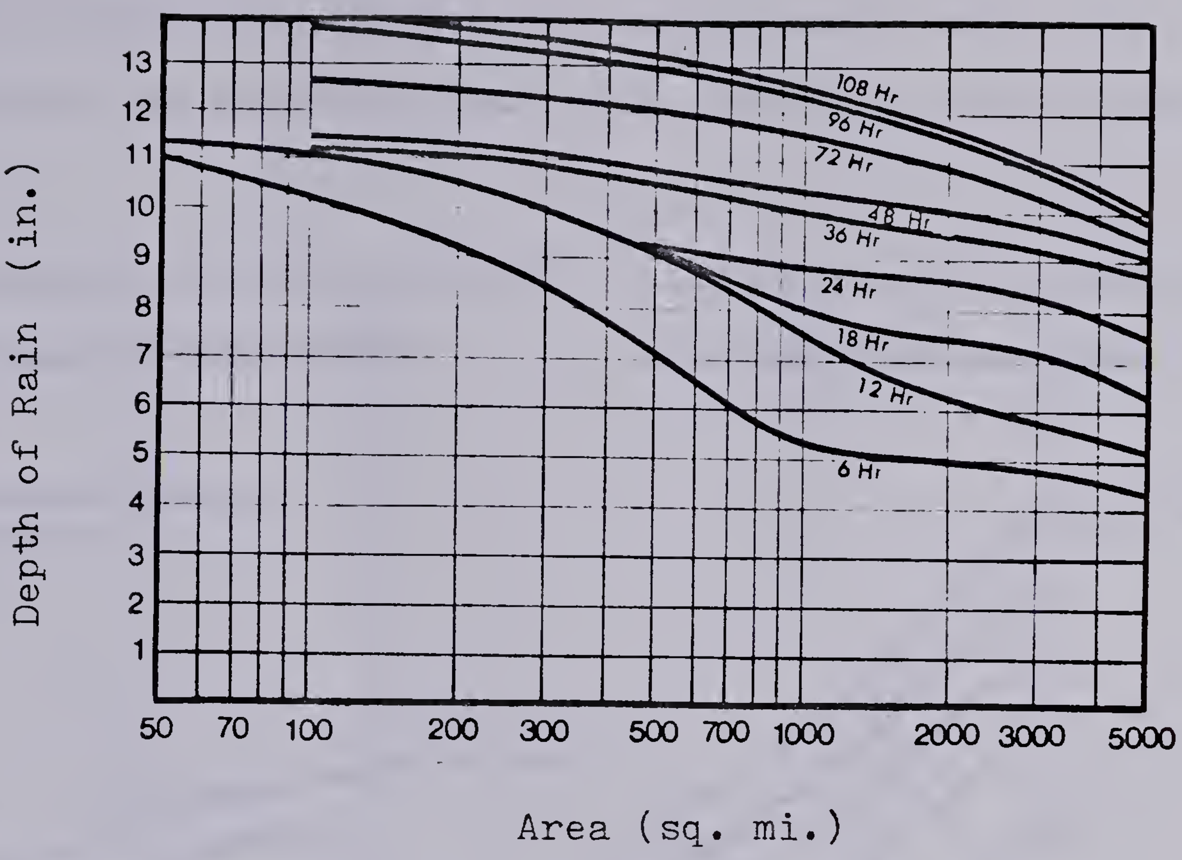

FIGURE 1.7. Maximum Possible Rainfall as a Function of Area for the Chaudiere and St. Francois Watersheds in Quebec (After Gagnon et al., 1970).

meteorological conditions that influenced the project design and PMF on the Paddle River, Alberta. Again the statistical approach was used to examine the 15 available severe storms analyses, including those storms within Alberta that the author believed could be transposable to the Paddle River area. In addition, the author computed snowmelt rates using generalized snowmelt equations and coefficients and combined these estimates with the snowmelt associated with a major spring storm. It should be pointed out that in this study no critical analysis was made of the coefficients in the generalized snowmelt equations, in particular of their validity for the basin being examined. Estimates of the

water yield from combined rain and snowmelt were also computed, as shown in Figure 1.8. The solid lines in the

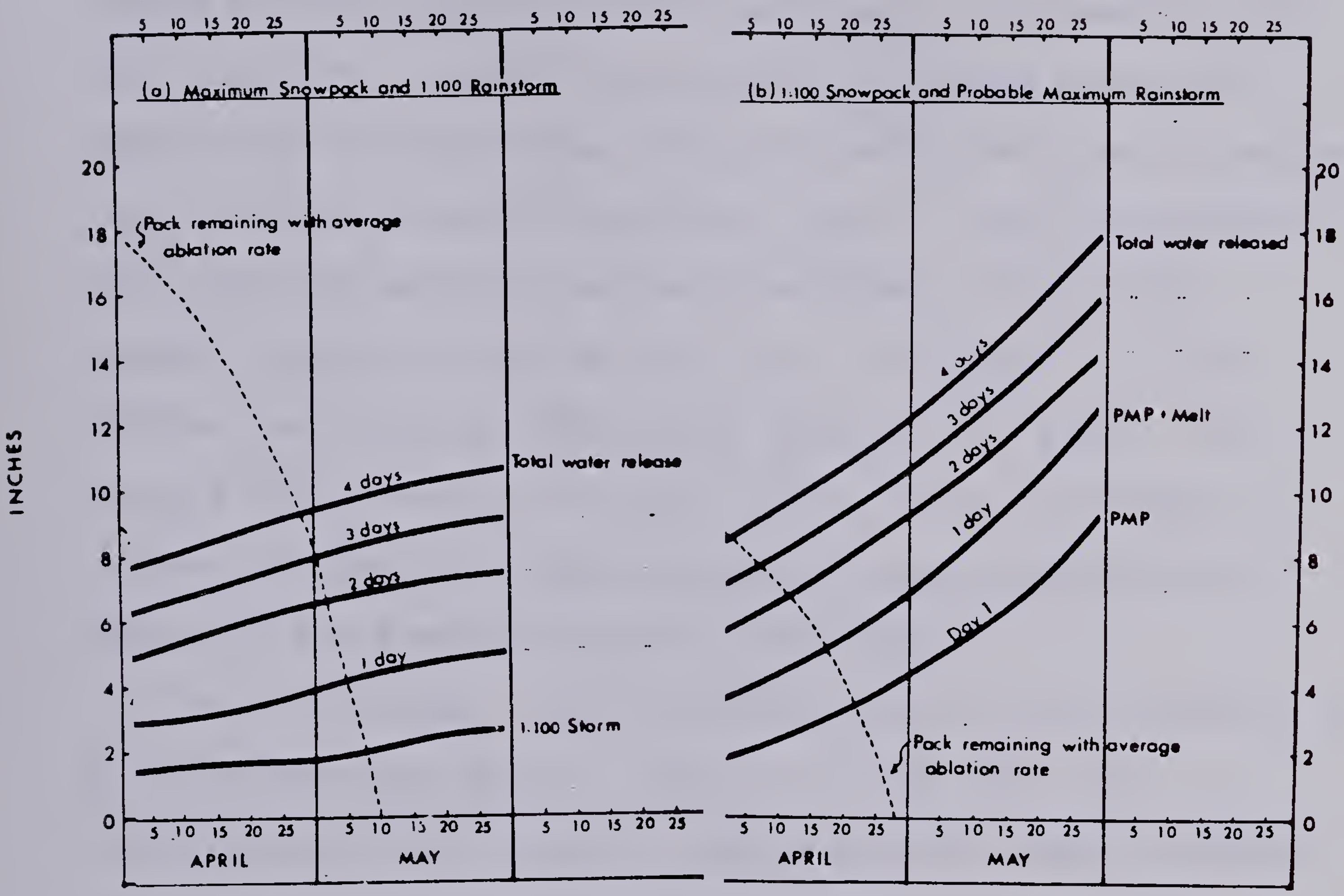

FIGURE 1.8. Snowmelt and Precipitation Computed for Various Combinations of Snowmelt (After McKay, 1968).

figure indicate the total water released from the storm, the storm plus 1-day melt, the storm plus 2-day melt, and so on. The broken line indicates how much snow can be expected to be on the ground under average ablation rate conditions.

Another study that examined critical meteorological conditions for maximum flow was that presented by Buckler

and Quine (1971) for the Pembina Valley north of Entwistle, Alberta. The authors estimated the probable maximum snow accumulation in the winter season and calculated the melt caused by the highest possible warm spell followed by a 3-day rainstorm. The melt rates were calculated using the generalized snowmelt equations and coefficients developed by the U.S. Army Corps of Engineers (1956). They estimated the PMP using the physical approach and for a 3-day storm suggest amounts of 368 mm (14.5 in.) of rainfall in the Pembina Basin (in a 1 554 km^2 or 600 sq. mi. area). The study's DAD curves for 24, 48, and 72 hours are shown in Figure 1.9. McKay's (1968) results (based on Hershfield's approach) are also displayed on the figure.

One of the most recent publications on PMP estimates is by Verschuren and Wojtiw (1980), in which both the traditional and statistical approaches were used to obtain estimates of PMP for the six main river basins in Alberta. The results of this work are discussed further under characteristics of PMP in Chapter 2.

1.2.4 Historical Flood Studies in Alberta

A number of publications have documented individual storms that have caused extensive flooding in Alberta. Although estimates of PMP or PMF were not discussed in these studies, it is important to recognize the work done in this area, for some of these storms play an important part in the PMP estimates and also demonstrate that rainstorms do cause

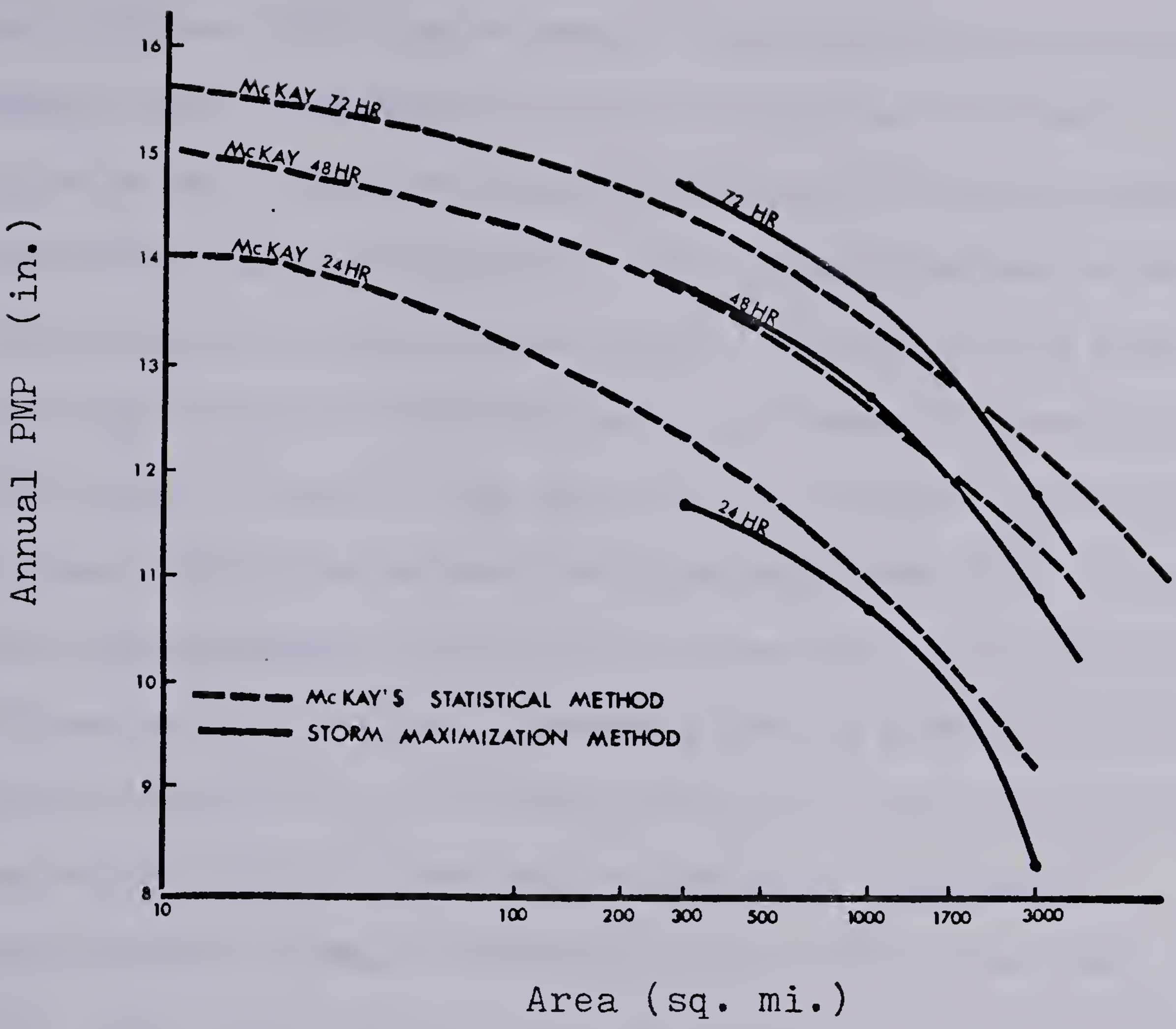

FIGURE 1.9. DAD Curves for 24-,48-,and 72-hour Durations for the Pembina Basin, Alberta (After Buckler and Quine, 1971; McKay, 1968).

extensive flooding. One such study was done by Thompson (1976), who used archive records to reconstruct three severe storms (June 1897, July 1902, and June 1915) on the Bow and North Saskatchewan rivers. The author concluded that the storm type that produced heavy rainfall in all three cases was a cold low. The rainfall that caused record floods from

the 1897 and 1915 storms was of extraordinary intensity [6], whereas the third storm (1902) was not as intense [7]. The latter event, however, was preceded by an exceptionally wet period during which the soil very likely became saturated and thereby enhanced storm runoff. The resulting peak discharge from the 1897 storm is believed to have produced the highest flood on the Bow River at Calgary dating back to at least 1884. The storm that preceded the 1915 flood on the North Saskatchewan River is believed to have produced extremely heavy rainfall amounts over a wide section of the Eastern Slopes of the Rockies and the foothills of Alberta. The instantaneous discharge recorded on the North Saskatchewan River at Edmonton was 5 806 m^3 per sec (205 000 cubic feet per second (cfs)) on 28 June 1915, and the daily discharge of 4 644 m^3 per sec (164 000 cfs) recorded on the following day is by far the highest on record for that location since 1911. The same storm produced the highest instantaneous discharge on the Red Deer River at Red Deer since records began in 1913, the fifth highest on the Bow River at Calgary since 1884, and very high discharges on the Macleod and Athabasca rivers.

Another example of a study where rare floods were examined is the report by Neill (1965), in which the author

---

[6] The 4-day rainfall amount in the 1897 storm exceeded a 1:100 year event, while in the 1915 storm the 2-day rainfall amount exceeded a 1:50 year value at Nordegg and Lovett.

[7] The heaviest 1- and 3-day amounts recorded during the storm are less than a 1:10 year event.

tabulated rare flood discharge data from 47 selected hydrometric stations in Alberta. In addition, the author plotted the 100-year mean daily flows against drainage areas and obtained a general empirical relationship of the form

$$Q_{100} = F A^{0.8} \tag{1.5}$$

where Q_{100} is the 100-year mean daily flow (cfs), F is a coefficient, and A is the drainage area (sq. mi.). The author also calculated the values of F for each station and depicted this on a map of Alberta. A plot of maximum recorded flows against drainage areas indicated an upper envelope curve with the equation

$$Q_{max} = 1588 A^{0.55} \tag{1.6}$$

A more recent example of a rainstorm that produced severe flooding occurred on 7-8 June 1964 (Warner, 1973) in the headwaters of many streams in Montana and southwestern Alberta. The main flood area in Alberta occurred in Waterton Lakes National Park. Flooding was primarily attributed to extreme rainfall (unofficially, over 250 mm (10 in.) in Waterton Park) influenced by the right combination of antecedent conditions: below-normal temperatures that delayed the usual snowmelt-runoff pattern (from March to May), and above-normal precipitation in May that resulted in large-scale melting of the snowpack in the latter part of

May, which continued into June at a sustained high rate. Although this storm occurred mainly in United States, with Alberta receiving only a small segment, the possible occurrence of such a storm further north cannot be ruled out.

Flood-producing rainstorms are not restricted to the southern part of the province. For example, Warner and Thompson (1974) presented a report on the 11-12 June 1972 rainstorm in which more than 150 mm (6 in.) of rain fell over parts of the Peace River Basin southwest of Grande Prairie, resulting in record flows in nearly all streams in that area. Other documented examples of rainstorms causing flooding conditions in northern Alberta include studies by McKay (1966) of the 30 July to 1 August 1953 storm on the Paddle River; by Froelich (1967) of the June 1965 storm in the Peace, Athabasca, and North Saskatchewan basins; and by Mustapha (1970b) of the 27 June to 1 July 1970 storm in the Lesser Slave Lake and Lac La Biche forestry regions.

A more recent publication on floods is the study by Mustapha et al. (1981) in which the authors presented a compilation of historical flood data and information concerning recorded floods within the North Saskatchewan River Basin. Data from 18 selected hydrometric stations in the basin with varying streamflow records between 1911 to 1978 were selected as representative of floods in the mountains, foothills, plains, and mainstream of the North Saskatchewan River. In the report the authors examined the

maximum annual flood discharge, the causes of floods, the effect of ice on recorded stages, the historical flood levels, flood damages, and flood frequency analyses. In the mountain region most of the volume of annual runoff and the annual flood peaks are due to snowmelt in the spring and summer. In the foothills, although snowmelt contributes to runoff, the major flood peaks are generated by heavy rainfall in this region. Runoff from mountain snowmelt combined with runoff from major storms in the foothills generally produced the largest flood peaks on the North Saskatchewan River. In this region, cold lows produce the major floods. In the plains region, snowmelt is the major contributing factor to the maximum annual flood peak, and this usually occurs in April or early May. On occasion, the early spring runoff from this region is due to a combination of rain and snowmelt. In some years the maximum annual flood peaks result primarily from heavy summer rainfall.

Mustapha et al. (1981) also discuss urban storms, in particular the storm that occurred in the Edmonton area on 10-11 July 1978 causing over $1.3 million damage. Although this storm did not produce very large recorded maximum point precipitation, it did produce extensive flooding in the city of Edmonton and surrounding towns. Urban flooding is generally caused by highly localized rainstorms whose intensity and subsequent runoff exceed the design capacity of the urban storm sewer system.

1.2.5 Snowmelt Studies

As was discussed earlier, some major floods result from melting snowpacks or from snowmelt combined with rain. To estimate the maximum floods in these regions it is necessary to consider the contributions of snowmelt water to major floods. This requires (1) determination of the maximum seasonal snow accumulation and (2) estimation of the critical melting rate of the snowpack.

Three methods have been used to estimate the upper limits of snow accumulation on watersheds: (a) partial season (or synthetic season) method, (b) snowstorm maximization method, and (c) statistical method.

In the partial season method an estimate of the physical upper limit of seasonal snow accumulation is made by assuming that the largest snowfalls for discrete intervals (i.e., 2, 4 days, or 1 month) during the recorded period can be combined, regardless of their year of occurrence, to produce a synthetic year of very high snowfall. The validity of such a synthetic year has been questioned, since different years are being combined. If a long recorded period is available, the upper limit obtained by this method would rarely be exceeded; however, for data bases with a short duration record this is not necessarily true, and hence caution must be applied in the interpretation of such results.

In the second method, the maximum snowfall is obtained by snowstorm maximization of all the snowfalls over the

basin for the entire winter. A factor is used to estimate the maximum moisture flow causing the snowfall. This factor, similar to that used for rainfall, is equal to the ratio between the maximum possible moisture content for the time of year when the snow fell and the moisture observed in the airmass that actually produced the snowfall.

The last approach, the statistical method, estimates the snowpack on the basis of a long return period, such as 100 or 1000 years, by applying the extreme value theory of Gumbel (1954) to the maximum annual water equivalent of snow cover. This approach is applied to point values, which are then translated into an areal estimate based on the assumption that there is little variation in the water equivalent of the snow cover. This assumption is usually correct for the plain areas; however, for mountainous regions it may not be applicable. The approach is also highly dependent on the recorded period, and caution should be used when obtaining estimates from stations with a short record length.

Some studies of eastern Canadian basins (Gagnon et al., 1970) suggest that the result obtained by the snowstorm maximization method corresponds fairly closely to the value derived by the partial season method; however, none of these methods is entirely satisfactory. Perhaps the second approach, the winter snowstorm maximization, has the most credibility, but there is the problem of compounding unlikely events by assuming that all winter storms in a

season occur with maximum water vapor content in the snow-producing air mass. Research on new and better methods of estimating maximum snow accumulation is needed.

For estimating critical snowmelt rates, two main approaches are commonly used. The first is the degree-day method, while the second is to apply generalized snowmelt equations based on energy balance considerations (U.S. Army Corps of Engineers, 1956).

In the degree-day method the melt (M) is expressed as a linear relationship of the daily air temperature and can be written as

$$M = C\sum T_a \qquad (1.7)$$

where C is an empirically determined coefficient and $\sum T_a$ is the sum of positive daily air temperatures (^{o}C) for a designated period. Either maximum or mean temperatures can be used for T_a. There is some physical justification for this approach, since air temperature is reasonably well correlated at a particular time and place with atmospheric factors that affect melt rates, such as solar radiation and vapor pressure. This is a simple and useful approach for calculating snowmelt but has some limitations because there is considerable variability in the coefficient C from basin to basin, year to year, and time to time within the snowmelt season, depending upon factors that cannot be represented by air temperature alone (i.e., albedo of the snow surface,

wind, dew point, and radiation). To date, little effort has been expended to justify the usage of the mean or maximum temperature in the interpretation of these quantities.

The other and more rigourous approach is to apply generalized snowmelt or energy balance equations, which can be written as

$$M = M_{rs} + M_{rl} + M_{ce} + M_{r} + M_{g} \qquad (1.8)$$

where M is the total snowmelt, M_{rs} is the short-wave radiation melt, M_{rl} is the long-wave radiation melt, M_{ce} is the melt due to convective heat transfer from the atmosphere and to latent heat of water vapor condensing onto the snow surface, M_{r} is the melt due to heat of raindrops, and M_{g} is the melt by heat conduction from the ground. Approximation of each of the various melts have been described by the U.S. Army Corps of Engineers (1956). Because these approximation were developed for a specific basin, the user must calibrate the coefficients for the basin being studied.

For both the energy balance equations and the degree-day method, curves of highest maximum (or mean) temperatures for the snowmelt season need to be developed for a representative long-term record station or stations within the basin. In using the degree-day method, the temperature sequence is all that is required. For the energy balance procedure, critical values of other meteorological factors (insolation and albedo, dew point temperatures, and wind)

are needed. The energy balance equations have been employed in Alberta by various authors (McKay, 1965b, 1968; Buckler and Quine, 1971; Storr, 1978) in computing snowmelt. In many of these studies, the coefficients given by the U.S. Army Corps of Engineers were used, and coefficients were not calibrated for the Alberta river basins.

1.2.6 Flood Estimates and PMF

To determine characteristics of a flood that would result from a given rainstorm and/or snowmelt period, it is necessary to estimate the percentage of basin water that will appear as surface runoff. Some of the rain or snowmelt water will infiltrate the soil and will not contribute directly to the flood rise; instead, it may recharge groundwater or be stored in the soil. The water that flows quickly into the stream channels mainly overland or as interflow is known as direct runoff. It is this volume that must be estimated. Direct runoff varies from time to time within a basin and from basin to basin. Each basin has a characteristic response depending on factors such as the permeability of the soils, the vegetation, the slopes of main land areas of the basin, the amount of the basin in swamp area or lakes, and the amount of small depression storage in the basin. Within a given basin the volume of direct runoff from a given amount of rain varies with the season, the antecedent conditions, and the duration and intensity of storm rainfall. Since all of these factors are

complex and some are interrelated, it is very difficult to estimate runoff volumes. For a particular river basin with records of streamflow and precipitation, a common procedure has been to develop multiple variable rainfall-runoff correlations either graphically or by empirical formulas (World Meteorological Organization, 1975).

Graphical relationships have been published by the U.S. Geological Survey (Chow, 1964) in flood-frequency reports for various states. From these the magnitude and probable recurrence interval of floods may be determined at any place on a stream, within the limits of the basic data. There are two discharge-frequency curves that are commonly used: the first expresses the flood discharge-time relationship and shows variation of peak discharge, which is expressed as a ratio of the mean annual flood, as well as recurrence interval [8] ; the second curve relates the mean annual flood [9] to the area alone or to the size of area and other significant basin characteristics.

From about 1913 to the 1930s, what is now known as the first flood frequency formula was developed by Fuller (1914) from the discharge records of hundreds of streams. The

---

[8] The average interval of time within which the given flood will be equalled or exceeded. A flood having a recurrence interval of 10 years is one that has a 10% chance of recurring in any year. Likewise, a 50-year flood has a 2% chance, and a 100-year flood has a 1% chance, of recurring in any year.

[9] The Gumbel distribution is used to express the mean annual flood, which is defined as the flood having a recurrence interval of 2.33 years.

formula is:

$$Q_T = \overline{Q}\,(1 + 0.8 \log_{10} T) \qquad (1.9)$$

where Q_T is the flood of return period T (in years), and $\overline{Q}$ is the mean highest annual flood. Fuller suggested using the above formula to estimate floods with as long a return period as 1000 years. As late as 1932, T = 1000 was recommended as the spillway design flood for certain classes of earth dams, together with a generous freeboard safety factor. This suggestion (i.e., T = 1000) is based not only on extrapolation of what appeared to be a law, but also on transposition and envelopment. It is now known that extrapolation to such return periods is uncertain.

With more discharge records, directly enveloping the records of peak discharges (normalized for area) rather than assigning specific frequencies became more popular in deriving the maximum flood. The most famous is the Myers' equation (Chow, 1964) in which peak discharge is proportional to the square root of the area drained and to a coefficient that varies with region and geology. Myers' formula is:

$$Q_m = C\,A^{0.5} \qquad (1.10)$$

where Q_m is the maximum discharge (cfs); C is an empirical coefficient varying with climate and geological

characteristics; and A is the drainage area (sq. mi.).

The second emphasis in the period from about 1914 to 1935 was on the use of probability theory to estimate magnitude of the flood. Curves were derived from past records on a stream, and the frequency was determined for the occurrence of a given flood. From data with a few years of records (i.e., seldom exceeding 20 years and rarely exceeding 30 or 40 years), probability curves were extrapolated to estimate the average expected discharge for longer time durations (i.e., once in 1 000, 5 000, or 10 000 years). This theory proved to be inadequate in that some of the floods that occurred in the 1930s, were estimated by the probability method to have a return period of once in millions or even billions of years, and not the usual assumed 1 000 to 10 000 years. One such example is the flood in 1935 on the Republican River in Nebraska, which was over 10 times larger than had occurred on that river during the previously recorded 40 years. The probability method would not have made provision for an adequate spillway for that flood.

The nature of flood analysis changed in the 1930s, with the increased knowledge of floods gained by superimposing the enveloping curves of record-breaking floods that occurred between 1890 to 1939 (Figure 1.10) (Craeger, 1939). With more gauging stations and longer records, the curves depict an upward trend in flood flows (there is no evidence that these changes were climatological). The increased data

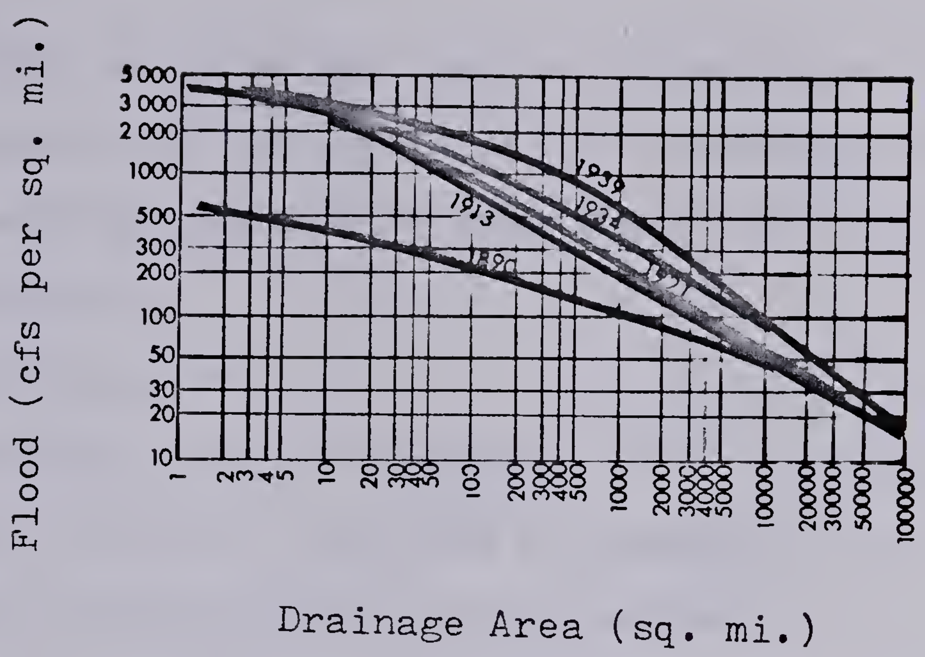

FIGURE 1.10. Enveloping Curves of Known Floods in the United States up to a Given Time Period (After Craeger, 1939).

significantly raised the records of flood flows for all drainage areas. For instance, the maximum flood for an area of 259 km^2 (100 sq. mi.) that in 1890 had a limit of 2.2 m^3 per sec per km^2 (200 cfs per sq. mi.) was increased about ninefold in 1939 to 19.7 m^3 per sec per km^2 (1800 cfs per sq. mi.). For larger areas the increase between the 1890 and 1939 results was less, for example, the flood for 25 900 km^2 (10 000 sq. mi.) being about double.

Many rainfall-runoff formulas have been derived for computing flood discharges since the 1940s, but most are considered inadequate for engineering design. Difficulties in the application of empirical relationships arise not so much from the empiricism of equations but more from the lack of knowledge of the exact conditions under which they may be applied. Peak flow formulas can be classified according to

the number of variables used in the equation. Listed below are examples of the functional relationships of the numerous peak formulas compiled by Gray (1970) in which flood flows are related to

(1) drainage area
(2) drainage area and frequency
(3) area, rainfall, and time paramaters
(4) basin width and rainfall parameters
(5) basin width, rainfall parameters, and slope
(6) area, slopes, and rainfall parameters
(7) area, elevation, length, and lakes.

A comparison of some of the flood formulas is presented in Figure 1.11 (Gray, 1970). No correlation relation between the various formulas is given and hence it is difficult to assess their reliability.

Another important characteristic of a flood to consider in spillway design is the hydrograph shape. The numerous papers published on the time distribution of runoff not only indicate the importance of hydrograph shape, but suggest that the techniques are far from being completely definitive. Where sufficient data on streamflow are not available to enable the shape of the flood hydrograph to be determined, simplified geometric forms have been used for approximation. It is obvious that simple geometrical forms are only first approximations and that more attention should be directed to the characteristics of the drainage area.

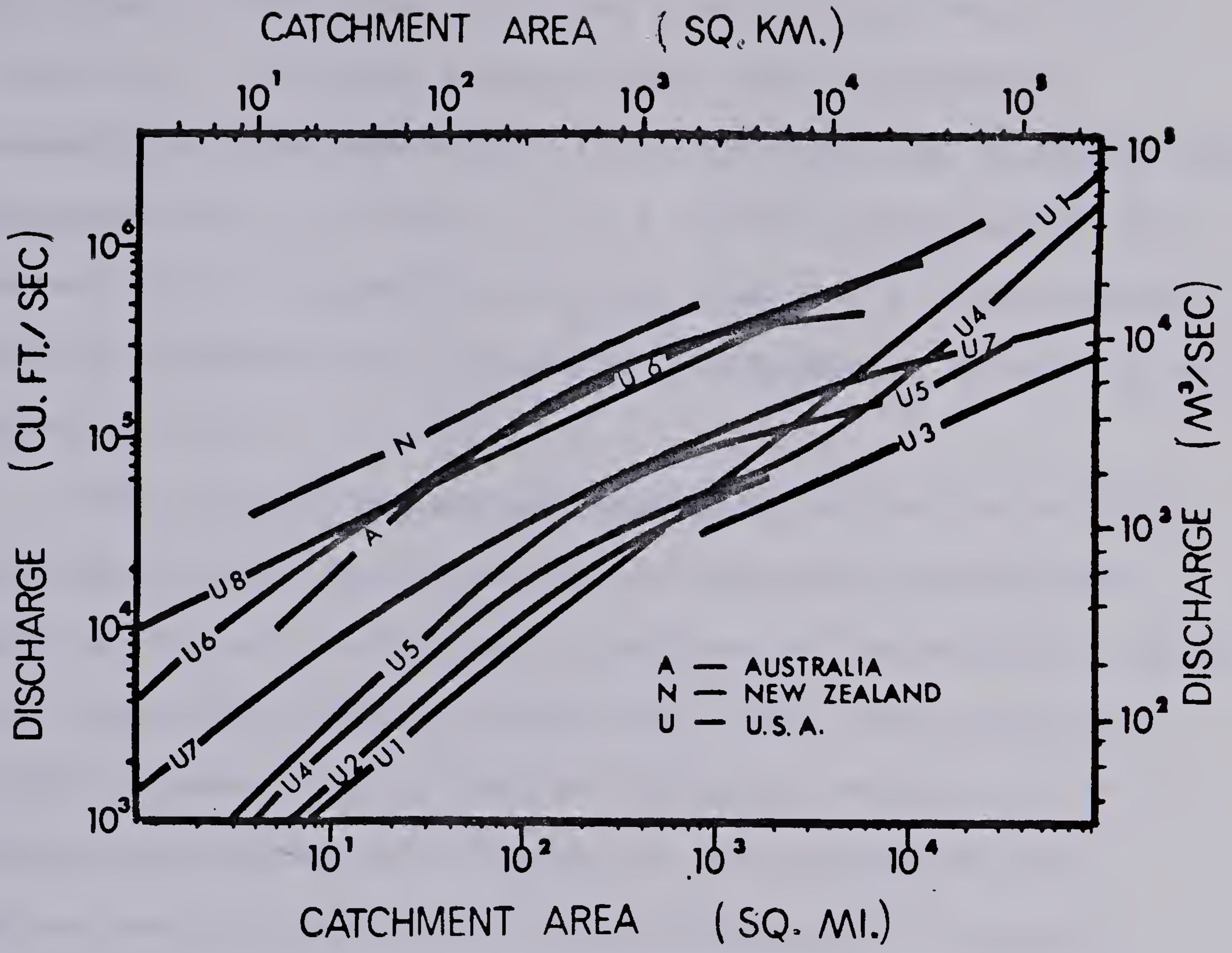

FIGURE 1.11. Comparison of Some of the Flood Formulas in General Use (After Gray, 1970).

The unit hydrograph method originally presented by Sherman (1932) has been the most widely used method of flood wave form computation. This method has been modified by many authors, but most of the basic principles have not changed. The unit hydrograph is defined as a hydrograph derived from storm rainfall of a specified duration, where the volume of surface runoff accounted for is of unit depth on the basin. The unit hydrograph method and its modifications are based on assumptions not entirely fulfilled in nature. Johnstone

and Cross (1949) give a fitting characterization of this situation: "All these propositions (unit hydrograph assumptions) are empirical. It is not possible to prove them mathematically. In fact, it is a rather simple matter to demonstrate by hydraulic analysis that not a single one of them is mathematically accurate. Fortunately, Nature is not aware of this."

The difficulties encountered with collection of data required for derivation of unit hydrographs caused many workers to seek further modifications of the method. Lack of sufficient precipitation and runoff data inspired Snyder (1938) to develop a synthetic hydrograph method. In this method the individual elements of the hydrograph are determined by computation. Peak discharge for a given duration was derived by Snyder from the equation

$$Q_m = 640\ c_p\ A_d \,/\, t_p \qquad (1.11)$$

where Q_m is the peak discharge (cfs); c_p the coefficient accounting for flood wave and storage conditions; A_d is the watershed area (sq. mi.); and t_p the lag time (hr). Values for c_p range from 0.4 to 0.8 and generally indicate retention or storage capacity of the watershed. Application to streams in other parts of the world requires different values of the c_p coefficient. The relation between the time of the center of precipitation period and the peak of the hydrograph rise (t_p) is given by the formula

$$t_p = c_t (L L_c)^{0.3} \qquad (1.12)$$

where c_t is a coefficient from 1.8 to 2.2 (dependent on slope of the drainage area); L is the total length of the main stream (miles); and L_c is the length of main stream from gauging station to cross section nearest to the centroid of the drainage area (miles).

The U.S. Department of Agriculture Soil Conservation Service (SCS, 1969) has developed a dimensionless unit hydrograph where ordinate and abscissa values are expressed as a nondimensionless relationship. Peak runoff and rise time depend on basin area, duration of rainfall excess, length of the main channel and slope of the watercourse. The peak flow of the unit hydrograph can be calculated using the following formula:

$$Q_p = 484 A / P_R \qquad (1.13)$$

where Q_p is the peak runoff, A is the area of the watershed (sq. mi.), and P_R is rise time (hours).

The Tennessee Valley Authority (1973) has developed a unit hydrograph using a double triangle defined at four points. Major elements corresponding to these four values are basin area, shape, length of the main watercourse, drainage density, percentage wooded area and soil type. Hoang (1977) has modified and applied this method to small watersheds in southern Quebec. The peak flow is calculated

using the following formula:

$$Q_p = K A^x \tag{1.14}$$

where Q_p is the peak flow of a unit hydrograph resulting from a net rainfall of 2 hours, K is a regional constant, A is the area of the watershed, and x is a regional constant. Hoang (1977) has developed by regression the values of the regional constants for southern Quebec.

It is interesting to compare the different formulas used to calculate peak flow. In all of these formulas, area is the common element. In the Snyder and SCS formulas, the flow varies linearly according to area, while the Hoang model contains an exponent of area that approaches unity.

Empirical formulas have been applied to watersheds in western Canada. McKay and Stichling (1961) obtained a relationship for the envelope curve of extreme flooding on the prairies, for which peak discharge and drainage area (Figure 1.12) are determined by Equation 1.10, with C equal to 400.

Another example is the work of Godwin (1975), who carried out regionalized estimates of PMF for 72 sites in the prairie provinces, primarily for the Saskatchewan Nelson Basin. The estimates were made for areas with floods from mountain and prairie streams. The results showed that for both types of streams the maximum mean daily peak flow per unit area (Figure 1.13) decreased exponentially with an

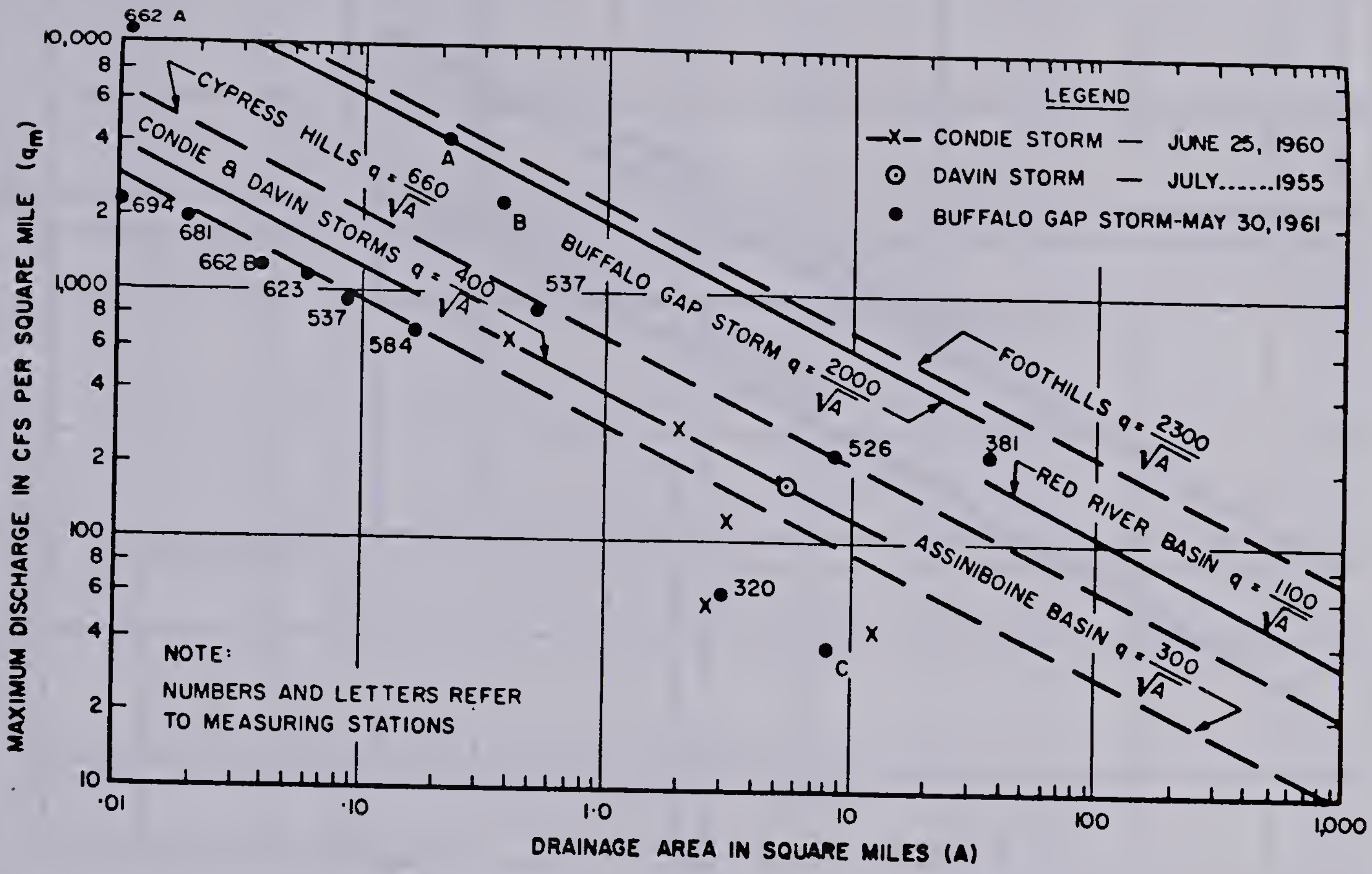

NOTE:
NUMBERS AND LETTERS REFER TO MEASURING STATIONS

FIGURE 1.12. Envelope Curves of Extreme Floods on Prairies (After McKay and Stichling, 1961).

increase in the drainage area, with the mountain-fed streams having a higher magnitude. The relationships for these curves also take the form of Equation 1.10.

1.2.7 Computer Simulation Modelling of PMF

The concept of a mathematical model for simulation of synthesized streamflow has become prominent in the past 20 years, primarily with the advancement of electronic computer technology. The basic concept involves simulating a

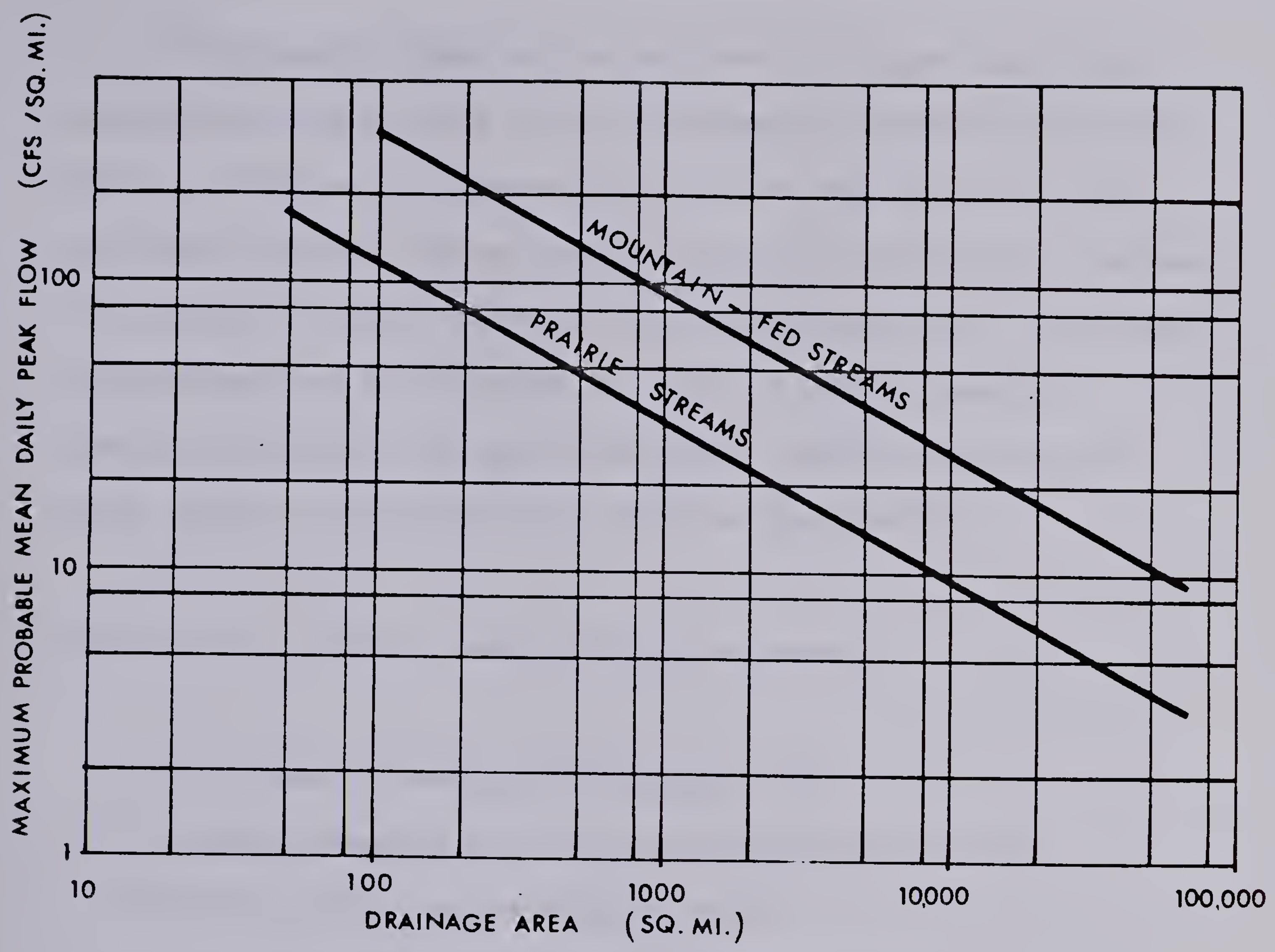

FIGURE 1.13. Mean Daily Peak Flow Versus Drainage Area for Probable Maximum Floods (After Godwin, 1975).

mathematical model comprising the physical processes involved in the hydrologic cycle. Such a model may include rainfall or snowmelt, effects of transpiration, interception losses, infiltration rates, soil moisture, depression storage, and groundwater storage. Usually the flow is then separated into its components of surface, subsurface, and base flow. Various versions of computer models have been developed with additions or updates of the various runoff processes.

At present, there are more than 20 major hydrologic simulation models (U.S. Army Waterways Experiment Station, 1974) available for representation of the hydrological processes. These can be subdivided into three main classes: (a) rainfall-runoff event simulation models, (b) continuous streamflow simulation models, and (c) urban runoff simulation models. Some of the more common models (with their abbreviated notation) are the following:

a) Rainfall-runoff event simulation models

HEC-1 Flood Hydrograph Package-(HEC-1)
Computer Program for Project Hydrology-(TR-20)
USGS Rainfall-runoff Model-(USGS)
Hydrologic Model Computer Language-(HYMO)
Storm Water Management Model-(SWMM)

b) Continous streamflow simulation models

Antecedent Precipitation Index Model-(API)
1970, 1973, 1974 Revised Watershed Hydrology-(USDAHL)
Stanford Watershed Model IV-(SWM-IV)
Kentucky Watershed Model-(KWM)
Self-optimizing Hydrologic Simulation Model-(OPSET)
Hydrocomp Simulation Program-(HSP)
Texas Watershed Model-(TWM)
National Weather Service Runoff Forecast System-(NWSRFS)

Streamflow Synthesis and Reservoir Regulation-(SSARR)
Ohio State University Version of SWM-IV-(OSUSWM)

c) Urban runoff simulation models

University of Cincinnati Urban Runoff Model-(UCUR)
Chicago Hydrograph Method-(NERO)
Quantity and Quality of Urban Runoff-(STORM)
Road Research Laboratory Model-(RRL)
MIT Catchment Model-(MITCAT)

A review of these models (U.S. Army Waterways Experiment Stations, 1974; World Meteorological Organization, 1975; Viessman et al., 1977) indicated a tremendous diversity in scope and purpose, mathematical detail, system elements, and hydrologic phenomena being modelled, size of the system that can be handled, data requirements, and computer output. These diversities are the result of the varying conditions and objectives that govern the design and evaluation of individual drainage systems. The state of development of these models also varies significantly. Some models have been developed and verified extensively, others have been developed but not verified, and some have been developed conceptually but not carried to the point of application. In addition, because no standards exist for evaluating and comparing models, differing criteria have been used in the evaluations. The rigor with

which the models have been tested varied greatly, from intuitive judgments to graphical comparisons and more demanding statistical analyses.

To provide a quick overview of the features of these models, a summary indicating the mathematical formulations used in the models is presented in Figure 1.14. It must be remembered that most of the models are being revised, expanded, and improved continuously by the model developers. A major drawback with many of the existing models is that they have not been developed for large rural drainage basins or have not incorporated snowmelt computations. The latter is important for estimating the PMP and PMF for watersheds in Alberta. Other models have extensive data requirements, are difficult to implement or modify, and may be very expensive for simulation.

The following are some of the above models and other minor models that have been employed to estimate floods design and in some cases PMF estimates:

(1) Stanford Watershed Model-used in Quebec for certain small watersheds,

(2) SSARR Model-used by Alberta Environment for design purposes on the Red Deer and Paddle rivers,

(3) CEQUEAU Model-used to determine the design floods of several rivers in northern Quebec (Morin et al., 1979),

(4) Hydro-Quebec Model-used to make real-time forecasts of floods in Quebec (Bisson, 1979),

(5) UBC Model (University of British Columbia)-used to

	HEC-1	TR-20	USGS	HYMO	SWMM	API	USDAHL	SWM-IV	KWM	OPSET	HSP	TWM	NWSRFS	SSARR	OSUSWM
Infiltration and Losses															
1. Holtan's Equation							X	X	X	X	X	X	X	X	X
2. Horton's Equation					X										
3. Phillip's Equation			X												
4. SCS Curve No. Method		X		X											
5. Variable Loss Rate	X							X	X	X	X	X	X	X	X
6. Standard Capacity Curves					X										
Unit Hydrograph						X									
1. Input	X	X													
2. Clark's	X		X												
3. Snyder's	X														
4. 2-Parameter Gamma Response				X											
5. Dimensionless Unit Hydrograph		X													
River Routing															
1. Hydraulic					X										
2. Muskingum	X														
3. Tatum	X														
4. Straddle-Stagger	X														
5. Modified Puls	X														
6. Working R and D	X														
7. Variable Storage Coefficients	X			X											
8. Convex Method		X													
9. Translation Only			X			X									
10. Lumped Parameter Approach								X	X	X	X	X	X	X	X
Base Flow															
1. Input			X												
2. Constant Value		X	X												
3. Recession Equation	X							X	X	X	X	X	X	X	X

FIGURE 1.14. Comparison of Mathematical Formulations in Models (After Viessman et al., 1977).

calculate the PMF in 10 subwatersheds of the Peace River (Fawkes, 1979),

(6) SWMM Model-used to establish the design flood in urban areas for small basins (Leclerc, 1979).

Many of the models described above are restricted to

small river basin studies since they were developed and modified for these needs. The two models that appear to have been used in large river basins studies are the SSARR and UBC models. Mustapha and Ojamaa (1975) used the UBC SASK6 simulation model to obtain estimates of PMF for the Red Deer River at the Raven. Using DAD analyses of four rainstorms, the authors estimated the PMP to be 292 mm (11.5 in.) near the Raven for a 48-hour duration, and distributed this precipitation on 2 consecutive days, with 229 mm (9 in.) in the first 24 hours. The PMP was converted to flood flows by use of the UBC model; the resulting PMF hydrograph for Raven is shown in Figure 1.15 (Muzik, 1975) and indicates an instantaneous peak discharge of 4 814 m^3 per sec (170 000 cfs).

The SSARR model has been and still is being used for various studies by Alberta Environment; however, only internal reports have been prepared on its usage. In the mid 1970s, the Alberta Flow Forecasting Branch of Alberta Environment conducted an investigation of several high-powered hydrologic computer models in order to choose a model for real-time flow forecasting in Alberta. The watershed models included in the investigation were HEC-1, Modified Stanford, UBC Watershed Model, and SSARR. The study concluded that while any of the models, if properly calibrated, could produce consistently better results than a unit hydrograph approach, the SSARR Model was the most flexible, comprehensive, and easiest to operate of the four.

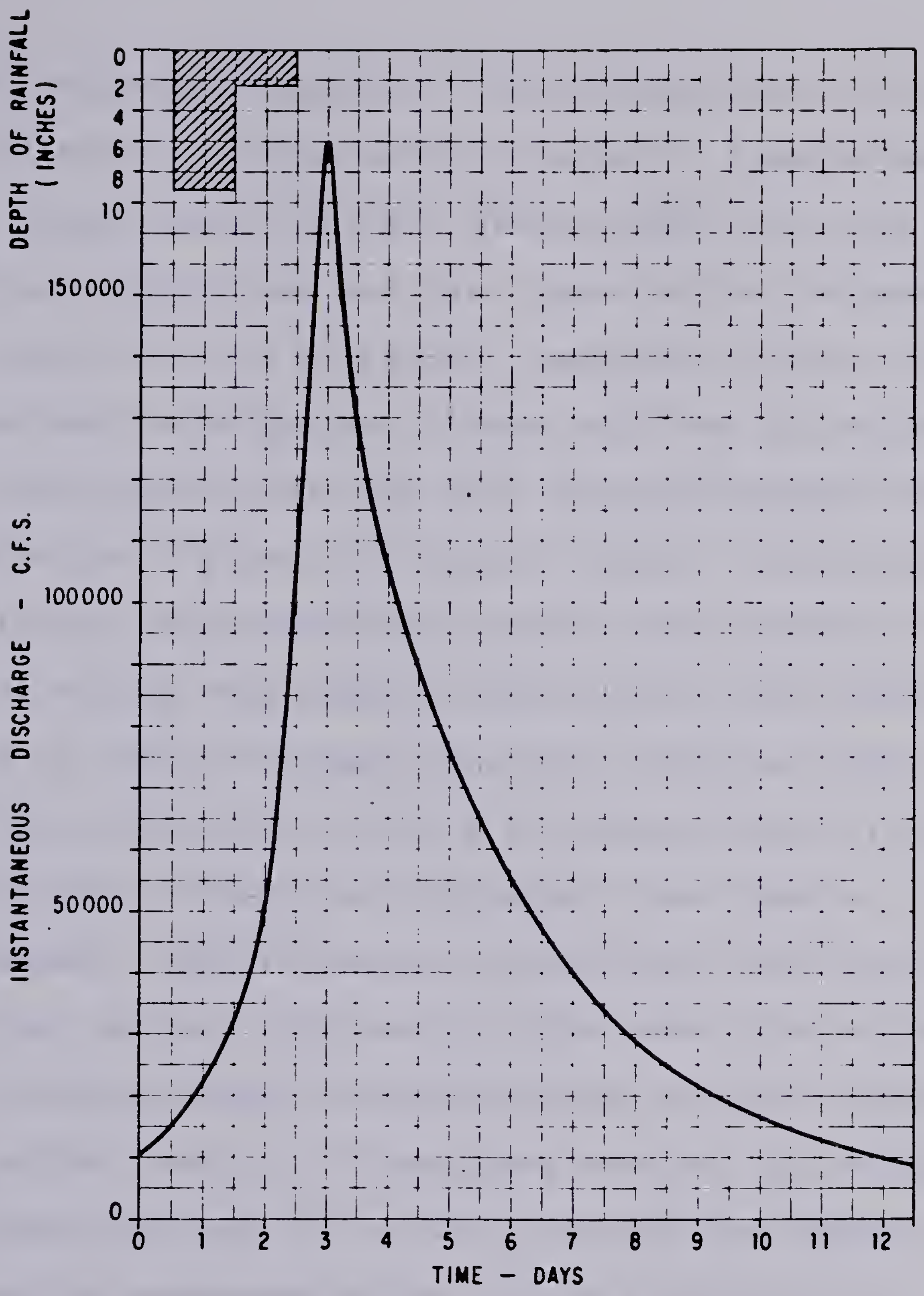

FIGURE 1.15. Probable Maximum Flood Hydrograph at Raven on the Red Deer River (After Muzik, 1975).

Because of its use by Alberta Environment and vast flexibility, the SSARR Model is used in this thesis.

1.3.0 Sources of Data and Models

A large number of different sources of data were used

in the analyses presented in this dissertation. Daily precipitation, maximum and minimum daily temperatures, dew point temperatures, and DAD analyses were obtained from the numerous publications and data tapes of the Atmospheric Environment Service of Canada, Downsview, Ontario. Daily streamflow discharges and stream and river characteristics came from publications and data sources produced and collected by the Water Survey of Canada, Inland Waters Directorate. River and hydrological characteristics were also extracted from numerous publications, and these are listed in the bibliography and are referenced where applicable. The SSARR model with appropriate write-up and descriptions of usage were obtained from Alberta Environment. The HYMO model was obtained from the City of Edmonton, Sanitary Engineering Department. The author would like to acknowledge the contributions of data, models and information from all of the above sources, for without this assistance the results in this dissertation together with the results presented in the author's publications (Verschuren and Wojtiw, 1980; and Wojtiw and Verschuren, 1981) would not have been possible.

CHAPTER 2

CHARACTERISTICS OF PMP

Probable Maximum Precipitation can be estimated by a number of methods, the two internationally accepted methods (World Meteorological Organization, 1973) are the physical (also called meteorological or traditional) and the statistical. Both of these methods have been examined extensively by Verschuren and Wojtiw (1980) in their publication dealing with Alberta river basins. In order not to duplicate this effort, only some of the results and figures are discussed and presented in this dissertation. The reader should refer to the above publication for an in-depth look at this topic. The results presented here deal only with the Red Deer River Basin, which is used as an example throughout this work. It should be noted that the sequence of major storm rainfalls was examined but not considered to be involved in PMP estimation.

2.1.0 Estimation of PMP by the Physical Method

The physical approach to obtaining an estimate of PMP was developed over a number of years. The method is indirect and is based on the analysis and maximization of the largest rainstorms that occurred during the period for which there are rainfall records. It assumes that the amount of rainfall

from a storm depends on two independent factors: 1) the moisture content of the air mass and 2) the efficiency of the rain-producing system. The procedure used for maximizing observed storm rainfall to estimate PMP involves moisture adjustments, storm transposition, and envelopment [1] . It further assumes that the largest rainstorm in the region has occurred during the period of record. This is an important assumption, which is open to criticism, especially regarding regions where scanty meteorological information is available. Because of its meteorological components, however, the method is much easier to relate to the physical occurrence and effect of rainfall from rainstorms and hence has been readily accepted by the meteorological and hydrological communities.

2.1.1 Estimation of Atmospheric Moisture

In production of precipitation, the moisture in the lower layers of the atmosphere is most important (Schwarz, 1967; U.S. Department of Commerce, 1960). Theoretical computations show that for excessive rain, air originally near the surface reaches within an hour or so the top of the layer from which the precipitation is falling. In the case of severe thunderstorms, surface air may reach the top of the storm in a matter of minutes because of the high-

---

[1] A process in which the largest value of PMP is selected from a set of data for a given area, and a smooth curve drawn is through the largest values.

velocity updrafts in such storms.

The most realistic assumption seems to be that the air ascends dry-adiabatically to the saturation level and then ascends moist-adiabatically. Thus hydrometeorologists generally postulate a saturated pseudoadiabatic atmosphere for extreme storms. To maximize the moisture of a storm, two saturation adiabats are required. The first gives a measure of the vertical temperature distribution in the storm to be maximized, and the second is the warmest saturation adiabat to be expected at the same location and time of year as the storm. In meteorology these two saturation adiabats are identified by the wet-bulb potential temperature, which corresponds with the dew point temperature at the 1000 mb level. The work by the U.S. Department of Commerce (1960) has shown that storm and extreme values of precipitable water may be approximated by estimates based on surface dew points when saturation and pseudoadiabatic conditions are assumed. An approximation based on surface dew point measurements is desirable since these measurements are more readily available than measurements at the 1000 mb level. Hence surface dew points are used in identifying the storm saturation adiabat for maximizing the moisture content of the storm. Both storm and maximum dew points can be reduced pseudoadiabatically to the 1000 mb level by use of Figure 2.1, so that dew points observed at stations of different elevations are comparable.

Since the moisture has an appreciable effect on the

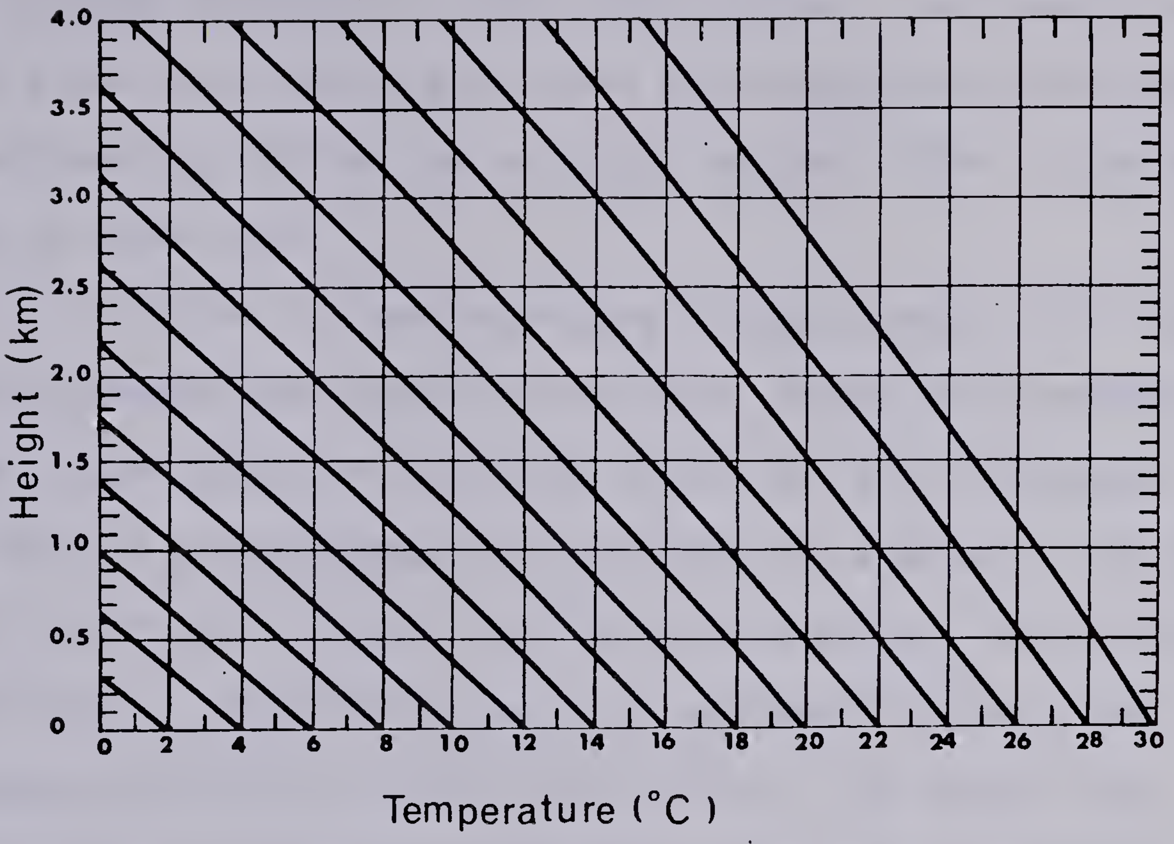

FIGURE 2.1. Pseudoadiabatic Diagram for Dew Point Reduction to 1000 mb at Height Zero (After World Meteorological Organization, 1973).

storm, precipitation must be that which persists for hours rather than minutes. Also, any single observation of dew point may be considerably in error; therefore, for estimating storm and probable maximum moisture the conventional procedure is to use dew point values on two or more consecutive measurements separated by a reasonable time interval. The adopted procedure is to use the so-called highest persisting 12-hour dew point. This is the highest value equalled or exceeded by all observations during a 12-hour period.

Paulhus and Gilman (1953) concluded that the 12-hour persisting dew point temperature was most representative of

the average moisture in the storm center. The results of this study have since been used and accepted internationally in estimating PMP by the physical method. This is the method used in this work.

It is from the maximum persisting 12-hour, 1000 mb dew point temperatures that the maximum values of atmospheric water vapor used for storm maximization are estimated. These dew points are obtained for stations in a given river basin. Since numerous estimates of PMP are required, each station must have an enveloping curve of semimonthly recorded maximum persisting 12-hour dew points. The author has produced such curves for Alberta (Verschuren and Wojtiw, 1980), with an example for the city of Red Deer given in Figure 2.2; graphs for the other stations can be found in the above publication. The 16 graphs produced in that report provide a comprehensive source of analyzed information for Alberta. Other studies had used only a few stations with less than half the record period, because of the limited data base available. With the aid of these curves, moisture adjustments can be made on the basis of the maximum persisting 12-hour dew point for the same time of year as the storm occurrence. Thus, for example, a May maximum dew point (and not one in September, for instance) would be used to maximize a May storm. Also prepared were monthly maps of maximum persisting 12-hour, 1000 mb dew points, which not only served as a convenient source of maximum dew points but aided in maintaining consistency between estimates for

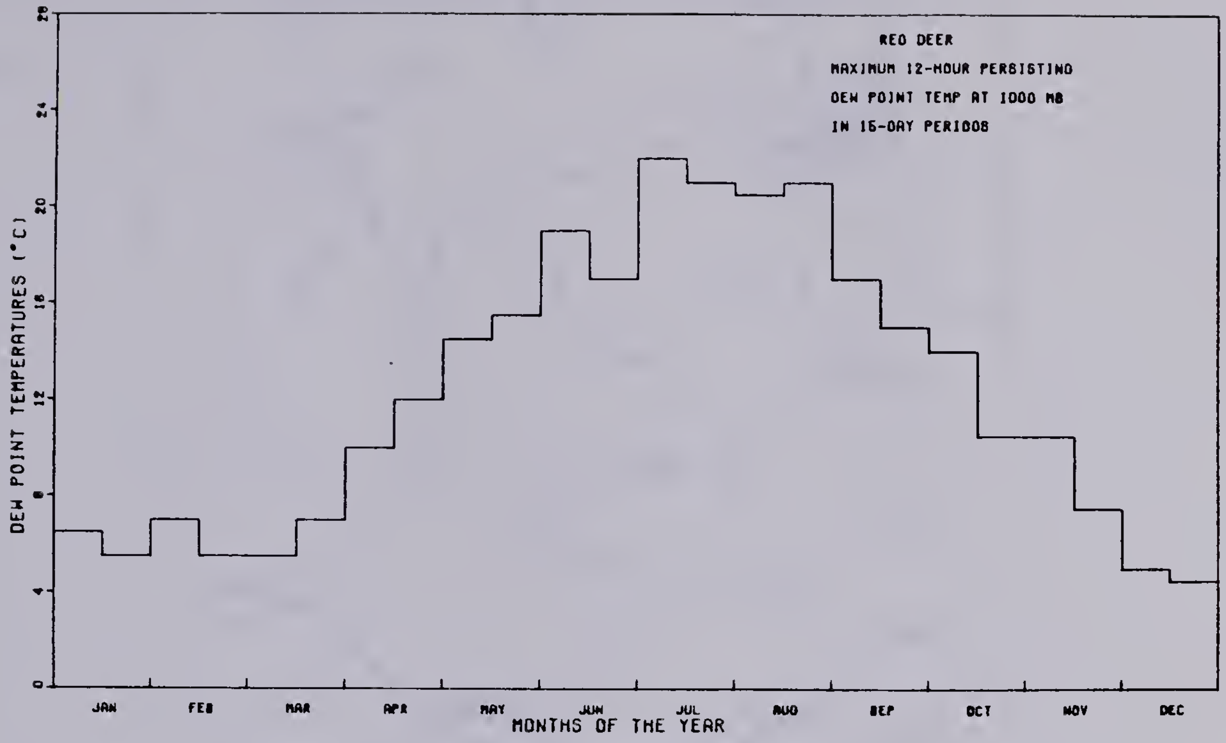

FIGURE 2.2. Maximum Recorded 12-hour Persisting Dew Point Temperatures at 1000 mb for the city of Red Deer (Verschuren and Wojtiw, 1980).

various basins. The maps were prepared by using the monthly maximum 12-hour dew point values, adjusting them to the 1000 mb level, plotting them at the locations of the observing stations, and drawing smooth isopleths. An example of such a map is shown in Figure 2.3 for the month of June in Alberta. The maps for other months can be found in Verschuren and Wojtiw (1980).

Before an estimate of the moisture maximization is obtained, it is necessary to find the amount of precipitable water available from the storm as well as the potential maximum amount produced at the maximum location. The amount of precipitable water, W (cm), can be computed by the

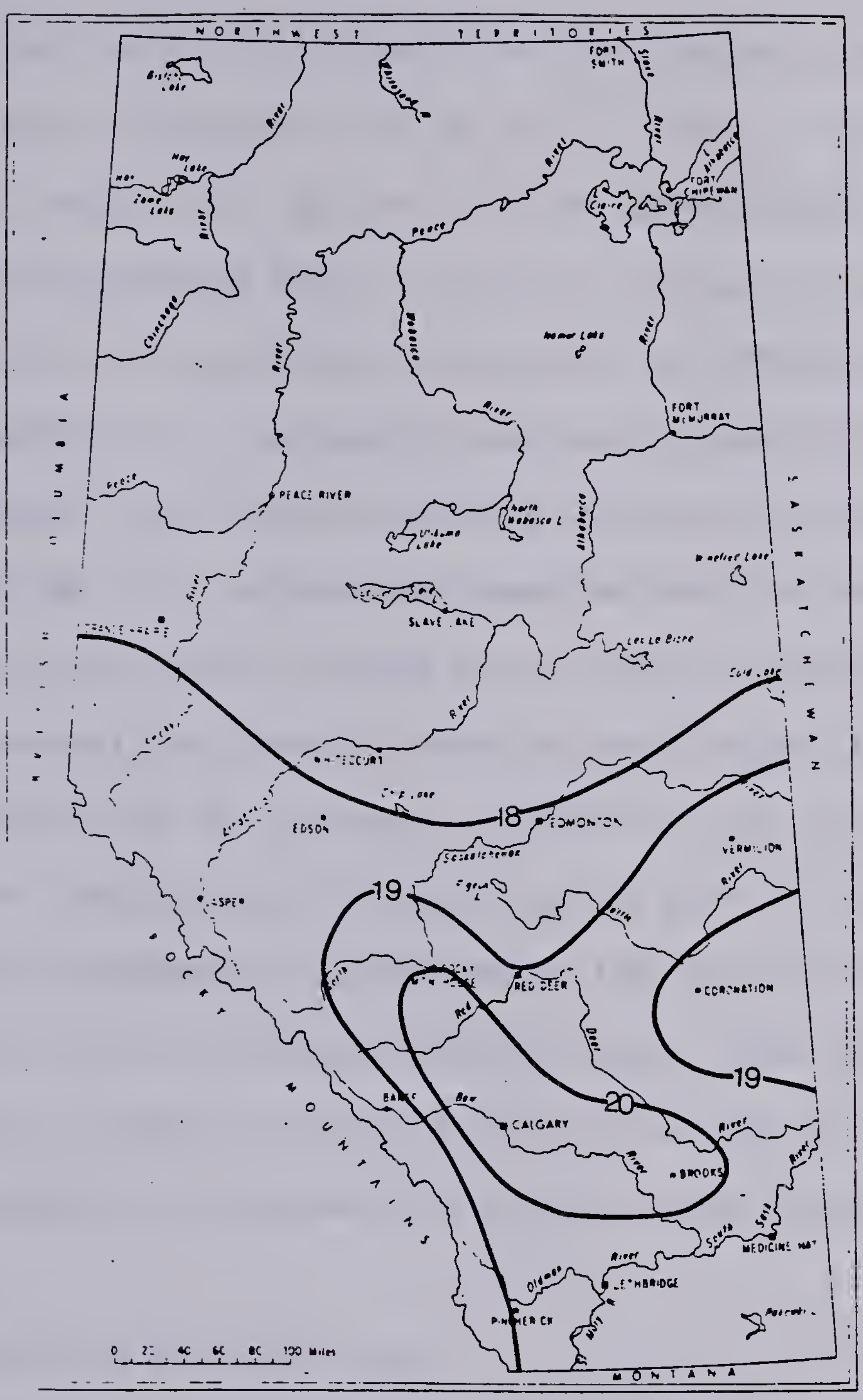

FIGURE 2.3. Isopleths of Maximum 12-hour Persisting Dew Point Temperatures for June (Verschuren and Wojtiw, 1980).

following general formula:

$$W = \frac{\bar{q}\,\Delta p}{g\rho} \qquad (2.1)$$

where $\bar{q}$ is the mean specific humidity in gm kg^{-1} of a layer

of moist air, Δp is the depth of the layer in mb, g is the acceleration of gravity in cm sec^{-2}, and ρ is the density of water (equal to 1 gm cm^{-3}). For convenience, Equation 2.1 can be pre computed and is usually listed in table or monogram form. Two tables are given in APPENDIX I: the first, Table A.I.1, presents values of precipitable water (mm) between the 1000 mb surface and various pressure levels up to 300 mb in a saturated pseudoadiabatic atmosphere as a function of the 1000 mb dew point. The second table, Table A.I.2, presents values of precipitable water (mm) for layers between the 1000 mb surface, assumed to be at zero elevation, and various heights up to 8 km (5 mi.). The 300 mb level is generally accepted as the top of the storm, but it makes little difference which level from 400 mb on up is selected, as there is very little moisture at those heights, and the effect on the moisture adjustment is negligible.

2.1.2 Moisture Maximization

Moisture maximization of rainstorms in place[2], consists of multiplying the observed storm rainfall amounts by the ratio (r_m) of the maximum precipitable water (W_m) indicated for the storm location over the precipitable water (W_s) estimated for the storm (World Meteorological Organization, 1973):

---

[2] Without change in location. Storm transposition requires a further moisture adjustment.

$$r_m = W_m / W_s \qquad (2.2)$$

2.1.3 Storm Transposition

Storm transposition refers to the transfer of storms from locations where they occurred to other areas where they could occur. The transposition procedure involves the meteorological analysis of the storm to be transposed, the determination of the limits of transposability, and the application of the proper adjustments for making the modifications required by the change in storm location. Two schools of thought seem to prevail on this topic in the hydrological community. The first advocates extensive transposition of storms over hundreds or thousands of kilometres. The greatest danger in this approach is deciding to transpose a storm when only limited analysis is planned or attempted. The second school of thought advocates limited transposition no more than a few hundred kilometres. The argument is that if no storms have occurred in the region in the last 50 years or so, they probably will not occur, since the topography is not conducive to such occurrences. The author in this study advocates the latter approach and hence has conducted limited storm transposition.

The storms that were transposed were adjusted according to the geographic features of that particular basin. The limits of transposability were governed not only by the constant lines of maximum persisting 12-hour, 1000 mb dew

point temperatures but also by the meteorology of the storms. After storm transportation the results of the PMP are usually depicted in a depth-area curve; an example of such a curve is shown in Figure 2.4.

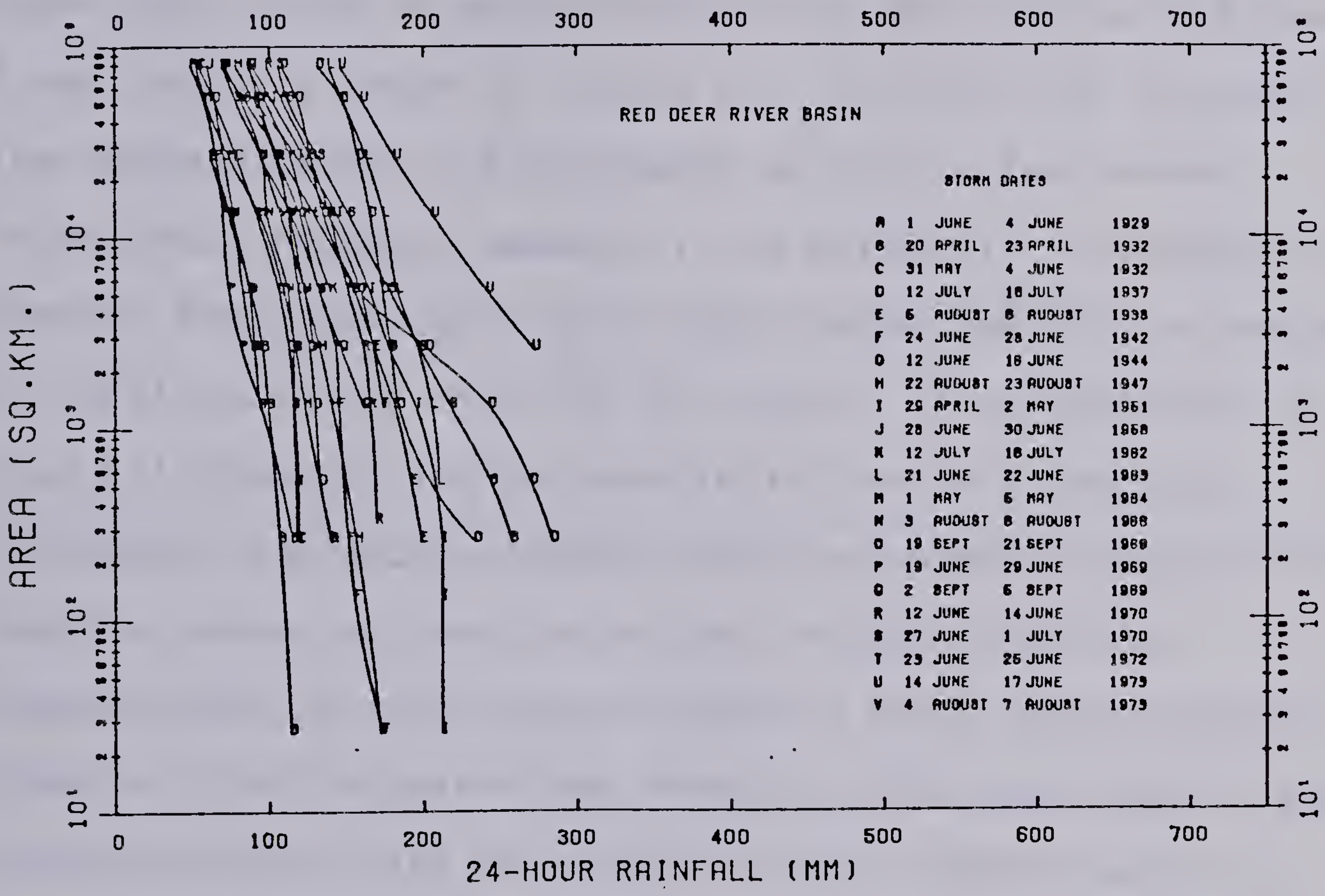

FIGURE 2.4. Depth-Area Curves of Maximized 24-hour PMP for the Red Deer River Basin (Verschuren and Wojtiw, 1980).

A single storm maximized and transposed to a basin gives the precipitation depth that could fall from that particular storm over that basin. In employing a single storm, there is no guarantee that the maximum magnitude of the precipitation has been achieved, since no single storm is likely to yield extreme rainfall values for all durations

and areal sizes. To obtain this maximum, all storms or as many as are available are plotted for the various durations and sizes of area. Some storms may not contribute at all to the enveloping curve, while others may contribute at certain durations. An example of a number of storms plotted on a depth-area curve of maximized 24-hour PMP for the Red Deer River Basin is shown in Figure 2.4. In the final analysis, the maximum values are dominated by only a few severe rainstorms; however, because it is difficult to determine whether the values of a particular rainstorm will be maximum in duration and/or area for the basin, it is necessary to plot all the most logical available rainfall analyses. Verschuren and Wojtiw (1980), wrote a computer program for rapidly producing such curves and included various combinations of durations for the six major river basins in Alberta. From the maximized rainfall data the largest value from any set of data is selected, and a smooth curve is drawn through the largest values (envelopment). A number of storms are plotted in Figure 2.5, where enveloping DAD curves for each specific duration are drawn for the Red Deer River Basin.

2.2.0 Estimation of PMP by the Statistical Method

Statistical procedures for estimating PMP may be best used wherever sufficient precipitation data are available. The method is useful for making estimates or when other meteorological data, such as dew point and wind records, are

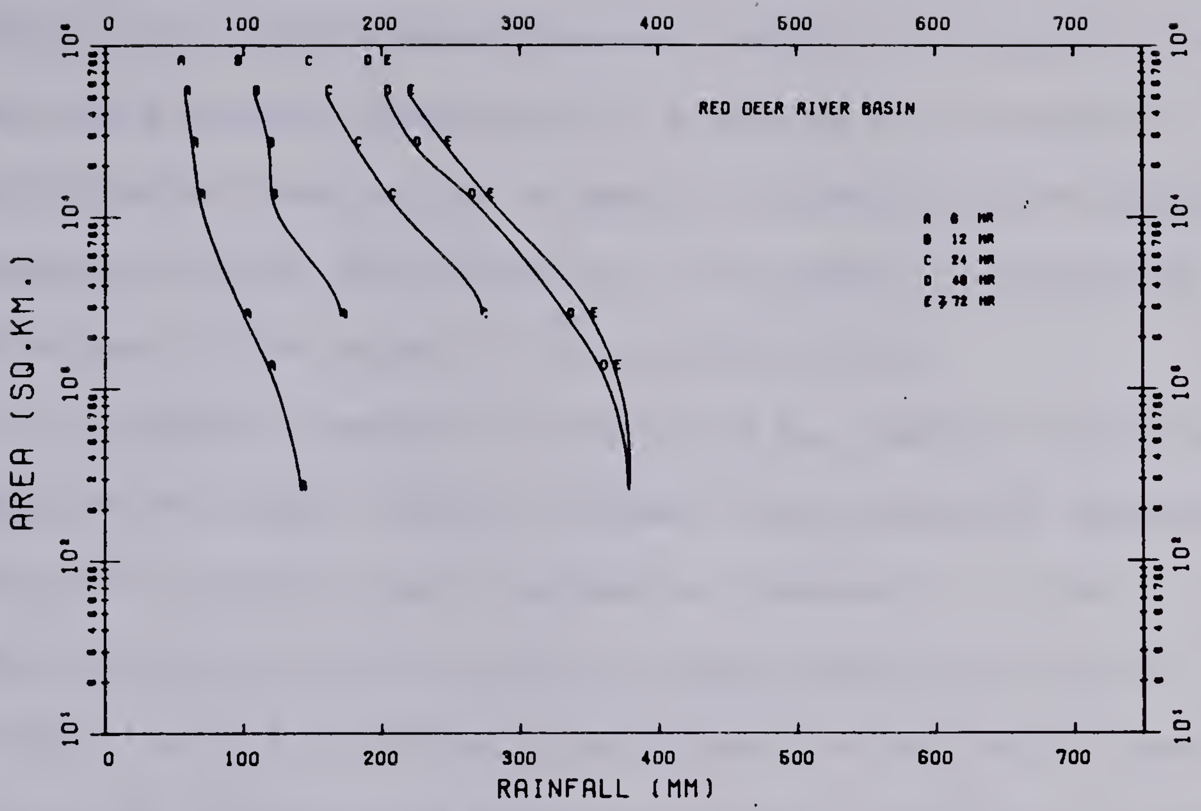

FIGURE 2.5. Enveloping Depth-Area-Duration Curves of PMP for the Red Deer River Basin (Verschuren and Wojtiw, 1980).

lacking. The procedure was developed by Hershfield (1961, 1965, and 1977), and though it is not the only approach, it is one that has received the widest acceptance, perhaps because it requires considerably less time to apply than does the physical approach, and needs only a limited understanding of meteorology.

2.2.1 Statistical Procedure

The statistical procedure, as developed by Hershfield and introducted in Section 1.2.3, is based on the general frequency equation (Equation 1.1) given by Chow (1951), which can be rewritten as

$$X_m = \overline{X}_n + K_m S_n \qquad (2.3)$$

where X_m is the maximum observed rainfall, $\overline{X}_n$ and S_n are the mean and standard deviation of a series of n annual precipitation maxima for a specific duration, and K_m is the frequency factor equivalent to the number of standard deviations to be added to $\overline{X}_n$ to obtain X_m.

To obtain a value for variable K_m, Hershfield first computed for each station the mean and standard deviation using the conventional precedures; however, in the computations he omitted the maximum observed rainfall. Then in Equation 2.3 he substituted these values for $\overline{X}_n$ and $S_n$in as well as the maximum observed rainfall for X_m to solve for K_m. This is equivalent to observing the maximum event after the values of the basic statistics have been established. The frequency factor has been observed to be a function of duration and the mean annual extreme rainfall (Hershfield, 1977). This relationship was given by Equations 1.2, 1.3, and 1.4.

Before PMP can be computed by the statistical procedure, a number of adjustments are required to the mean and standard deviation for maximum observed event and sample size.

2.2.2 Adjustment of $\overline{X}_n$ and S_n for Maximum Observed Event

Hershfield (1961) states that extreme rainfall amounts of rare magnitude (i.e., with return periods of 500 or more years) are believed to have occurred during a much shorter period of record, for example, 30 years. Such rare events,

or outliers, may have an appreciable effect on the mean $(\overline{X}_n)$ and standard deviation (S_n) of the annual series. The magnitude of the effect is less for long records than for short, and it varies with the rarity of the event. This effect has been studied by Hershfield (1961) using hypothetical series of varying lengths and can be summarized by the relationship of the maximum observed event to the

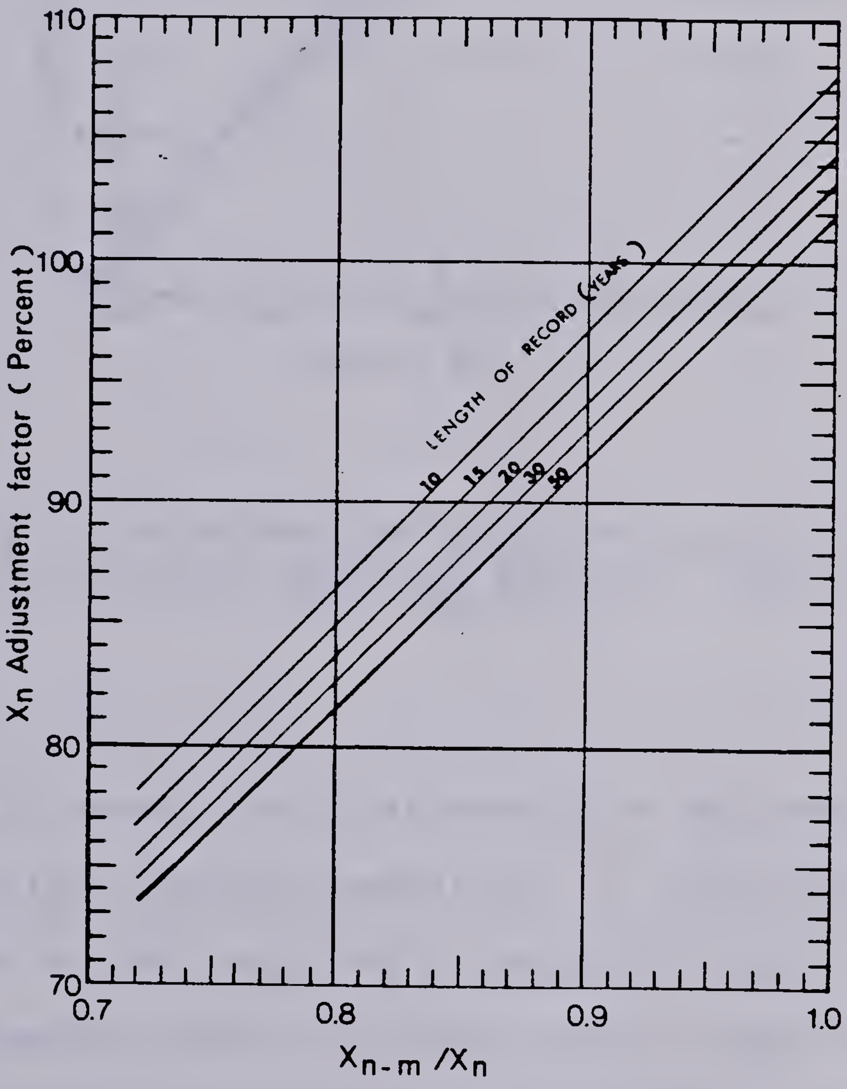

FIGURE 2.6. Adjustment of Mean of Annual Series for Maximum Observed Rainfall (After Hershfield, 1961).

mean, as shown in Figure 2.6. Similiarly, Figure 2.7 (after

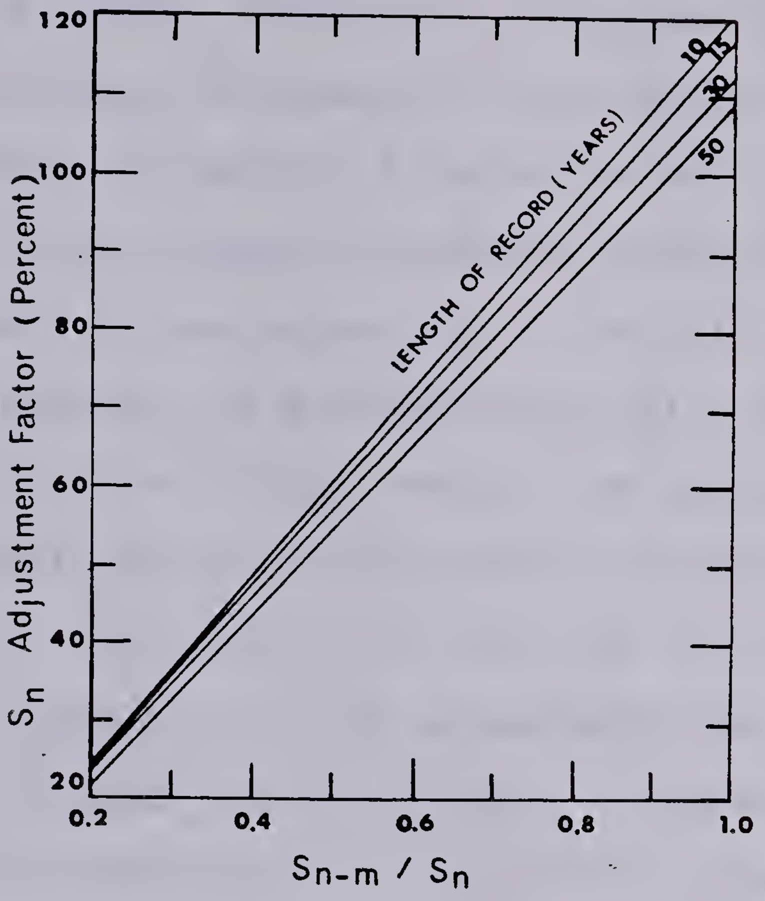

FIGURE 2.7. Adjustment of Standard Deviation of Annual Series for Maximum Observed Rainfall (After Hershfield, 1961).

Hershfield) shows the relationship of maximum observed events on the standard deviation. In these figures X_{n-m} and S_{n-m} refer to the mean and standard deviation of the annual series computed after excluding the maximum item in the series. In both diagrams, the relationships are for only the effect of the maximum observed event; no consideration was given to other anomalous-appearing observations.

2.2.3 Adjustment of $\bar{X}_n$ and S_n for Sample Size

The mean ($\bar{X}_n$) of the annual series may tend to increase with record length, because the frequency distribution of rainfall extremes is skewed to the right so that there is a greater chance of getting a larger rather than a smaller extreme as record length increases. Using data from 198 key weather stations and adjusting for an outlier, Hershfield (1961) determined the average ratios of a 50-year mean to 10-, 15-, 20-, and 30-year means; the adjustment necessary for the length of record is shown in Figure 2.8. In his computations, the statistics from the 50-year records were used as a standard, so that adjustments were required for those with shorter record periods. A comparison of a small number of available means for records longer than 50 years with the 50-year means showed only a negligible difference. Similiarly, the necessary standard deviation adjustment for length of record was computed, and the results are shown in Figure 2.8. The effect of the record length is much more pronounced on the standard deviation than on the mean. The few records for longer than 50 years indicate the need for only a slight adjustment from the values for the 50-year records.

2.2.4 Adjustment for Fixed Observational Time Intervals

Precipitation data are usually recorded on a fixed time interval, e.g., hourly, six-hourly, or daily. Such data rarely yield the true maximum rainfall amounts for the

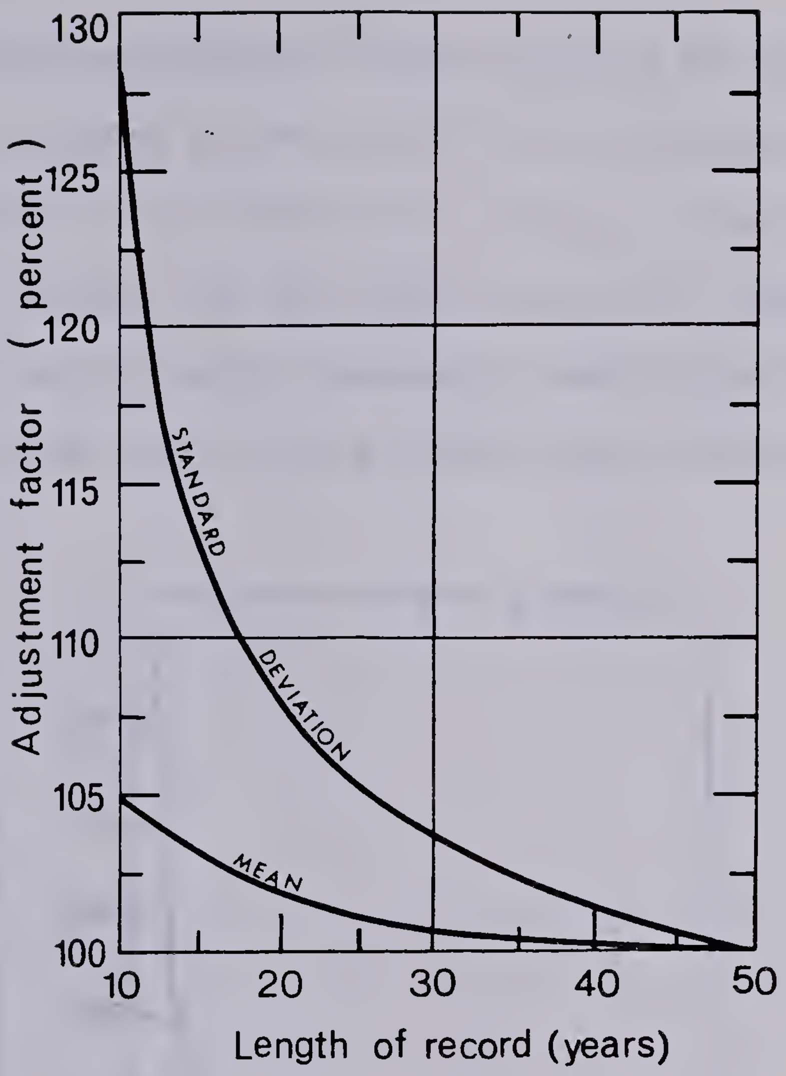

FIGURE 2.8. Adjustment of Mean and Standard Deviation of Annual Series for Length of Record (After Hershfield, 1961).

indicated durations. As an example, the annual maximum observational day amount is very likely to be appreciably less than the annual maximum 24-hour amount determined from intervals of 1440 consecutive minutes unrestricted by any particular observation time. Studies by Weiss (1964) indicate that when the results of a frequency analysis of annual maximum rainfall amounts for a single, fixed-time interval of any duration from 1 to 24 hours are multiplied by 1.13 they will yield values closely approximating those

obtained from an analysis based on true maxima. Hence, the PMP values yielded by the statistical procedure should be multiplied by 1.13 if data for single, fixed-time intervals are used in compiling the annual series. Figure 2.9 shows the smaller adjustments necessary when durations are determined from two or more fixed-time intervals. As an example, maximum 24-hour amounts determined from 24 consecutive, 1-hour rainfall increments requires an adjustment by a factor of 1.01. The results from these studies show the importance to the user of understanding the

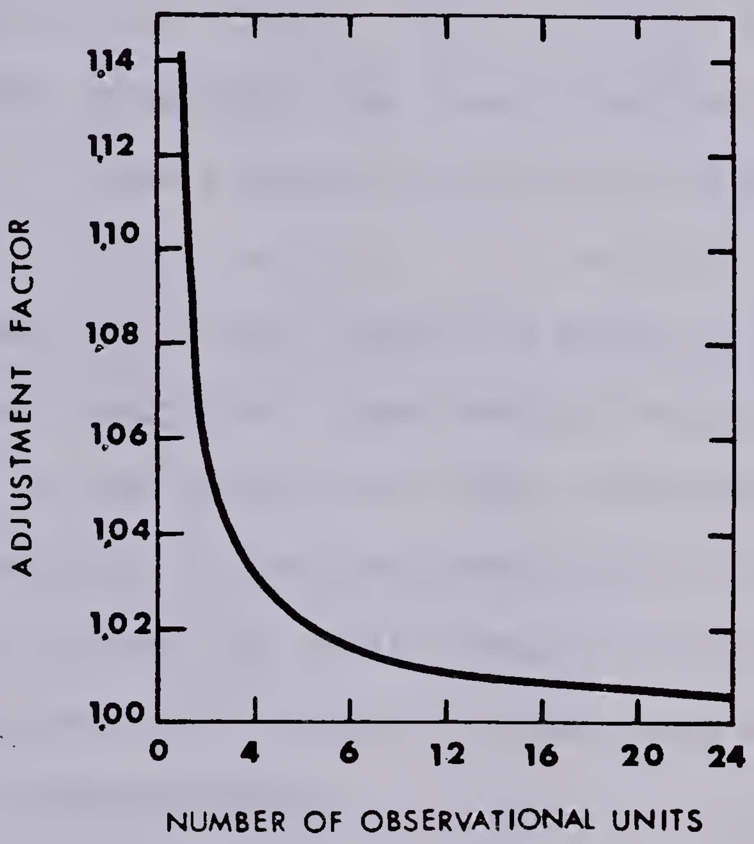

FIGURE 2.9. Average Adjustment of Fixed Interval Precipitation Amounts for Number of Observational Units within the Interval (After Weiss, 1964).

time collection of precipitation data.

2.2.5 Area-Reduction Curves

One of the shortcomings of the statistical procedure is that it yields only point values of PMP and thus requires area-reduction curves for adjusting the point values to various sizes of area. A number of variations of depth-area relationship exist (Court, 1961). For the prairie provinces, McKay (1965b) developed the area-reduction curves shown in Figure 2.10. These curves relate point values to areas up to 129 500 km^2 (50 000 sq. mi.). For rainfall, point values are often assumed to be applicable to areas up to 65 km^2 (25 sq. mi.) without reduction. These reductions can be called areal in nature, in the sense that once a maximum point value is defined spatially it can be converted to an estimate for a larger area. These are called reductions because the maximum point value has been observed to decrease with an increase in area of representation.

2.2.6 Statistical Estimates for Alberta River Basins

Employing the various concepts described above, Verschuren and Wojtiw (1980) obtained statistical PMP estimates for the major river basins in Albera. For each recorded year, maximum 24-, 48-, 72-, and 96-hour rainfalls were calculated for 27 first-order weather stations in Alberta. Then the statistical estimates were computed using the procedure developed by Hershfield. An example of the 24-

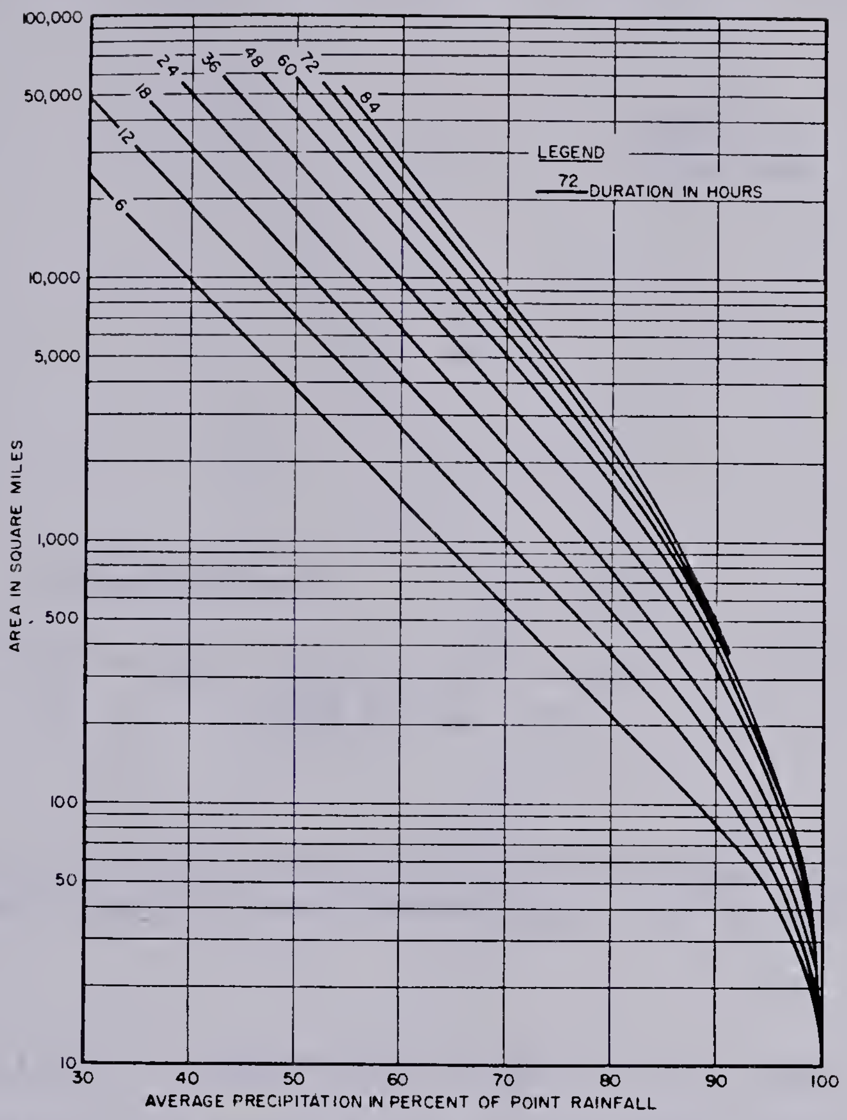

FIGURE 2.10. Depth-Area, or Area-Reduction, Curves (After McKay, 1965b).

hour enveloping depth-area curve for the Red Deer station is shown in Figure 2.11. In general, for the six river basins the statistical approach produced results that were slightly higher than those calculated by the physical approach.

2.2.7 Spatial Characteristics of PMPs

The results seem to suggest that in Alberta the PMP

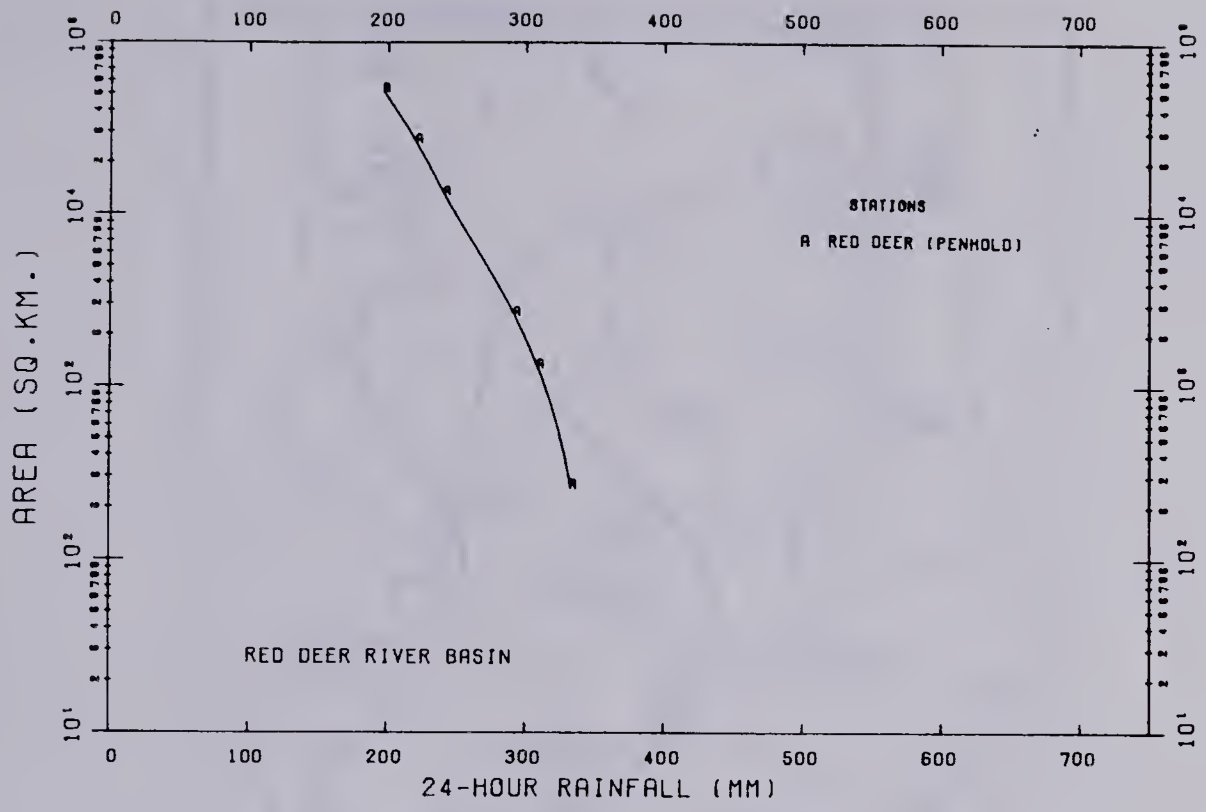

FIGURE 2.11. 24-hour Enveloping Depth-Area Curves for the Red Deer River Basin (Verschuren and Wojtiw, 1980).

varies spatially in each basin, as can be seen from the 24-hour estimates in Figure 2.12. The largest PMP estimates are observed in the South Saskatchewan River Basin, while the smallest are in the eastern and northern portions of the province. Generally, two characteristic variations can be defined: the first, also being the most predominant, is the variation from west to east in the basin, while the second is the variation northward. The west-east variation exibits two main features. First, there is a strong decreasing gradient in the southern parts of the province (namely, the South Saskatchewan River Basin). PMP values decrease from over 500 mm (20 in.) in the western portion to about 100 mm (4 in.) in the eastern portion of the river basin. The

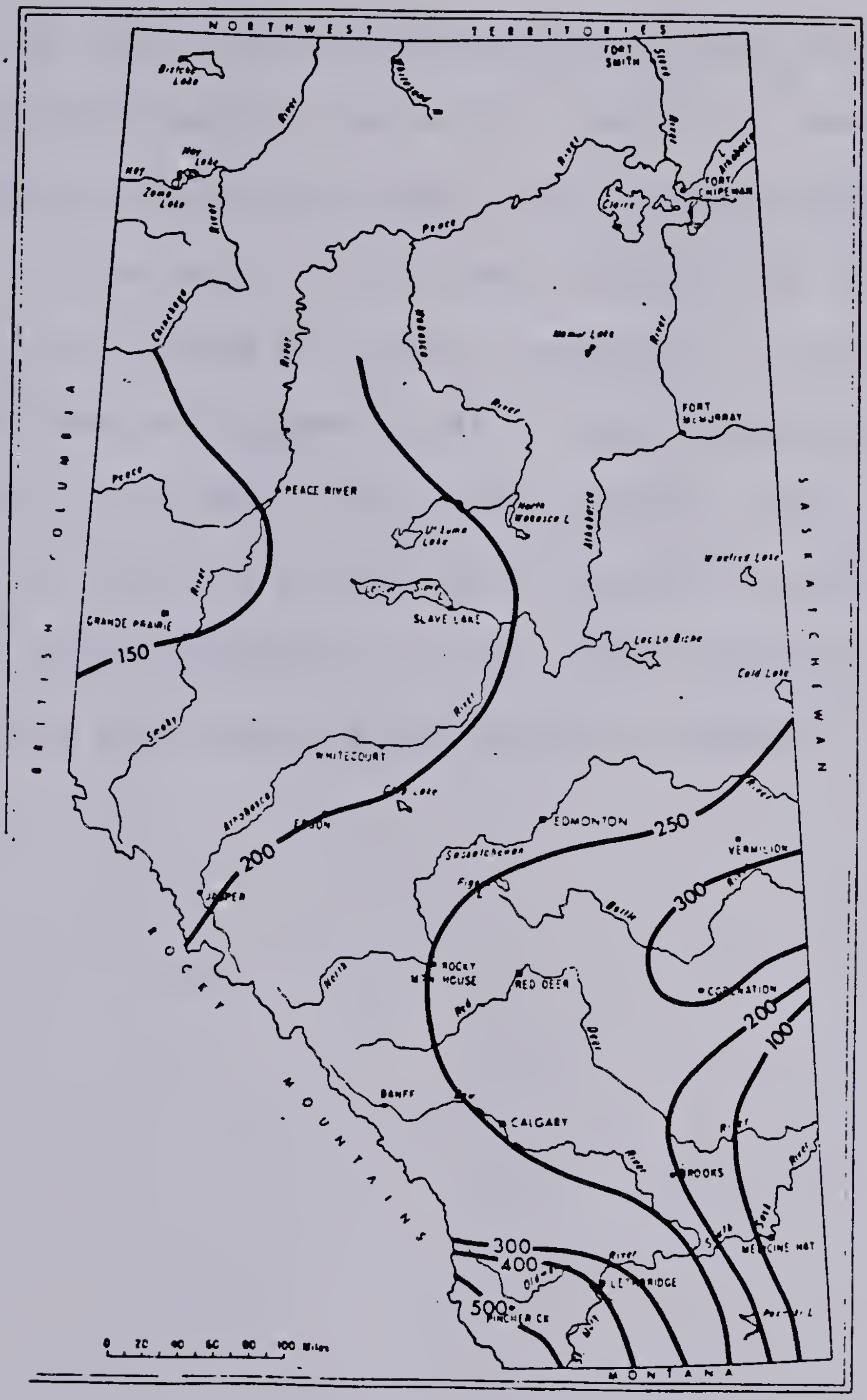

FIGURE 2.12. Spatial Variation (mm) of the Maximized 24-hour PMP (Verschuren and Wojtiw, 1980).

second feature is an increase (about 50%) in the central and northern river basins. The variation northward is important mainly in the southern basins of the province, where changes of about 40% are not uncommon. For basins in central and northern Alberta only slight variations are observed and

these are of very little consequence in the PMP estimate.

The coefficient of variation, which is the ratio of the standard deviation to the mean, has been used (McKay, 1965b) to obtain estimates of the climatological day 24-hour precipitation extreme of given frequency. To examine this aspect, extreme value series of 24-hour precipitation were used from all available long-term weather stations in Alberta. The isolines of the coefficient of variation (expressed in percentage) for the annual 24-hour precipitation extremes are depicted in Figure 2.13.

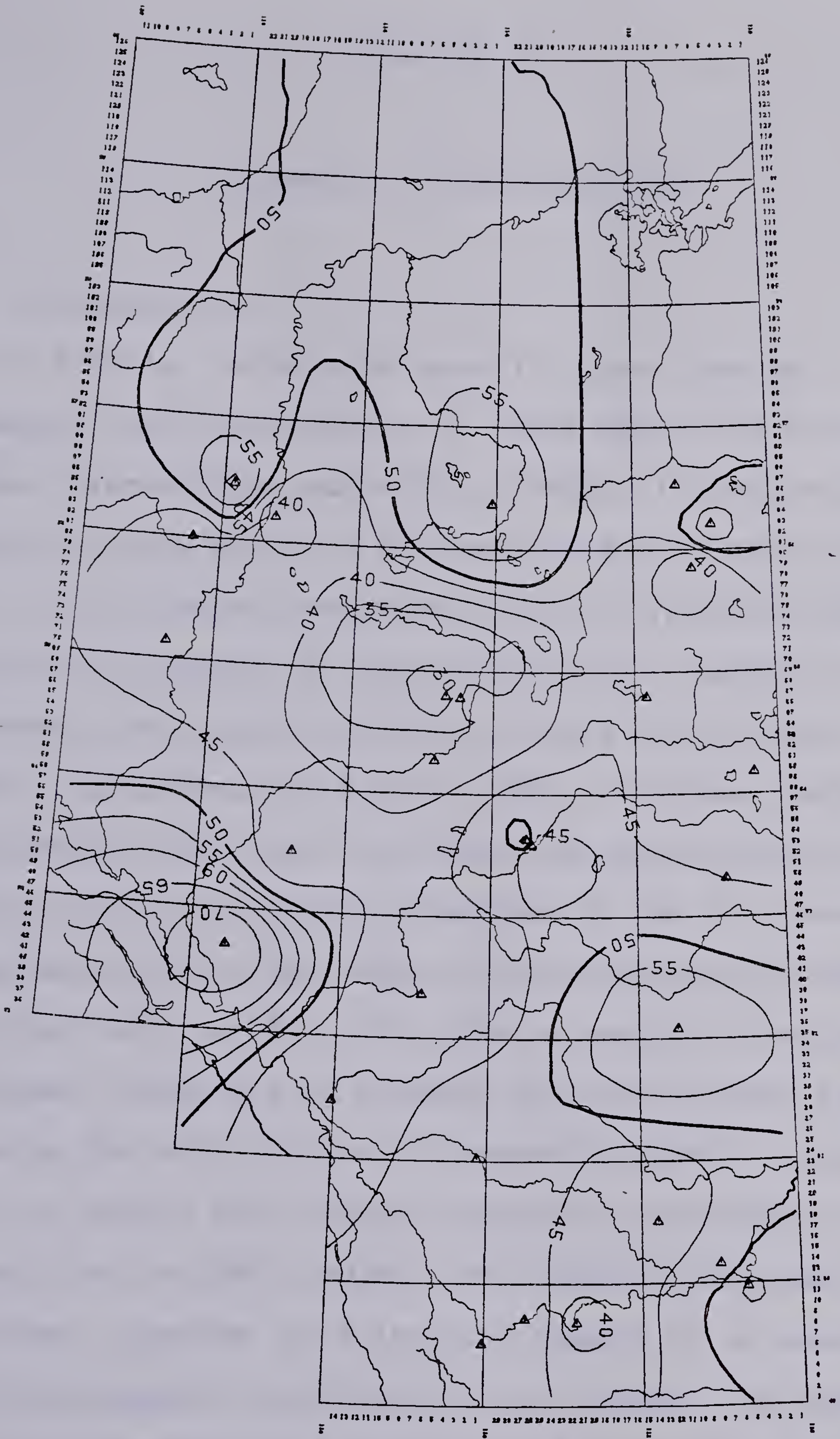

FIGURE 2.13 Coefficients of Variation of Annual 24-hour Precipitation Extremes.

CHAPTER 3

SNOWMELT WITH PMP LOADING

3.1.0 Introduction

In Alberta, rainstorms usually occur from April to September, with the majority of these occurring during June and July (Verschuren and Wojtiw, 1980). Of these rainstorms, the rain-on-snow event is believed by many authors (McKay, 1965b, 1968; Buckler and Quine, 1971) to have the best potential for producing the maximum water loading on the watersheds; this usually occurs in late May or early June in Alberta (Verschuren and Wojtiw, 1980). The few studies that have examined this event have used the generalized snowmelt equations and coefficients developed by the U.S. Army Corps of Engineers (1956) for basins in United States, without examining their validity for Alberta basins. An objective in the present study was to examine the rain-on-snow event and determine the contribution of snowmelt to PMF. It was also useful to define the relevant processes contributing to snowmelt for the PMP loading. This chapter discusses these objectives, together with the development of an equation for computing snowmelt for Alberta river basins. The snowmelt equation presented can be expressed by meteorological parameters; which in turn can be expressed in terms of location, elevation, and drainage area. A number of relationships between these latter parameters can be

developed to provide spatial estimates of the meteorological parameters (Section 3.3). These relationships can then be used to examine the snowmelt for spatial variability and maximum melt rate, and to obtain estimates for watersheds lacking meteorological data.

3.2.0 Rain-on-Snow Event

The generation of snowmelt at a point location in a snowpack is essentially a thermodynamic process, with the amount of melt produced being dependent on the net heat exchange between the snowpack and its environment. To represent physical processes that are not easily measured, indexes expressed in terms of readily observed measurements between the snowpack and its environment are usually used. The reliability of the indexes depends upon (a) how well the physical process is described by the measured variable, (b) the random variability of the measurement, (c) the variability between point values and areal values, and (d) the validity of the measured value. The index relationship may be described by a coefficient and may be either constant or variable, depending upon the variability of associated factors.

The atmospheric temperature is a useful parameter in snowmelt determination and has been used as an index, because it is generally thought to be the best index of the heat transfer processes associated with snowmelt and is a reliable and regularly available meteorological variable.

Snowmelt is the overall result of many different processes of heat transfer: shortwave and longwave radiation, condensation of vapor, convection, air and ground conduction, and rainfall. What follows is an examination of each of these melt contributions in terms of PMP loading.

3.2.1 Radiation Melt

The amount of incoming solar (shortwave) radiation received by a snowpack can be a very important source of heat energy for snowmelt. The net amount of heat absorbed by the snowpack depends on latitude, orientation and slope, season, time of day, atmospheric conditions (clouds, fog, rain), forest cover, and reflectivity of the snow (albedo). Of these, cloud cover and albedo have been identified as being significant to snowmelt. The intensity of insolation or shortwave solar radiation is normally expressed in langleys (ly) (calories per square centimetre) per unit of time (minute, hour, or day) and abbreviated, for example, as ly/hr. The most simple and accurate measurement of net insolation uses pyrheliometers; these instruments are calibrated to give the shortwave radiation intensity in ly/hr or ly/day.

The snowmelt by shortwave radiation, M_{rs}, can be approximated by (U.S. Army Corps of Engineers, 1956)

$$M_{rs} = \frac{(1-a)\ R_{si}}{203.2\ B} = 0.00508\ R_{si}\ (1-a) \qquad (3.1)$$

where M_{rs} is the snowmelt in inches due to shortwave radiation, a is the albedo written as a decimal fraction, R_{si} is the effective solar radiation in ly/day, and B is the thermal quality of the snowpack (defined as the ratio of heat required to melt a unit weight of snow to that of ice at 0°C or 32°F). The thermal quality averages from 0.97 to 0.95, for a snowpack with 3-5% liquid water and is usually assumed to be 0.97 for a melting snowpack. The constant, 203.2, is the heat input in langleys required to produce one inch of water from ice at 32°F; it is in term of ly/in..

Since the snowmelt depends upon the air temperature over the snow and the temperature of the cloud base, the maximum snowmelt rate in most cases would probably occur under clear skies as compared to under skies with a complete or partial cloud cover. The albedo is commonly considered 80% for fresh snow and is assumed to decrease exponentially to about 40% for melting, late-season snow (Figure 3.1). Equation 3.1 indicates that the melt increases with a decrease in albedo and that the greatest melt would be produced when the smallest value of albedo is used. Insolation during rain conditions is commonly assumed to be close to 40 ly/day for an open area, and an albedo of roughly 65% gives a contribution of M_{rs} equal to 1.78 mm per day (0.07 in. per day) using Equation 3.1 (Gray, 1970). The albedo value of 65% has been shown to be much too high for Alberta (especially from April to June) by Hay (1970). Hay estimated regionally representative monthly mean albedo

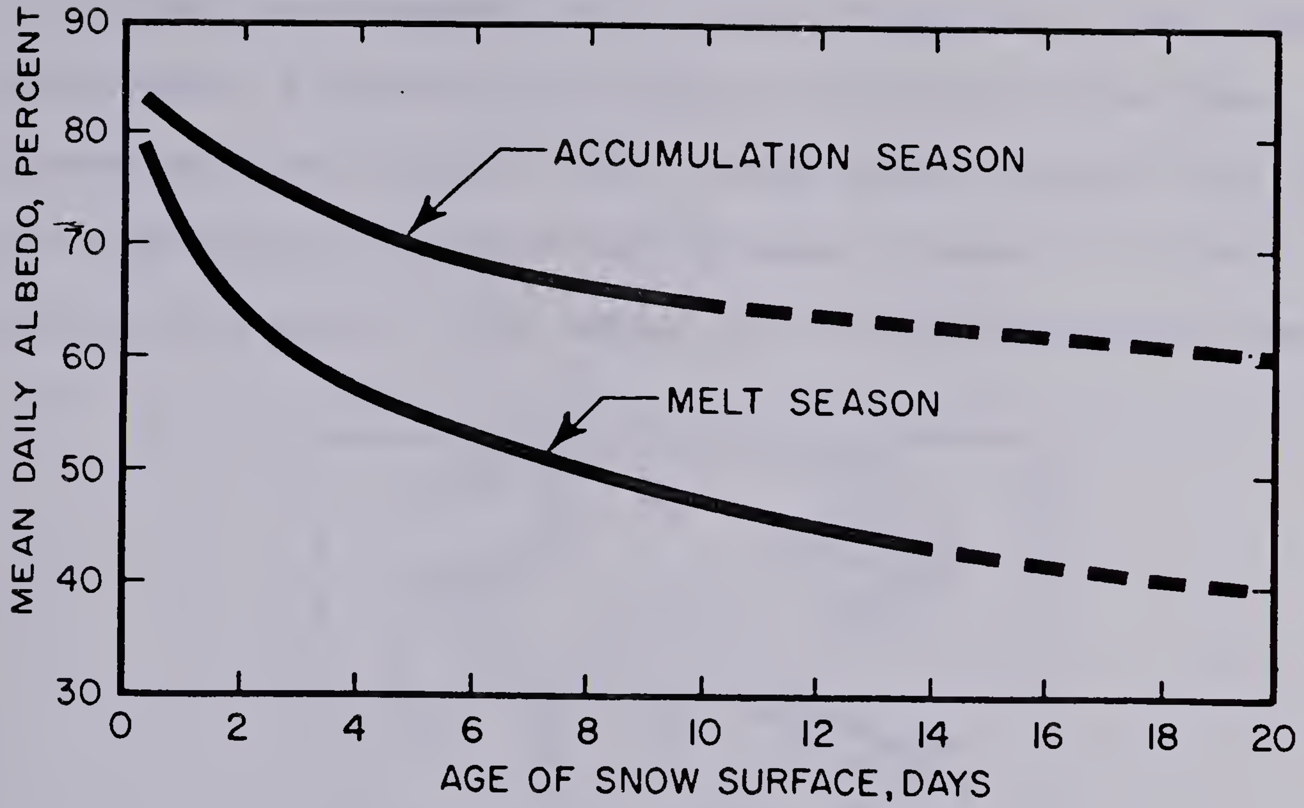

Figure 3.1. Variation in Snow Surface Albedo with Time (After U.S. Army Corps of Engineers, 1956).

values for selected Alberta locations. Mean values are used because rainstorms that may produce precipitation approaching the PMP are on a scale of days as compared to minutes or a few hours. For June, Hay gives mean values of 20% for Beaverlodge and 23% for Edmonton and Suffield. About 20% seems as a reasonable value to use as a minimum value for Alberta, since there is little variation in the values between the northern and the southern stations. Although zero in the smallest value that can be achieved under specific conditions, it is not a practical value since it is rarely recorded in nature during precipitation events. The relationship (if one exists) between albedo and precipitation events is not well understood.

A maximum snowmelt rate can be expected in late May or early June, since the coincidence of severe rainstorms (Verschuren and Wojtiw, 1980), snow cover (Figure 3.2), and air temperatures above freezing seem to occur in Alberta during this period. The amount of radiation reaching the surface is usually expressed in terms of the average cloudless day's insolation; in Alberta these values increase

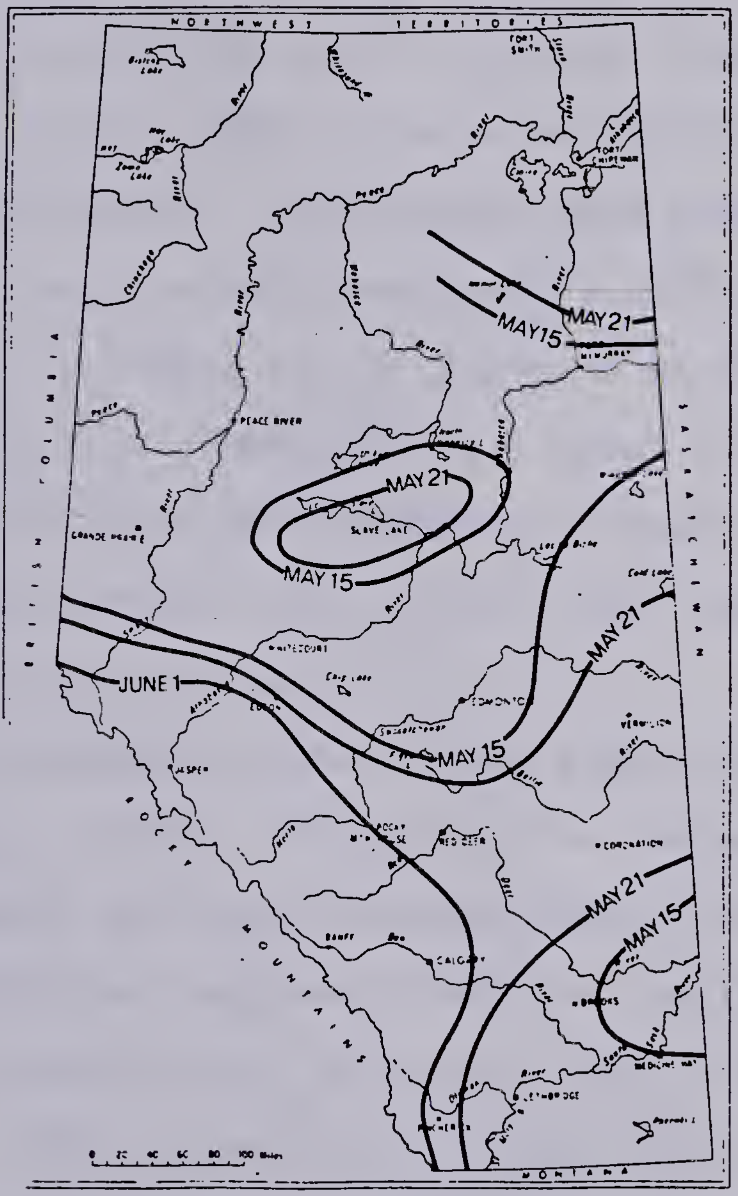

Figure 3.2. Date of last snow cover of 25 mm (1 in.) or more for Alberta (Verschuren and Wojtiw, 1980).

from May to June (Figure 3.3). Average values between 760 and about 800 ly/day seem to be representative of prairie basins in Alberta (Gray, 1970), with the large insolation values being observed at the head of the basins (that is, near the mountains) while the lower values occur at the mouth of the basins (usually in the plains). Hence a value of 800 ly/day is used for prairie basins, compared to 40 ly/day given in Gray (1970). The value of 40 ly/day may be an interpretation error. Exactly the same number appears in the U.S. Army Corps of Engineers report (1956, page 196); however, there it refers to the standard error of the estimated insolation. Substituting a value of 800 ly/day into Equation 3.1, the melt component produced by shortwave radiation is 82.6 mm per day (3.25 in. per day) or 3.4 mm per hour (0.14 in. per hour).

Snow is considered to be a nearly perfect black body with respect to longwave radiation. The longwave radiation emitted by a snow surface can be estimated using Stefan's law (total radiation is proportional to the fourth power of temperature) (Shortley and Williams, 1961; U.S. Army Corps of Engineers, 1956). Computation of net longwave radiation involves estimation of back radiation from the atmosphere under clear or cloudy skies and from beneath forest cover, and these evaluations are difficult to calculate and usually not used in practical snow hydrology. Instead, U.S. Army Corps of Engineers (1960) recommends the use of simplified linear relationships in terms of temperature. Longwave

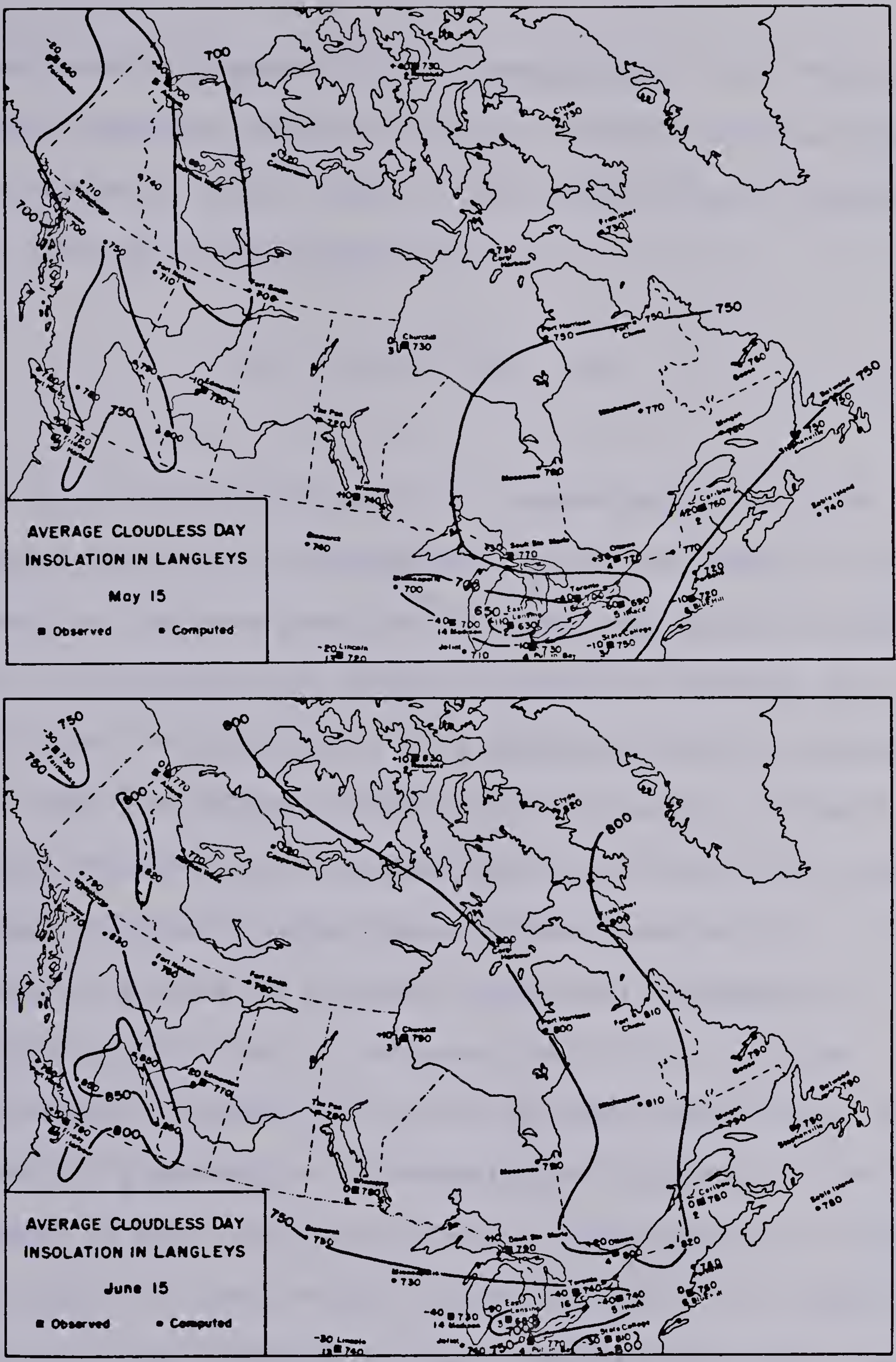

Figure 3.3. Average Cloudless Day Insolation in Langleys for May 15 and June 15 for Canada (After Gray, 1970).

radiation melt for rain conditions can be considered to be under complete cloud cover; also, the cloud base temperature

is approximately equal to air temperature. The relationship between longwave radiation and air temperature was found experimentally to be linear (U.S. Army Corps of Engineers, 1956) and can be expressed as

$$M_{rl} = 0.029\ (T_M - 32) \tag{3.2}$$

where M_{rl} is the daily melt in inches resulting from longwave radiation exchange and T_M is the mean of the daily maximum air temperatures in °F during the specific month. There is no indication in the literature whether the coefficient in Equation 3.2 is dependent upon parameters other than the sky conditions and the canopy. Hence it is probably reasonable to assume that the coefficient can be applied to Alberta watersheds. Above-freezing air temperatures make up the most important component in determining melt due to longwave radiation, with an approximation representative of maximum conditions. The mean of the daily maximum air temperatures is used, since this is believed to best represent the air temperature. In Alberta, this value for June in most cases is about 20% higher than a mean of all maximum and minimum temperatures and is about 30% lower than the extreme maximum temperature. Another approximation that was considered but not used was the extreme maximum temperature. The typical values recorded at many stations in June in Alberta (sometimes during the period of record) are greater than 32 °C (90 °F). The use of

these temperatures was ruled out since in reality such values are usually only attained after prolonged warm spells lasting beyond the 2 days or more duration used here; in such cases the snow cover probably disappeared long before this.

3.2.2 Condensation and Convection Melt

Two other processes that must be considered in determining snowmelt are the condensation of vapor and convection (U.S. Army Corps of Engineers, 1956). The term for the combined convective-condensation process, M_{ce}, can be divided into two components; a condensation component denoted by M_e and a convective component denoted by M_c .

When water vapor from the atmosphere condenses on a snow surface, the heat of condensation of water is absorbed by the snowpack. The theory behind the condensation processes producing snowmelt is quite complex; generally, temperature and wind velocity are considered to be the principal parameters influencing this process. The snowmelt produced by condensation may be estimated from the derived relation

$$M_e = 0.054 \, (z_a \, z_b)^{-1/6} \, (e_a - e_o) \, u_b \qquad (3.3)$$

where M_e is the snowmelt due to condensation in inches per day, z_a and z_b are the heights (ft.) above the snow surface of the air vapor pressure and wind speed, respectively, e_a

is the air vapour pressure in mb, e_o is the snow surface vapor pressure in mb (6.11 mb at a melting snow surface), and u_b is the wind speed in miles per hour.

Melt produced by convection results mainly from heat transferred from warm air advected over the snow surface. The theory of turbulent transfer in the atmosphere is complex, but experiments have indicated that simple approximations can be used that consider chiefly the temperature gradient of the air above the snow surface, the wind speed, and the air density (taken as a function of air pressure). Convection melt may be estimated from the equation (U.S. Army Corps of Engineers, 1956)

$$M_c = 0.00629\ (\frac{p}{p_o})\ (z_a\ z_b)^{-1/6}(T_a - T_o)\ u_b \qquad (3.4)$$

where M_c is the snowmelt due to convection in inches per day, p and p_o are the air pressure at the site and at sea level, respectively, z_a and z_b are the heights (ft.) above the snow surface of air temperature and wind speed, respectively, T_a and T_o are the air and snow surface temperature in °F, with the snow surface temperature being normally taken as 32 °F (0 °C), and u_b is the wind speed in miles per hour. For practical application, in hydrology Equations 3.3 and 3.4 can be further simplified.

The ratio (p/p_o) varies from 1.0 at sea level to 0.7 at an elevation of 10 000 ft. (3 km). For moderate topographic

changes a value of 0.8 is usually used and is appropriate for application in Alberta. Condensation-convection melt during rain is assumed to occur under saturated air, hence vapor pressures can be assumed to be adequately represented by dew point temperatures, and these in turn by air temperatures. Fixing heights of measurement of T_a and T_o in °F at 10 ft. (3 m) and the height of wind speed at 50 ft. (15 m) as well as replacing air temperatures by the mean daily maximum temperatures and wind speed by the maximum of the average daily wind speed results in the reduction of Equations 3.3 and 3.4 to

$$M_{ce} = 0.0084\, u_M\, (T_M - 32) \qquad (3.5)$$

where M_{ce} is the snowmelt due to convection-condensation in inches per day; u_M is the maximum average daily wind speed in miles per hour; T_M is the mean of the daily maximum air temperatures in °F during the specific month. Thus condensation of vapor and convection are two important sources of heat energy that affect snowmelt.

3.2.3 Melt from Rainfall

Rain falling on the snow surface at temperatures above 32°F (0°C) transfers heat to the snow and thus produces melt. The amount of heat given up to the snow by the rain is directly proportional to the quantity of rain and to its temperature excess above that of the snowpack. For a melting

snowpack, each centimetre depth of rainfall releases one langley (cal per cm²) for each °C above freezing:

$$H_p = (T_r - T_s)\ P_r \qquad (3.6)$$

where H_p is the heat released by the rainfall in langleys, T_r and T_s are the temperatures of the rain and the snowpack, respectively, in °C, and P_r is the depth of rainfall in centimetres. Substituting English units (since computations in the present work are in English units) in the above equation and setting $T_s = 32°F$, Equation 3.6 becomes

$$M_p = \frac{H_p}{203.2\ B} = \frac{\frac{5}{9}\ (T_r - 32)\ (2.54)\ P_r}{203.2\ (0.97)} \qquad (3.7)$$

$$= 0.00716\ (T_r - 32)\ P_r$$

where M_p is the daily snowmelt due to rainfall in inches, H_p is the heat released by rainfall in langleys, T_r is the temperature of the rain in °F, and P_r is the rainfall in inches. Substituting the PMP loading for P_r, replacing the wet bulb temperature by the mean daily maximum temperature, and assuming 0.97 for the thermal quality of the snowpack results in the equation

$$M_r = 0.007\ P_{MP}\ (T_M - 32) \qquad (3.8)$$

where M_r is the daily snowmelt from rain in inches, P_{MP} is the daily probable maximum precipitation in inches, and T_M is the mean of the daily maximum air temperatures in °F during the specific month. This equation provides a tool for calculating the effect of rainfall on snowmelt.

3.2.4 Ground Conduction

Ground conduction is another process involved in the heat transfer associated with snowmelt. The melt produced by this process is the result of the upward transfer of heat from ground to snowpack due to thermal energy stored in the ground during the preceding summer and early fall. Heat transfer by ground conduction can be expressed by the following relationship (U.S. Army Corps of Engineers, 1956)

$$H_q = K \frac{dT}{dz} \qquad (3.9)$$

where H_q is the heat transfer by ground conduction, K is the thermal conductivity of soil, and $\frac{dT}{dz}$ is the temperature gradient perpendicular to soil surface. The thermal conductivity of a soil varies directly with its density and its moisture content. Generally, the snowmelt from ground conduction is exceedingly small. Wilson (1941a) found that there was an insignificant heat transfer from ground to snow after about 30 days of continuous snow cover. The U.S. Army Corps of Engineers (1960) estimated the snowmelt from ground

conduction to be approximately 0.5 mm per day (0.02 in. per day). The snowmelt from ground heat, M_g, contributes very little to the melt and about $2.1 \times 10^{-2} D$ mm ($8.3 \times 10^{-4} D$ in.) to the total melt, where D is the duration of melt in hours.

Combining the five components of snowmelt (i.e., Equations 3.1, 3.2, 3.5, 3.8, and the snowmelt from ground conduction), the total melt for PMP loading at a point location can be expressed as

(a) daily melt in inches

$$M_{PMP} = M_{rs} + M_{rl} + M_{ce} + M_p + M_g$$

$$= (T_M - 32)\ (0.029 + 0.0084\ u_M + 0.007\ P_{MP}) + 3.271 \tag{3.10}$$

(b) hourly melt in inches

$$M_{PMP} = 10^{-4}\ (T_M - 32)\ (12.0 + 3.5\ u_M + 2.9\ P_{MP}) + 0.136 \tag{3.11}$$

For rain-on-snow events under a PMP loading, the predominant heat transfer processes are due to convection and condensation, shortwave (solar) radiation, rainfall, and longwave radiation; heat input by the other processes is relatively minor. The relative importance of the heat

processes can be examined by considering the following values for a 24-hour PMP loading for a specific location in Alberta (for example): $T_M = 65^{o}F$ ($18^{o}C$), $P_{MP} = 12.0$ in. (305 mm), and $u_M = 15$ miles per hour. Using these values, Equations 3.11 becomes

$$
\begin{aligned}
M_{PMP} &= 0.135 + 0.040 + 0.173 + 0.116 + 0.0008 \\
&= 0.465 \qquad \text{(in./hr.)}
\end{aligned}
$$

For the above values, the total snowmelt equals 0.46 in. per hour (11.7 mm per hour). Of this total, convection and condensation account for 37.2% of the total melt; shortwave (solar) radiation for 29.0%; rainfall for 24.9%; longwave radiation for 8.6%; and ground conduction for 0.2%. For rain-on-snow events not subject to PMP loading, the U.S. Army Corps of Engineers (1956) and Gray (1970) state that only convection and condensation are important to the total melt, but from the values obtained by using Equation 3.11 it becomes obvious that other processes are also important.

From Equation 3.11, the total hourly melt can be estimated by knowing the temperature (T_M) in ^{o}F, probable maximum precipitation (P_{MP}) in inches, and the wind speed (u_M) in miles per hour, for a duration (D) in hours. This is expressed by variables that are readily available and are not considered to be subject to large spatial and temporal variability. The parameters u_M, P_{MP}, and T_M can be called meteorological parameters, since they are functions of the

meteorological situation. As such, they can be expressed in terms of a location in the river basin or watershed.

The total snowmelt computed by Equation 3.11 is a point estimate representing a probable maximum rate of melt for a given location. This point estimate is probably representative of the location, since the meteorlogical parameters comprising the estimate are generally considered to be representative by the collecting agency. For hydrological application, point estimates need to be examined for the basin in terms of (a) the spatial variability, (b) the maximum melt rate, and (c) obtaining estimates for watersheds lacking meteorological data. Although the basic meteorological parameters of temperature, wind, and precipitation are believed to vary spatially slightly throughout the plains of Alberta, it is worthwhile to verify the parameters used in computation of the snowmelt to see if they behave similarly. In a basin a number of point estimates may be computed using Equation 3.11; hence it is desirable to find the maximum value for a watershed with and without available meteorological data. One approach is to correlate the point values for available meteorological data in order to obtain a relationship and then to investigate the relationship for various data values. The next section discusses the use of this approach to determine relationships of the meteorological parameters.

3.3 Relationships of Meteorological Parameters

In order to obtain relationships for the three meteorological parameters, the daily maximum air temperature, the average daily wind speed, elevation, and probable maximum precipitation for various lengths of time were examined, analyzed, and correlated for all first-order weather stations and other available meteorological data for major Alberta river basins. These data were obtained from the numerous Atmospheric Environment Service publications, as discussed in Section 1.3. Regarding the best way to stratify and represent this information, since one of the desired results is a streamflow hydrograph of the PMF, the most logical stratification seemed to be by river basin. Stratification by other means, for example by PMP or temperature distribution, would imply some form of interbasin transfer, which was not one of the objectives in this study.

In comparing the values of the above parameters, it was noted that they varied by several orders of magnitude, suggesting the need to use a logarithmic form. Analysis using a multilinear regression approach was carried out using both the original and those values converted to logarithmic form. The relationships obtained by using the logarithmic values had much higher correlation coefficients than the relationships with unconverted data, confirming the original observations about the data. A large number of comparisons were made, and a summary of the relationships obtained in the analysis of the three meteorological

parameters for the various basins is presented in Appendix II.

3.3.1 Relationship of the Air Temperature

The mean daily maximum air temperature (T_M) was found to vary with location (which in turn can be expressed in terms of latitude and longitude) and elevation, and can be represented in the functional form

$$T_M \propto f(L_A, L_o, E) \qquad (3.12)$$

where T_M denotes the mean of the daily maximum air temperature in $^\circ$F, L_A is the latitude in degrees, L_o is the longitude in degrees, and E is the elevation above sea level in feet. Because very little temperature data are available for the Red Deer River Basin, the data from the North Saskatchewan River and Red Deer River basins were combined, and a relationship was obtained. This expression can be written mathematically as

$$T_M = 12339.6 \left(\frac{L_o^{1.3476}}{L_A^{2.3768} \, E^{0.27242}} \right) \qquad (3.13)$$

where T_M is the mean of the daily maximum air temperature in $^\circ$F, L_A is the latitude in degrees, L_o is the longitude in degrees, and E is the elevation above sea level in feet.

This relationship has a high multicorrelation coefficient of 0.995, which seems to suggest that this quantity is well defined by the variables considered. Elevation seems to be important in the computation of the air temperature, for without this parameter the relationship had a correlation coefficient about 30% lower (see Appendix II). The computations of Equation 3.13 can be depicted graphically; these are shown in Figure 3.4. The values give the air

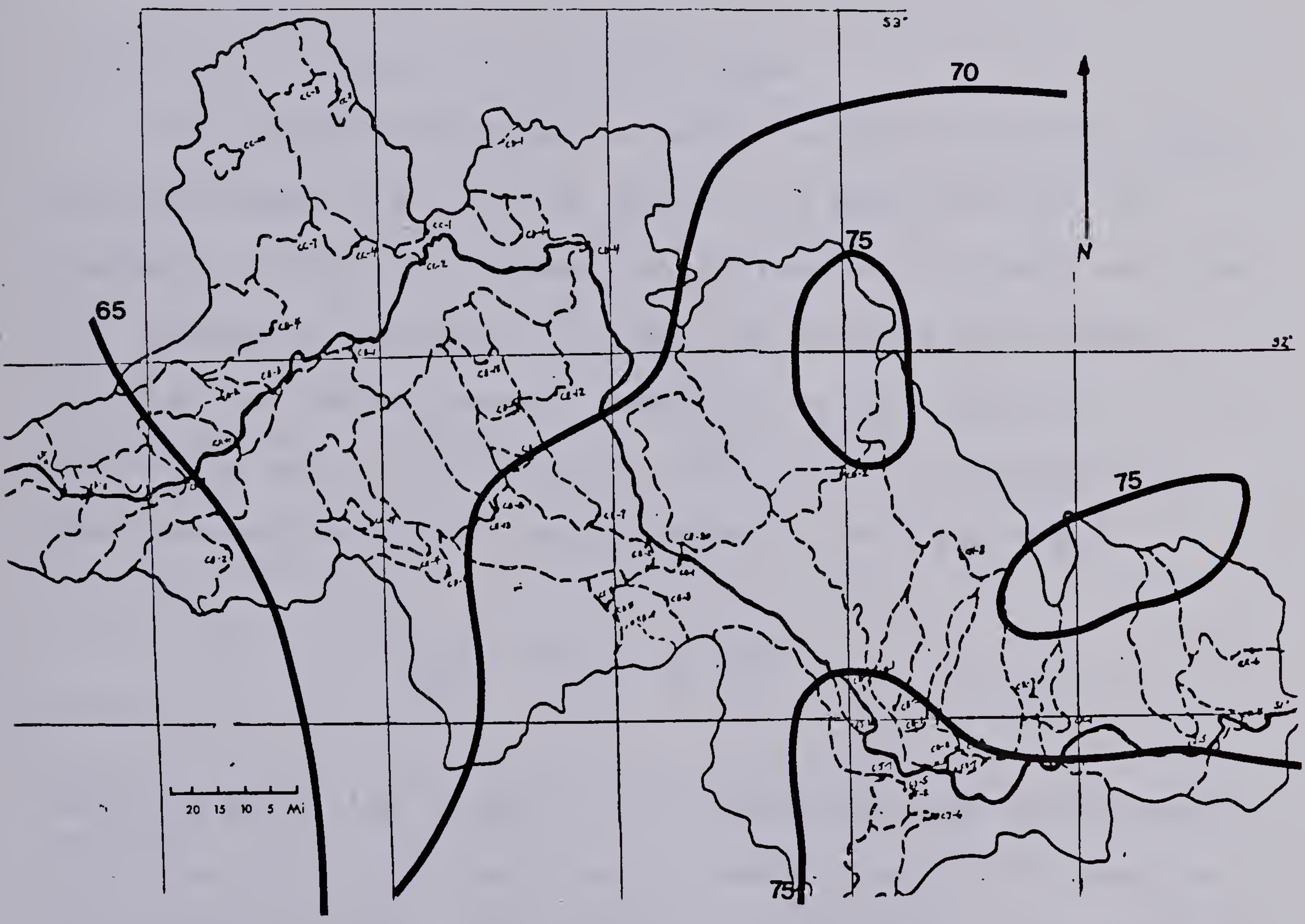

Figure 3.4. Temperature Variation (°F) for the Red Deer River Basin.

temperature loading for the Red Deer River Basin and show that the greatest decrease in air temperature occurs in the westward direction and is dependent upon elevation. The main advantage of such a relationship is that estimates of temperature can be made at locations where no meteorological data is available. No relationship is presented for the mountainous areas, because very little meteorological data are available for these areas.

3.3.2 Relationship of the Wind Speed

The second parameter for which a spatial relationship was developed was the wind speed. The magnitude of the largest average wind speed integrated over an hour was used for computing snowmelt. The maximum average wind speed, similar to the maximum air temperature was found to correlate well with location and elevation (Appendix II), and this relationship can be generally expressed as

$$u_M \propto f(L_A, L_o, E) \qquad (3.14)$$

with u_M being the value of the largest average wind speed in miles per hour and the other parameters being the same as in the previous case. The functional relationship suggested for the Red Deer River basin has a correlation coefficient of 0.800 and can be expressed as

$$u_M = 8.42 \left(\frac{L_o^{36.01}}{L_A^{34.01} E^{4.461}}\right) \qquad (3.15)$$

where u_M the average wind speed in miles per hour, L_A is the latitude in degrees, L_o is the longitude in degrees, and E is the elevation above sea level in feet. Examination of the existing wind speed data showed that this quantity varied with location in May and June. The approach used in the generalized snowmelt equations is to consider wind speed as a constant (i.e., assign a value of 5 miles per hour). From the examination and analysis of meteorological data, the values that emerge for average wind speeds are up to three times larger than those used in generalized snowmelt equations. For the Red Deer River Basin, the spatial distribution of values of wind speed are graphically shown in Figure 3.5; these appear to be dependent on the elevation. For this river basin the average wind speed seems to vary from about 12 to 18 miles per hour, with most of the lower values computed in the eastern portions of the river basin. The value of 18 miles per hour is over three times the 5 miles per hour value commonly used in the generalized snowmelt equations. Maximum observed hourly speeds are also available; however, these were not used because the values are very large and occur in a much shorter time period than was considered in this work. A summary of wind speed relationships for other river basins is provided in Appendix II. No relationship was obtained for the Peace River Basin

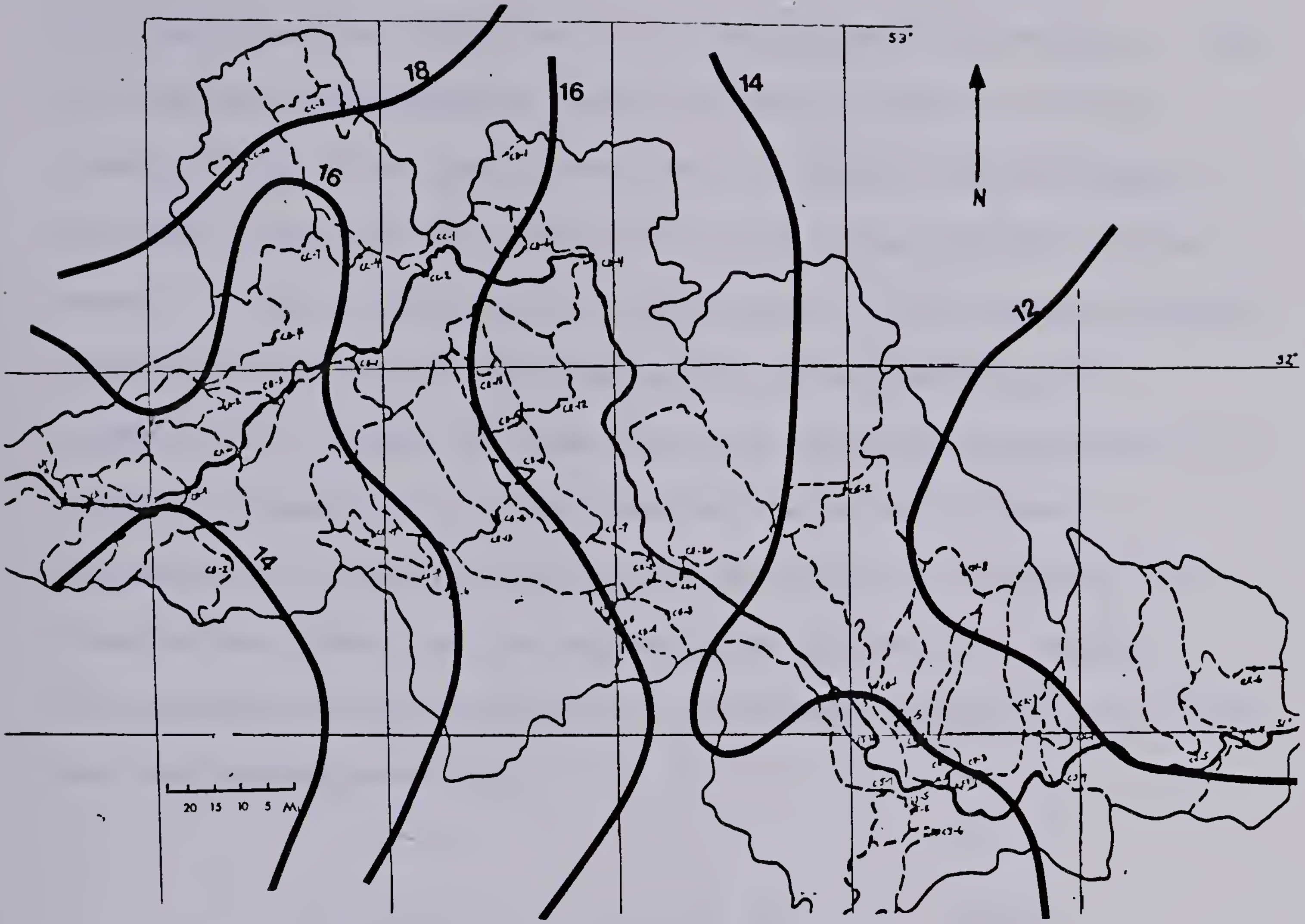

Figure 3.5. Variation of the Wind Speed (miles per hour) for the Red Deer River Basin.

because of the lack of meteorological data; for this area, values obtained for the Athabasca River Basin are recommended.

3.3.3 Relationship of the Precipitation

The third and last parameter examined was the point values of PMP as obtained by the statistical approach. The factors that can be identified in determining the PMP are the location (which can be expressed in terms of latitude and longitude), duration, storm area, and the elevation. In

the DAD analyses (Chapter 2 and Verschuren and Wojtiw, 1980) the PMP was observed to vary with the duration of the rainfall and with the storm area. Although the decrease in the PMP value was not expected to be large for the storm area, it was considered in the analysis. The elevation and location were considered necessary in estimating PMP. A summary of a number of combinations of these parameters is given in Appendix II. The combination of all these parameters (a sample size of 75 values with 5 degrees of freedom was used for the regression) gives the largest correlation coefficient in a multilinear regression analysis and can be expressed by

$$P_{MP} \propto f(L_A, L_o, D, E, A) \qquad (3.16)$$

where P_{MP} is the PMP in inches, L_A is the latitude in degrees, L_o is the longitude in degrees, D is the duration in hours, E is the elevation above sea level in feet, and A is the watershed area in sq. mi.. For the Red Deer River Basin, the mathematical expression has the following equation

$$P_{MP} = \frac{4.246 \times 10^{-3} \, L_o^{33.455} \, D^{0.419}}{L_A^{31.584} \, E^{3.257} \, A^{0.071}} \qquad (3.17)$$

and produces a correlation coefficient of 0.940. The watershed area does not contribute significantly to the PMP estimate in this basin. This is also true for the other basins (Appendix II). The other three variables (location, elevation, and duration) do contribute substantially, and the elimination of any of these variables would significantly decrease the correlation coefficient. For a number of locations in the Red Deer River Basin this equation was computed with the contoured results depicted in Figure 3.6, which shows a gradual decrease in the 24-hour PMP from over 305 mm (12 in.) in the headwater of the basin to about 230 mm (9 in.) in the eastern portions of the basin. This relationship provides spatial estimates of PMP for a watershed within a basin when meteorological data are lacking, since the four remaining unknown parameters (L_A ,L_o ,D , and E) can be determined from topographical maps. This type of relationship provides a graphical or numerical method of determining the maximum PMP in the basin. Without such a relationship it is not certain if the PMP estimate obtained by either the statistical or the physical method has been computed for maximum value.

3.4 Maximum Water Loading

The maximum water loading can now be determined, since this is a combination of the PMP and maximum snowmelt (that is, the summation of Equations 3.11 and 3.17). These two quantities can be defined in terms of the air temperature,

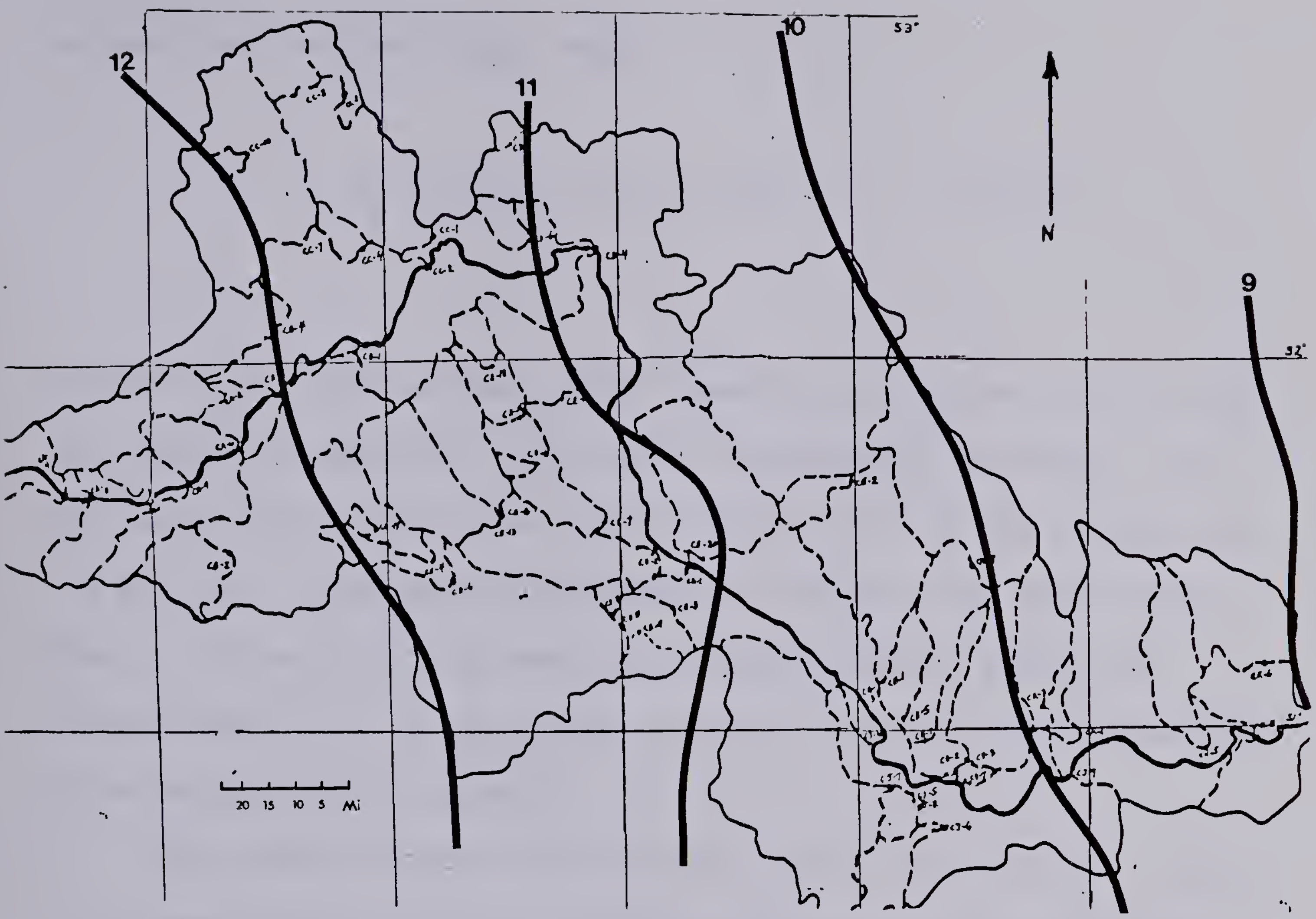

Figure 3.6. 24-hour Spatial PMP Variation (inches) in the Red Deer River Basin.

wind speed, and probable maximum precipitation for a given duration, which in turn can be expressed by functional relationships for more easily obtainable parameters, i.e., location, elevation, and drainage area of the watershed. Elevation and area of basin can be predetermined for a given location from topographic and drainage maps. Minimum elevation is used since it gives the maximum result. Thus the maximum water loading lasting for D hours for a given watershed area reduces to a simple functional relationship in terms of the location (i.e., latitude and longitude),

elevation, and drainage area:

$$W_M \propto f(L_A, L_o, E, A) \qquad (3.18)$$

where W_M is the maximum water loading in inches, L_A is the latitude in degrees, L_o is the longitude in degrees, E is the elevation above sea level in feet, and A the storm area in sq. mi.. The numerical equation for the Red Deer River basin can be obtained easily using the above equations (Equations 3.11, 3.13, 3.15, and 3.17) but is not presented here because of complexity.

The use of a functional relationship for water loading is advantageous in that spatial estimates can be obtained for a watershed where meteorological data are lacking and can provide an estimate of the maximum value.

The concept of functional relationship discussed in this chapter has been presented in a general form to suggest that this concept can be applied to other basins. The relationships depend upon the quality and quantity of data available and on the homogeneity of meteorological conditions and topographical features within the basin.

CHAPTER 4

THE TIME-AREA PROBABLE MAXIMUM FLOOD MODEL

4.1 Introduction

As was noted in the literature review, there have been few estimates of PMP and PMF for Alberta river basins. One of the reasons for this is the lack of a simplified method or model that can be modified for PMP conditions and from which a PMF hydrograph can be estimated. It was also believed that the computations of the slope of the watershed would significantly influence the PMF estimate.

To address these concerns (and as an objective of this thesis), it was necessary to develop a numerical model for estimating PMF. The resulting model had to incorporate an estimate of the shape of the watershed. A model with this requirement is presented in this chapter; it has been termed the Time-Area Probable Maximum Flood Model (TAPMF Model). Because it was also desirable to examine two commonly used models for PMP loading and to compare the peak discharges, the SSARR and HYMO models are presented in Chapter 5, and the results from all three models are compared in Chapter 6.

4.2.0 The TAPMF Model

The TAPMF model is graphically depicted in Figure 4.1. Functional relationships are used to obtain estimates of PMP and the maximum snowmelt for locations within the watershed

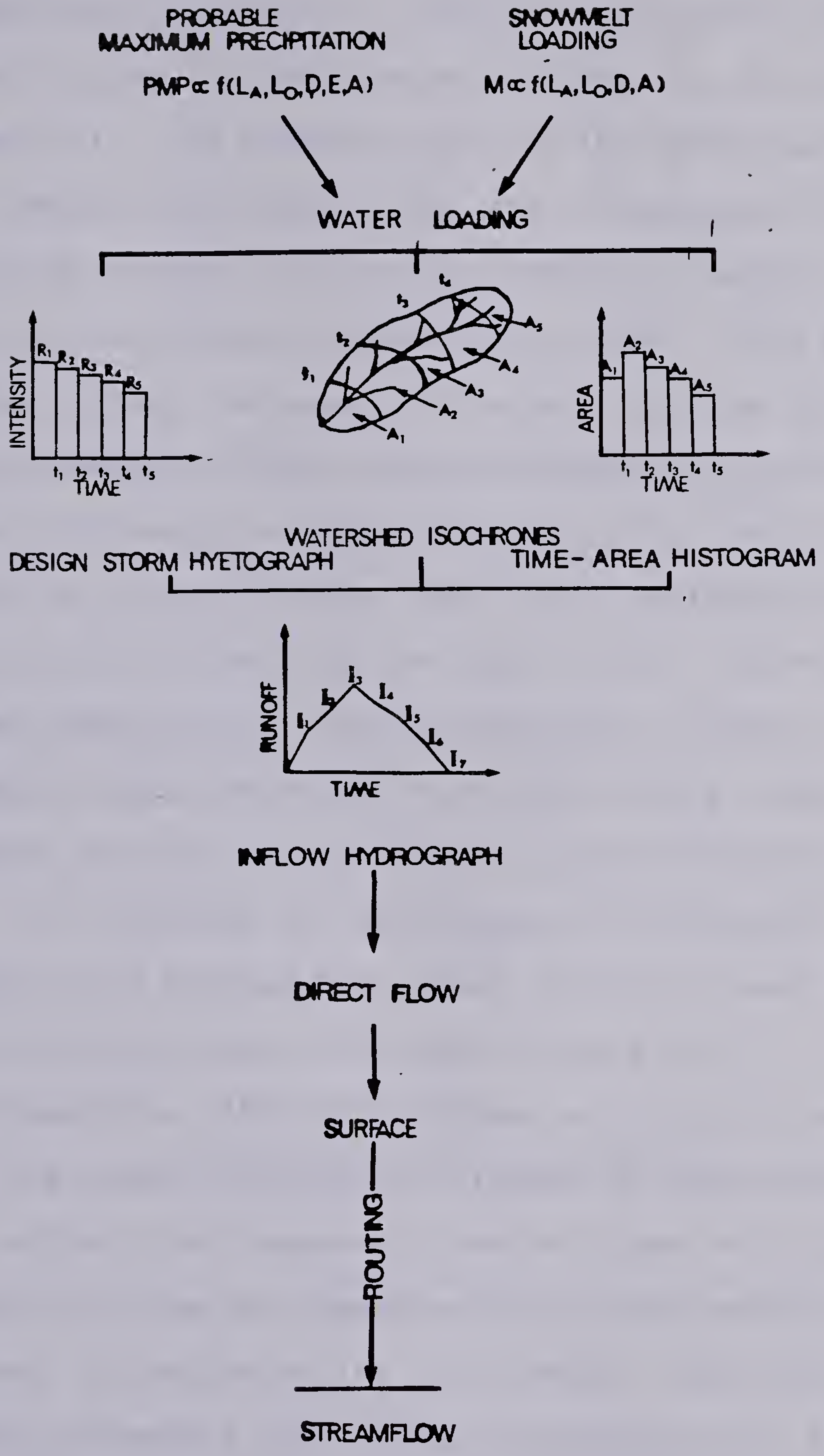

Figure 4.1. The TAPMF Model.

(as presented in Chapter 3), and these estimates are combined to give the total water loading for the watershed. For simplicity, the maximum value in the watershed is used. Using a design storm hyetograph and a time-area histogram, an inflow hydrograph is obtained from this loading, which yields the total water available for runoff. This hydrograph is routed through the watershed as surface flow by using a modified storage-outflow relationship and the continuity equation to produce the PMF hydrograph. The runoff is expressed as direct surface flow, since saturated soil conditions are assumed for the PMP loading. The resulting flow then generates an outflow hydrograph termed as the PMF. For computations, the basin is divided into a number of watersheds, so that the drainage is toward the main river system. To illustrate the development of the model, watersheds from the Red Deer River Basin are used, as defined by Water Survey of Canada (Figure 4.2).

Although the TAPMF Model presented in this thesis follows the overall design of a number of hydrological models, not all the components can be found in a single model, nor are they estimated or calculated using the same procedures. In designing the TAPMF Model, the author has used parts of models that seemed appropriate for Alberta river basins, that is, components that seemed physically suitable. The main features of the design are simplicity of data requirements, usage, and potential for modification.

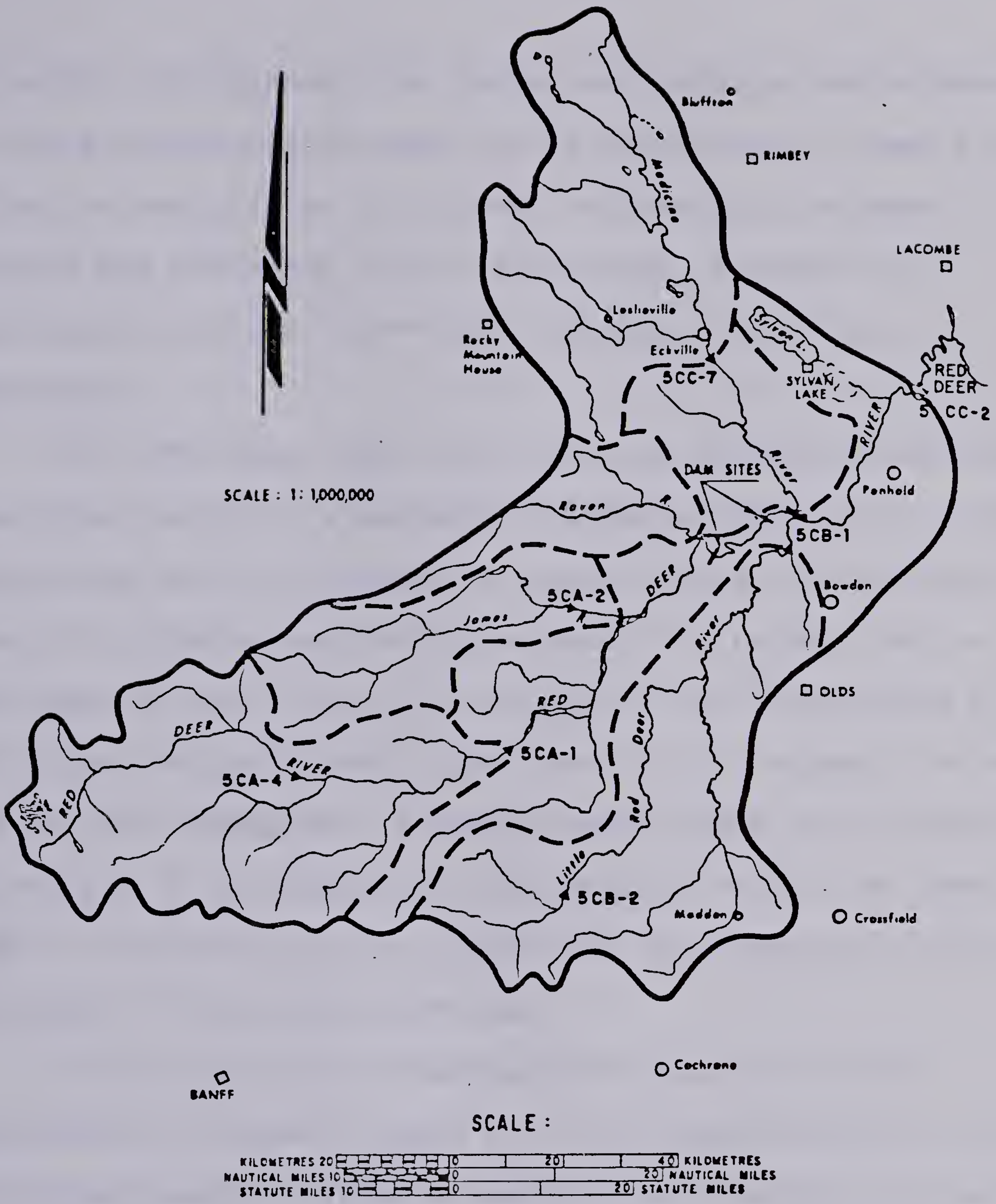

Figure 4.2. Map of the Watersheds of the Red Deer River Basin (After Muzik, 1975).

4.2.1 Determination of the Inflow Hydrograph

Watershed simulation generally utilizes some form of synthesizing technique to predict the temporal and spatial variations of a flood wave as it traverses the watershed. Hydrologic techniques are usually applied to the synthesis

of runoff hydrographs from gauged and ungauged watersheds. In these techniques an equation of continuity is used with either an analytic or an assumed relationship between storage and discharge within the system. A number of techniques exist for hydrologic synthesizing of the watershed.

The TAPMF Model uses the time-area histogram technique, also known as Clark's method (Viessman et al., 1977). This method was selected because by construction of isochrones it directly incorporates the basin shape in its application. The shape of the basin is a parameter that is believed by the author to contribute significantly to the peak discharge and the PMF hydrograph. Although basin shape is considered indirectly in the SSARR and HYMO models, in both of these models it is not easy to isolate the contribution of this parameter to the peak discharge.

In the time-area histogram technique, an inflow hydrograph is needed (Figure 4.1) The construction of this hydrograph requires three elements: (a) creation of a design storm hyetograph, (b) separation of the watershed into isochrones, and (c) construction of a time-area histogram.

4.2.2 Design Storm Hyetograph

The design storm hyetograph (Figure 4.1) can be considered the water loading for a given time period. The total water loading for a watershed is a combination of the PMP loading and the maximum snowmelt. (The latter was

discussed in Chapter 3 and can be estimated for a watershed by functional relationships.) As part of the PMP loading, the precipitation distribution (the variation of the depth of precipitation with time) affects the shape, peak, and lag time of the resultant flow. The time distribution of precipitation with large recorded depths seems to be ignored in the literature, however, this distribution plays an important part in PMF estimates. In the few PMF studies (e.g., Muzik, 1975), the usual approach was to distribute the total precipitation equally in a number of daily periods, which resulted in a uniform and low-intensity loading on the watershed.

As an alternative, the author grouped Alberta rainstorms that produced depths of 100 mm (4 in.) or more in 6-hour intervals and stratified these for different storm durations. The maximum mass distribution for durations of 24-72 hours at the maximum recorded depth is shown in Figure 4.3. This can provide an indication of when the intense rainfall occurred. Durations greater than 72 hours were also examined; however, these are not included here because the author was unable to define a representative curve for rainstorms with these durations, because of the limited available data in Alberta.

For rainstorm durations of 48 hours or more, small percentages of rain occur in the first 18 hours, and the precipitation is produced gradually with time, as is indicated in Figure 4.3. These storms lack the high-

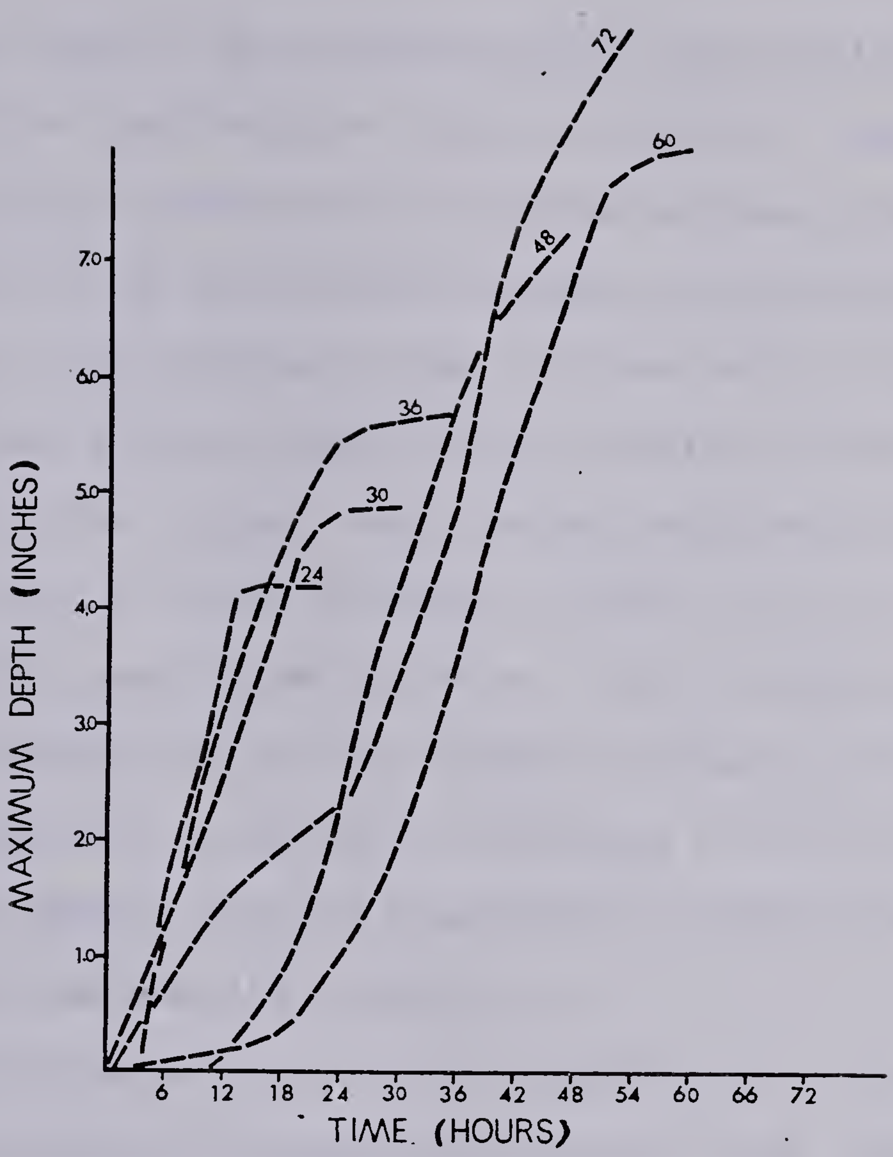

Figure 4.3. Maximum Mass Distribution at the Recorded Maximum Depth for Various Durations.

intensity characteristics evident in some thunderstorms and rainstorms with durations less than 48 hours. Rainstorms with durations of 48 hours or more are termed the cold lows (Chapter 1) and are capable of producing precipitation over 150 mm (6 in.) at the maximum depth. For short-duration rainstorms (36 hours and less) most of the precipitation occurs at the beginning of the storm and is produced in a very short period of time. This suggests that for rainstorms with durations of 36 hours and less, short-duration

intensity rainfall data could be used for obtaining the precipitation distribution. The use of short-time intensity data is further advocated because the maximum discharge would result from the greatest amount of precipitation occurring in the shortest time. The available intensity data were examined for stations in the vicinity of the Red Deer River Basin. The largest recorded maximum depths were 29 mm (1.14 in.) for a 1-hour duration, 49 mm (1.94 in.) for a 6-hour duration, and 73 mm (2.89 in.) for a 12-hour duration. Although intensities for durations in minutes are available, hourly values are used here to coincide with the time period used in the models and for practical considerations (computing time and the results).

Three parameters need to be considered in the design of the precipitation distribution: the total PMP loading, duration, and intensity. Expression of these parameters needs to be such that the product of the duration and intensity is equal to the total PMP loading. Various combinations of these parameters are possible, the simplest being division of the total PMP loading by the duration, which produces a low average intensity compared to the 1-hour intensity-duration data. Such an average intensity would in most cases coincide with a frequent event (one in 2 years or one in 5 years) and not an extremely rare event (as the PMP is considered to be). A more logical approach, and one that is advocated here, is to use the largest recorded 1-hour intensity (since this is the shortest time used) and

distribute this value over the shortest duration period possible for total PMP loading. For example, for a 24-hour PMP loading of 343 mm (13.5 in.) with an intensity of 38 mm (1.5 in.) per hour, the storm-design distribution would consist of rainfall intensity of 38 mm (1.5 in.) per hour for the first 9 hours and a zero intensity for the remaining 15 hours. For validity, this approach can be compared to analyzed short-duration intensity data, depicted in Figure 4.4 for the Edmonton Municipal Airport (with 45 years of record). Unfortunately, few intensity-frequency-duration graphs are available for Alberta; hence it was necessary to select the station nearest to the watershed that had a long record of data. In this case the Edmonton Municipal Airport was chosen (Figure 4.4). In terms of the shortest time period considered (1 hour), the 38 mm (1.5 in.) per hour intensity suggests about a 1 in 100 year event, while a 6- or 12-hour duration comparison suggests that the 38 mm (1.5 in.) per hour intensity may occur once in several thousand or even a million years. The use of the largest recorded 1-hour intensity seems to provide a practical aspect to the storm-design hyetograph.

4.2.3 Separation of Watershed into Isochrones

The second requirement for devising an inflow hydrograph for the TAPMF Model is the separation of the watershed into isochrones. The watershed is first divided into a number of time zones separated by isochrones, or

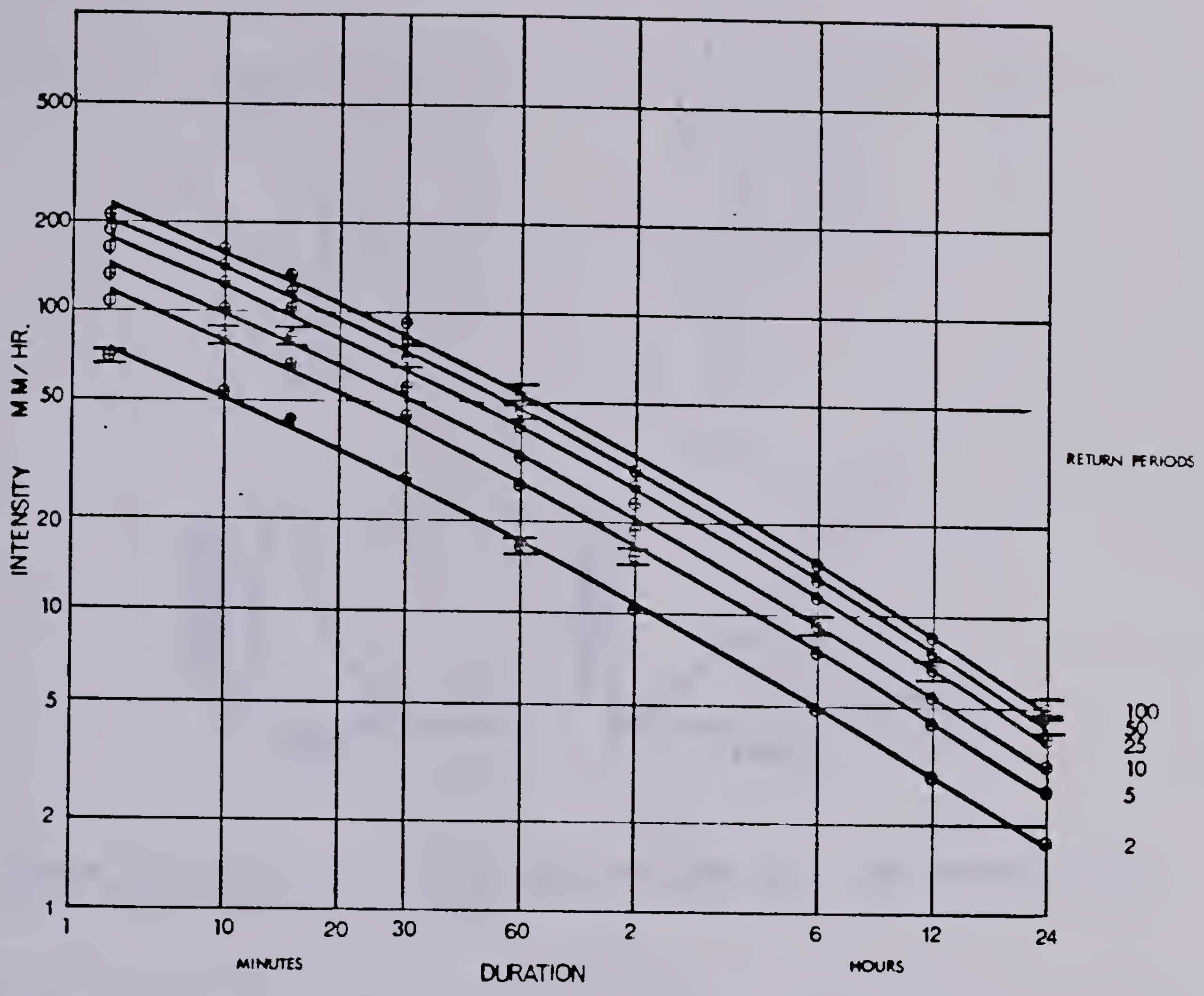

Figure 4.4. Intensity-Frequency-Duration Curves for Edmonton Municipal Airport (Data from Atmospheric Environment Service).

lines of equal travel time from the watershed outlet, as shown in Figure 4.1. The maximum isochrone is believed to be an approximation of the watershed shape that affects the peak flow. Numerous authors have attempted to obtain a bulk parameter for the watershed shape, and although some have had moderate success with particular watersheds, no universal parameter has been found. The importance of the shape of the watershed on the outlet hydrograph can be seen in Figure 4.5, which illustrates two different watershed shapes. This figure shows that the larger the value of the

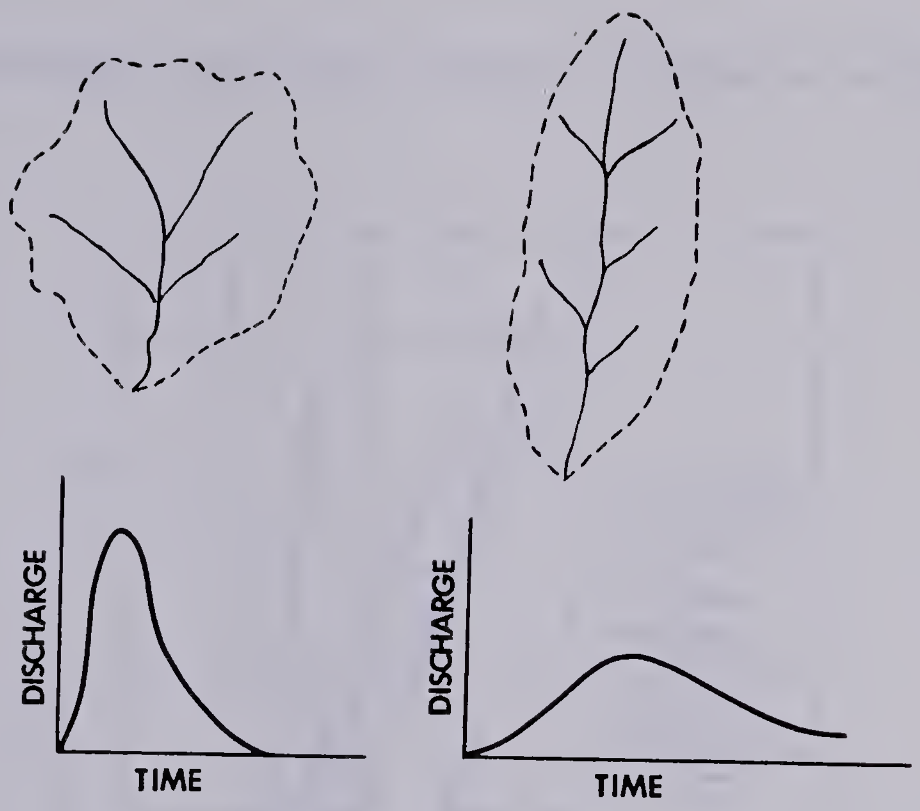

Figure 4.5. Effect of Shape on the Outflow Hydrograph.

maximum isochrone, the greater the peak discharge. The time-area approach is believed to provide a reasonable representation of the shape of the watershed. The areas between the isochrones can be determined and plotted against the travel time (i.e., time-area histogram).

To divide the watershed into equal time zones, an estimate of the speed of water flow in the streams of the watershed is needed. The velocity of water in a stream or river has been approximated by a logarithmic relationship (Water Survey of Canada, 1977), that is, a straight line is obtained when logarithmic values of velocity are plotted against the logarithmic values of discharge. Figure 4.6 illustrates this dependency (from graphs produced by Inland Water Survey) for a number of streams in the Red Deer River

Basin watersheds. From this figure, a value of stream

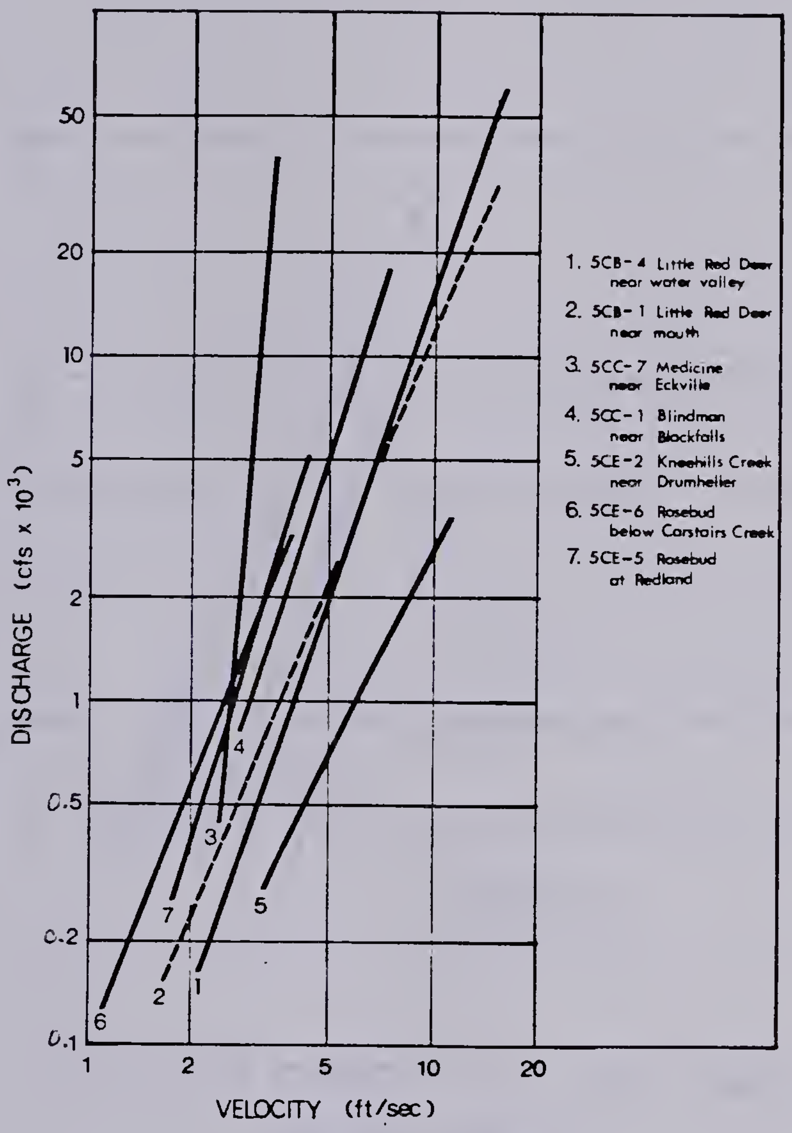

Figure 4.6. Discharge-Velocity Distributions for a Number of Streams in the Red Deer River System (Data from Water Survey of Canada, 1977).

velocity can be estimated, and this in turn can be used to calculate the distance water travels for a specified time interval. From this, isochrones for the watershed can be drawn. The water travel time on the river can be similarly obtained by considering discharge-velocity distributions for

the river. This is illustrated for the Red Deer River system in Figure 4.7. In most models, the velocity is often

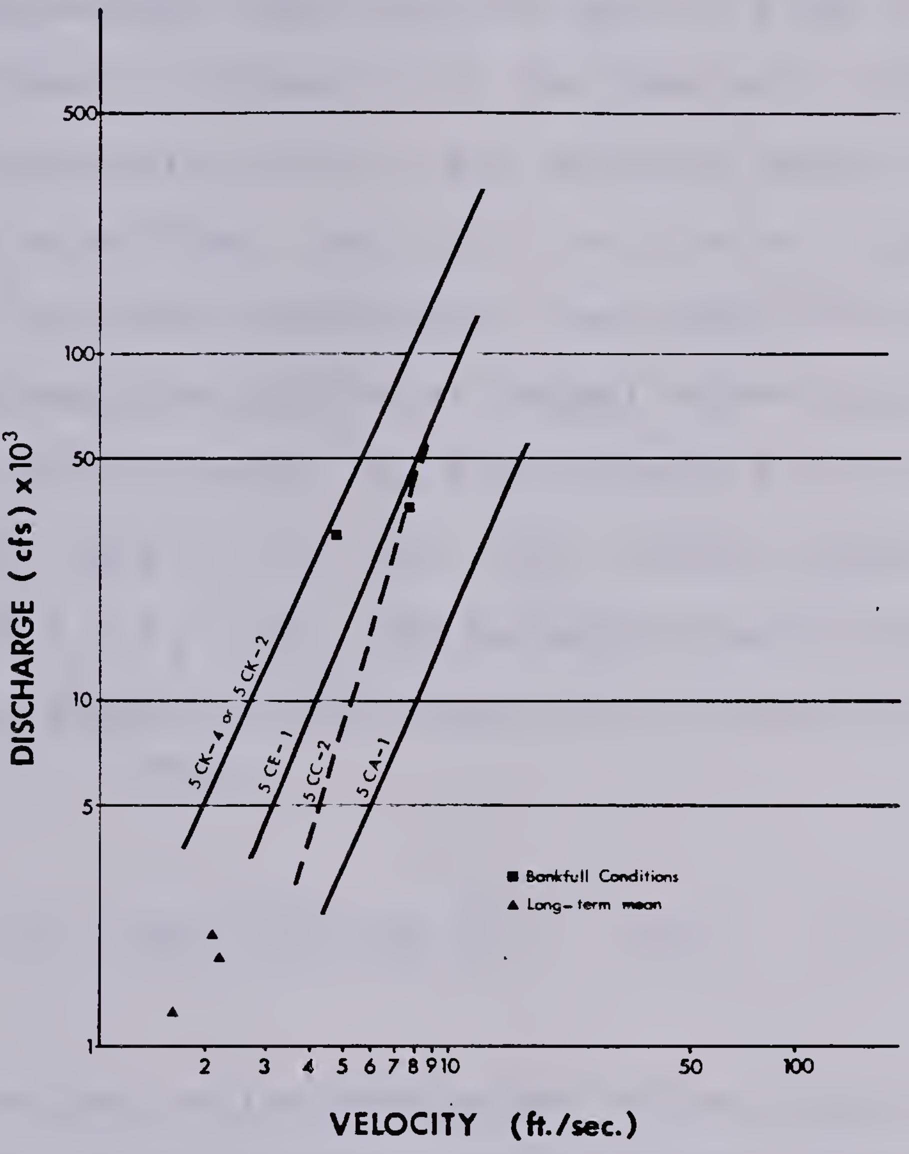

Figure 4.7. Discharge-Velocity Distribution at a Number of Locations on the Red Deer River (Data from Water Survey of Canada, 1977).

approximated by a velocity-discharge relationship with a fixed upper limit.

4.2.4 Time-area Histogram

In creating an inflow hydrograph for the TAPMF Model,

the third requirement is to obtain a time-area histogram. From the watershed isochrones, the area for each time zone can be planimetered; when plotted against time, a time-area histogram results (Figure 4.1). The reservoir inflow hydrograph ordinates (I) for any selected design hyetograph can now be determined. Each block of rain in Figure 4.1 is applied to the entire watershed; the runoff from each subarea reaches the outflow at lagged intervals defined by the time-area histogram. The simultaneous arrival of the runoff from areas A_1, A_2, etc., for various design storm intensities R_1 ,R_2 ,etc., can be determined by properly lagging and adding contributions, as expressed by the equation

$$I_i = R_iA_1 + R_{i-1}A_2 + \dots + R_1A_i \quad (4.1)$$

where I_i are the inflow hydrograph values in cfs, R_i are the design storm intensity values in inches per hour, and A_i are the time-area histogram values in acres. By applying Equation 4.1 it is possible to compute the inflow hydrograph shown in Figure 4.1. The time-area histogram method (although a little tedious to apply) is easier to interpret.

4.2.5 Flow Separation

Anticipating no evapotranspiration losses, the total generated runoff can be partitioned into the components of base, surface, and subsurface flow runoff. For PMF estimates

the maximum surface runoff would occur when base and subsurface flows are assigned zero flows (equivalent to saturated soil conditions). Hence, the total generated runoff is expressed as surface runoff.

4.2.6 Routing Method

The basic routing method used in the TAPMF model is similar to that described by Wilson (1941), expanded upon by Rockwood (1958) and used in the SSARR Model (U.S. Army Corps of Engineers, 1972). In this method, routing through watershed, river system, and reservoir components of the model, relies on the use of the law of continuity in the storage relationship

$$\left(\frac{I_n + I_{n+1}}{2}\right) \Delta t - \left(\frac{O_n + O_{n+1}}{2}\right) \Delta t = S_{n+1} - S_n \quad (4.2)$$

where I_n is the inflow at the beginning of the time period, I_{n+1} is the inflow at the end of the period, O_n is the outflow at the beginning of the period, O_{n+1} is the outflow at the end of the period, S_n is the storage at the beginning of the period, S_{n+1} is the storage at the end of the period, and Δt is the duration in hours.

The inflow at time t (I_t) can be expressed by

$$I_t = O_t + \frac{dS}{dt} \quad (4.3)$$

In natural lakes, where storage is a function of outflow at any given elevation, K represents the proportionality factor between storage and outflow:

$$S = K\ O \qquad (4.4)$$

Differentiating with respect to time, the following relationship is obtained:

$$\frac{dS}{dt} = K\ (\frac{dO}{dt}) \qquad (4.5)$$

Substituting this expression into Equation 4.3 and rewriting the terms results in

$$\frac{dO}{dt} = \frac{I_t - O_t}{K} \qquad (4.6)$$

which represents the basic form of the storage equation. Watershed routing can be evaluated through successive increments of lake-type storage. A watershed can be considered a series of small lakes that represent the natural delay of runoff from upstream to downstream points. During the routing computation, the computer operates on each specified increment of storage consecutively, one period at a time. The equation used by the computer (in the TAPMF Model and also in SSARR Model) can be derived by considering Equation 4.2, the storage routing equation.

Setting $I_m = (I_n + I_{n+1}) / 2$

and substituting this in Equation 4.2 gives

$$(I_m)\,\Delta t \;-\; \left(\frac{O_n + O_{n+1}}{2}\right)\Delta t \;=\; S_{n+1} - S_n$$

Dividing by Δt , and subtracting O_n from both sides, the equation becomes

$$I_m - O_n \;=\; \left(\frac{S_{n+1} - S_n}{\Delta t}\right) \;+\; \left(\frac{O_{n+1} - O_n}{2}\right)$$

Multiplying both sides by $\frac{\Delta t}{(O_{n+1} - O_n)}$ and rearranging the terms results

$$I_m - O_n \;=\; \left(\frac{O_{n+1} - O_n}{\Delta t}\right) \left(\frac{S_{n+1} - S_n}{O_{n+1} - O_n} \;+\; \Delta t / 2\right)$$

With $K = (S_{n+1} - S_n) / (O_{n+1} - O_n)$

the above equation can be re-written as

$$\frac{O_{n+1} - O_n}{\Delta t} \;=\; \frac{I_m - O_n}{K + \Delta t/2}$$

Solving for O_{n+1} the equation in the TAPMF model becomes

$$O_{n+1} = \left(\frac{I_m - O_n}{K + \Delta t/2}\right) \Delta t + O_n \qquad (4.7)$$

where O_{n+1} is the outflow at the end of the period, I_m is the mean inflow, O_n is the outflow at is the beginning of the period, Δt is the time duration of computational period, and K is the storage coefficient. For given values of inflow and outflow at the beginning of the period, the outflow at the end of the period (O_{n+1}) is found by Equation 4.7. In the computer program, the value of $\Delta t / (K + \Delta t/2)$ is evaluated for a specified condition, and multiplied by the difference between I_m and O_1 to obtain the change in outflows. The outflow (O_2) computed from the first incremental routing is then saved and converted to initial outflow (O_1) for the next period routing.

The coefficient K must be estimated and can be a few hours to a month or more. For watersheds where hydrograph data are not available, K can be estimated from an empirical equation by equating this quantity with the basin lag time. A number of equations are available. The equation that is used in the TAPMF Model is the one developed by the Soil Conservation Service (1969):

$$t_1 = \frac{1^{0.8} (S + 1)^{0.7}}{1900 \, Y^{0.5}} \qquad (4.8)$$

where t_1 is the lag time in hours, 1 is the length to the divide in feet, Y is the average watershed slope in percent,

and S is the potential maximum retention in inches. The potential maximum retention is equivalent to (1000/CN)-10, where CN is a curve number. For saturated soil conditions, CN = 100, and hence S becomes equal to zero. Substituting S = 0.0 reduces Equation 4.8 to:

$$t_1 = \frac{l^{0.8}}{1900\ Y^{0.5}} \qquad (4.9)$$

For a watershed in the Red Deer River Basin with an area of 2470 km² (954 sq. mi.) an average slope of 5.7 m per km (30.1 ft. per mi) or 0.5701 expressed as a percentage, and l equal to 85 km (53 mi.), a lag time of 16 hours is calculated from Equation 4.9. This lag time can be used as an estimate of the storage coefficient in Equation 4.7.

4.2.7 Operations and Data Requirements

The above components are then organized and coordinated to produce a river basin model. The system configuration (similar to Figure 5.7 for SSARR Model) essentially describes to the computer the physical layout and relationships of all components of the system. The configuration is in upstream to downstream order of all watersheds, lakes, reservoirs, channel reaches, and confluence points for a particular basin. The hierarchical procedure involves, first, watershed routing, then consecutive channel routing, and finally combining until all

operations are complete. The computer model then integrates the two hierarchies and performs the model simulation of the river basin system.

The input data needed for operation of the TAPMF Model include: (a) nonvariable characteristics data which describe physical features such as drainage area, (b) time variable data which include physical data expressed as time series; for example, probable maximum precipitation, snowmelt loading, storm hyetograph, and time-area histogram, and (c) miscellaneous job control and time control data which specify such items as total computation period, routing intervals, and special computer instructions to control input-output alternatives.

Results obtained using the TAPMF Model are compared with those from the SSARR and HYMO models in Chapter 6.

CHAPTER 5

THE SSARR AND HYMO MODELS

5.1.0 Introduction

An objective in this study was to compare the predicted PMF peak discharge from the TAPMF Model (presented in Chapter 4) with that obtained from two commonly used models in Alberta (SSARR and HYMO). Before the comparison is presented in Chapter 6, the PMP loading for the SSARR Model is discussed in Section 5.2 and for the HYMO Model is discussed in Section 5.3.

The SSARR (Streamflow Synthesis and Reservoir Regulation) Model was one of the earliest continuous streamflow simulation models using a lumped parameter representation; its primary strength lies in its verified accuracy. Successful tests have been conducted in several large drainage basins, including the Columbia River Basin (NW United States) and the Mekong River Basin (SE Asia) (U.S. Department of Commerce, 1970). This model has also been used by Alberta Environment in hydrological studies on several river basins in Alberta (Alberta Environment, 1980). For these reasons, this model was chosen for comparison in this work. The success of any model is usually dependent upon the applicability of the relationships to a watershed or basin; these relationships are examined in some detail in Section 5.2. For PMF estimates, the sensitivity of a model

response to parameter changes is important, since some parameters may affect the shape of the resulting hydrograph and the peak estimate of the PMF. The parameterization and sensitivity of the SSARR and HYMO models for PMP loading are emphasized here, since this is important to an understanding and interpretation of the estimates of PMF.

5.2.0 SSARR Watershed Model

The SSARR Model is a widely used, continuous streamflow simulation model designed for large basins. It was developed by the U.S. Army Corps of Engineers (1972) for streamflow and flood forecasting and for reservoir design and operation studies. It is a mathematical hydrologic model of a river basin system throughout which streamflow can be synthesized by evaluating snowmelt and rainfall.

Applications of the model begin with a subdivision of the drainage basin into homogeneous hydrologic units of a size and character consistent with subdivides, channel confluences, reservoir sites, diversion points, soil types, and other distinguishing features. The streamflows can be computed for all significant points throughout the river system. An SSARR watershed model flow chart is shown in Figure 5.1.

Rainfall data can be supplied at any number of stations in the watershed. The part that will run off is divided into the base flow, subsurface or interflow, and surface runoff. The separation is based on indexes and on the intensity of

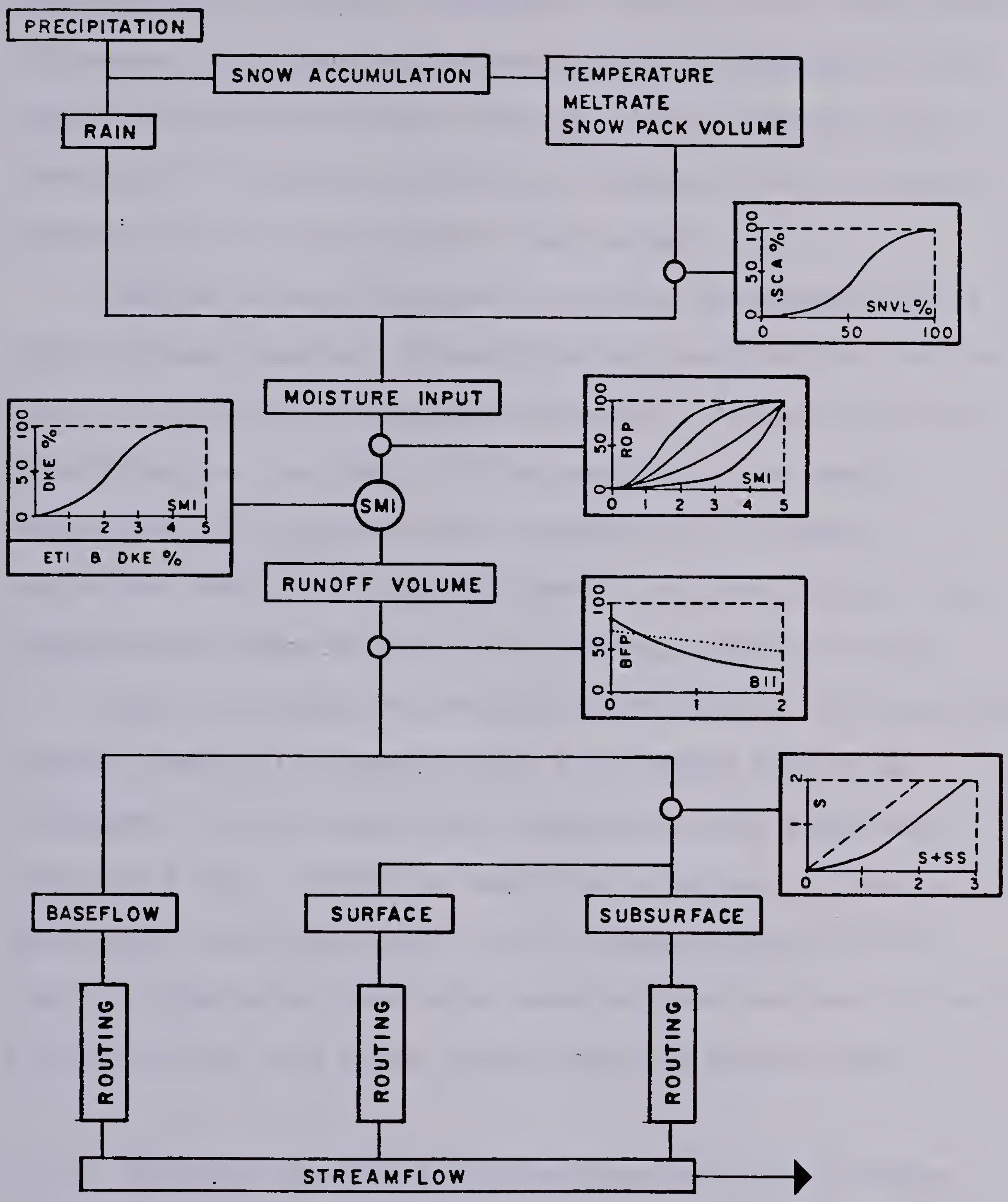

Figure 5.1. SSARR Watershed Model Flow Chart (After Alberta Environment, 1977b).

the direct runoff. Each component is simply delayed according to different processes, and all are then combined to produce the final watershed outflow hydrograph. This runoff can then be routed through stream channels and combined with other watershed hydrographs, all of which become part of the resultant hydrograph.

Routing through channels requires an assumption of short stream reaches. Streamflows are synthesized on the basis of rainfall and snowmelt runoff. Snowmelt can be determined on the basis of the precipitation depth, elevation, air and dew point temperatures, albedo, radiation, and wind speed. Snowmelt options include the temperature index method or the energy budget method.

Input includes the precipitation depths; the watershed-runoff indexes for subdividing flow among the three processes; initial reservoir elevations and outflows; drainage areas; bounds on usable storage and allowable discharge from reservoirs; total computation periods; routing intervals; and other special instructions to control plots, prints, and other input-output alternatives.

5.2.1. Rainfall-Runoff Relationships for PMF Estimates

Rain falling on a watershed must either be (a) runoff, (b) retained in the soil system, (c) intercepted and evaporated from trees and other plants, (d) evaporated from pond, lake, and stream surfaces, (e) evaporated from the soil, (f) returned to the atmosphere by transpiration from

trees and other plants, or (g) percolated into the groundwater system and thereby lost to the surface water system. If percolation to the groundwater is considered negligible; this rainfall input can be grouped into three classes: (1) runoff, (2) soil moisture increases, and (3) evapotranspiration losses.

The percentage of water available for runoff is found from empirically derived relationships of the Soil Moisture Index (SMI) versus Runoff Percent (ROP), with intensity as a third variable. In the SSARR Model this is entered into the program in the form of a table for each watershed. These values are usually developed by trial and error. Before a design curve for PMF estimates is provided, two examples of SMI-ROP relationships are cited. The first example is a three variable SMI relationship developed for the Bird Creek Basin near Sperry, Oklahoma (Figure 5.2) (U.S. Army Corps of Engineers, 1972). This basin is characterized by hot summer temperatures, long dry periods, high evapotranspiration rates, and high intensity, short-duration rainfall. The SMI-ROP relationship was developed by trial and error. For saturated soil conditions (equivalent to SMI greater than 100 mm (4 in.)) a large percentage of the precipitation is runoff; for very low precipitation intensity (0.25 mm (0.01 in.) per hour) about 30% is runoff; while for high-intensity values (25.4 mm (1.0 in.) per hour and greater) the runoff is 100%.

The second example is the relationship calibrated by

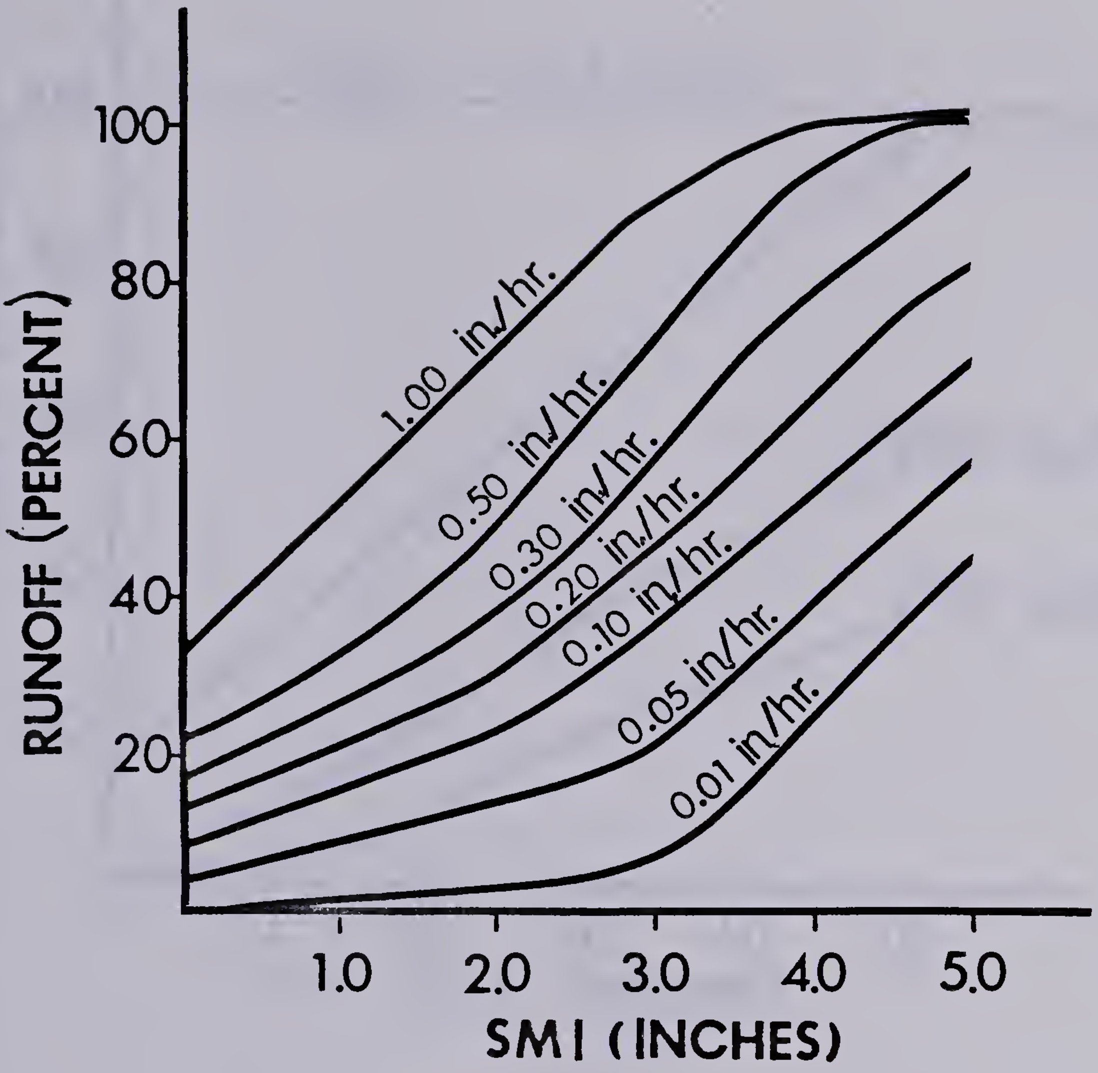

Figure 5.2. Three Variable Soil Moisture Index Relationships Developed for Bird Creek Basin (After U.S. Army Corps of Engineers, 1972).

Alberta Environment (1980) for the Little Red Deer River watershed in the Red Deer River Basin, as illustrated in Figure 5.3. This watershed, because it is located much farther north than the basin in the previous example, is characterized by a moderate climate with moderate summer temperatures, intermediate evapotranspiration rates, and low-intensity duration rainfall. The main difference between these two examples is that in the latter case the lower intensity of the rainfall would produce a greater runoff,

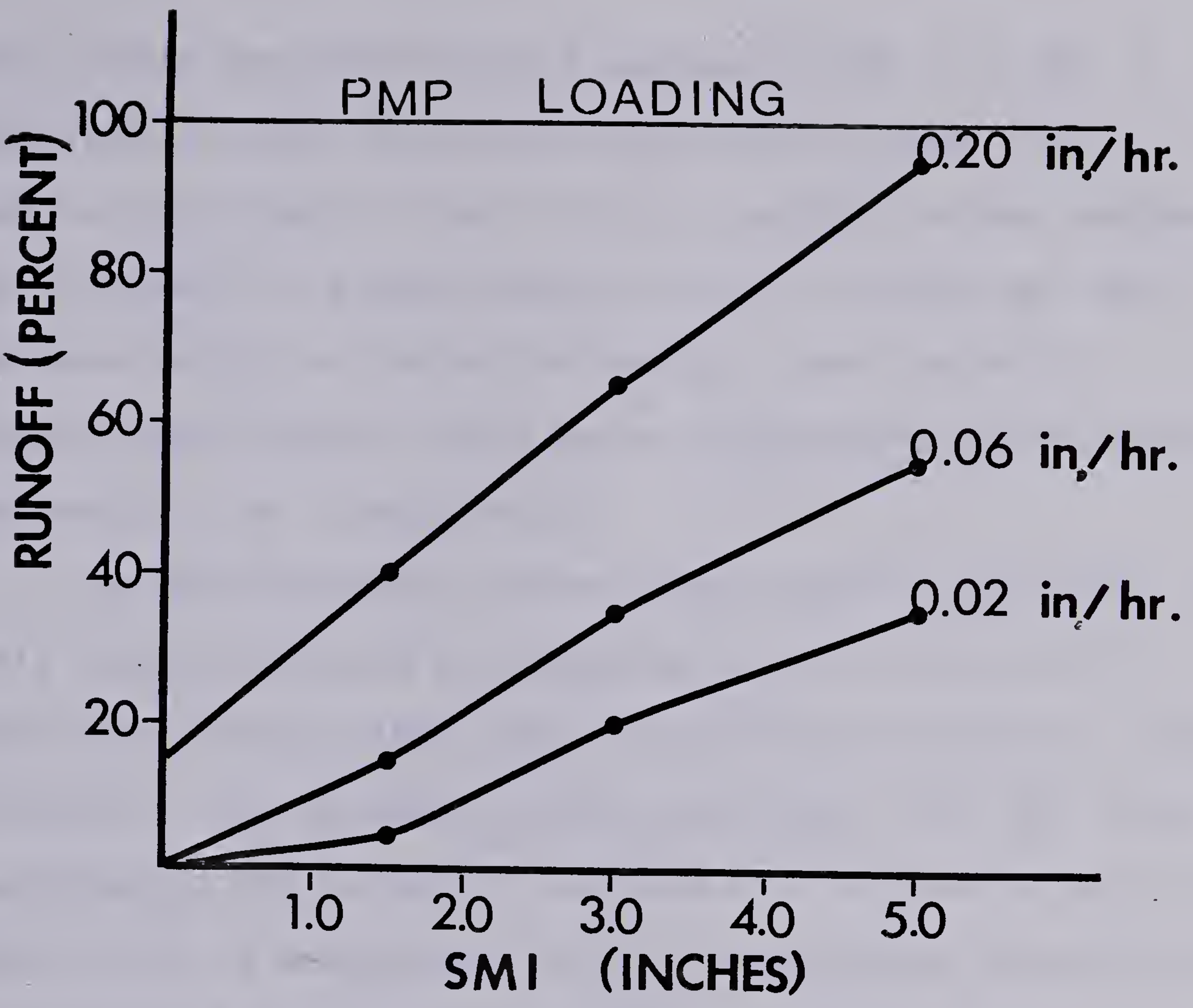

Figure 5.3. Three-variable Soil Moisture Index Relationship for the Little Red Deer River and a Design Curve for PMP Loading (After Alberta Environment, 1980).

probably because of the lack of long dry periods in central Alberta.

The SMI is an indicator of the relative soil wetness and is used to determine runoff. When the soil moisture is depleted to approximately the permanent wilting point, the SMI is a small number associated with little or no runoff. When precipitation recharges soil moisture, the value of the SMI increases until it reaches a maximum value considered to represent its field capacity or water holding capacity. At

this value the runoff would approach 100%. The SMI is depleted only by the evapotranspiration index (ETI). The ETI can be specified in table form as monthly versus average daily potential evapotranspiration (in inches per day). Maximum runoff is characterized by a zero value of evapotranspiration, which means there would be no losses to evaporation or transpiration.

For PMF estimates the maximum runoff is desired, and this can be achieved by assuming (a) that the soil is saturated and (b) that the precipitation occurs at a high intensity. To represent these conditions, all SMI values are assigned an ROP value of 100% and ETI is given a value of zero. This is equivalent to the relationship shown by the solid line (labelled PMP loading) in Figure 5.3.

5.2.2 Flow Separation

In the SSARR Model, the rainfall that will run off is divided into three parts: a) base flow, b) subsurface or interflow, and c) surface runoff. Because of antecedent conditions (i.e., saturated soil), the maximum runoff for PMF estimates would occur when there were no base and subsurface flows. This is equivalent to the 1-to-1 broken line in Figure 5.4 and is specified for the SSARR Model in the form of a table. The solid line depicts a calibrated curve that has been used in the Red Deer River Basin for natural flows during the summer (Alberta Environment, 1980).

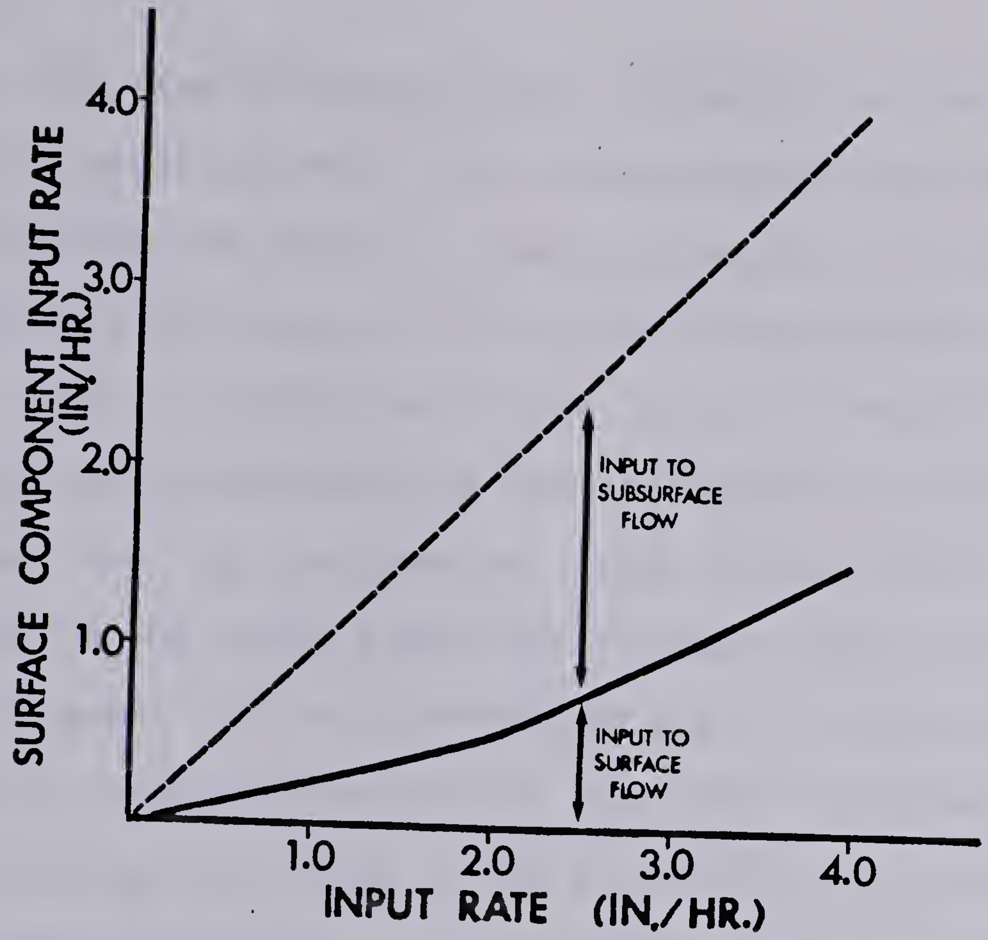

Figure 5.4. Surface-Subsurface Separation Curve (After Alberta Environment, 1980).

5.2.3 Routing of Surface Flow

In the SSARR Model, each component of surface flow is computed as input rates, expressed in inches per period. Each period value is converted to the equivalent inflow rate in cfs, based on the drainage area and the length of the period in hours. Each component of inflow is routed through a specified number of increments of storage. These increments can be considered a series of small lakes that delay runoff. Routing is accomplished by solution of the basic storage equation in finite time periods for each increment of storage routing (Section 4.2.6). Inflows are computed as mean values for the period for watershed

routing. The time of storage per increment can be a few hours to a month or more. The routing specifications determine the time delay to the outflow point of the watershed and the shape of the outflow hydrograph. In this model, virtually unlimited flexibility in time distribution of runoff can be achieved by the incremental storage routing technique. The lag time and unit peak relationships available in the SSARR Model for various combinations of multi-increment routing coefficients are illustrated in Figure 5.5. The intersection of the number of phases and the time of storage per phase in this figure give the lag time and the peak discharge. In this model, the time of storage per phase and the number of phases need to be determined. The first of these two parameters is usually computed by an empirical relationship similar to Equation 4.9, while the second parameter can be obtained through calibration of the model.

The typical routing specifications for surface flow that have been calculated for a 539 km^2 (208 sq. mi.) watershed in Oregon are four phases and 2.5 hours storage per phase (U.S. Army Corps of Engineers, 1972). For the Red Deer River watershed at Sundre, the values that have been calibrated and calculated for a 2471 km^2 (954 sq. mi.) watershed are two phases and 16 hours storage per phase (Alberta Environment, 1980).

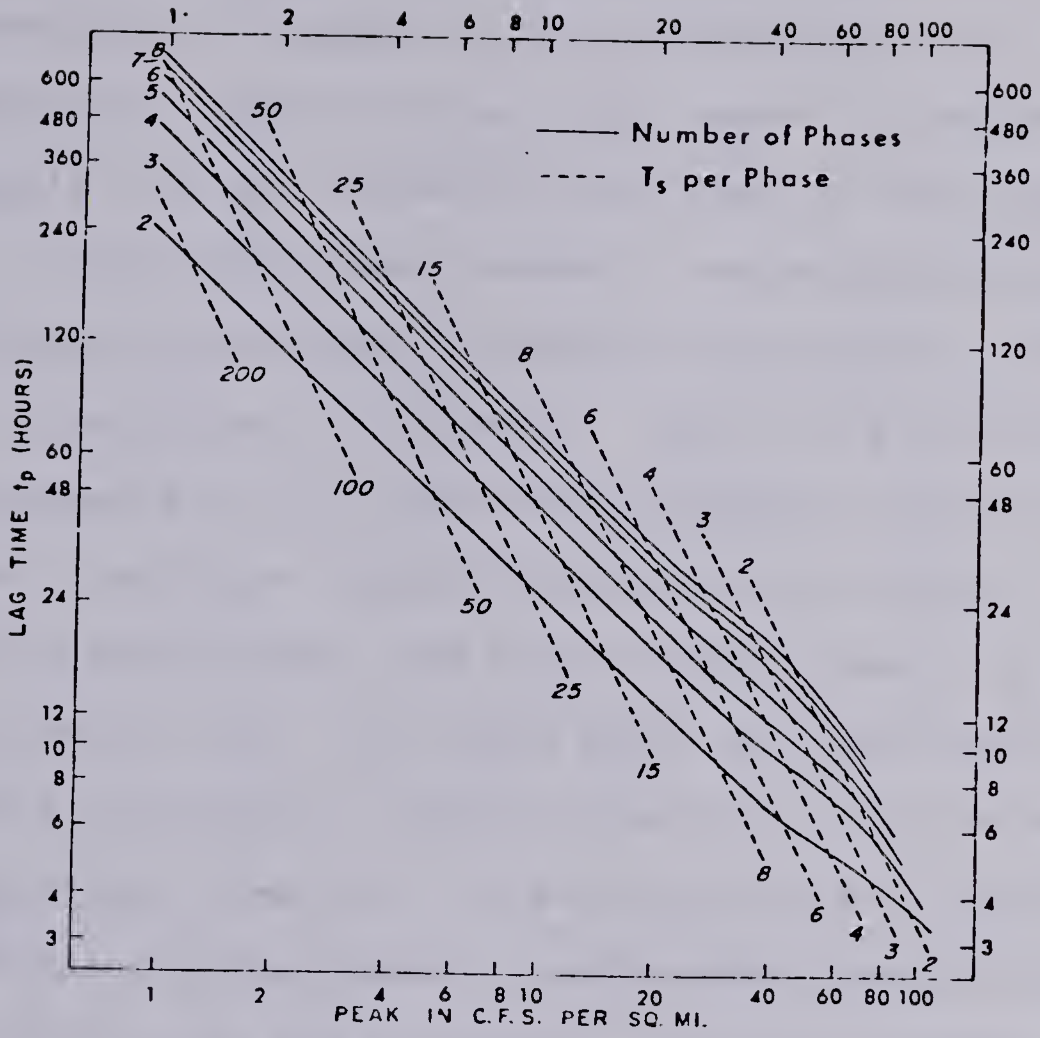

Figure 5.5. Watershed Multiple Phase Storage Routing Available in SSARR (After U.S. Army Corps of Engineers, 1972).

5.2.4 Runoff from Snowmelt

Runoff from snowmelt may contribute significantly to streamflow in Alberta, and hence an applicable model for this province must consider this component. In the SSARR Model, extensive routines are programmed for computation of runoff from snowmelt. Because snowmelt runoff poses complex problems for the hydrologist, this aspect has been ignored by many modellers in their design.

Unlike rainfall, snowmelt is not generally measured

quantitatively; it must be estimated indirectly from observations of meteorological parameters (e.g., air temperature, depth of snow, wind speed) to determine the snowmelt rate and the water equivalent of the snowpack.

In the SSARR Model snowmelt can be calculated by use of the generalized snowmelt equation for a partly forested area (U.S. Army Corps of Engineers, 1956). This equation requires measurements of air temperature, dewpoint temperature, wind speed, insolation (solar radiation on horizontal surface), snow surface albedo, and forest canopy cover, for estimating the snowmelt rate. The SSARR Model has been modified by Alberta Environment (1977b) to perform split-watershed computations, that is, the snow-covered and snow-free areas are treated as two separate watersheds, each with its own characteristics and parameters. Since the number of watersheds is doubled, this approach is more cumbersome and requires more data for simulation; however, it does allow for separate accounting of the SMI in the snow-free and snow-covered areas. The various hydrologic options available in the split watershed approach are illustrated in Figure 5.6. These options are specified for the model in either tabular form or as part of the data.

5.2.5 Channel Routing

The time rate of change of streamflow in a river reach is evaluated by first dividing the reach into a series of increments. The increments should be small enough so that

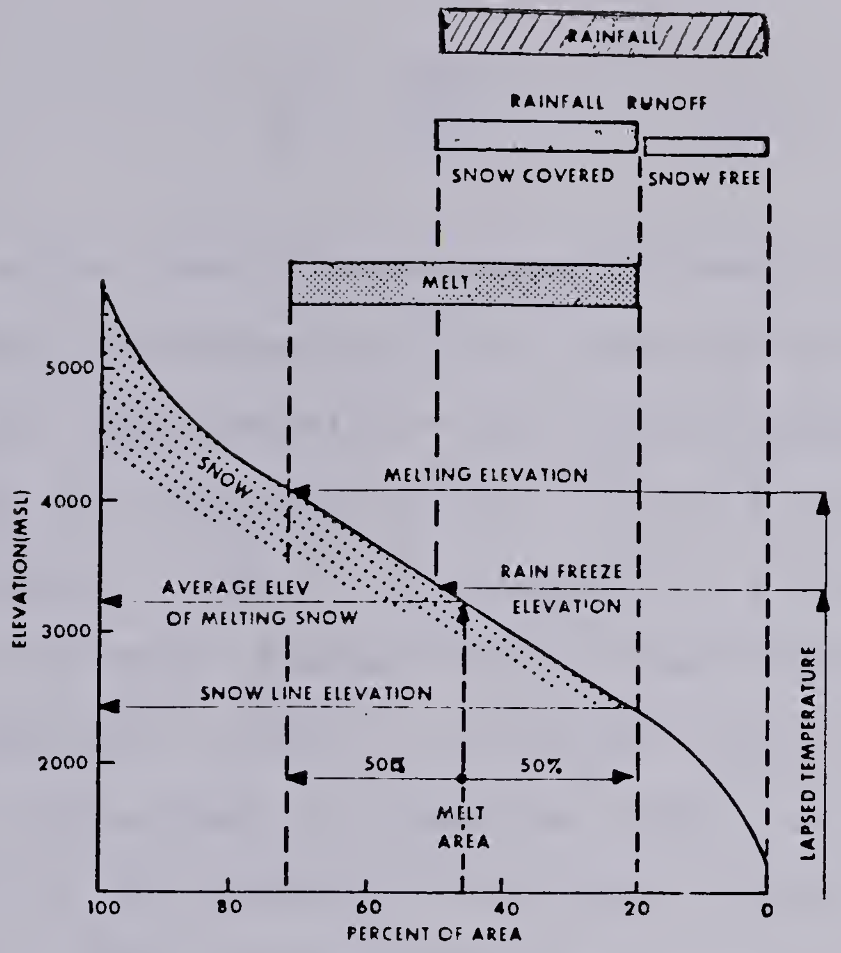

Figure 5.6. Split Watershed Option of the Snow Cover Depletion Method Available in the SSARR Model (After U.S. Army Corps of Engineers, 1972).

wedge [1] storage is negligible compared to prismatic storage. Inflows are computed at point values in time for channel routing. Outflow from each increment serves as inflow to the next downstream increment. Time of storage for channel routing may vary inversely or directly as a power function of discharge and is expressed as the following relationship:

---

[1] Linsley et al. (1949) showed that the storage in a channel reach may be considered to be the sum of two portions: prism storage, or the water below an imaginary line drawn parallel to the channel bottom; and wedge storage, or the water between that line and the actual water surface profile.

$$T_s = \frac{KTS}{Q^n} \qquad (5.1)$$

where T_s is the time of storage per increment in hours, KTS is a constant determined by trial and error or estimated from physical measurements of flow and corresponding routing times, Q is the discharge in cfs, an n is a coefficient usually between -1 and +1. A value of n = 0.20 was found reasonable for most streams in the Columbia Basin (U.S. Army Corps of Engineers, 1972); n = 0.35 was found for the Mekong River (U.S. Department of Commerce, 1970); and n = 0.13 was determined for the Red Deer River Basin (Alberta Environment, 1980). Although the last appears to be low with respect to the other two values, it has been obtained by Alberta Environment from calibration for the Red Deer River Basin.

Routing of flow is accomplished by an iterative solution of the storage equation. A backwater mode exists for cases in which elevation and discharge are affected by backwater from a downstream time-variant source. Examples of such occurrences are river estuaries affected by tidal fluctuations, river reaches upstream from a junction with a major tributary, and the upstream reaches of a reservoir or a lake whose outflow is affected by the elevation of another lake just downstream. This model utilizes a three-variable relationship between upstream elevation, downstream elevation or flow, and discharge from the upstream location.

The above components are organized and coordinated to

produce a river basin model that simulates the hydrologic response of the physical system. The system configuration essentially describes to the computer the physical layout and relationships of all components of the system. The configuration is in upstream to downstream order of all watersheds, lakes, reservoirs, channel reaches, and confluence points for a particular basin. The hierarchical procedure involves, first, watershed routing, then consecutive channel routing, and finally combining until all operations are complete. The computer model then integrates the two hierarchies and performs the model simulation of the river basin system.

An example of a configuration for the watersheds of the Red Deer River Basin from the headwaters, through Sundre, to Red Deer is depicted in Figure 5.7. In this figure, four watersheds are simulated: headwater watershed to Sundre (drainage area of 2471 Km^2 or 954 sq. mi.), Little Red River watershed (drainage area of 2392 Km^2 or 924 sq. mi.), James River watershed (drainage area of 821 Km^2 or 317 sq. mi.), and Medicine River watershed (drainage area of 655 Km^2 or 253 mi^2). Because of the snowmelt computations, each of the above watersheds is treated as two separate watersheds (one for the snow-free area and the other for the snow-covered area). For example, in Figure 5.7 the number 301 is assigned to the snow-covered area for the Little Red Deer River watershed, while the number 302 refers to the snow-free area for the same watershed.

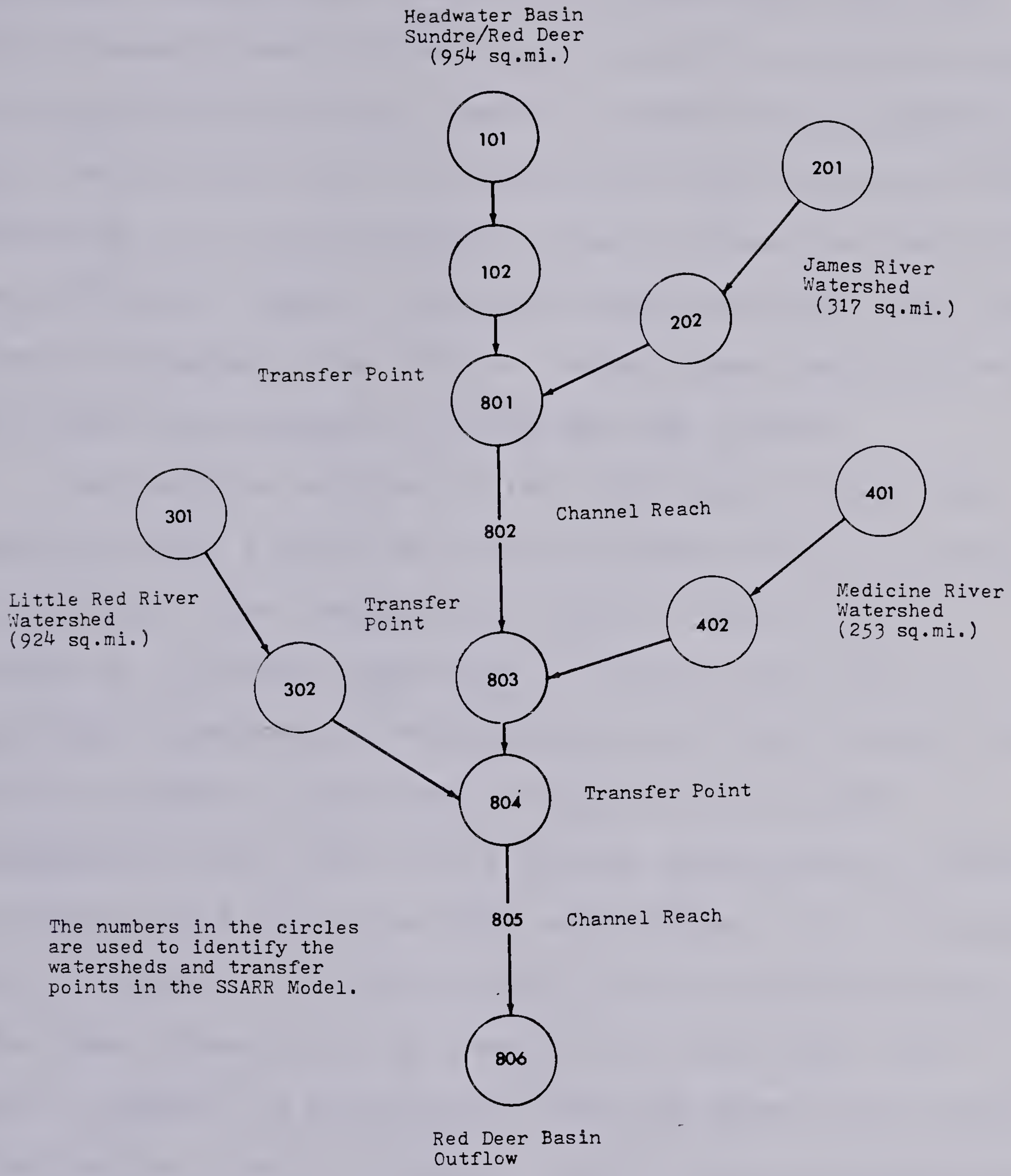

Figure 5.7. A Watershed Configuration Used in the SSARR Model for the Red Deer River Basin.

5.2.6 PMF Estimates from the SSARR Model

The various parameters and relationships discussed previously are first maximized and then used in the SSARR Model to produce a PMF hydrograph and a peak discharge. In

the above computations the soil is considered saturated, with no evapotranspiration losses, and all available water is translated as surface runoff. An underlying assumption is that the surface area of precipitation and the area of the watershed are interchangeable. Usually these two quantities are different, however, under maximum conditions they are commonly assumed to be similar. Hence these terms can be and are used interchangeably in PMP and PMF studies.

The computer program of the SSARR Model allows the results of the simulation to be produced either in tabular or graphical form. Because the tabular results are extensive, graphical depiction is usually desirable. A graphical example of a PMF hydrograph for the Red Deer River Basin at Sundre is depicted in Figure 5.8. The PMF hydrograph is the result of a 24-hour precipitation loading of 340 mm (13.4 in.) on a 2471 Km^2 (954 sq. mi.) drainage area at Sundre. The precipitation loading is distributed at a maximum intensity of 30.5 mm (1.2 in.) per hour for 11 hours. Snowmelt is calculated using the generalized snowmelt equation for a partly forested area. In future discussions of the watershed at Sundre it can be assumed that the above values of precipitation loading apply. Any deviation from these values will be mentioned in the discussion. The largest recorded hydrograph at Red Deer is shown on the same diagram (Figure 5.8) for comparison. The Red Deer station was used because it is the only station with long-term discharge data in the Red Deer River Basin. The hydrograph

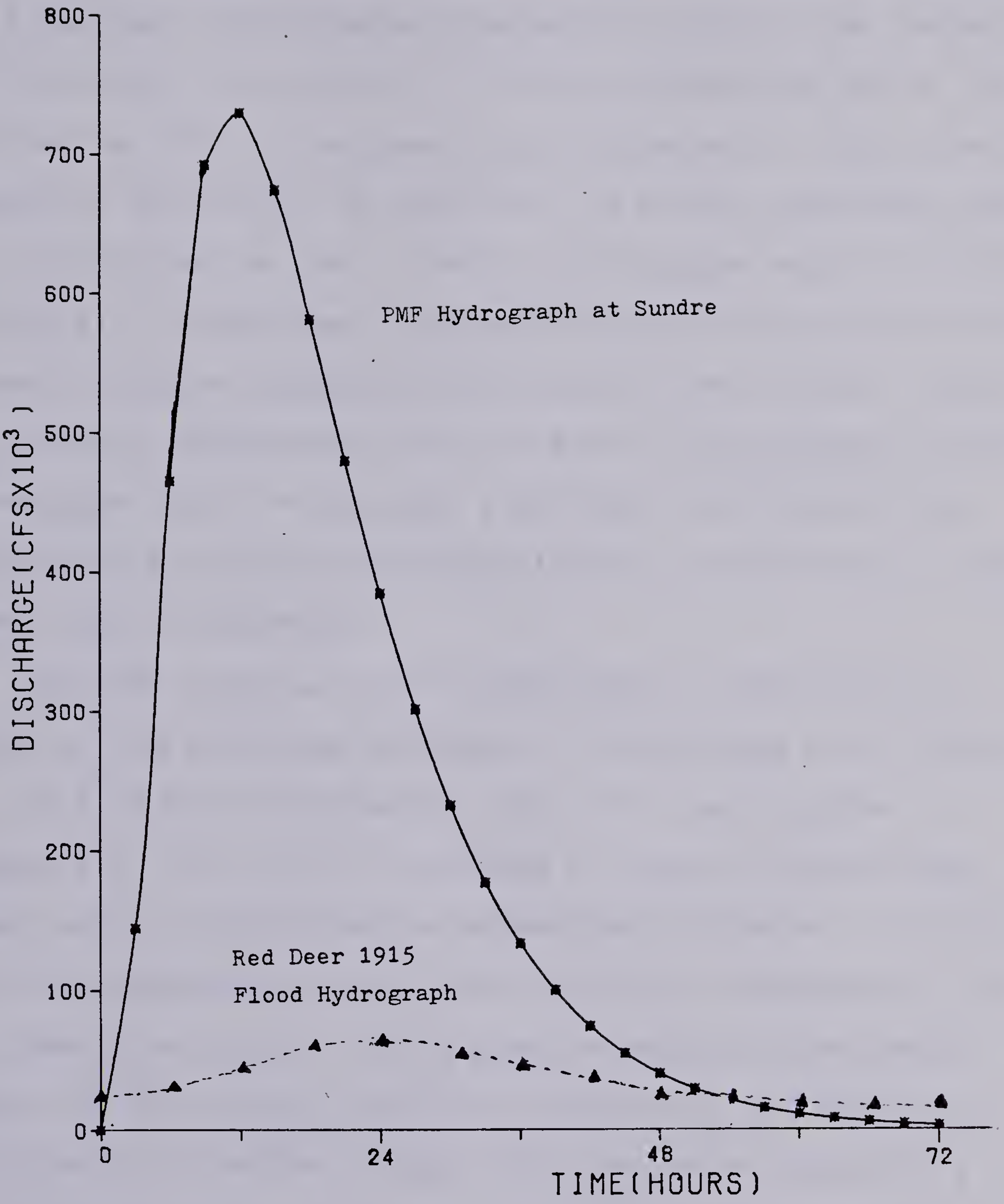

Figure 5.8. PMF Hydrograph at Sundre and the Largest Recorded Hydrograph at Red Deer.

recorded at Red Deer (drainage area of 11 600 km² or 4480 sq. mi.) occurred from 26 June to 2 July 1915 and resulted in a maximum instantaneous discharge of 1933 m³ per second or 68 250 cfs (a ratio of 0.17 m³ per second per km² or 15.2 cfs per sq. mi.), a maximum daily discharge of 1586 m³ per second or 56 000 cfs (a ratio of 0.14 m³ per second per km² or 12.5 cfs per sq. mi.), and a record gauge height of 5.8 m (19.05 ft.) at Red Deer. Historical reconstruction of this record rainstorm suggests that probably the rainfall (which is unknown) associated with this event also produced record hydrograph flows in the entire Red Deer River Basin, but because of a lack of recording stations in the basin at that time, this is uncertain.

The PMF results can be summarized by comparing the ratio of the discharge divided by the drainage area (cfs per sq. mi.) to the drainage area (sq. mi.), as is shown in Figure 5.9. This ratio (discharge divided by the drainage area) can be interpreted as normalized discharge. In Figure 5.9, the recorded and computed results are compared for the Red Deer River Basin. The largest recorded instantaneous flows for the various recording stations in the basin are depicted by triangles. These flows can be enveloped by a relationship of the form $Q = 1000\ A^{0.5}$, where Q is the instantaneous maximum discharge (cfs) and A is the drainage area (sq. mi.). Also shown in the figure are the PMF estimates obtained from the SSARR Model for some of the watersheds (displayed by stars).

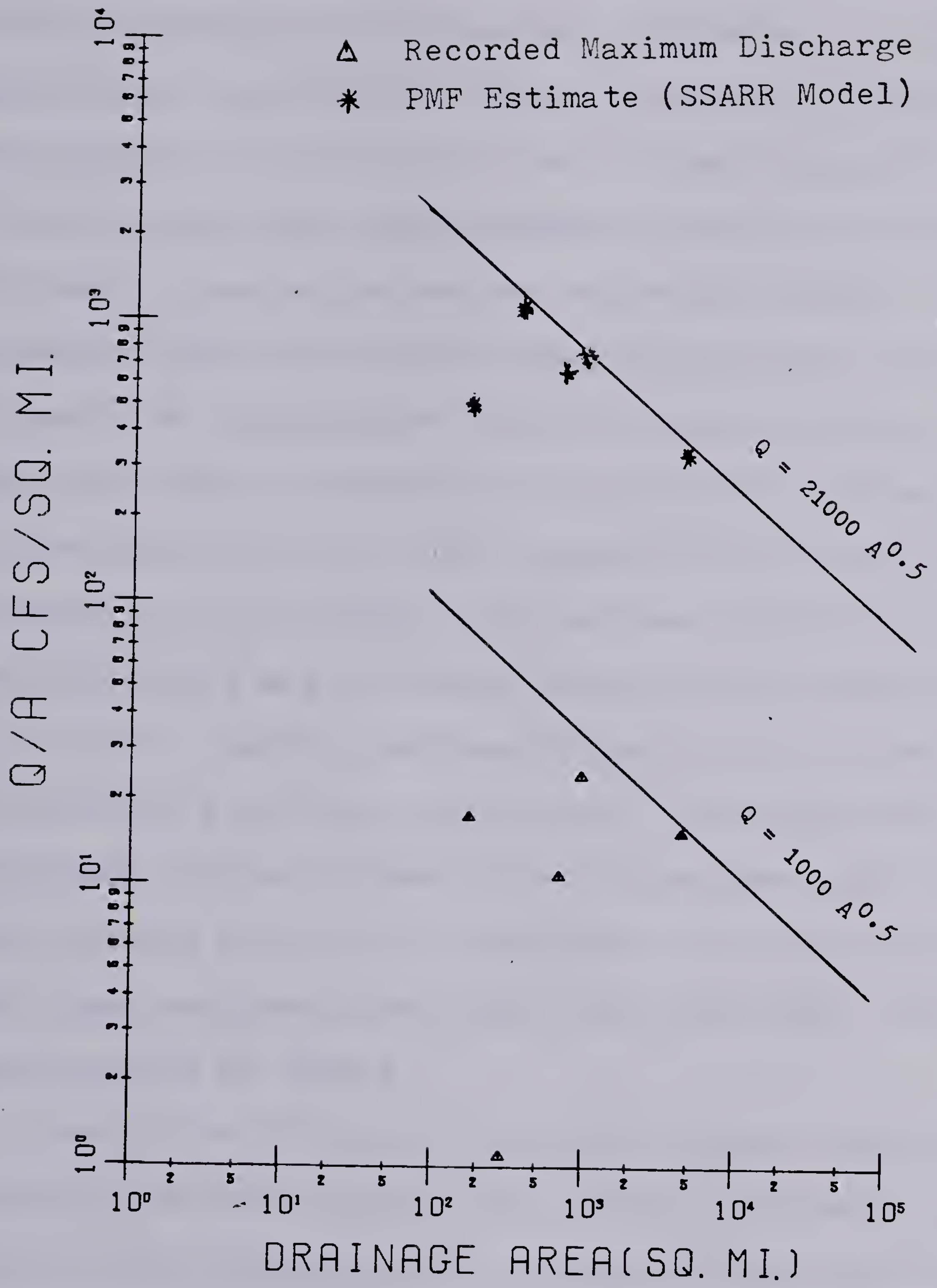

Figure 5.9. Variation of the Discharge-drainage Area Ratio with Drainage Area.

5.2.7 Sensitivity of SSARR Model.

The sensitivity of the SSARR Model to parameter changes for PMP loading are discussed next in terms of a number of hypothetical simulations. Because the model allows the user considerable flexibility to simulate hydrologically different watersheds, good judgment and logic are essential to properly develop parameters and relationships. Various parameters and relationships were examined for the watershed at Sundre on the Red Deer River. The sensitivity of the model was tested by holding all parameters constant at maximum conditions and then changing only the desired parameter or relationship. The maximum conditions used in the simulations are a 24-hour precipitation loading of 340 mm (13.4 in.) (with a maximum intensity of 30.5 mm (1.2 in.) per hour) on a 2471 Km^2 (954 sq. mi.) drainage area. Other watersheds in the Red Deer River Basin were also tested, but those results are not included here since they showed the same shape and peak discharge in the resultant hydrograph as the watershed at Sundre.

One of the first relationships examined was the three-parameter SMI-ROP relationship. This relationship for natural flows determines the volume of runoff and affects the shape of the hydrograph. Two quantities seem to be important: the SMI value and the average intensity of the loading. The SMI can be any value from 0 to 127 mm (5 in.) depending upon the antecedent conditions. The upper value was chosen as an arbitrary upper limit for the tests

conducted in this work because others (U. S. Army Corps of Engineers, 1972; Alberta Environment, 1980) have used this value. For PMP loading, because saturated soil conditions are assumed, the SMI is assigned the upper limit value of 127 mm (5 in.). Using this upper value a number of different average intensities were tested. The results were identical to those shown in the PMF hydrograph depicted in Figure 5.8. This was because of the allocation of the total flow to surface flow in the surface-separation relationship. Hence, for upper limit values of SMI, the SMI-ROP relationship has no effect on PMF estimates in the SSARR Model.

A second relationship that was tested was the daily evapotranspiration. Values of evapotranspiration from 0 to 10 mm (0.4 in.) per day were used, and these had no effect on the PMF hydrograph. Furthermore, the resultant hydrographs were identical to that shown in Figure 5.8. Although this index may be important for long-term simulations, it is not believed to be critical for PMP loading.

A third relationship investigated was the surface-subsurface separation curve. For PMF estimates this relationship was represented by the 1-to-1 broken line in Figure 5.4 and corresponded to saturated soil conditions and maximum runoff. For natural flow conditions, such a curve would rarely be attained. Instead, for those conditions the expected curve would be similar to the solid line curve shown in Figure 5.4 and is usually determined by

calibration, through a trial-and-error procedure. This relationship can be examined hypothetically for a water loading with different surface-subsurface curves, which will provide insight into the effects of these curves on the shape and peak discharge of the resultant hydrograph. The relationship was examined by decreasing the surface curve with each simulation. As the surface component of the relationship is decreased, the subsurface component is increased, since the total sum of surface and subsurface is constant. Three different surface-subsurface curves were tested, and the resulting hydrographs are illustrated in Figure 5.10. The effects of varying the surface-subsurface separation relationship on streamflow depends on the magnitude of the surface to subsurface components. When most of the flow is allocated to surface and little to the subsurface flows, a higher and earlier peak results in the hydrograph. The largest peak in magnitude occurs when 100% is allocated to surface flow and 0% to subsurface flow, as is the case for PMP loading (Curve A). The other extreme is allocating 100% of the flow to the subsurface and 0% to surface, and a straight-line hydrograph results. In between these two extremes are the curves depicted by B and C, equivalent to what may be called unsaturated soil conditions. The variation of the surface-subsurface separation relationship would only be important to PMF estimates if unsaturated soil conditions exist.

In addition to the three relationships above, a number

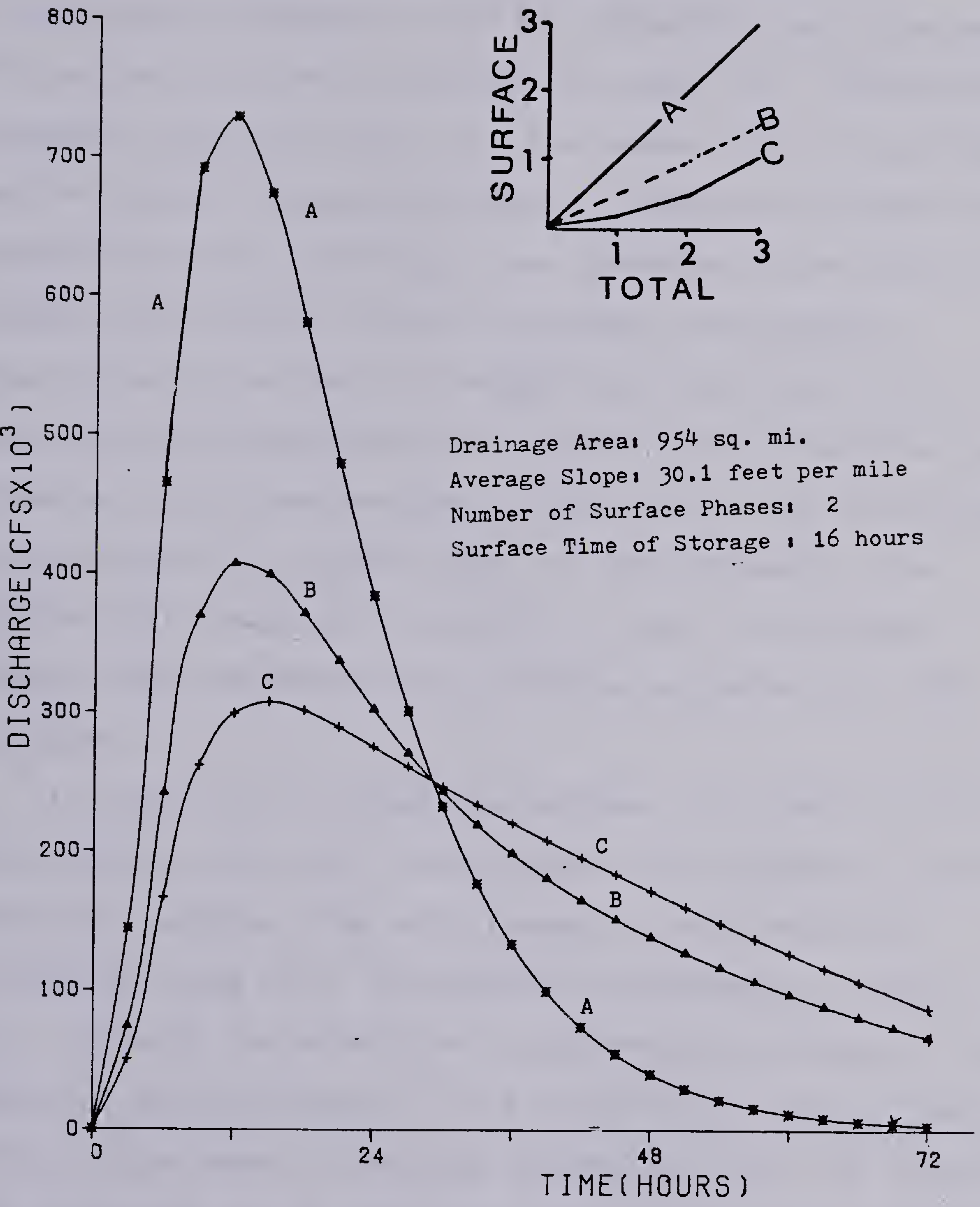

Drainage Area: 954 sq. mi.
Average Slope: 30.1 feet per mile
Number of Surface Phases: 2
Surface Time of Storage : 16 hours

Figure 5.10. Effect on Streamflow of Varying the Surface-Subsurface Separation Relationships.

of routing parameters were examined. The effects on the outflow hydrograph shape and timing response can be observed by changing the number of routing phases for each component of flow and the time of storage per phase (T_s). Because two parameters are involved (i.e., the number of routing phases and the time of storage per phase), there are a number of possibilities for examining these parameters. One way to display any possible effect is to keep one parameter constant while varying the second, and vise versa. The simulations discussed here are hypothetical, since the two parameters are predetermined by computation and calibration, which results in a fixed value for each parameter. The hypothetical simulation is useful in that it provides insight into the sensitivity of these parameters for PMF estimates.

In the first of these simulations, all coefficients and relationships were kept constant while the number of routing phases for surface flow was allowed to vary from the calibrated value of 2. The results, displayed in Figure 5.11, indicate two effects arising from an increase in the number of routing phases: (a) a delay in the time of peaking and (b) a decrease in the peak discharge. Thus the largest peak discharge can be obtained using the smallest possible number of phases. In all of these examples the total volume of runoff was the same.

In the second simulation, the time of storage per phase (T_s) was varied from the 16-hour calibrated value. This

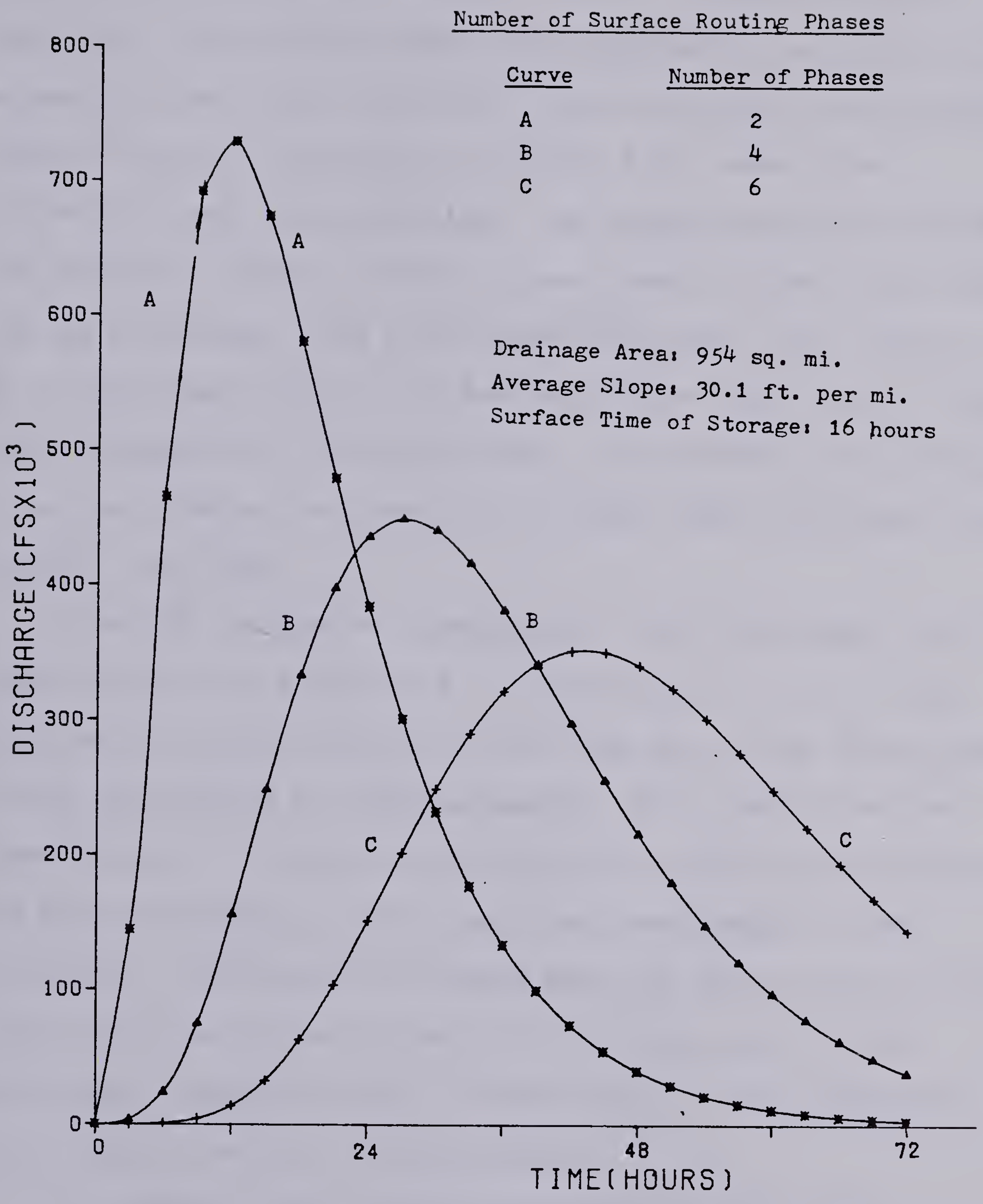

Figure 5.11. Effect on Streamflow of Varying the Number of Surface Routing Phases.

variation can also result in significant changes in timing and in the hydrograph characteristics. To examine this parameter, the surface phase time was varied while all other parameters were kept constant. The variation of the surface phase time is illustrated in Figure 5.12, where two different times were selected. The values selected varied by 50% from the 16-hour surface phase time. Sixteen hours was the surface phase time calibrated for a 2471 km^2 (954 sq. mi.) watershed area in the Red Deer River Basin and is the value suggested for PMF estimates. As expected, an increase in surface phase time results in lower peak discharges and greater lag times.

The last parameter examined for the SSARR Model was the coefficient n in Equation 5.1. The value of n (0.13) was obtained from calibration for the Red Deer River Basin and can be considered a fixed parameter. This coefficient was examined for $n = 0.26$ to determine the effect on the shape and peak discharge of the resultant hydrograph for PMF estimates. The resultant hydrographs for both values of the coefficient were nearly the same in shape and in peak discharge, suggesting that changes only in this parameter are insignificant for PMF estimates.

In summary, for a given watershed area and mass precipitation distribution with the same intensity loading and for saturated soil conditions, two parameters affect the PMF peak discharge for PMP loading: the number of surface routing phases and the time of storage per phase. These two

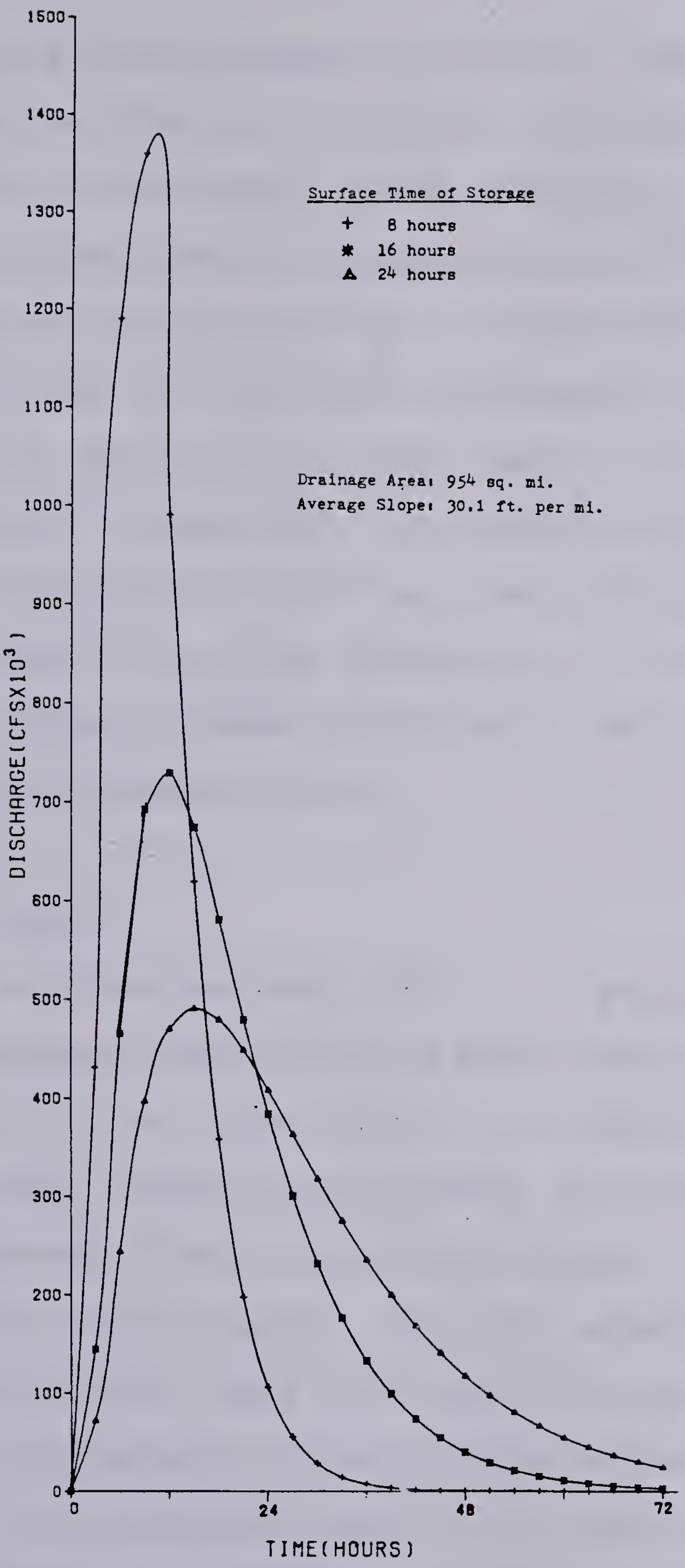

Figure 5.12. Effects on Streamflow of Surface Time of Storage.

parameters are interrelated (Figure 5.5), and an effect on one produces an effect on the other. The other relationships examined have little effect on PMF estimate in the SSARR Model. The values used and suggested for a PMF estimate for a 24-hour precipitation loading of 340 mm (13.4 in.) on a 2471 km^2 (954 sq. mi.) drainage watershed at Sundre in the Red Deer River Basin are: (1) SMI equal to 127 mm (5 in.) for all rainfall intensities, (2) evapotranspiration value of 0, (3) 100% of the total flow to be allocated to surface flow, (4) number of routing phases is 2, (5) the time of storage per phase is equal to 16 hours, and (6) the coefficient n is equal to 0.13.

5.3.0 HYMO Model

HYMO (Williams and Hann, 1973) is a problem-oriented computer language consisting of a main program and 16 subroutines that when combined for watersheds result in a hydrologic model, hence the name HYMO. This model can be used for planning flood prevention projects, forecasting floods, and research studies. The HYMO language was designed to transform rainfall data into runoff hydrographs and to route these hydrographs through streams and valleys or reservoirs. The procedures used in this model were selected by Williams and Hann (1973) because of their accuracy, general applicability, practicality of inputs, and computational efficiency.

The HYMO language is based on hydrologic techniques

suggested by the Soil Conservation Service (SCS, 1969) for the prediction of flood hydrographs on ungauged basins. The main features in this model include (a) ability to subdivide the drainage area into various subareas, (b) ability to account for the effect of various land uses, (c) ability to estimate the time of concentration for each subwatershed, which in turn is a function of the flood travel time, (d) ability to account for the effects of channel storage in each river reach, and (e) ability to produce flood hydrographs at any point in the watershed. The main conceptual and computational features include the peak flow rates (q_p) and the unit hydrograph. The peak flow rates from individual watershed subareas can be computed by the equation

$$q_p = \frac{BAQ}{t_p} \qquad (5.2)$$

where q_p is the peak flow rate, B is a statistically based watershed parameter computed within the model as a function of watershed characteristics, A is the watershed area (sq. mi.); Q is the volume of runoff (in.), and t_p is the time to peak (hours). The unit hydrographs are divided into three parts for computation (Figure 5.13).

In the first part (from the beginning of the rise to the inflection point, t_o), the hydrograph is computed by the two-parameter gamma distribution equation

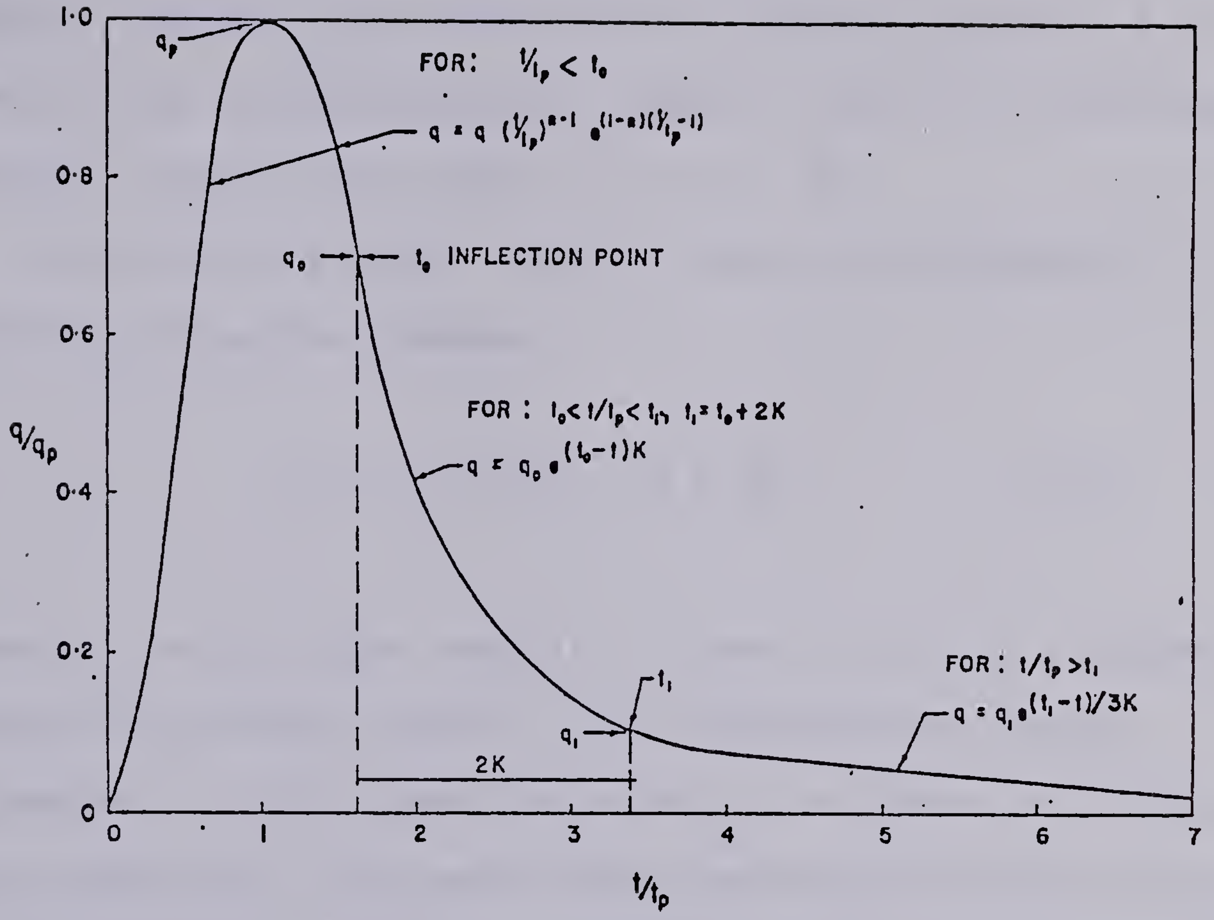

Figure 5.13. Dimensionless Unit Hydrograph Used in the HYMO Model (After Williams and Hann, 1973).

$$q = q_p \left(\frac{t}{t_p}\right)^{n-1} e^{(1-n)(t / t_p - 1)} \qquad (5.3)$$

where q is the flow rate at time t, q_p is the peak flow rate, t_p is the time to peak (hours), and n is a dimensionless parameter determined from watershed characteristics.

For the second part, from t_o to t_1, the recession depletion equation is used to compute the hydrograph:

$$q = q_o \, e^{(t_o - t) / K} \qquad (5.4)$$

where q is the flow rate at the inflection point, t_o is the time at the inflection point (hours), and K is the recession constant (hours) such that $t_1 = t_o + 2K$.

In the third part, from t_1 to ∞, the recession depletion equation becomes

$$q = q_1 \, e^{(t_1 - t) / K_1} \qquad (5.5)$$

where q_1 is the flow rate at t_1, and $K_1 = 3K$ is a second recession constant (hours). The dimensionless shape parameter, n, is a function of K/t_p, as shown in Figure 5.14; therefore, the entire unit hydrograph can be computed if K and t_p are known. To compute K and t_p for ungauged watersheds, HYMO uses the equations

$$K = 16.1 \, A^{0.24} \, S^{-0.84} \qquad (5.6)$$

and

$$t_p = 6.54 \, A^{0.39} \, S^{-0.50} \qquad (5.7)$$

where A is the watershed area (sq. mi.), and S is the difference in elevation in feet, divided by flood-plain distance in miles, between the watershed outlet and the most distant point on the watershed. Calculating the peak flow using equation 5.2, the volume of runoff (Q) in inches is computed by utilizing the SCS rainfall-runoff relationship

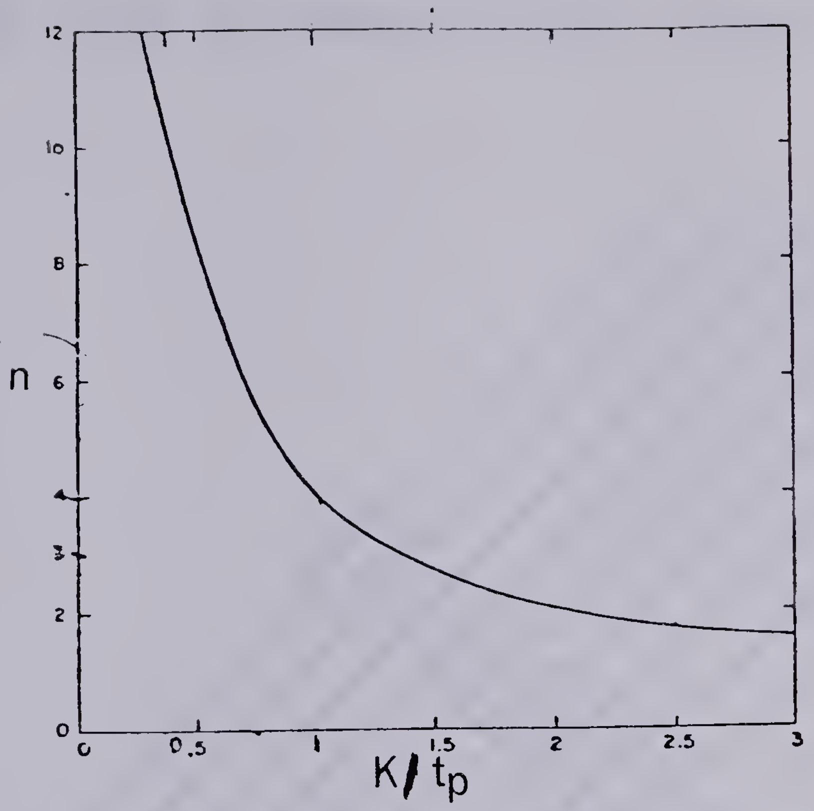

Figure 5.14. Relationship Between Dimensionless Shape Parameter n and Recession Constant/Time to Peak (After Williams and Hann, 1973).

(Soil Conservation Service, 1969). This can be obtained by the following equations

$$Q = \frac{(P - 0.2\ S)^2}{P + 0.8\ S} \quad (\text{for } P > 0.25) \qquad (5.8)$$

and

$$S = \frac{1000}{CN} - 10 \qquad (5.9)$$

where P is the rainfall (inches), S is the rainfall retention parameter, and CN is the soil-cover complex number determined from actual soil types and land cover for each subwatershed. The SCS rainfall-runoff relationship is

expressed by a set of numbered curves (Figure 5.15). In the

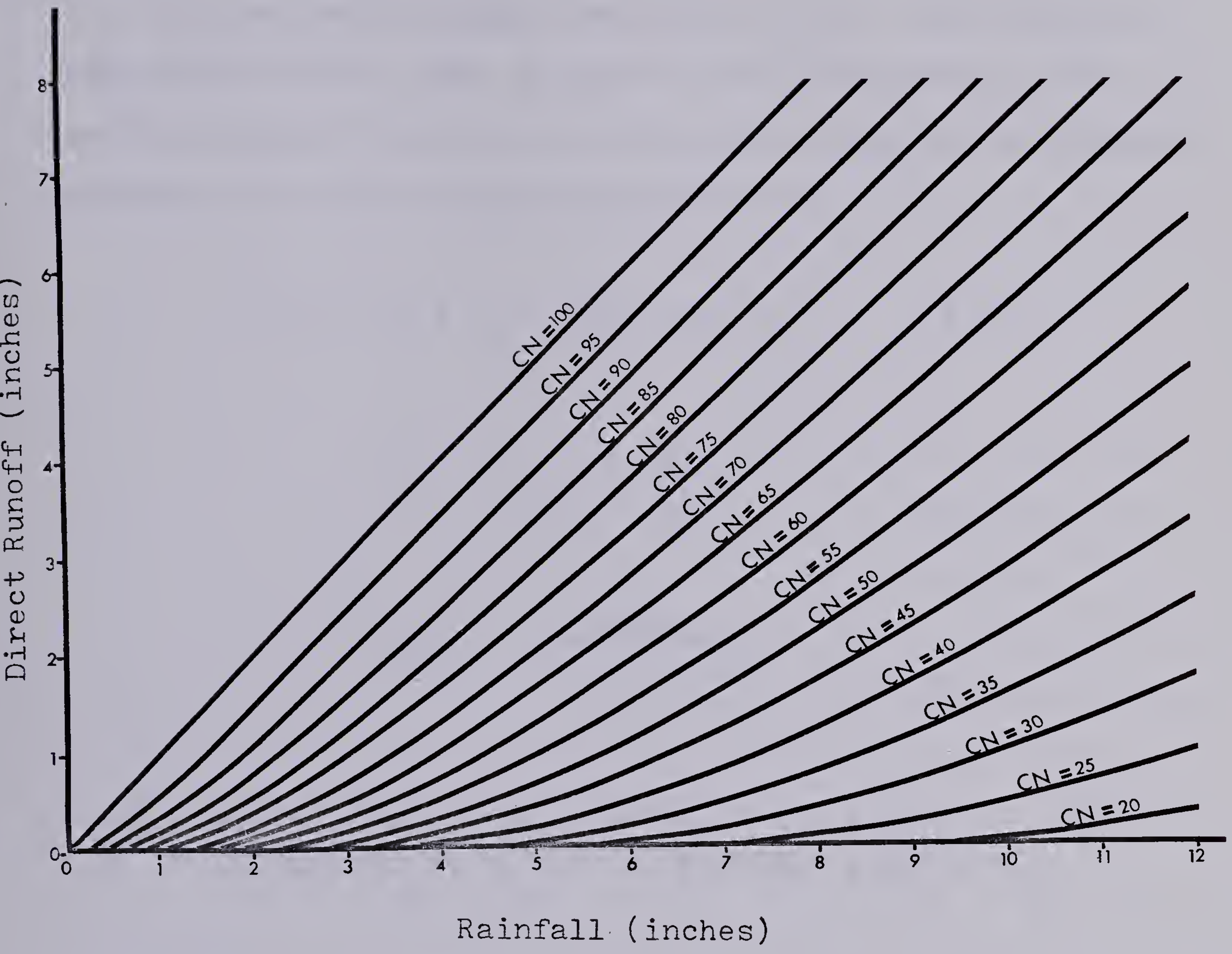

Figure 5.15. Graphical Solution of Rainfall-runoff Equation (After Soil Conservation Service, 1969).

SCS method the change in S (actually in CN) is based on the soil antecedent moisture condition, determined by the total rainfall preceding the storm. For best estimates of peak flood flows, the watershed should be subdivided into subcatchment areas, each of which is homogeneous with respect to soil type, topography, vegetation cover, land

use, and drainage pattern.

The variable storage coefficient (VSC) flood-routing method (Williams, 1969) is used in the HYMO method. This method uses an iterative solution and is free of convergence problems. The VSC routing equations are

$$O_2 = C_2 \left(I_a + \left(\frac{1}{C_1} - 1\right) O_1 \right) \qquad (5.10)$$

$$C_1 = \frac{2\,\Delta t}{2\,T_1 + \Delta t} \qquad (5.11)$$

$$C_2 = \frac{2\,\Delta t}{2\,T_2 + \Delta t} \qquad (5.12)$$

$$T_1 = \left(\frac{L}{1800\,(V_{I_1} + V_{O_1})}\right) \times \left(\frac{L \times SLP_o}{L \times SLP_o + D_{I_1} - D_{O_1}}\right)^{1/2} \qquad (5.13)$$

$$T_2 = \left(\frac{L}{1800\,(V_{I_2} + V_{O_2})}\right) \times \left(\frac{L \times SLP_o}{L \times SLP_o + D_{I_2} - D_{O_2}}\right)^{1/2} \qquad (5.14)$$

where I is the inflow rate (cfs), O is the outflow rate (cfs), I_a is the average inflow rate (cfs), C is the storage coefficient, T is the travel time through the reach (hours), L is the reach length (ft.), V is the velocity (ft. per second), SLPo is the normal slope, and D is the depth (ft.). In the above equations the subscripts 1 and 2 refer to the beginning and end of the time interval, Δt. Subscripts I_1 ,I_2 ,O_1 , and O_2 are also used in conjunction with the normal depth, D, and velocity, V, to define the spatial and temporal values of these quantities. Since T_2 and C_2 are dependent upon O_2 , an iterative technique is required to solve the routing equations. In Equation 5.10, I_a and O_1 are known, and C_1 can be computed from Equation 5.12. Hence only O_2 and C_2 are unknown. O_1 can be used as a first approximation of O_2 . The normal depth and velocity for the approximate value of O_2 are entered into Equation 5.14 for computing T_2 . Then Equation 5.11 is used to compute C_2 . The second approximation of O_2 is obtained from Equation 5.10. This iterative process continues until there is a difference of about 0.1% or less between successive O_2 values.

HYMO uses the storage-indication method to route floods through reservoirs. This method has been widely used and accepted because it is practical and accurate. The model requires rating curves along a valley to adequately describe the hydraulics of the stream and valley. The model also uses Manning's equation (Viessman et at., 1977) to compute the

normal flow-rating curves that are used in the VSC flood-routing method. A normal flood plain slope is determined for each valley section by plotting a profile of the flood plain. The normal channel slope is determined by plotting a profile of the flood plain with channel distances. Since flow-rating curves are needed in this model but are not always available, this tends to make the HYMO Model less effective. Also, the user needs to describe the valley section to the computer, which may not always be possible. This model has an advantage in that it is a user-oriented model, with a smaller data requirement than the SSARR Model. Because of its simplicity, however, it lacks powerful methods for sophisticated hydrological simulation, including snowmelt computations.

5.3.1 PMF Estimates from the HYMO Model

A PMF estimate can be computed with the HYMO Model by (1) assigning the curve number (CN) a value of 100, which represents saturated soil conditions and (2) distributing the PMP loading to produce the maximum discharge. Snowmelt can be simulated by adding the melt rate to the precipitation mass distribution. The precipitation distribution can be specified in the model by the time period (DT) and the mass distribution. To investigate the choice of the time period, three different time periods were tested for a 24-hour water loading of 645 mm (25.4 in.) over a 2471 km^2 (954 sq. mi.) watershed area with a slope of 5.69

m per km (30.1 ft. per mi.) in the Red Deer River Basin. The water loading consisted of a PMP loading of 340 mm (13.4 in.) and a snowmelt of 305 mm (12 in.). The precipitation loading of 340 mm (13.4 in.) is distributed at a maximum intensity of 30.5 mm (1.2 in.) per hour for 11 hours. The resultant PMF hydrographs are depicted in Figure 5.16 for DT = 1, 3, and 6 hours. For the different DT values the results show only a slight difference in the shape of the hydrograph and in the peak discharge. Hence, using a time period of 1, 3, or 6 hours will result in comparable hydrographs and peak discharges. Because the largest peak discharges were obtained with the 1- and 3-hour time periods, these periods were used in analysis in this work.

5.3.2 Sensitivity of the HYMO Model

In the HYMO Model a number of parameters are needed for simulation of the PMF hydrograph, and these quantities are either recorded, measured, or calculated. For a particular watershed, specific values of these parameters are obtained that are called fixed quantities, that is, they do not vary within measuring tolerance. Even though these parameters are fixed, it is still possible to examine the model's sensitivity to parameter variation by considering hypothetical simulations. These simulations are advantageous in that they can provide insight into variations of the magnitude of the peak discharge. The same watershed as was described in sections 5.2.6 and 5.3.1 is used here for the

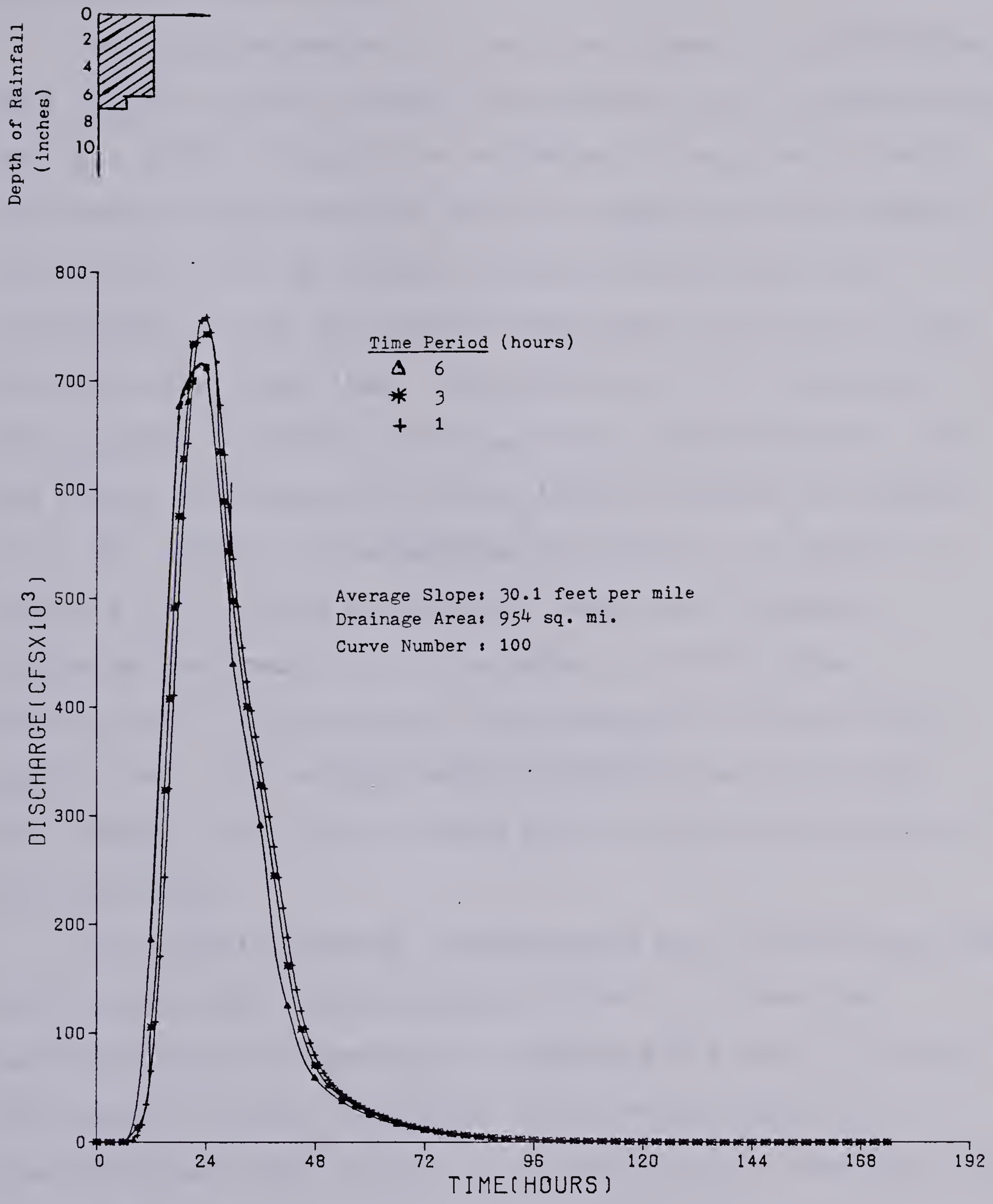

Average Slope: 30.1 feet per mile
Drainage Area: 954 sq. mi.
Curve Number : 100

Figure 5.16. Variation of the Time Period for a 24-hour Water Loading of 645 mm (25.4 in.) over a 2471 km² (954 sq. mi.) Watershed Area in the Red Deer River Basin.

hypothetical simulations.

The first parameter is the curve number. The HYMO Model uses the SCS rainfall-runoff relationship (Soil Conservation Service, 1969) to obtain an estimate of the direct runoff, and hence an approximation of CN is required in the model. A value of CN = 100 gives the maximum direct runoff and corresponds to the soil being saturated. For natural flows, CN is usually lower than 100; therefore, it is important to investigate the effect of using lower values than CN = 100. The effect is examined by using three different CN numbers (100, 80, and 65, corresponding to curves A, B, and C in Figure 5.17). Curves A, B, and C show that the peak discharge decreases with a decrease in the CN value (equivalent to progressing from saturated to unsaturated conditions). The maximum peak discharge occurs with CN = 100; hence, this value is used for the other simulations of the HYMO Model.

The second parameter investigated was the average slope of the watershed, represented by K and t_p. These two quantities can be computed by equations 5.6 and 5.7 in the HYMO Model. For any watershed, the average slope is a predetermined fixed value. It is possible to investigate the effect of this fixed value on the PMF estimate by considering hypothetical simulations in which all parameters are kept constant while the average slope is varied with each simulation. To test any possible effect, two average slopes (ranging from 0.95 to 5.69 m per km) were simulated

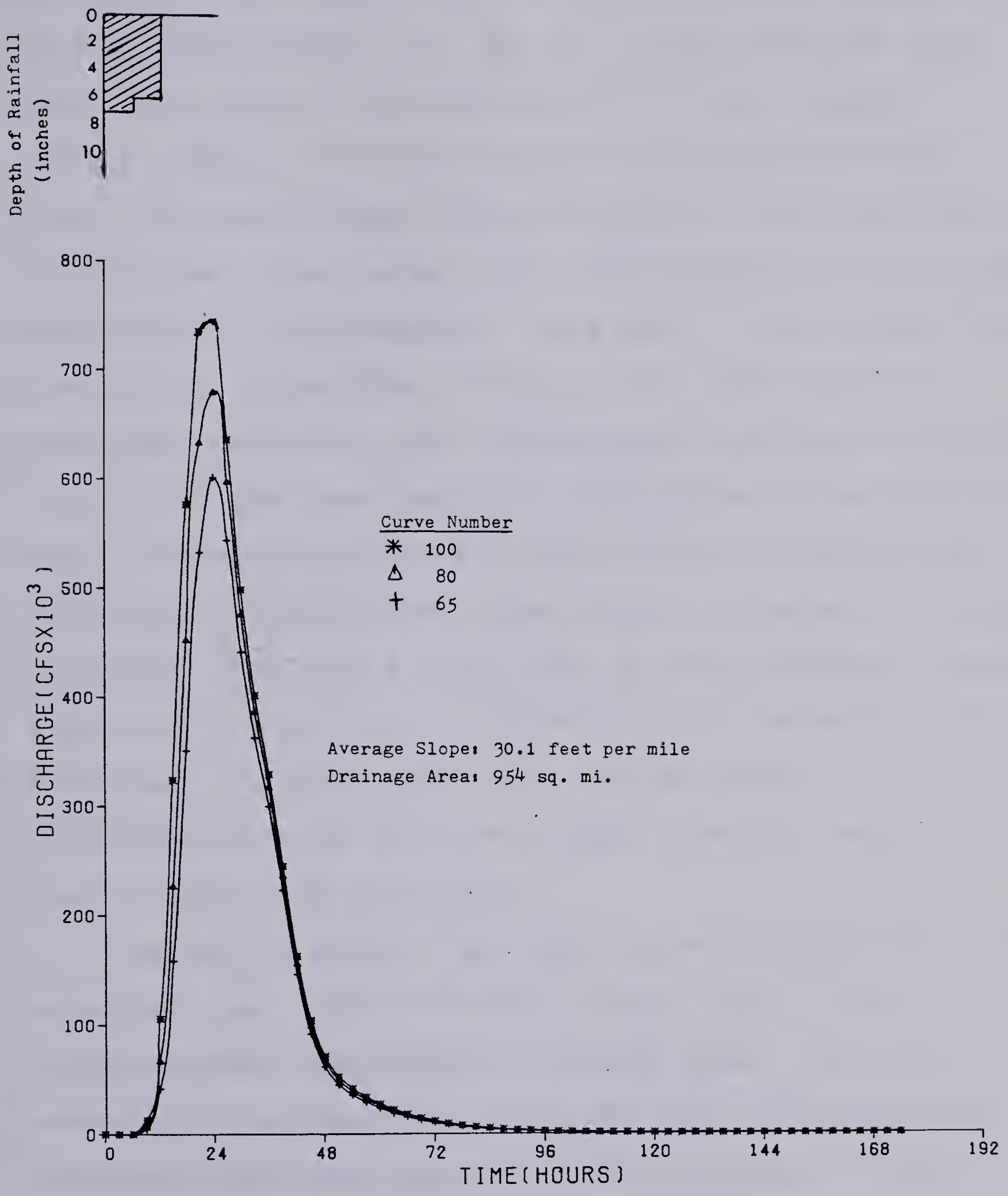

Figure 5.17. Effect on the Resultant Hydrograph by Variation of the Curve Number in HYMO Model.

for the 2471 km^2 (954 sq. mi.) watershed with average slope of 5.69 m per km (30.1 ft. per mi.) in the Red Deer River Basin. The 2471 km^2 watershed has one of the steepest average slopes of the watersheds in the Red Deer River Basin. Thus the average slopes selected in the simulation are arbitrary lower values than the estimated value of 5.69 m per km for this watershed. The effect of the hypothetical simulations is depicted in Figure 5.18. The resultant hydrograph shows that the largest peak discharge coincides with the largest average slope, and similarly the smallest peak discharge coincides with the smallest average slope. Increases in the average slope produce increases in the peak discharge. This figure shows that in the HYMO Model, average slope not only affects the shape but also the peak of the hydrograph. Two watersheds with similar areal characteristics but different slopes therefore would not have the same peak discharge.

The third parameter was the area of the watershed. The watershed area, similar to the average slope, is a predetermined fixed value in the HYMO Model. For this parameter it was desirable to investigate the effect the watershed area might have on the PMF estimate. In this investigation the watershed at Sundre was again used, and two different watershed areas were hypothetically simulated, with all other conditions being the same. The results, as shown in Figure 5.19, indicate a logarithmic increase in area with peak discharge. Two watersheds with similar

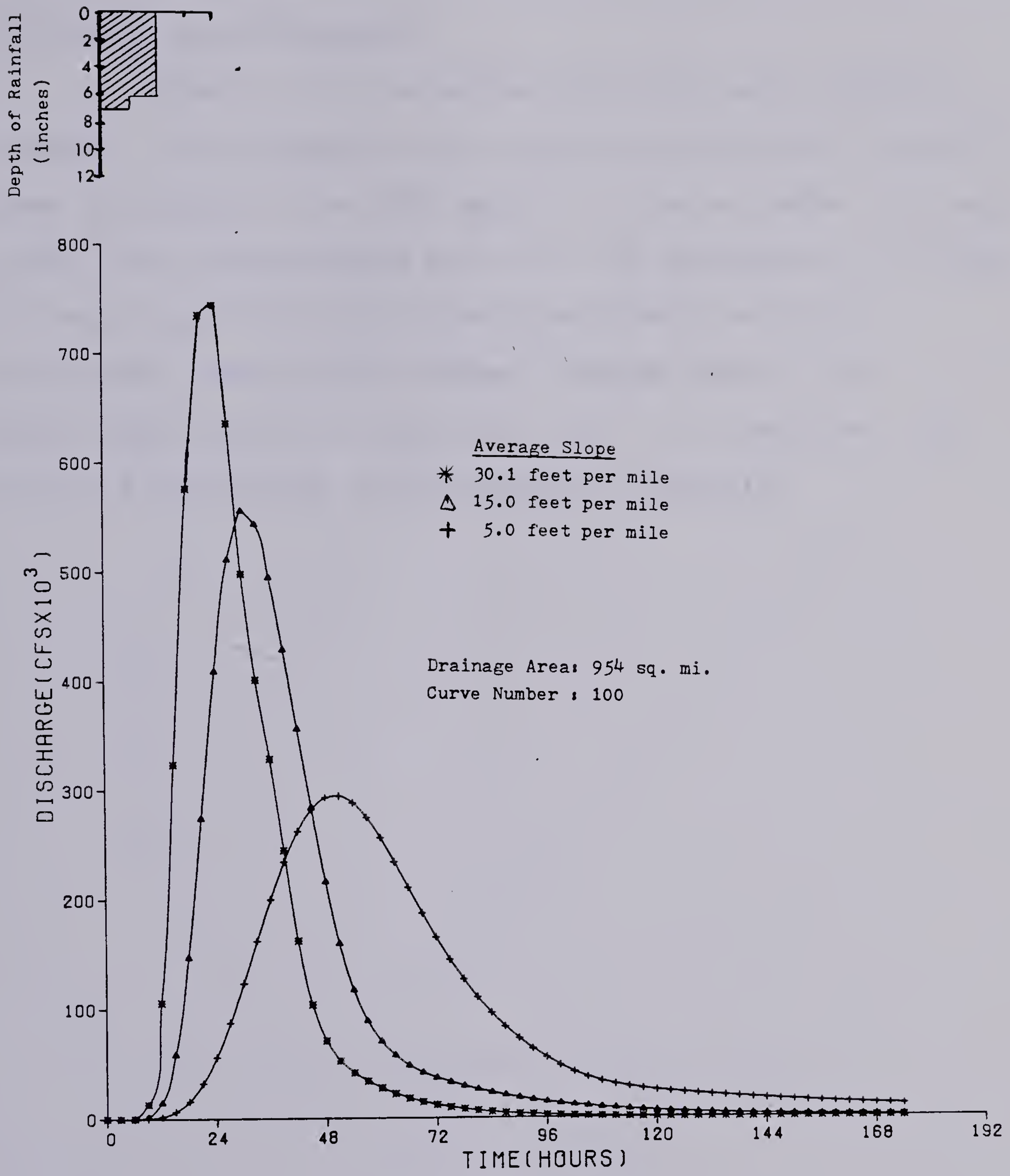

Figure 5.18. Effect of Average Slope of the Watershed on the Resultant Hydrograph.

watershed parameters but of different areas would also have different peak discharge.

In summary, for a watershed with the same intensity loading, three parameters can significantly affect the PMF peak discharge in the HYMO Model: the curve number, average slope, and the watershed area. For PMF estimates, all three of these parameters are fixed quantities, and once determined, they do not change. Because these fixed quantities affect the resultant PMF, it is important that they are determined as accurately as possible.

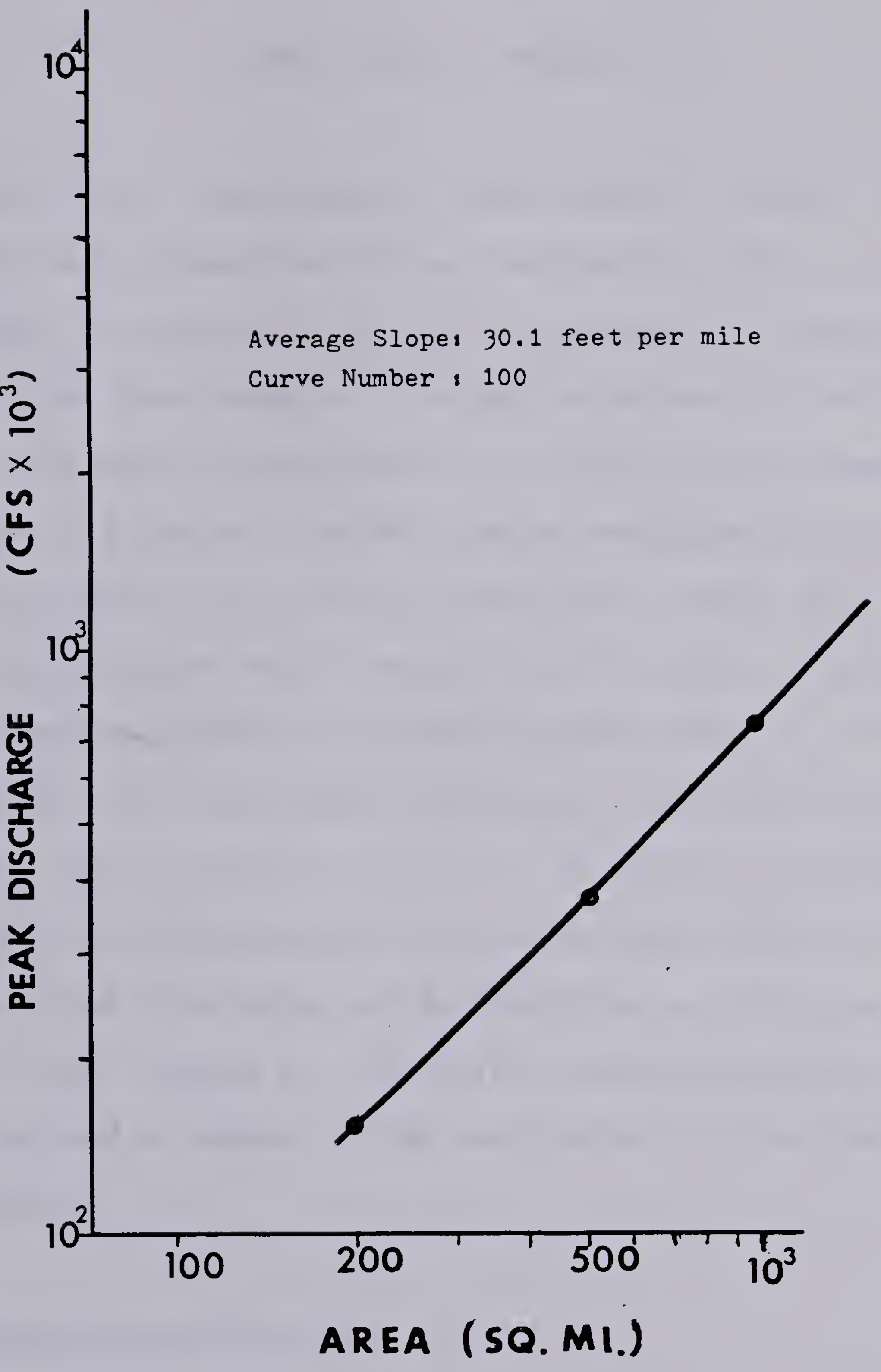

Figure 5.19. Area Versus Peak Discharge Relationship for PMF Estimates in the HYMO Model.

CHAPTER 6

COMPARISON OF MODELS

In the last two chapers, three models (TAPMF, SSARR, and HYMO) were presented for estimating the PMF for gauged watersheds. An objective in this study was to compare the results from these models in order to determine which model would be the most appropriate for estimating the peak PMF discharge in Alberta. The PMF can be regarded as an extreme event and probably has not yet occurred, hence only comparisons between model results can be made. A graphical approach was selected for comparing the results. In such comparisons, the normalized discharge (expressed as m^3 per second per km^2 or cfs per sq. mi.) is usually plotted against the drainage area of the watershed (km^2 or sq. mi.). The normalized discharge can be regarded as the discharge per unit area. Figure 6.1 presents recorded maximum discharges and a number of PMF estimates for the Red Deer River Basin.

6.1 Recorded Maximum Discharges

The available maximum recorded discharges are indicated by triangles in Figure 6.1. The enveloping curve, a curve in which all discharge values are equalled or exceeded, is commonly used in hydrological studies to identify a relationship between discharge and area. This curve is

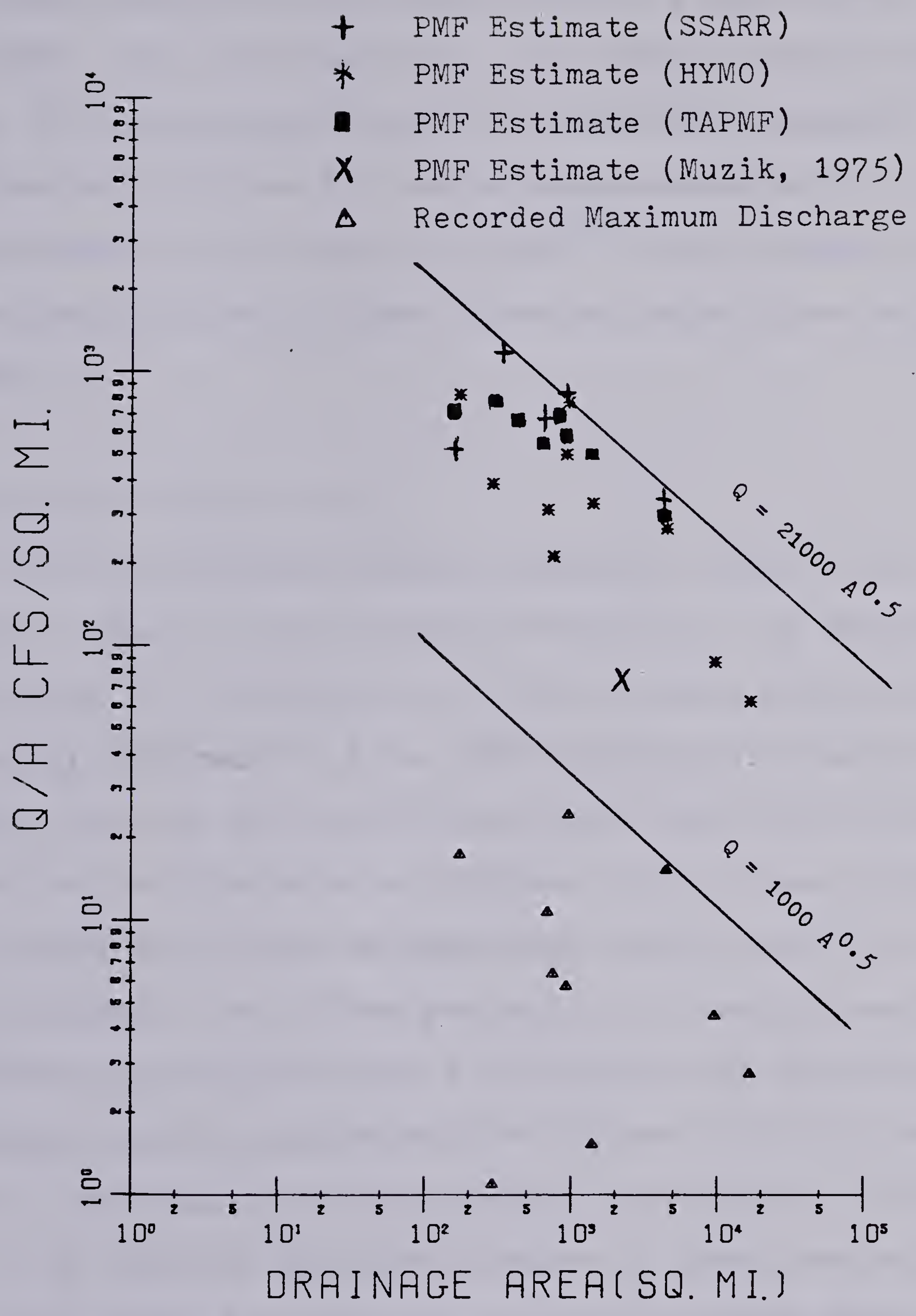

Figure 6.1. Comparison of Recorded Maximum Discharge and PMF Estimates for the Red Deer River Basin.

obtained graphically and may be either a curved or a straight line. For simplicity, the latter is most frequently used. The enveloping curve for the maximum recorded discharges in Figure 6.1 can be approximated by a relationship of the form $Q = 1000A^{0.5}$; this straight line coincides with the 100-year flood estimates given by Neill (1965).

6.2 Muzik's PMF Estimate

The PMF estimate obtained by Muzik (1975) (from Figure 1.15) at Raven in the Red Deer River Basin, is designated by the letter "X" in Figure 6.1. This estimate was obtained by imposing a 292 mm (11.5 in.) PMP loading distributed over a 48-hour period, so that 228 mm (9 in.) were distributed the first day and the balance of 64 mm (2.5 in.) was distributed the second day. Since no mass distribution was given with this estimate, the 228 mm precipitation loading was probably uniformly distributed over a 24-hour period (giving an average intensity equivalent to 9.65 mm (0.38 in.) per hour). The resulting instantaneous discharge of 4 814 m^3 per sec (170 000 cfs) obtained by Muzik is consistent with results obtained by the author using the SSARR Model (not presented here) for a similar average-intensity PMP loading at Raven in the Red Deer River Basin. It would seem from the literature (Muzik, 1975) that this estimate is strictly due to a PMP loading without the snowmelt loading.

6.3 PMF Estimates from TAPMF, SSARR, and HYMO Models

PMF estimates for a number of watersheds in the Red Deer River Basin as obtained from the three models (TAPMF, SSARR, and HYMO) are also presented in Figure 6.1. For a given drainage area, all three models produced greater normalized discharge than either the maximum recorded discharge or the PMF discharge estimate by Muzik (1975). The estimates from the three models seem to be comparable in value. Any differences can be attributed to the data required and the mathematical approximations used in the models. For example, in the HYMO Model a value of the average slope is used for simulation, but this parameter is not needed in the other two models. In the SSARR Model, snowmelt is estimated using the generalized snowmelt equation for a partly forested area, while in the HYMO and TAPMF models the snowmelt is simulated by adding the melt rate (Chapter 3) to the precipitation mass distribution. Another example of a difference between the models is in the technique used for routing of floods. In the HYMO Model, the variable storage coefficient flood-routing method (Williams, 1969) is used for routing of floods through streams and valleys (Section 5.3.0). This method accounts for the variation in water surface slope during a flood. In the SSARR and TAPMF models, routing is accomplished by solution of the basic storage equation in finite time periods for each increment of storage routing (Sections 4.2.6 and 5.2.3).

It was originally expected by the author that the results from the SSARR Model would be vastly different from those of the HYMO Model, since the former model is considered by many users to be a more superior hydrological model. The comparison in Figure 6.1 seems to suggest that, to the contrary, either of the three models can be used for PMF estimates. It was also believed that the computations of the shape of the watershed would significantly influence the PMF estimate. To test this concept the TAPMF Model was developed. Comparison of the results from the TAPMF Model with the results obtained from the other two models seems to dismiss this belief. Because the results were comparable, it is not practical (due to time and resource constraints) to estimate the PMF for the other watersheds in Alberta by using all three models. Instead, it was decided to use the model requiring the least amount of data and with minimal computational costs for estimating the PMF for all other watersheds in Alberta. The model that best met these requirements was the HYMO Model; hence this model was used for other simulations in this thesis. The HYMO Model requires less data, or at least data that are more easily accessible, for simulation than either the SSARR and the TAPMF models. The HYMO Model also costs approximately the same as the TAPMF Model and less than the SSARR Model for computer simulation.

6.4 Ratio of PMF to Maximum Recorded Discharge

A second comparison of the three models' results involved examining the ratio of the PMF estimate (Q_R) to the maximum recorded discharge (Q_{MR}) for each watershed. This ratio gives the number of times the PMF estimate is greater than the recorded discharge. Figure 6.2 shows that the PMF estimates from the HYMO Model are from over 10 to several 100 times the recorded values. The recorded discharges are the largest available values, and for many stations these values are small because large discharges have not yet been recorded due to the short record period.

For completeness, the PMF estimate from the HYMO Model was compared to recorded flows using a frequency analysis for the Red Deer River at the Red Deer station (Figure 6.3). This station was chosen because of its long record length compared to the other stations in the basin and also because this station had the largest recorded discharge in the Red Deer River Basin. A frequency analysis is usually displayed on Gumbel extreme-value logarithmic probability paper, where discharge data from a small period (say, 50 years or so) is extrapolated to return periods of thousands or millions of years. The plotting positions on Figure 6.3 were determined by ranking the extreme yearly values of the discharge, from the highest to the lowest ($m = 1,2,\ldots,n$) and calculating the probability (e.g., $P = m / (n + 1)$). In Figure 6.3, extrapolating a straight line through the points for the Red Deer station suggests that the PMF estimate of 21 041 m^3 per second (743 482 cfs) would have a return period of 9×10^6

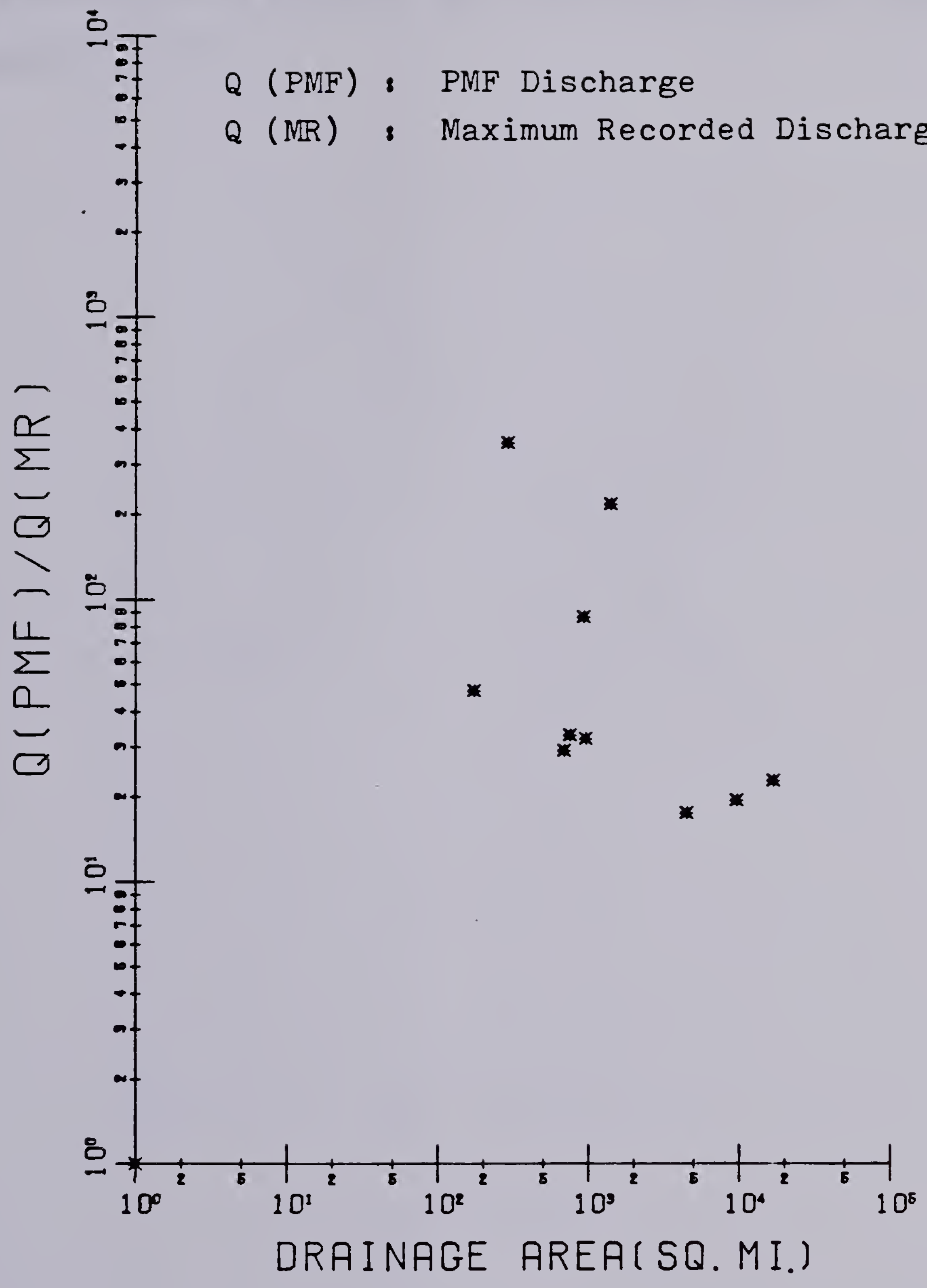

Figure 6.2. Ratio of the PMF to Recorded Discharge for Watersheds in the Red Deer River Basin.

years. As a general rule, however, a frequency analysis is not recommended by statisticians when the return periods to be estimated are greater than twice the record length (Pugsley, 1981).

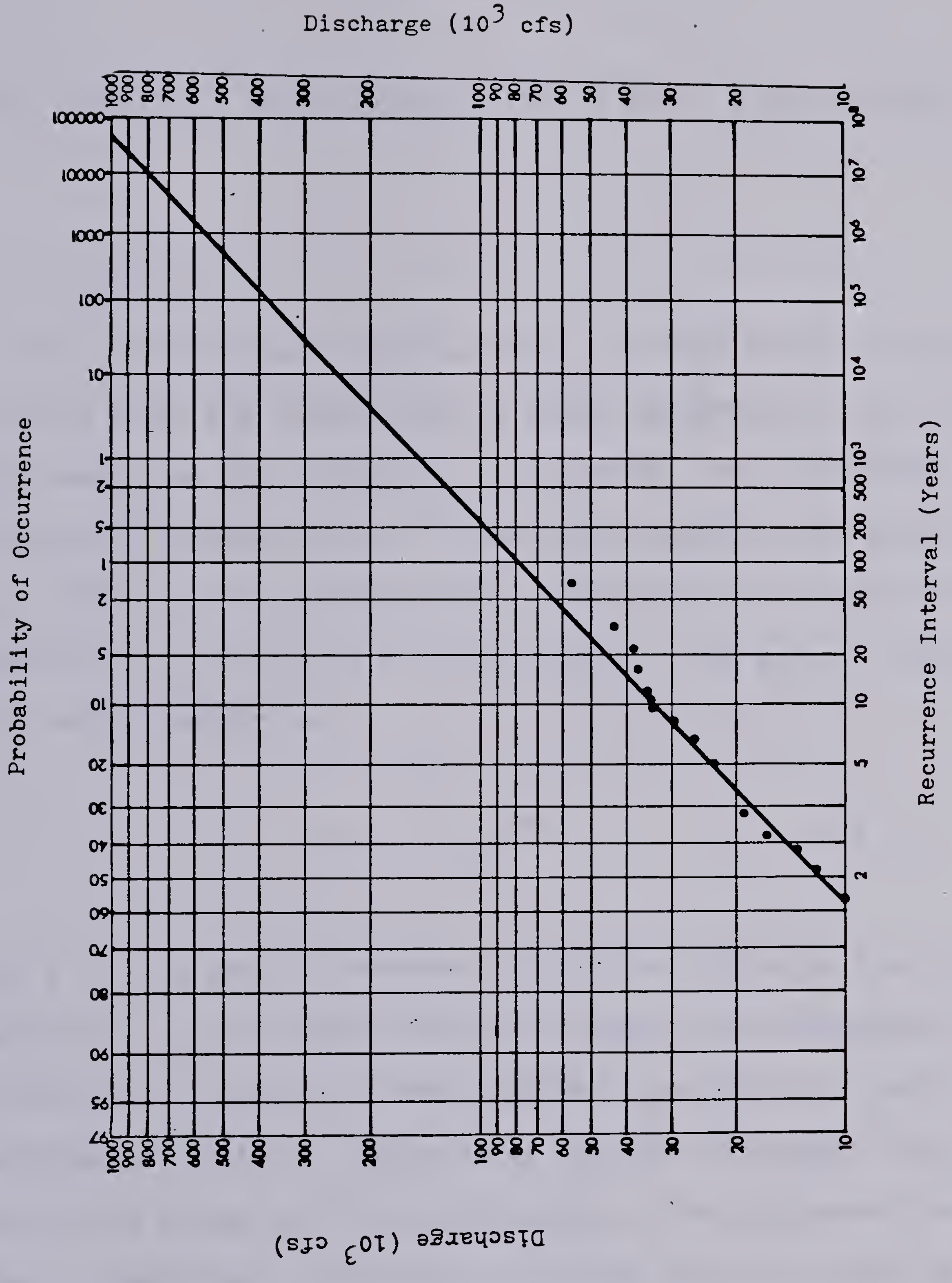

Figure 6.3. Frequency Analysis of the Annual Maxima Discharges of the Red Deer River at Red Deer.

CHAPTER 7

PMF EMPIRICAL RELATIONSHIPS FOR ALBERTA RIVER BASINS

7.1.0 Introduction

For hydrological applications a relationship is desired to relate peak PMF discharge to other parameters that can be easily measured or computed. A parameter that has been considered by many authors (numerous examples are given in Gray, 1970) is the drainage area. An equation using this parameter is called a Q-A relationship. The general form of a Q-A relationship is

$$Q = c_1 A^m \qquad (7.1)$$

where Q is the peak discharge, A is the drainage area of the watershed, c_1 is a coefficient believed to be dependent on various meteorological, hydrological, geological, and watershed parameters, and m is a constant exponent that governs the slope of the relationship. The exponent can be either a positive or a negative value, thus allowing an infinite number of combinations relating the discharge to area. Many different combinations have been suggested by various authors, and the two that are frequently advocated are the relationships with $m = 0.5$ and $m = 1.0$. These two forms of Equation 7.1 are examined using the HYMO Model for

gauged watersheds in the five major river basins in Alberta to define the coefficient c_1 for estimating the PMF. Once a coefficient is defined for gauged watersheds in a basin, it may be possible to use this value to obtain PMF estimates for ungauged watersheds in the same basin.

The work discussed in this chapter is divided into three sections. In the first section (7.2.0) the square-root approximation (or $m = 0.5$ in Equation 7.1) is examined. Some authors (e.g., McKay and Stichling, 1961) have suggested that this approximation defines the enveloping curve of the Q-A relationship. A multilinear regession analysis of peak discharge and area gave a value of $m = 0.51$ for Alberta. This value suggests that a square-root approximation may be a valid consideration to define the enveloping curve in the Q-A relationship.

In the second section (7.3.0) the second form of Equation (7.1) (called the Rational Formula) is investigated. The Rational Formula has been used for estimates of peak discharge. The formula is obtained by setting $c_1 = KCI$ and $m = 1.0$ in Equation 7.1 so that

$$Q = K\,C\,I\,A \qquad (7.2)$$

where Q is the peak discharge, K is the conversion constant (equivalent to 0.278 if Q is in m^3 per second and 645.3 if Q is in cfs), C is the runoff coefficient, and I is the average rainfall intensity lasting for period of time t

(time of concentration). Equation 7.2 is investigated (Section 7.3.0) to define the spatial distribution of the runoff coefficient for PMF estimates in Alberta river basins.

In the third section the normalized discharge and the runoff coefficient are examined. Because these vary within a basin and from basin to basin a further objective of this study was to investigate the spatial distribution of the normalized discharge and the runoff coefficient for the river basins in Alberta. This work is presented in Section 7.4.0.

7.2.0 PMF Relationship (m = 0.5)

The coefficent c_1 is believed by many authors (e.g., McKay and Stichling, 1961) to be a function of many variables, including the climate, geology, and hydrology of a given watershed. For PMF estimates, because of the requirement for saturated soil conditions, a number of these variables become less important and contribute little to the estimation of the coefficient. Slope and the intensity of the precipitation loading were identified as important parameters affecting the PMF estimates. Parameters such as maximum watershed width and length are to some degree covered by the $A^{0.5}$ approximation and hence are not expected to significantly influence the coefficient.

Three types of intensities can be identified: (1) the intensity for precipitation loading, (2) the intensity for

snowmelt loading, and (3) the sum of the precipitation and snowmelt loading, i.e., the intensity for water loading. Of these three, the intensity of the precipitation loading was selected for analysis in this work for simplicity. Either of the other two intensities could also have been used.

7.2.1 Relationship of Coefficient c_1 with Slope

A watershed characteristic that can be easily estimated is the average slope. The average slope of watersheds in the Red Deer River Basin was plotted against the coefficient c_1 (Figure 7.1) to investigate any possible relationship between the two parameters. The coefficient was calculated from Equation 7.1, using the PMF discharge (data given in Appendix II) from the HYMO Model and the drainage area for each watershed. The results of these computations, as displayed in Figure 7.1, indicate a logarithmic increase in the coefficient with an increase in slope. These results further suggest that the slope may contribute to the estimation of coefficient c_1.

7.2.2 Relationship of Coefficient c_1 with Intensity

The second parameter believed to affect the coefficient c_1 is the intensity of the precipitation loading. To investigate this aspect, three different simulations using the HYMO Model were carried out for the Sundre watershed of the Red Deer River Basin. In these simulations all parameters were kept constant, and only the intensity of the

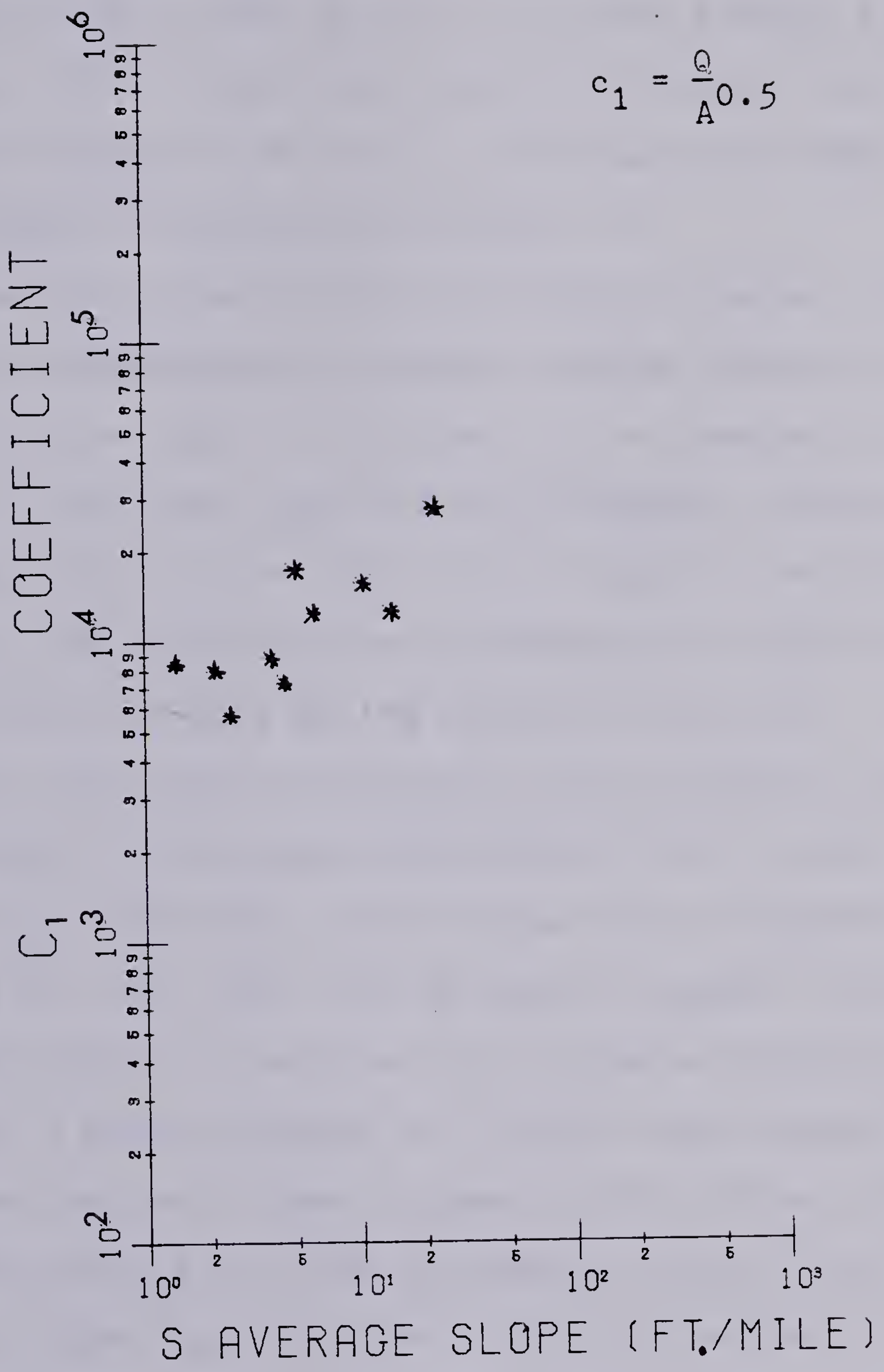

Figure 7.1. Relationship between Slope and Coefficient c_1.

precipitation loading was varied from simulation to simulation. The constant parameters were (a) the drainage area (2471 Km² or 954 sq. mi.), (b) the average slope (5.7 m per Km or 30.1 ft. per mi.), and (c) 24-hour total water loading (645 mm or 25.4 in.). The results of these three simulations are depicted in Figure 7.2.

The first simulation is depicted by Curve A, the resultant hydrograph of a water loading intensity of 43.2 mm (1.70 in.) per hour. This intensity is composed of a 12.7 mm (0.5 in.) per hour (for 24 hours) snowmelt loading and a 30.5 mm (1.20 in.) per hour (for 9 hours) precipitation loading. The resulting peak discharge of 21 055 m³ per second (743 482 cfs) giving c_1 equal to 24 071.

For the second simulation, Curve B depicts the hydrograph for the same watershed but with a water loading intensity of 35.6 mm (1.40 in.) per hour, composed of a 12.7 mm (0.5 in.) per hour (for 24 hours) snowmelt loading and a 22.9 mm (0.90 in.) per hour (for 9 hours) precipitation loading. A peak discharge of 19 829 m³ per second (700 183 cfs) and the coefficient c_1 equal to 22 669 were obtained.

The third simulation is shown by Curve C for a water loading intensity of 26.9 mm (1.06 in.) per hour, composed of a 12.7 mm (0.5 in.) per hour (for 24 hours) snowmelt loading and a 14.2 mm (0.56 in.) per hour (for 24 hours) precipitation loading. A peak discharge of 16 735 m³ per second (590 910 cfs) and a coefficient value of 19 131 were obtained.

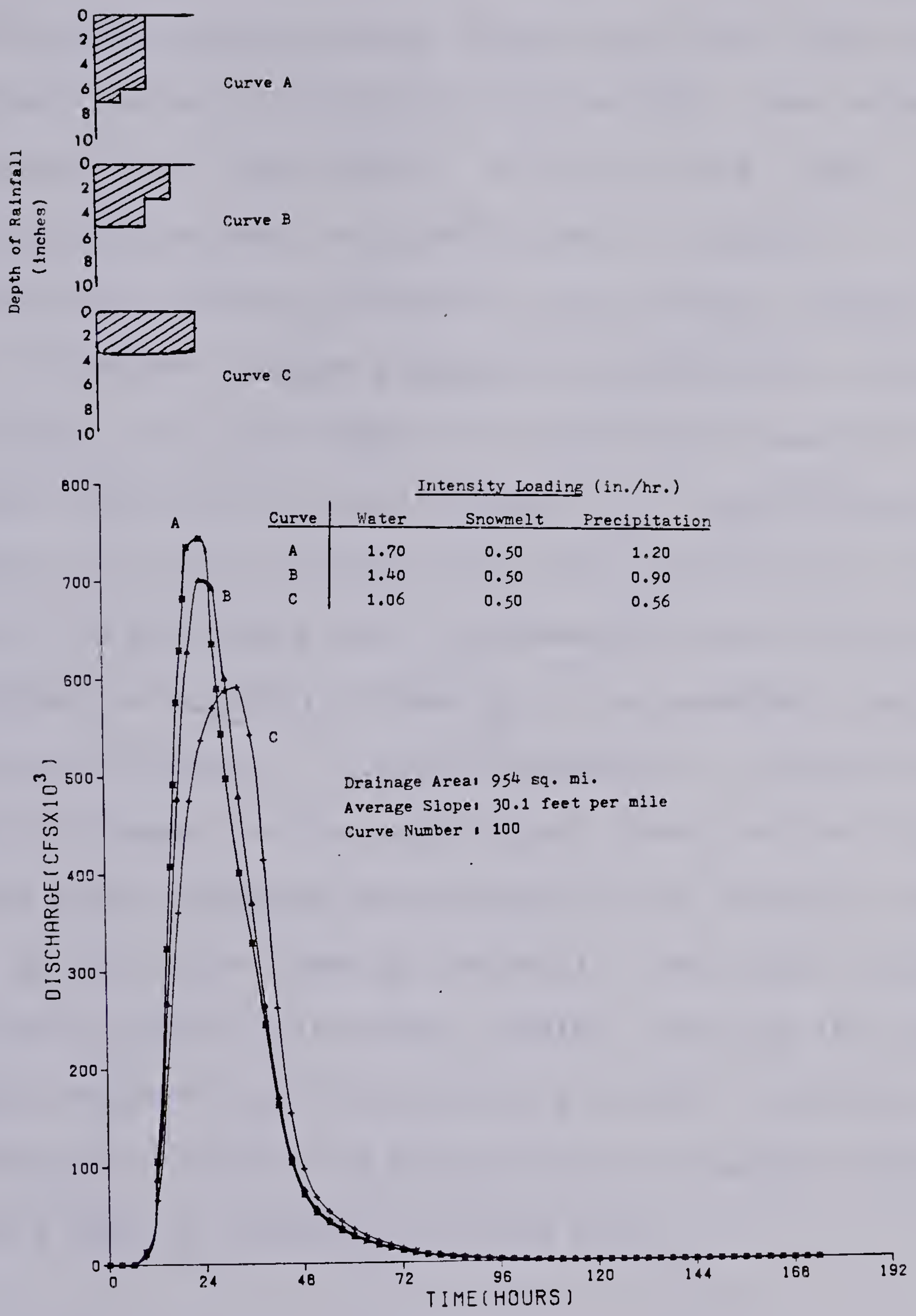

Curve	Intensity Loading (in./hr.) Water	Snowmelt	Precipitation
A	1.70	0.50	1.20
B	1.40	0.50	0.90
C	1.06	0.50	0.56

Drainage Area: 954 sq. mi.
Average Slope: 30.1 feet per mile
Curve Number : 100

Figure 7.2. Variation of the PMF Discharge with Changes in Intensity of the Water Loading.

The three curves in Figure 7.2 show that the PMF peak discharge increases with an increase in the intensity of the precipitation loading (even though the total water loading remained constant for the 24-hour period). The increase is suspected to be logarithmic. To verify this, the relationship between the coefficient c_1 and the precipitation loading intensity was plotted (Figure 7.3). Three different average slopes were simulated, since it was suspected that slope might also affect the results. Figure 7.3 confirms that the coefficient c_1 is logarithmically related to (a) the intensity of the precipitation loading and (b) the average slope. Of these two quantities, the precipitation loading intensity is the dominant contributor to the coefficient c_1, since increases in intensity produce larger increases in the coefficient than similar increases for the slope. Because the precipitation loading intensity makes up the water loading intensity, the above statments can also be applied to water loading. Varying the snowmelt loading intensity will also have an effect (probably similar to that observed for the precipitation loading intensity), but this was not examined in this work.

7.3.0 PMF Relationship (m = 1.0)

The second Q-A relationship investigated is Equation 7.2, or Equation 7.1 with $m = 1.0$ and $c_1 = KCI$. The coefficient C (called the runoff coefficient) is divided into three parts: (1) K, the conversion constant, (2) C, the

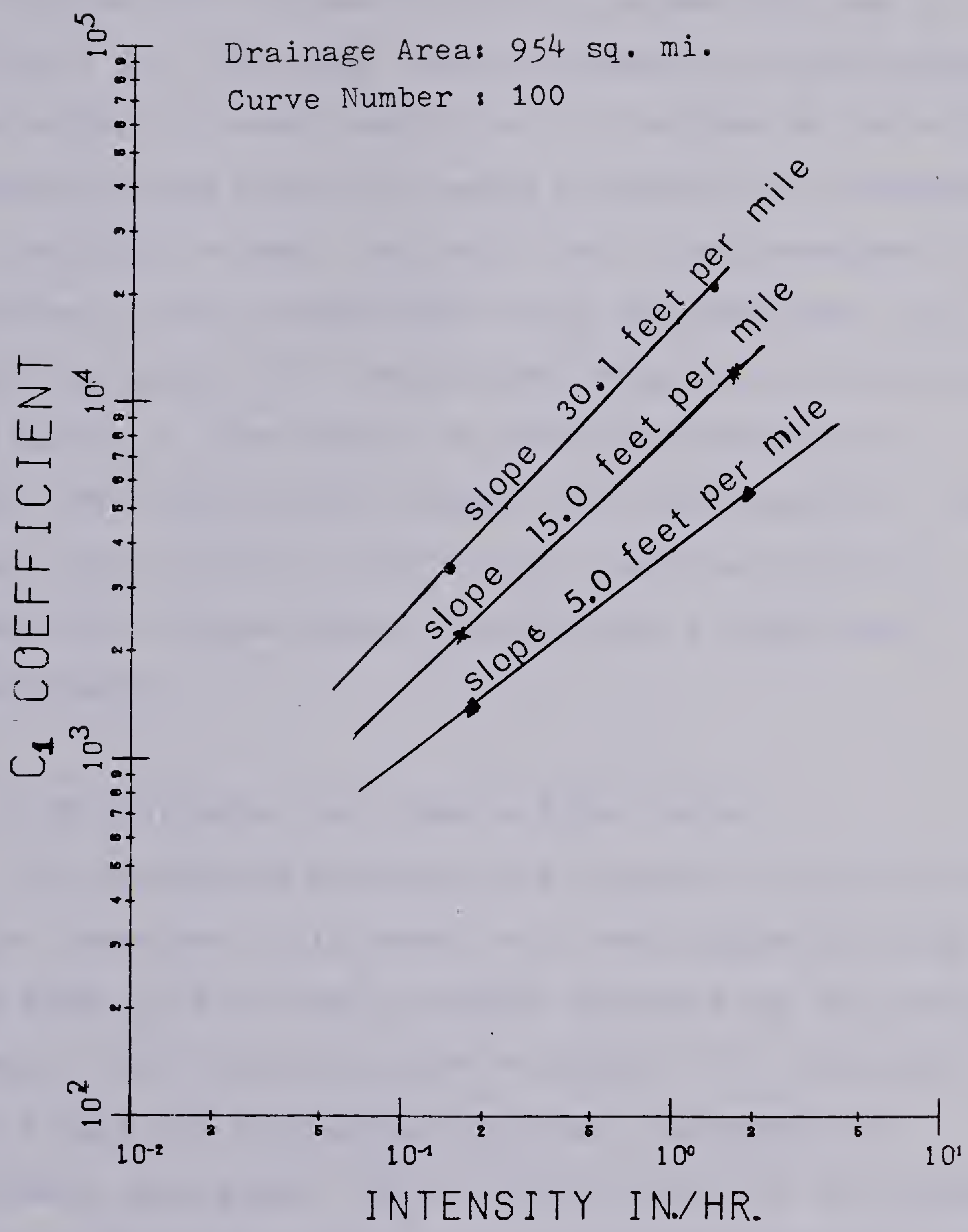

Figure 7.3. Relationship of the Water Loading Intensity with the Coefficient C_1 .

runoff coefficient, and (3) I, the water loading intensity. In Equation 7.2 intensity is considered a variable parameter and not part of the coefficient c_1, as was the case in Section 7.2.0. The water loading intensity is considered here since the runoff coefficient is defined as the ratio between surface runoff following a rainfall on a snowpack and the total volume. The coefficient C was examined in relation to the average slope using the HYMO Model, and the resulting scatter for the Red Deer River Basin is depicted in Figure 7.4. The results in the figure indicate a logarithmic relationship between the two parameters. The graphs for the other Alberta river basins are given in Appendix IV. These graphs also indicate a logarithmic relationship.

7.4.0 PMF Estimates for Alberta River Basins

The normalized discharge was thought to vary within a basin; therefore, this aspect was investigated by using the HYMO Model with the PMF estimates obtained for the various Alberta river basins depicted in Figure 7.5. Also given in this figure are the maximum recorded discharges for available watersheds. The enveloping curve for the maximum recorded discharges seems to be well approximated by the equation $Q = 2000A^{0.5}$. The enveloping curve for the PMF estimates can be approximated by an equation $Q = 1.35 \times 10^5 A^{0.29}$, suggesting a relationship with a smaller exponent value (m = 0.29) than the square-root value obtained for the

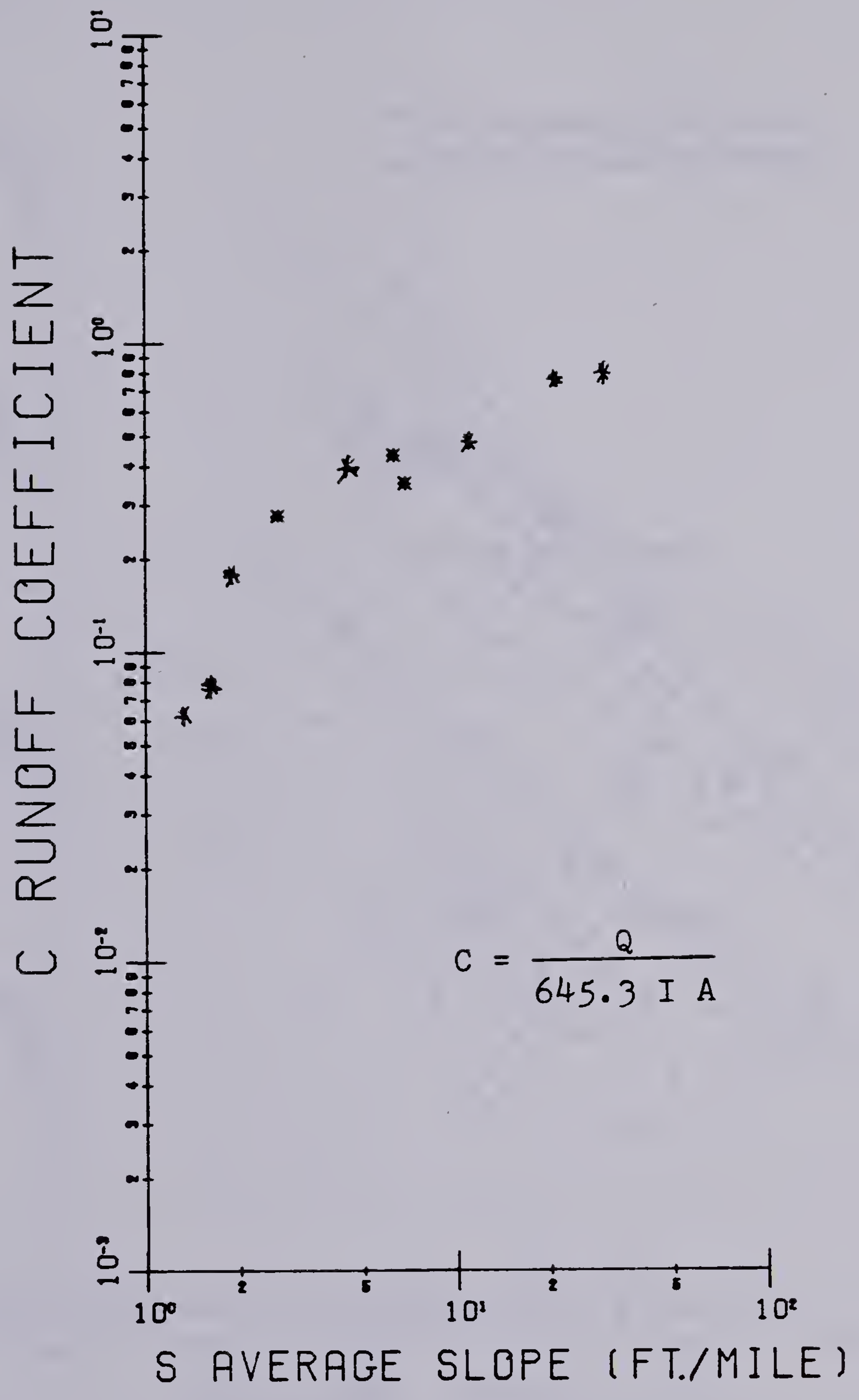

Figure 7.4. Variation of the Runoff Coefficient C with Average Slope for the Red Deer River Basin.

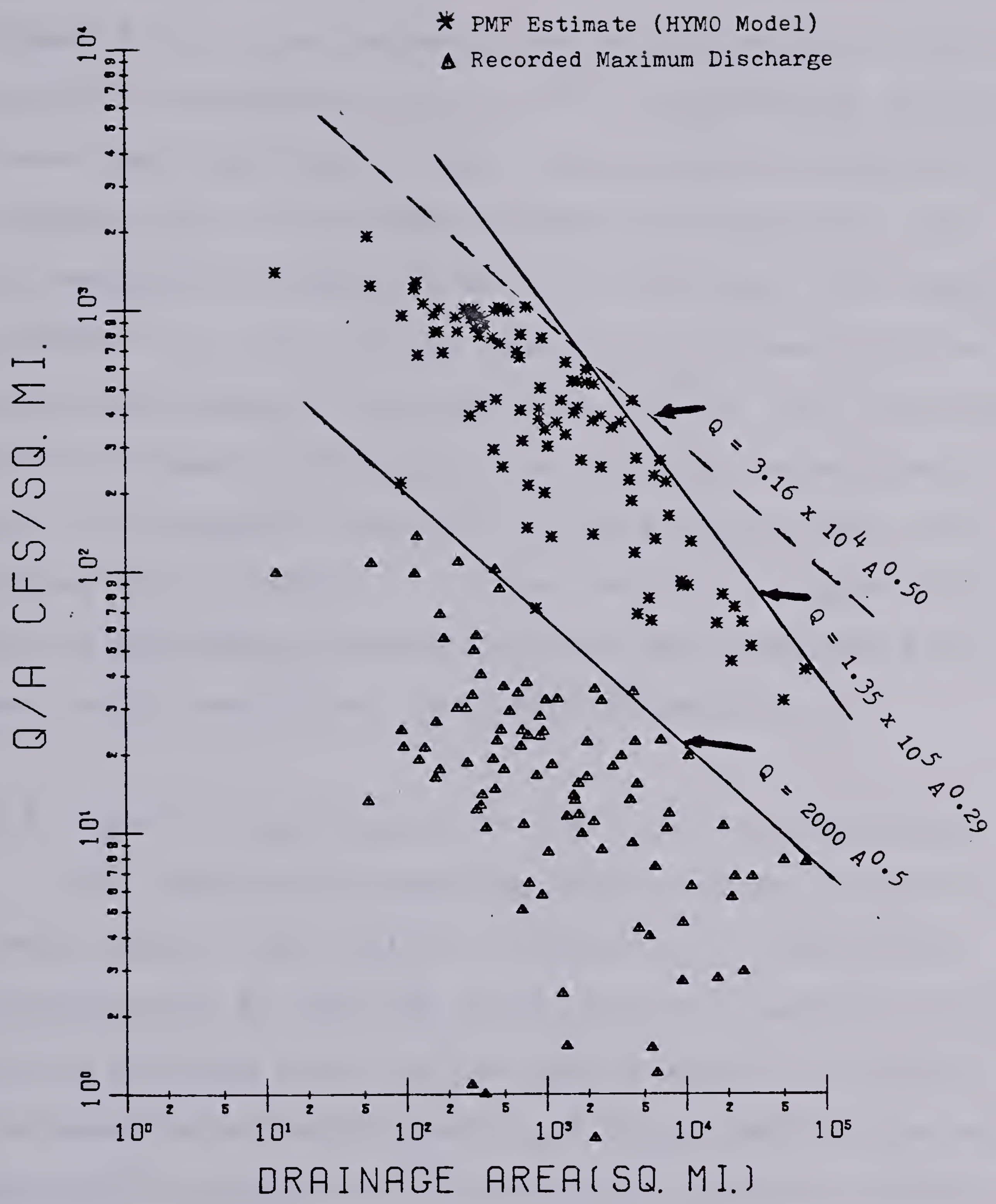

Figure 7.5. Relationship Between Normalized Discharge and Drainage Area for Alberta River Basins.

recorded discharges. An equation with a square-root approximation (i.e. $Q = 3.16 \times 10^4 A^{0.5}$) is also drawn on Figure 7.5 to show the deviation of this equation from the one with an exponent of $m = 0.29$. The separation of the normalized discharge by basin is presented in APPENDIX IV, together with the maximum recorded discharges for the corresponding drainage areas. For individual river basins (APPENDIX IV), the results seem to be represented by an enveloping curve of the form $Q \propto f(A^{0.5})$. The large spread in the values of the normalized discharge is believed to be due to the spatial variation of the average slope. Also presented in APPENDIX IV is the graphical representation of the relationships between slope and PMF discharge and slope and runoff coefficient for the different basins.

7.4.1 Spatial Distribution of the Normalized Discharge

The normalized discharges were examined in terms of their spatial distribution in Alberta. The normalized discharge can be computed by dividing the peak PMF discharge by the drainage area from the data provided in APPENDIX III. The computer contoured results of these computations are depicted in Figure 7.6. The computer contouring system used in this analysis was developed for the Kansas Geological Survey and is presented by Sampson (1975) in the user's manual, "SURFACE II Graphics System". SURFACE II is a computer software system for creation of displays of spatially distributed data. The form of graphic display

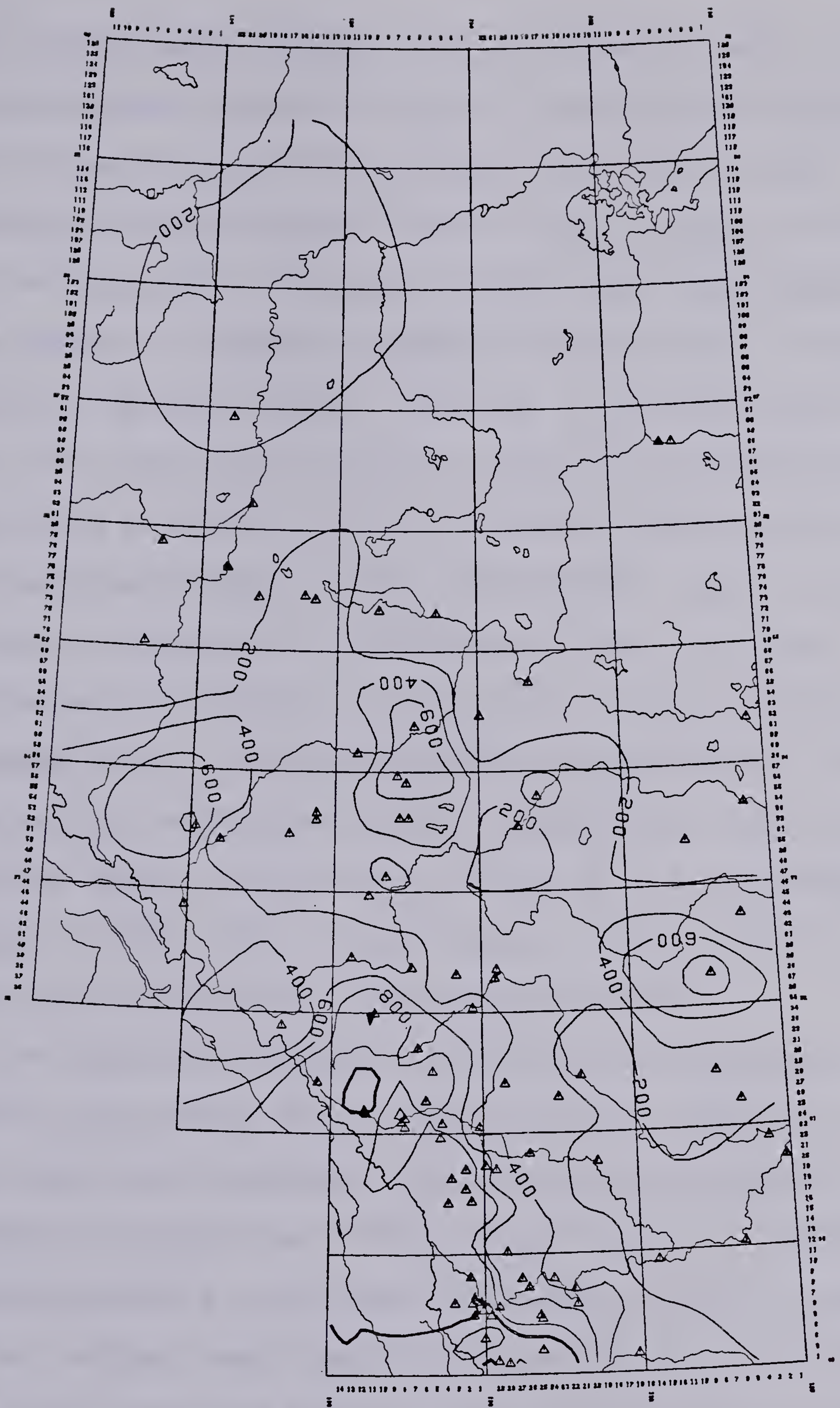

Figure 7.6. Spatial Distribution of Normalized Discharge for Alberta River Basins.

shown in this work (Figure 7.6) is a contour map, a plot of two coordinates (values of spatial coordinates x and y) on which values of the third variable (variable to be contoured) are defined by lines of equal values. In Figure 7.6, the contoured lines depict the normalized discharge. A large number of computer commands are available in the SURFACE II graphic system. The user first generates a grid matrix of normalized discharge values from irregularly spaced data points by using a distance weighting function in the averaging process. Sample data points used in the estimation procedure are weighted so their influence declines with distance from the point being estimated. Following this, a contour map from the grid matrix is generated by the graphic system. Smoothing is done by piecewise Bessel intepolation (a spline fitting method) (Sampson, 1975) within the grid cell, which results in a smooth path of contour line through the grid.

The results in Figure 7.6 show that watersheds in the foothills and along the continental divide generally have high normalized discharge values ranging from several hundred to slightly over 1000 cfs per sq. mi.. The high values coincide to watershed with steep average slopes. Smaller (values less than 200 cfs per sq. mi.) of the normalized discharge were obtained for the northern and eastern sections of the province.

7.4.2 Spatial Distribution of the Coefficients

Another aspect examined was the spatial distribution of the coefficients c_1 and C using the SURFACE II Graphic System. These results are depicted in Figures 7.7 and 7.8., respectively. Generally, high coefficient values are found for the foothills and along the continental divide coinciding with watersheds of high average slopes. Low coefficient values were obtained for watersheds in the eastern and northern sections of the province, coinciding with watersheds with low average slopes.

7.4.3 Topic for Future Research

The results obtained in Section 7.2.1 suggest that the average slope may contribute to the estimation of the peak discharge and needs to be considered in a Q-A relationship. To examine this aspect a preliminary investigation was conducted using a multilinear regression analysis with the three parameters (peak discharge, average slope, and drainage area as given in APPENDIX A.3) expressed in logarithmic form. Using this analysis the following equation was obtained for Alberta with a multicorrelation coefficient of 0.97:

$$Q = 505\ A^{0.78}\ S^{0.57} \qquad (7.3)$$

where Q is the peak discharge (cfs), A is the drainage area (sq. mi.), and S is the average slope (feet per mile). Equation 7.3 was computed for average slopes of 1.0, 10.0,

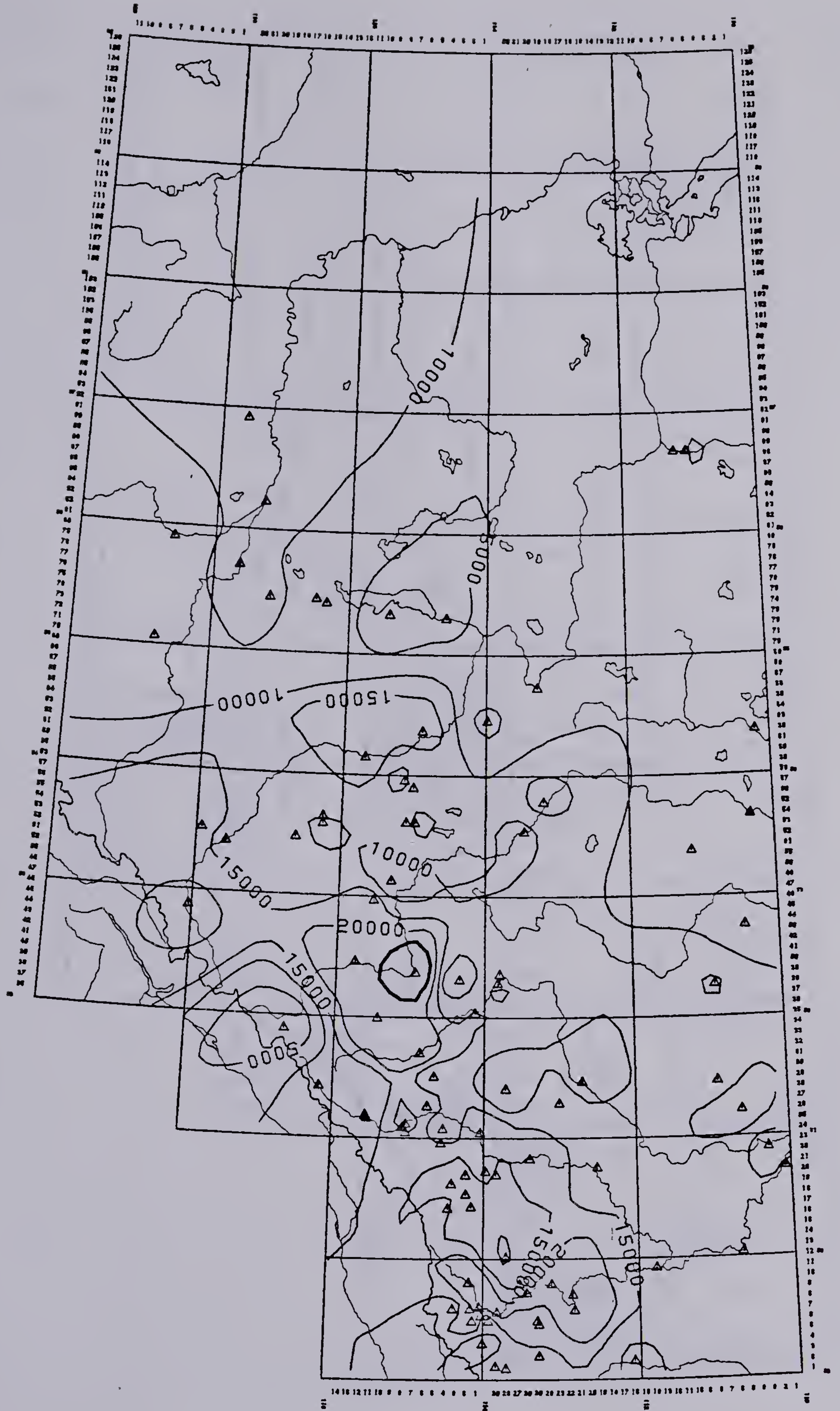

Figure 7.7. Spatial Distribution of the Coefficient c_1 for Alberta River Basins.

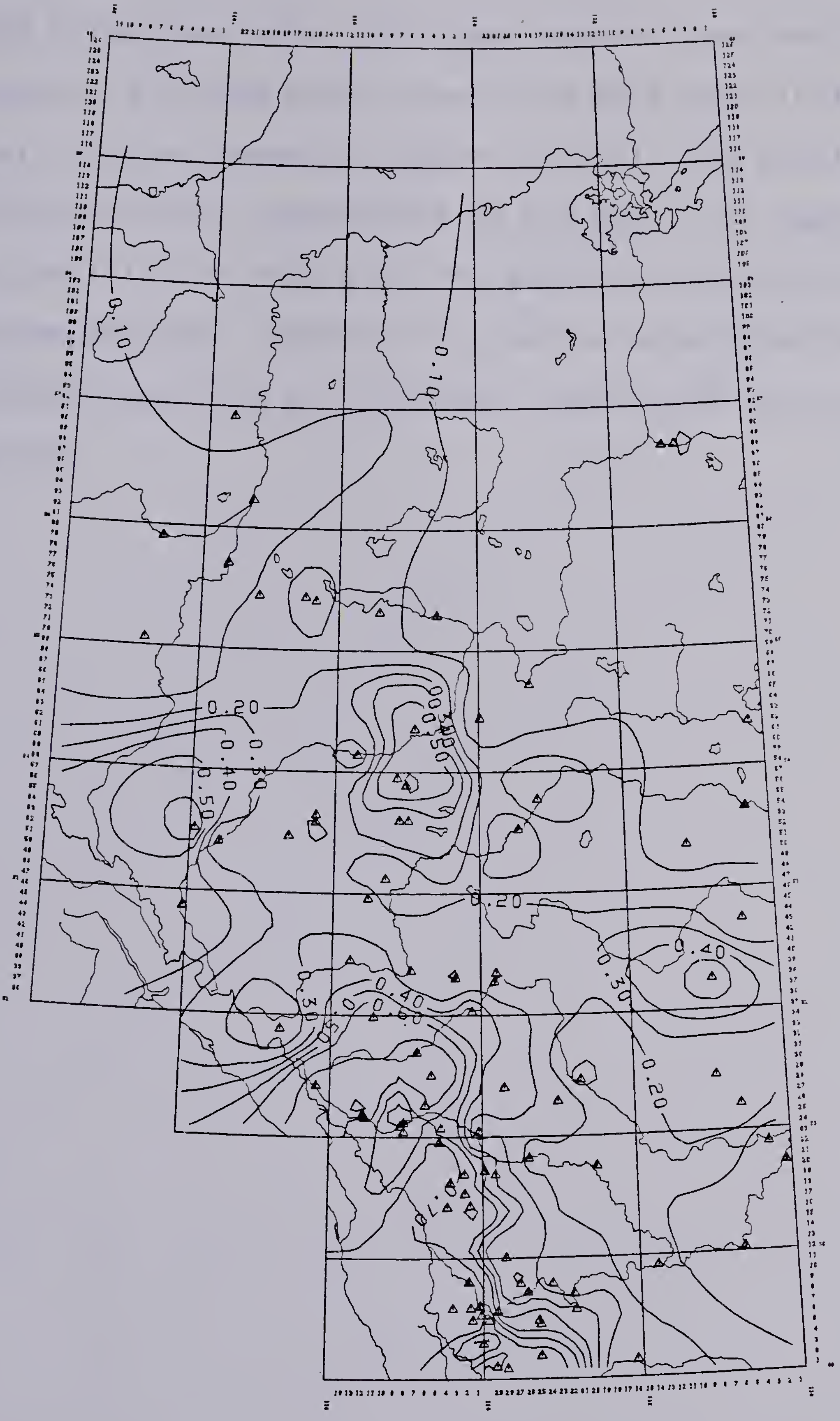

Figure 7.8. Spatial Distribution of the Runoff Coefficient C for Alberta River Basins.

and 100.0 feet per mile, and these computations are depicted in Figure 7.9 by the solid lines. The data used in the analysis is also shown in Figure 7.9, with the position of the various values represented by the dots. The numerical values next to the dots give the average slope for a given discharge and area. Equation 7.3 can be considered as a preliminary analysis on this topic and further work is suggested.

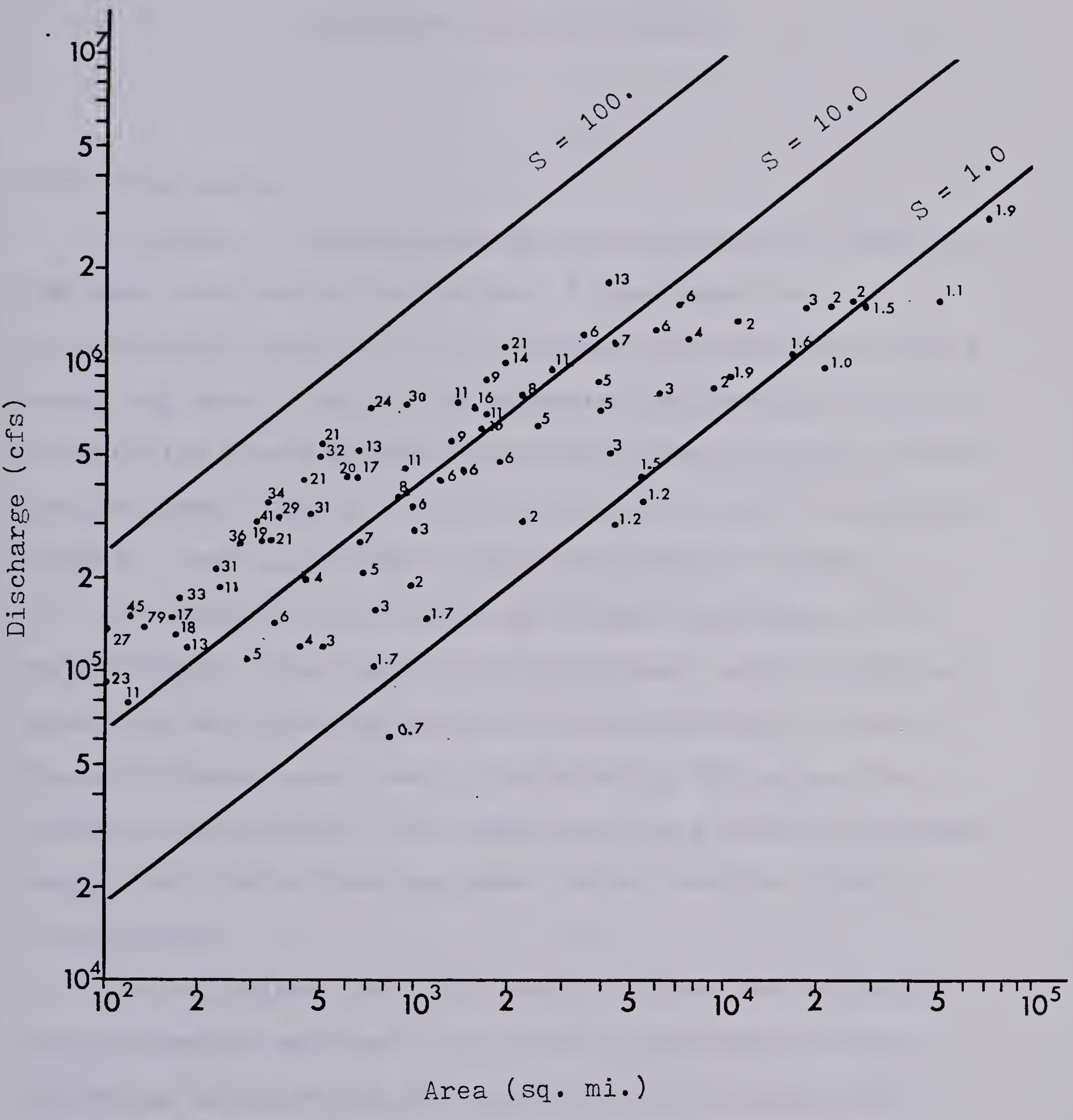

Figure 7.9. Relationship between Peak Discharge, Average Slope, and Drainage Area for Alberta River Basins.

CHAPTER 8

DISCUSSION AND CONCLUSIONS

8.1.0 Discussion

A number of topics dealing with estimation of PMP and PMF were examined by the author. A comprehensive climatological analysis of rainstorms was conducted using a novel approach in which the isohyetal patterns and rainfall intensities from rainstorms were digitized in spatial blocks and analyzed. Such an analysis is the first of its kind for Alberta, and is lacking for many provinces in Canada.

PMP was estimated using two common approaches, the meteorological and statistical techniques, and included an extensive analysis and graphical representation of the (a) dewpoint temperature, and (b) enveloping PMP curves for Alberta river basins. Both techniques gave similar estimates suggesting that either approach can be used for Alberta river basins.

PMP estimates were also used to obtain PMF estimates. A unique concept employed the spatial relationship of PMP estimates to determine the location of the largest PMP loading in a basin. In the study, the author found that such a relationship was well correlated within a river basin and mainly dependent on position and elevation of the location for which the estimate is required.

The rain-on-snow event is believed to produce the largest water loading on watersheds in Alberta. The important processes contributing to snowmelt were defined, and an equation was developed to estimate maximum snowmelt. Previously, convection and condensation were identified as necessary to the total melt in the rain-on-snow event; however, analysis showed that shortwave radiation and rainfall are also important.

To investigate the effect of watershed shape on PMF, the TAPMF Model was developed. PMF estimates obtained from this model were comparable to those obtained by the SSARR and HYMO models. The lack of a significant difference in the estimate, attibutable to the watershed shape, is probably due to the dominance of area on the shape parameters. The sensitivity of the SSARR and HYMO models was also investigated hypothetically and the results show the importance of accurately determining the required model parameters. All three models gave about three times larger than a previous PMF estimate in the Red Deer River Basin; this is mainly due to the difference in the precipitation intensity loading.

Two empirical Q-A relationships were investigated with exponents equal to 0.5 (a square-root approximation) and 1.0 (Rational Forumla). The Rational Formula was selected because the coefficient is dimensionless and hence easily interpretable. Also, the Q-A relationship obtained by other investigators have exponent values less than 1.0 and hence

the exponent equal to 1.0 can be considered an upper limit in the relationship.

The spatial distributions of the coefficients in the two Q-A relationships and the normalized discharge are also presented. The Q-A relationship with an exponent equal to 0.29 best represents the data for all the river basins in Alberta, while for many individual river basins a square-root relationship best describes the enveloping curve of PMF. The square-root relationship seems to vary logarthmically with slope and intensity.

This study presents PMP and PMF estimates, previously lacking, for Alberta river basins.

A number of conclusions were reached during the course of this study pertaining to the climatological, meteorological, PMP, and PMF estimates; these are summarized below.

8.2.0 Conclusions

8.2.1 Climatology and Meteorology

1. Rainstorms with depths of 50 mm (2 in.) and more are frequent in Alberta (average of 11 occurrences per year), while rainstorms with depths of 150 mm (6 in.) and more are uncommon (average of an occurrence per two year).
2. The majority of rainstorms occur in June and July, with only a small percentage occurring in April and September.

3. The greatest frequency of rainstorms is in the mountainous area in the southern part of the province (i.e., Waterton Lakes National Park) with an average of two rainstorms a year with depths 50 mm (2 in.) and more. In this area a rainstorm with a depth of 100 mm (4 in.) or more occurs on the average once every 3 years, while one with a depth of 150 mm (6 in.) or more, occurs once every 10 years.
4. The frequency of rainstorms decreases eastward and northward from the continental divide in Alberta.
5. Severe rainstorms (rainstorms with depths of 150 mm (6 in.) and more) occur in four main regions (or belts) of the province: the first extends through southern Alberta, just south of Calgary; the second is in central Alberta from south of Edson eastward to the Edmonton region; the third is from Lesser Slave Lake northeastward to Fort McMurray; and the fourth is around the Fort Vermilion area.
6. In Alberta, heavy precipitation events (depths of 150 mm (6 in.) or more) are produced by a cold low system.

8.2.2 PMP and PMF Estimates

Several conclusions can be drawn from the analyses of the depth-area-duration curves and the estimates of PMP and PMF.

1. DAD analyses using the physical approach show that only a few rainstorms contribute to the estimate of the PMP. The storms that contribute to the PMP are not obvious, hence the

procedure of plotting DAD curves is an important and necessary part.

2. The maximum estimates of the PMP occur in June for the basins in the southern portion of the province, while in central and northern Alberta these occur in July.

3. Estimates of PMP vary spatially within each river basin in Alberta. Generally, two characteristic variations can be defined: the first and the most predominant is a decrease west to east in the basin, while the second is a decrease from south to north.

4. For many of the river basins in Alberta, estimates from the statistical technique produced results similar to those from the physical approach.

5. Maximum water loading on a watershed can be expected in late May or early June in Alberta, since the coincidence of severe rainstorms, snow cover, and air temperatures above freezing seems to occur during this period.

6. For rain-on-snow events under a PMP loading, the predominant heat transfer processes are due to convection and condensation, shortwave and longwave radiation, and rainfall. Maximum snowmelt can be expressed as a function of meteorological parameters (temperature, PMP, and wind speed), which were observed to be well correlated with the location, elevation, duration, and rainstorm area.

7. Sensitivity of model response to parameter changes is an important feature of the SSARR and HYMO models, since some parameters affect the shape of the resulting hydrograph and

the peak PMF discharge.

8. The three models for PMF produced comparable results, indicating that any one can be used effectively for watersheds in Alberta.

9. The Q-A relationship expressed as $Q = c_1 A^{\frac{1}{2}}$ defines the enveloping curves for the maximum recorded flows and PMF estimates for watersheds in Alberta.

10. The coefficients c_1 in $Q = c_1 A^{\frac{1}{2}}$ and C (the runoff coefficient) in Q = KCIA in the Q-A relationship are logarithmically related to the average slope of the watersheds.

11. High normalized discharge and runoff-coefficient values are mainly observed in the foothills and along the continental divide where watersheds exhibit high average slopes. Lower values of the these parameters were obtained for watershed in the eastern and northern portions of the province (coinciding with watersheds of lower average slopes).

BIBLIOGRAPHY

Ackermann, W.C. 1964. Application of severe rainstorm data in engineering design. Bulletin of the American Meteorological Society 45:204-206.

Alberta Environment. 1975. Red Deer River flow regulation planning studies. Vol. I. Technical Services Division. Hydrology Branch. Edmonton, Alberta 184 pp.

Alberta Environment. 1977a. Flood information index. Environmental Engineering. Technical Services Division, Hydrology Branch. Edmonton, Alberta 45 pp.

Alberta Environment. 1977b. Modification of SSARR Watershed Model for flow forecasting in Alberta Alberta Environment. Technical Services Division, Edmonton, Alberta. 10 pp.

Alberta Environment. 1978. Areas of drainage basins within Alberta. Technical Services Division, Hydrology Branch. Edmonton, Alberta. 16 pp.

Alberta Environment. 1980. Private communication.

Alexander, G.N. 1963. Using the probability of storm transposition for estimating the frequency of rare floods. Journal of Hydrology. North-Holland Publishing Co., Amsterdam. I(1):46-57.

Alexander, G.N. 1967. Application of probability to spillway design flood estimation. Presented at UNESCO-WMO Symposium, Leningrad, U.S.S.R..

Atmospheric Environment Service. 1888- . Monthly record of meteorological observations in Canada. Environment Canada. Downsview, Ontario.

Atmospheric Environment Service. 1961- . Storm rainfall in Canada. Environment Canada. Downsview, Ontario.

Atmospheric Environment Service. 1970a. Extremes of snowfall and snow cover at selected stations in Canada. Environment Canada. Downsview, Ontario. CDS Nos. 3-70.

Atmospheric Environment Service. 1970b. Extremes of snowfall-Canada. Environment Canada. Downsview, Ontario. CDS Nos. 5-70.

Atmospheric Environment Service. 1975a. Canadian normals, temperature. 1941-1970. Environment Canada. Downsview, Ontario. Vol. 1-SI. 198 pp.

Atmospheric Environment Service. 1975b. Canadian normals, precipitation. 1941-1970. Environment Canada. Downsview, Ontario. Vol. 2-SI. 333 pp.

Atmospheric Environment Service. 1975c. Canadian normals, wind, 1955-1972. Environment Canada. Downsview, Ontario. Vol. 3-SI. 142 pp.

Bailey, S.M. and G.R. Schneider. 1939. The maximum probable flood and its relation to spillway capacity. Civil Engineering. 9(1):32-35.

Beard, L.R. 1954. Estimation of flood probabilities. Proceedings of the American Society of Civil Engineers. 80(438). 21 pp.

Bernard, M. 1936. The unit-hydrograph method and storm transposition in flood problems relating to great storms in the eastern and central United States. Pages 218-244 in Floods in the United States. Water Supply Paper 772. U.S. Geological Survey.

Bernard, M. 1944. Primary role of meteorology in flood flow estimating. Transactions of the American Society of Civil Engineers. 109:311-382.

Bisson, J.L. 1979. Modèle de prévision des apports naturels de l'Hydro-Québec. Hydro-Québec. Montreal, Qué.

Bristol, M. 1975. A method to determine flood hydrographs for ungauged watershed. M.Sc. thesis. Department of Civil Engineering, University of Alberta. Edmonton, Alberta. 123 pp.

Bruce, J.P. 1957. Preliminary estimates of probable maximum precipitation over southern Ontario. Engineering Journal. 40(7):978-984.

Bruce, J.P. 1959a. Storm rainfall transposition and maximization. Pages 162-170 in Proceedings of 1st Canadian Hydrology Symposium, Spillway Design Floods. National Research Council. Ottawa, Ontario..

Bruce, J.P. 1959b. Rainfall intensity-duration-frequency maps for Canada. Meteorological Branch, Atmospheric Enviornment Service. CIR-3243. TEC-308. 27 pp.

Bruce, J.P. 1961. Frequency of heavy rainfalls in the lower Fraser valley. Meteorological Branch, Atmospheric Enviornment Service. CIR-3468. TEC-354. 21 pp.

Bruce, J.P. 1962. Snowmelt contributions to maximum floods. Proceedings of the Eastern Snow Conference. 20:85-104.

Bruce, J.P. 1964. Large scale atmospheric circulations affecting floods on the Fraser River. Proceedings of the 32nd Western Snow Conference. Nelson B.C. 44-51.

Bruce, J.P. 1968. Atlas of rainfall intensity-duration-frequency data for Canada. Climatological Studies. Atmospheric Environment Service, Downsview, Ontario No. 8. 31 pp.

Bruce, J.P. and D.V. Anderson. 1957. The storm and floods of October, 1954 in southern Ontario. International Association Scientific Hydrology. IUGG. General Assembly, Toronto. 3:331-341.

Bruce, J.P. and R.H. Clark. 1966. Introduction to hydrometeorology. Pergammon Press, Toronto. 319 pp.

Bruce, J.P., T.L. Richards, and U. Sporns. 1965. Critical meteorological conditions for maximum inflow, wind set-up and waves, Portage Mountain Reservoir, Peace River, B.C. Meteorological Branch. Climatological Studies. Atmospheric Environment Service, Downsview, Ontario No. 2. 26 pp.

Bruce, J.P. and U. Sporns. 1962. Maximum snow accumulation and melt rates in the Canadian portion of the Columbia River Basin. Meteorological Branch, Atmospheric Enironment Service. CIR-3766. TEC-436. 13 pp.

Bruce, J.P. and U. Sporns. 1963. Critical meteorological conditions for maximum floods in the Saint John River Basin. Meteorological Branch, Atmospheric Environment Service. Canadian Meteorological Memoirs. Atmospheric Environment Service. Downsview, Ontario. No. 14. 81 pp.

Buckler, S.J. 1968. Probable maximum snowpack, spring melt and rainstorm leading to probable maximum flood, Elbow River, Alberta. Hydrometeorological Report No. 1. Department of Transport. Meteorological Branch. 25 pp.

Buckler, S.J. 1969. Probable maximum rainfall for the Bighorn power development. Hydrometeorological Report. Prairie Farm Rehabilitation Administration. Regina, Sask. 23 pp.

Buckler, S.J. 1973. Spring runoff from a forested basin on the eastern slopes of the Rockies. Canadian Meteorological Research Report 3/73. Atmospheric Environment Service, Downsview, Ontario. 19 pp.

Buckler, S.J. and J.F. Quine. 1971. Critical meteorological conditions for maximum flow in the Pembina valley above Entwistle. Canadian Meteorological Research Report 2.

Atmospheric Environment Service, Downsview, Ontario. 46 pp.

Burrows, W.R. 1966. Heavy rainfalls in Edmonton. Meteorological Branch, Atmospheric Environment Service. CIR 4477. TEC-626. 33 pp.

Chow, V.T. 1951. A general formula for hydrologic frequency analysis. Transactions of the American Geophysical Union. 32:231-237.

Chow, V.T. 1964. Handbook of Applied Hydrology. McGraw-Hill, New York, N.Y.. 29 Sections.

Church, J.E. 1941. The melting of snow. Proceeding of the Central Snow Conference. I:21-32.

Clark, C.O. 1945. Storage and the unit hydrograph. Transactions of the American Society of Civil Engineers. 110:1419-1446.

Clarke, D.K. 1968. Applications of Stanford watershed model concepts to predict flood peaks for small drainage areas. Division of Research. Kentucky Department of Highways.

Collier, E.P. 1965. Flood of June 1953 in the south Saskatchewan River Basin. Water Resources Paper 113F. Water Resources Branch. Department of Northern Affairs and Natural Resources, Ottawa, Ont. 228 pp.

Court, A. 1961. Area-depth rainfall formulas. Journal of Geophysical Research. American Geophysical Union. 66:1823-1832.

Craeger, W.P. 1939. Possible and probable future floods. Civil Engineering. 9(11):668-670.

Crawford, N.H. and R.K. Linsley, Jr.. 1966. Digital simulation in hydrology: Stanford Watershed Model IV. Department of Civil Engineering. Stanford University, Stanford, California. Technical Report No. 39.

Davies, L.B. and D.M. Rockwood. 1966. A hydrometeorlogical analysis of a maximum probable flood for the Portage Mountain project, Peace River B.C. Pages 57-58 in Proceedings of the 34th Western Snow Conference. Seattle, Washington. 57-68.

Dooge, J.C.I. 1959. A general theory of the unit hydrograph. Journal of Geophysical Research. 64(1):241-256.

Durrant, E.F. and S.R. Blackwell. 1961. The magnitude and

frequency of floods on the Canadian prairies. Proceedings of Hydrology Symposium No. 1. National Research Council Associate Committee on Geodesy and Geophysics. Subcommittee on Hydrology. Ottawa, Ont., Canada. 1:101-154.

Fawkes, P.E. 1979. Probable maximum flood for the Peace River at Site C. Proceeding Canadian Hydrology Symposium - 79. National Research Council. Ottawa, Ont.

Flavell, D.R. and R.O. Lyons. 1973. Probable maximum floods for the Fraser River at Hope and Mission. Inland Waters Directorate. Environment Canada. Vancouver, B.C.

Froelich, C.R. 1967. June 1965 storm in the southern Peace, Athabasca and North Saskatchewan basins of Alberta. Alberta Department of Agriculture, Water Resources Division. Edmonton, Alberta.

Fuller, W.E. 1914. Flood flows. Transactions of the American Society of Civil Engineers. 77:564-617.

Gagnon, R.W., D.M. Pollock and D.M. Sparrow. 1970. Critical meteorological conditions for maximum flows, the St. Francois and Chaudiere River basins, Quebec. Climatological Studies. Atmospheric Environment Service, Downsview, Ont. No. 16. 85 pp.

Godwin, R.B. 1975. Regionalized estimates of probable maximum floods. National Research Council. Canada. Canadian Hydrology Symposium. Winnipeg, Manitoba. 213-217.

Grainge, J.W. 1963. Preliminary report on flood Habay, Alberta. Report of the Department of National Health and Welfare. Edmonton, Alberta.

Granger, R.J. and D.H. Male, 1977. Melting of a prairie snowpack. Pages 261-267 in Proceedings of the Second Conference on Hydro-Meteorology, Toronto, Ontario.

Gray , M.G. (ed.) 1970. Handbook on the principles of hydrology. 13 Sections.

Gumbel, E.J. 1941. The return period of flood flows. Annals of Mathematical Statistics. 12:163-190.

Gumbel, E.J. 1954. Statistical theory of extreme values and some practical applications. National Bureau of Standards. Applied Mathematics Series 33. Washington, D.C.

Gumbel, E.J. 1966. Extreme value analysis of hydrologic

data. Pages 147-181 in Poceeding Hydrology Symposium No. 5.

Harris, J.D. 1978. Design flood estimation for medium and large watersheds. Bridge Hydraulics Manual. Chapter C. Second Edition. Ontario Ministry of Transportation and Communications. Downsview, Ont.

Hathaway, G.A. 1939. The importance of meteorological studies in the design of flood control structures. Bulletin of the American Meteorological Society. 20:248-253.

Hathaway, G.A. 1944. Discussion of primary role of meteorology in flood flow estimating. Transactions of the American Society of Civil Engineers. 109:370-375.

Hay, J.E. 1970. Precipitable water over Canada. Part 1, Computation. Atmosphere. 8(4):128-143.

Hay, J.E. 1971. Precipitable water over Canada. Part 2, Distribution. Atmosphere. 9(4):101-111.

Hay, J.E. 1977. A tabulation and analysis of solar radiation data for Alberta. Alberta Research Council and Alberta Environment. Edmonton, Alberta. 124 pp.

Hershfield, D.M. 1961. Estimating the probable maximum precipitation. Journal of Hydraulics Division. Proceedings of the American Society of Civil Engineers. 87(HY5):99-116.

Hershfield, D.M. 1965. Methods for estimating probable maximum precipitation. Journal of American Waterworks Association. 57:965-972.

Hershfield, D.M. 1977. Some tools for hydrometeorologists, Preprints, 2nd Conference on Hydrometeorology. American Meteorological Society. Boston, Mass.

Hershfield, D.M. and W.T. Wilson. 1960. A comparison of extreme rainfall depths from tropical and nontropical storms. Journal of Geophysical Research. 65:959-982.

Hoang, V.D. 1977. Méthode permettant la construction d'un hydrogramme de crue pour les petits bassins versants. Compte-rendu du Symposium canadien d'Hydrologie-77. Conseil national de la recherche. Ottawa, Ont.

Hogg, W.D. 1977. Probable maximum precipitation in the McGregor River Basin. Atmospheric Environment Service. Downview, Ont.. Unpublished report. 11 pp.

Hogg, W.D. 1980a. Critical meteorological conditions for maximum inflow Stikine River, B.C. above Grand Canyon. Atmospheric Environment Service. Downview, Ont. Unpublished report.

Hogg, W.D. 1980b. Time distribution of short duration storm rainfall in Canada. Proceeding of the Canadian Hydrology Symposium 80 (Toronto). National Research Council. Ottawa, Ont.

Holtan, H.N. and N.C. Lopez. 1973. USDAHL-73 revised model of watershed Hydrology. U.S. Department of Agriculture. Plant Physiology Institute. Report No.1.

Horton, R.E. 1936. Hydrologic conditions as affecting the results of the application of methods of frequency analysis to flood records. Pages 433-450 in Floods in the United States. Water Supply Paper 771. U.S. Geological Survey.

Huff, F.A. 1967. Time distribution of rainfall in heavy storms. Water Resources Research. American Geophysical Union. 3:1007-1019.

Huff, F.A. 1979. Precipitation relations for use in dam safety project. Illinois State Water Survey. 10 pp.

Huff, F.A. and J.C. Neil. 1956. Frequency of point and areal mean rainfall rates. Transactions of the American Geophysical Union. 37:678-681.

Huschke, R.E. 1970. Glossary of meteorology. American Meteorological Society, Boston, Mass. 638 pp.

Johnstone, D., and W.P. Cross. 1949. Elements of appled hydrology. The Ronald Press Company, N.Y..

Kellerhals, R., C.R. Neill, and D.I. Bray. 1972. Hydraulic and geomorphic characteristics of rivers in Alberta. Research Council of Alberta. River Engineering and Surface Hydrology Report 72-1. Edmonton, Alberta. 52 pp.

Kemball, B.F. 1942: Limited type of primary probability distribution applied to annual maximum flood flows. Annals Mathematical Statistics. 13:318-325.

Kendall, G.R. 1959: Statistical analysis of extreme values. National Research Council. Pages 54-78 in Proceedings of Hydrology Symposium No. 1.

Kendall, G.R. 1966. Probability distribution of a single variable. Pages 37-54 in Proceedings of Hydrology

Symposium No. 5.

Koelzer, V.A. and M. Bitoun. 1964. Hydrology of spillway design floods: Large structures-limited data. Journal of Hydraulics Division. Pages 261-293 in Proceedings of the American Society of Civil Engineers. Paper No.3913.

Kozub, G.C. 1964. Heavy snowfalls at Edmonton, Canada. Meteorological Branch. Atmospheric Environment Service, Downview, Ont. CIR-4076. TEC-526. 35 pp.

Laycock, A.H. 1964. Water deficiency patterns in the prairie provinces. Report No. 8. Prairie Farm Rehabilitation Administration. Regina, Sask. 53 pp.

Laycock, A.H. 1967. Water deficiency and surplus patterns in the prairie provinces. Report No. 13. Prairie Farm Rehabilitation Administration. Regina, Sask. 185 pp.

Leclerc, G. and P. Purene. 1979. Critère de selection d'un modèle de simulation du ruissellement urbain. Proc. 2e colloque sur le drainage urbain. AQTE, Montréal, Que.

Linsley, R.K., M.A. Kohler, and J.L. Paulhus. 1949. Applied hydrology. McGraw-Hill Book Co., Inc., New York.

Linsley, R.K. 1971. A critical review of currently available hydrologic models for analysis of urban stormwater runoff. Hydrocomp International, Inc., Palo Alto, California.

Longley, R.W. 1972. The climate of the prairie provinces. Environment Canada. Climatological Studies. Atmospheric Environment Service, Downsview, Ont. No. 13. 79 pp.

Longley, R.W. 1974. Spatial variation of precipitation over the Canadian prairies. Monthly Weather Review. 102(4):307-312.

Lott, G.A. and V.A. Myers. 1956. Meteorology of flood-producing storms in the Mississippi River valley. Hydrometeorological Report No. 34. U.S. Weather Bureau.

Louie, P.Y.T. and W.D. Hogg. 1980. Extreme value estimates of snowmelt. Proceedings Canadian Hydrology Symposium 80 (Toronto). National Research Council. Ottawa, Ont.

McKay, G.A. 1962. Statistical estimates of probable maximum rainfall in the prairie provinces. Department of Agriculture, Prairie Farm Rehabilitation Administration, Hydrology Division. Regina, Sask. 10 pp. and 5 fig.

McKay, G.A. 1963. Persisting dewpoints in the prairie provinces. Meteorology Report No.11. Hydrometeorological Division. Prairie Farm Rehabilitation Administration, Regina, Sask. 21 pp.

McKay, G.A. 1964. Statistical estimates of probable maximum rainfall in the prairie provinces. Prairie Farm Rehabilitation Administration. Meteorology Report No.7. Regina, Sask. 10 pp.

McKay, G.A. 1965a. Probable maximum snowpack and rainstorm, Penticton Creek, B.C. Canada. Prairie Farm Rehabilitation Administration. Report No. 8. Regina, Sask. 43 pp.

McKay, G.A. 1965b. Statistical estimates of precipitation extremes for the prairie provinces. Prairie Farm Rehabilitation Administration. Regina, Sask. 29 pp.

McKay, G.A. 1966. Meteorological conditions leading to the project design and probable maximum flood-Paddle River, Alberta, Canada. Prairie Farm Rehabilitation Administration Meteorology Report No. 19. Regina, Sask. 54 pp. and 25 fig.

McKay, G.A. 1968. Meteorological condition leading to the project design and probable maximum flood on the Paddle River. Transactions of the American Society of Agricultural Engineering. 11(6):821-825.

McKay, G.A. and W. Stichling. 1961. Rainfall and runoff from a prairie thundershower. Meteorological Branch. Atmospheric Environment Service, Downsview, Ont. CIRC-3524. TEC-368. 11 pp.

McKay, G.A. and H.A. Thompson. 1968. Snow cover in the prairie provinces of Canada. Transactions of the American Society of Agricultural Engineering. 11(6):812-815.

McMorine, J.G.S. and G.A. McKay. 1962. Storm rainfall and runoff at Buffalo Gap, Saskatchewan May 30, 1961. Meteorological Report No.2. Hydrology Division. Prairie Farm Rehabilitation Administration, Regina, Sask. 12 pp.

Miller, J.F. 1964. Two-to ten day precipitation for return periods of 2 to 100 years in the contiguous United States. Department of Commerce, Weather Bureau Technical Paper No. 49. 29 pp.

Mokievsky-Zubak, O. 1975. Sudden flood and sorted debris over the winter snowpack within Sentinel Glacier Basin,

British Columbia. Canadian Journal of Earth Sciences, 12(5):878-879.

Mokosch, E. 1961. Location of lows east of the Rockies. Meteorological Branch. Atmospheric Environment Service, Downsview, Ont. CIRC 3575. TEC-386. 10 pp.

Mokosch, E. 1962. Mean pressure maps for summer rain in southern Alberta. Meteorological Branch. Atmospheric Environment Service, Downsview, Ont. CIR 3594. TEC-393. 13 pp.

Morin, G., J.P. Forten, J.P. Lardeau and W. Sochanska. 1979. Modèle hydrologique CEQUEAU. Manuel d'utilisation. Université du Québec. INRS-EAU. Québec.

Mowchenko, M. 1965. Magnitude and frequency of floods on major prairie streams. Prairie Farm Rehabilitation Administration. Regina, Sask. Report No. 42. 46 pp.

Murray, W.A. 1964. Rainfall-intensity-duration-frequency maps for British Columbia. Meteorological Branch. Atmospheric Environment Service, Downsview, Ont. CIR-4031. TEC-518. 20 pp.

Mustapha, A.M. 1970a. Probable maximum floods on the Pembina River near Entwistle. Hydrology Branch. Alberta Environment. Edmonton, Alberta.

Mustapha, A.M. 1970b. June 1970 storms in Lesser Slave Lake and Lac La Biche forestry regions. Hydrology Branch. Alberta Environment Edmonton, Alberta. 18 pp.

Mustapha, A.M. and P.M. Ojamaa. 1975. Probable maximum flood-Red Deer River flow regulation proposal. Technical Services Division. Alberta Environment. Edmonton, Alberta.

Mustapha, A.M., G.W. Samide and W.H. Kuhnke. 1976. Flood forecasting-Oldman River Basin. Pages 101-105 in Proceedings of the 44th Western Snow Conference. Calgary, Alberta. 101-105.

Mustapha, A.M., S. Figliuzzi, H. Rickert, and G. Coles. 1981. History of floods in the North Saskatchewan River Basin. Alberta Environment. Edmonton, Alberta. 124 pp.

Muttitt, G.H. 1961. Spring and summer rainfall patterns in Alberta. Meteorological Branch. Atmospheric Environment Service, Downsview, Ont. CIRC 3512. TEC-361. 22 pp.

Muzik, I. 1975. Red Deer River flow regulation planning study, hydrologic study. Alberta Environment, Technical

Services Division. Edmonton, Alberta.

Myers, V.A. 1959. Meteorology of hypothetical flood sequences in the Mississippi River basin. Hydrometeorological Report No. 35. U.S. Weather Bureau.

Myers, V.A. 1966. Criteria and limitations for the transportation of large storms over various size watersheds. Pages 45-66 in Symposium on Consideration of Some Aspects of Storms and Floods in Water Planning. Texas Water Development Board. Report 33.

Myers, V.A. 1967. Meteorological estimation of extreme precipitation for spillway design floods. U.S. Department of Commerce. Technical Memorandum WBTM HYDRO-5. 29 pp.

Nash, J.E. 1957. The form of the instantaneous unit hydrograph. International Association of Scientific Hydrology. Publication 45. 3:14-121.

Neill, C.R. 1965. A comparison of rare floods on larger streams in Alberta. Alberta Research Council Open File Report 1965-1. Edmonton, Alberta. 11 pp.

Neill, C.R., D.P. Bray, M.F. Schouten, and J.R. Card. 1970. Selected characteristics of streamflow in Alberta. Alberta Research Council. River Engineering and Surface Hydrology Report 70-1. Edmonton, Alberta.

Neill, C.R. and G.V. Gehmlich. 1965. Hydrologic data on flood in the North Saskatchewan River. Alberta Research Council. Unpublished Report. Highway Research Division. Edmonton, Alberta.

Neill, C.R., G.V. Gehmlich and E.F. Taylor. 1964. Hydrologic data on floods in the Red Deer River. Alberta Research Council. Unpublished Report. Highway Research Division. Edmonton, Alberta.

Newton, D.W. 1960. Storms and floods on small areas. Journal of Geophysical Research. 65(7):2117-2123.

Nicks, A.D. and M.A. Hartman. 1966. Variation of rainfall over a large gages area. Transactions of the American Society of Agricultural Engineering. 9(3):437-439.

Nkemdirim, L.C. and P.W. Benart. 1975. Heavy snowfall expectations for Alberta. The Canadian Geographer. 19:60-72.

Overton, D.E. 1966. Muskingum flood routing of upland streamflow. Journal of Hydrology. 4(3):185-200.

Papadakis, C. and H.C. Preul. 1972. University of Cincinnati urban runoff model. Journal of Hydraulics Division. Proceedings of the American Society of Civil Engineers. 98(HY10):1789-1804.

Paulhus, J.L.H. and C.S. Gilman. 1953. Evaluation of probable maximum precipitation. Transactions American Geophysical Union. 34(5):701-708.

Pollock, D.M. 1975. An index to storm rainfall in Canada. Environment Canada. CLI-1-75. Downsview, Ontario. 37 pp.

Pollock, D.M. and G.J. Gaye. 1973. One-day extreme rainfall statistics for the prairie provinces. Environment Canada. CLI-5-73. Downsview, Ontario.

Pollock, D.M. and T.F. Gigliotti. 1975. Critical meteorological conditions for maximum flows on the Pine, Beatton and Halfway Rivers in British Columbia with an estimate of associated conditions for the Peace River above the W.A.C. Bennett Dam. Unpublished report. Atmospheric Environment Service. Downsview, Ont.

Potter, J.G. 1965. Snow cover. Climatological Studies No. 3, Department of Transport. Meteorological Branch. Atmospheric Environment Service, Downsview, Ont.. 69 pp.

Preul, H.C. and C.N. Papadakis. 1973. University of Cincinnati urban runoff (UCUR) model-user's manual. University of Cincinnati, Ohio. Department of Civil Engineering.

Pugsley , W.I. (ed.) 1981. Downsview, Ontario. Flood hydrology guide for Canada: Hydrometeorological design techniques. Environment Canada. CLI3-81. 102 pp.

Quick, M.C. and A. Pipes. 1975. U.B.C. watershed model. Proceedings WMO/IAHS Symposium on the Application of Mathematical Models in Hydrology and Water Resources System. Bratislava, Czechoslovakia.

Reich, B.M. 1963. Short-duration rainfall-intensity estimates and other design aids for regions of sparse data. Journal of Hydrology. 1:3-28.

Reid, T.C. and K.G. Brittain. 1962. Design concepts of the Brazeau development including river and hydrology studies. The Engineering Journal. 45(10):60-66.

Ricca, V.T. 1972. The Ohio State University version of the Stanford streamflow simulation model, Part I-Technical

Aspects. Ohio State University, Columbus.

Riedel, J.T., J.F. Appleby, and R.W. Schloemer. 1956. Seasonal variation of the probable maximum precipitation east of the 105th meridian for areas from 10 to 100 square miles and durations of 6,12, 24, and 48 Hours. Hydrometeorological Report No. 33. U.S. Weather Bureau.

Riedel, J.T., F.K. Schwarz, and R.L. Weaver. 1969. Probable maximum precipitation over the South Platte River, Colorado, and Minnesota. River, Minnesota Hydrometeorological Report No. 44. U.S. Weather Bureau.

Rockwood, D.M. 1958. Columbia basin streamflow routing by computer. Journal of Waterways and Harbors Division. American Society of Civil Engineers. Vol. 84. Part 1. Paper No. 1874. Also published in American Society of Civil Engineers. Transactions Paper No. 3119, 1961.

Rockwood, D.M. and J.A. Anderson. 1969. Probable maximum floods for Mekong river projects. American Society of Civil Engineers. National Meeting on Water Resources Engineering. New Orleans, Louisiana.

Sampson, R.J. 1975. Surface II Graphics System. Kansas Geological Survey. Lawrence, Kansas. 240 pp.

Schwarz, F.K. 1961. Meteorology of flood-producing storms in the Ohio River Basin. Hydrometeorological Report No. 38. U.S. Weather Bureau.

Schwarz, F.K. 1967. The role of persistence, instability and moisture in the intense rainstorm in eastern Colorado, June 14-17, 1965. Technical Memorandum WBTM HYDRO-3. ESSA. U.S. Department of Commerce.

Schwarz, F.K. 1977. Probable maximum precipitation for southeast Alaska. Pages 97-103 in Second Conference on Hydro-Meteorology. Toronto, Ontario.

Sherman, L.K. 1932. Stream-flow from rainfall by the unit-graph method. Engineering News Record. 108:501-505.

Sherman, L.K. 1944. Discussion of primary role of meteorology in flood-flow estimating. Transactions of the American Society of Civil Engineers. 109:369.

Shortley, G. and D. Williams. 1961. Elements of Physics. Third Edition. Prentice-Hall, Inc.. Englewood Cliffs, N.J. 928 pp.

Showalter, A.K. 1945. Quantitative determination of maximum

rainfall. Section in: Handbook of Meteorology. Edited by F.A. Berry, E. Bollay and N.R. Beers, McGraw-Hill. New York. 1015-1027.

Showalter, A.K. 1954. Precipitable water template. Bulletin of the American Meteorological Society. 35:129-131.

Showalter, A.K. and S.B. Solot. 1942. Computation of maximum possible precipitation. Transactions of the American Geophysical Union. Part 2. 258-274.

Simmons, G.E. 1959. Snowmelt runoff-Fraser River Basin. Pages 227-254 in Proceedings of Hydrology Symposium No. 1. Spillway Design Floods. Ottawa. National Research Council.

Sittner, W.T., C.E. Schauss, and J.C. Monro. 1969. Continuous hydrograph synthesis with an API-type hydrologic model. Water Resources Research. No.5. 1007-1022.

Slade, J.J. 1936. The reliability of statistical methods in the determination of flood frequencies. U.S. Geological Survey. Water Supply Paper 771. 421-432.

Snyder, F.F. 1938. Synthetic unit-graphs. Transactions American Geophysical Union. 19:447-454.

Soil Conservation Service. 1969. Hydrology. Section 4. National Engineering Handbook. U.S. Department of Agriculture, Washington, D.C.

Sporns, U. 1962. Occurrence of severe storms in the lower Fraser valley, B.C.. Meteorological Branch. Atmospheric Environment Service, Downsview, Ont. CIR-3631. TEC-404. 11 pp.

Sporns, U. 1963a. Frequency and severity of storms in the lower Fraser valley, B.C.. Meteorological Branch. Atmospheric Environment Service, Downsview, Ont. CIR-3848. TEC-469. 44 pp.

Sporns, U. 1963b. Rainfall-intensity-duration-frequency maps for Ontario. Meterological Branch. Atmospheric Environment Service, Downsview, Ont. CIR-3895. TEC-480. 14 pp.

Sporns, U. 1964. Transposition of short duration rainfall intensity data in mountainous areas. Meteorological Branch. Atmospheric Environment Service, Downsview, Ont. CIR-4032. TEC-519. 6 pp.

Storr, D. 1963. Maximum one-day rainfall frequencies in

Alberta. Meteorological Branch. Atmospheric Environment Service, Downsview, Ont. CIR 3796. TEC-451. 27 pp.

Storr, D. 1964a. Maximum one-day rainfall frequencies in northeastern B.C. Meteorological Branch. Atmospheric Environment Service, Downsview, Ont. CIR-4015. TEC-513. 3 pp.

Storr, D. 1964b. Maximum one-day rainfall frequencies in Saskatchewan. Atmospheric Environment Service, Downsview, Ont. Meteorological Branch CIR 4078. TEC-528. 26 pp.

Storr, D. 1967. A frequency analysis of maximum two-day and three-day rainfalls in Saskatchewan, Alberta and northeastern British Columbia. Meteorological Branch. Atmospheric Environment Service, Downsview, Ont. TEC-654. 17 pp.

Storr, D. 1978. A comparision of daily snowmelt calculated by the U.S. Corps of Engineers theoretical model With measured amounts on a snowpillow, Alberta Environment. Technical Services Division, Flow Forecasting. Edmonton, Alberta. 30 pp.

Tennessee Valley Authority. 1973. Storm hydrographs using a double-triangle model. Knoxville, Tenn.

Thomas, M.K. 1964. Snowfall in Canada. Meteorological Branch. Atmospheric Environment Service, Downsview, Ont. TEC-503. 16 pp.

Thomas, M.K. and J.P. Bruce. 1957. Storm Audrey in Ontario, June 1957. Meteorological Branch. Atmospheric Environment Service, Downsview, Ont. TEC-256. 13 pp.

Thompson, C.E. 1950. Cold lows affecting Alberta in summer (June-September). Meteorological Branch. Atmospheric Environment Service, Downsview, Ont. CIR 1813. TEC-76. 12 pp.

Thompson, H.A. and U. Sporns. 1964. Critical durations of snowmelt periods in the Liard and Hay River floods. Meteorological Branch. Atmospheric Environment Service, Downsview, Ont. CIR-4030. TEC-517. 22 pp.

Thompson, W.C. 1974. Rainfall intensities and topographical features. Technical Report No. 46 to the Prairie Provinces Water Board Committee on Hydrology. 120 pp.

Thompson, W.C. 1976. Three early severe flood producing storms in Alberta. Meteorological Branch. Atmospheric Environment Service, Downsview, Ont. TEC-827. 19 pp.

U.S. Army Corps of Engineers. 1952. Standard project flood determinations. Civil Engineering Bulletin 52(8).

U.S. Army Corps of Engineers. 1956. Snow hydrology summary report of snow investigations. Portland, Oregon. 433 pp.

U.S. Army Corps of Engineers. 1959. Flood hydrograph analysis and computations. EM1110-2-1405.

U.S. Army Corps of Engineers. 1960. Runoff from snowmelt. Engineering and Design Manuals. EM1110-1-1406.

U.S. Army Corps of Engineers. 1972. Program description and user manual for SSARR model streamflow synthesis and reservoir regulation. Program 724-K5-G0010.

U.S. Army Corps of Engineers. 1973. HEC-1 flood hydrograph package, users and programmers manuals. HEC Program 723-X6-L2010.

U.S. Army Waterways Experiment Station. 1974. Models and methods applicable to Corps of Engineers urban studies. Miscellaneous Paper H-74-8. National Technical Information Service.

U.S. Department of Commerce. 1941. Maximum possible precipitation over the Ohio River Basin above Pittsburg, Pa. Hydrometeorological Report No. 2. 21 pp.

U.S. Department of Commerce. 1943. Maximum possible precipitation over the Sacramento Basin of California. Hydrometeorological Report No. 3. 225 pp.

U.S. Department of Commerce. 1948. Highest persisting dew points in western United States. Technical Report No. 5. 27 pp.

U.S. Department of Commerce. 1951. Tables of precipitable water and other factors for a saturated pseudsadiabatic atmosphere. Technical Report No. 14. 27 pp.

U.S. Department of Commerce. 1956. Seasonal variation of the probable maximum precipitation east of the 105th meridian for areas from 10 to 1000 square miles and durations of 6, 12, 24, and 48 hours. Hydrometeorological Report No. 33. 58 pp.

U.S. Department of Commerce. 1960. Generalized estimates of probable maximum precipitation for the United States west of the 105th meridian. Technical Report No. 38.

U.S. Department of Commerce. 1961a. Interim report-probable

maximum precipitation in California. Hydrometeorological Report No. 36. 202 pp.

U.S. Department of Commerce. 1961b. Generalized estimates of probable maximum precipitation and rainfall-frequency Data for Puerto Rico and Virgin Islands. Technical Paper No. 42. 97 pp.

U.S. Department of Commerce. 1966a. Probable maximum precipitation, north-west states. Hydrometeorological Report No. 43. 228 pp.

U.S. Department of Commerce. 1966b. Meteorological conditions for the probable Maximum flood on the Yukon River above Rampart, Alaska. Hydrometeorological Report No. 42. 97 pp.

U.S. Department of Commerce. 1969. Probable maximum precipitation over South Platte River, Colorado and Minnesota River, Minnesota. Hydrometeorological Report No. 44. 114 pp.

U.S. Department of Commerce. 1970. Probable maximum precipitation, Mekong River Basin. Hydrometeorological Report No. 46.

U.S. Department of Commerce. 1973a. Meteorological criteria for extreme floods for four basins in Tennessee and Cumberland River watersheds. Hydrometeorological Report No. 47. 59 pp.

U.S. Department of Commerce. 1973b. Probable maximum precipitation and snowmelt criteria for Red River of the North above Pembina, and Souris River above Minot, North Dakota. Hydrometeorological Report No. 48, 69 pp.

U.S. Department of Commerce. 1978. Probable maximum precipitation estimates, United States east of the 105th meridian. Hydrometeorological Report No. 51. 87 pp.

U.S. Weather Bureau. 1947. Generalized estimates of maximum possible precipitation over the United States east of the 105th meridian. Hydrometeorological Report No. 23, 62 pp.

Verschuren, J.P. and L. Wojtiw. 1980. Estimate of the maximum probable precipitation for Alberta river basins. Alberta Environment, Hydrology Branch. RMD-80/1. Edmonton, Alberta. 307 pp.

Viessman, W., J.W. Knapp, G.L. Lewis, and T.E. Harbaugh. 1977. Introduction to Hydrology. Dun-Donnelley

Publisher. N.Y., 2nd Edition. 704 pp.

Warner, L.A. 1973. Flood of June 1964 in the Oldman and Milk River Basins, Alberta. Environment Canada. Technical Bulletin No. 73 (Inland Water Directorate). 89 pp.

Warner, L.A. and W.C. Thompson. 1974. Flood of June 1972 in the southern Peace (Smoky River) Basin, Alberta. Water Resources Branch. Technical. Bulletin No. 87. 51 pp.

Water Survey of Canada, Surface Water Data, Alberta, Environment Canada. Annual Publication.

Water Survey of Canada. 1977. Velocity and cross section data for selected Alberta stream gauging stations. Environment Canada. 8 pp. and 73 pp of Graphs.

Weaver, R.L. 1962. Meteorology of hydrological critical storms in California. Hydrometeorological Report No. 37. U.S. Weather Bureau.

Weaver, R.L. 1968. Meteorology of major storms in western Colorado and eastern Utah. Technical Memorandum WBTM HYDRO-7. ESSA. U.S. Department of Commerce.

Weiss, L.L. 1955. A nomogram based on the theory of extreme values for determining values for various return periods. Monthly Weather Review. 83:69-71.

Weiss, L.L. 1964. Ratio of true to fixed-interval maximum rainfall. Proceedings of the American Society of Civil Engineers. Journal of Hydrology Division. 90:77-82.

Williams, J.R. 1969. Flood Routing with Variable Travel Time or Variable Storage Coefficients. Transactions of the American Society of Agricultural Engineers. 12(1):100-103.

Williams, J.R. and R.W. Hann, 1973. HYMO: Problem-oriented computer language for hydrologic modeling. U.S. Department of Agriculture. Agriculture Research Service.

Wilson, W.T. 1941a. An outline of the thermodynamics of snowmelt. Transactions of the American Geophysical Union. 22:182-195.

Wilson, W.T. 1941b. A graphical flood-routing method. Transactions of the American Geophysical Union. Part III.

Wilson, H.P. 1948. Investigation of an August storm over western prairies. TEC-42. Report No. 10.

Wisler, C.O. 1951. Estimating floods of rare frequency. International Association of Scientific Hydrology. Brussels, Belgium. 4:71-75.

Wojtiw, L. and J.P. Verschuren. 1981. Climatology of severe rainstorms in Alberta, Canada. Fourth Conference on Hydrometeorology. Reno, Nevada. American Meteorological Society. 21-26.

World Meteorological Organization. 1967. Assessment of the magnitude and frequency of flood flows. Water Resources Series No. 30. 15 pp.

World Meteorological Organization. 1969a. Hydrological forecasting. Technical Note No. 92. 325 pp.

World Meteorological Organization. 1969b. Estimation of maximum floods. Technical Note No. 98. 288 pp.

World Meteorological Organization. 1969c. Manual for depth-area-duration analysis of storm Precipitation. Technical Note No. 129. 114 pp.

World Meteorological Organization. 1973. Manual for estimation of probable maximum precipitation. Operational Hydrology. Report No. 1. 190 pp.

World Meteorological Organization. 1974. Guide to hydrological practices. Report No. 168.

World Meteorological Organization. 1975. Intercomparison of conceptual models used in operational hydrological forecasting. Operational Hydrology. Report No. 7. 172 pp.

APPENDIX A.1

This appendix contains tables used in estimating the PMP by the physical approach.

Table A.1.1 presents values of precipitable water (mm) between the 1000 mb surface and various pressure levels up to 300 mb in a saturated pseudoadiabatic atmosphere as a function of the 1000 mb dew point. Table A.1.2 lists similiar values for layers between the 1000 mb surface, assumed to be at zero elevation, and various heights up to 8 km.

Table A.1.1. Precipitable water (mm) between 1000 mb surface and indicated pressure (mb) in a saturated pseudoadiabatic atmosphere as a function of the 1000 mb dew point (°C)

mb	2	4	6	8	10	12	13	14	15	16	17	18	19	20	21	22	23	24
990	0	0	1	1	1	1	1	1	1	1	1	1	1	1	1	2	2	2
980	1	1	1	1	1	2	2	2	2	2	2	2	3	3	3	3	3	4
960	2	2	2	3	3	3	4	4	4	4	5	5	5	6	6	6	7	7
940	2	3	3	4	4	5	5	6	6	7	7	7	8	9	9	10	10	11
920	3	4	4	5	6	7	7	8	8	9	9	10	10	11	12	13	14	14
900	4	4	5	6	7	8	9	9	10	11	11	12	13	14	15	16	17	18
880	4	5	6	7	8	9	10	11	12	12	13	14	15	16	17	19	20	21
860	5	6	7	8	9	11	12	12	13	14	15	16	18	19	20	21	23	24
840	6	7	8	9	10	12	13	14	15	16	17	19	20	21	23	24	26	28
820	6	7	8	10	11	13	14	15	17	18	19	20	22	24	25	27	29	31
800	7	8	9	11	12	15	16	17	18	19	21	22	24	26	28	29	32	34
700	8	10	12	14	16	19	21	23	24	26	28	31	33	35	38	41	44	47
600	9	11	13	16	19	23	25	27	29	31	34	37	40	43	46	50	54	58
500	10	12	14	17	20	24	27	29	32	34	37	41	44	48	52	56	61	66
400	10	12	15	18	21	25	28	30	33	36	39	43	47	51	55	60	65	71
300	10	12	15	18	21	25	28	30	33	36	40	44	48	52	57	62	67	71

TABLE A.1.2 Precipitable water (mm) between 1000 mb surface and indicated height (m) above that surface in a saturated pseudoadiabatic atmosphere as a function of the 1000 mb dew point (°C)

(m)	2	4	6	8	10	12	14	15	16	17	18	19	20	21	22	23
200	1	1	1	2	2	2	2	2	3	3	3	3	3	4	4	4
400	2	2	3	3	4	4	5	5	5	5	6	6	6	7	7	8
600	3	3	4	5	5	6	7	7	7	8	8	9	10	10	11	11
800	4	4	5	6	7	8	9	9	10	10	11	12	13	13	14	15
1000	4	5	6	7	8	9	10	11	12	13	13	14	15	16	17	18
1200	5	6	7	8	9	11	12	13	14	15	16	17	18	19	20	21
1800	6	7	8	9	10	12	14	15	16	17	18	19	20	22	23	24
1600	6	7	9	10	11	13	15	16	17	19	20	21	23	24	25	27
1800	7	8	9	11	12	14	17	18	19	20	22	23	25	26	28	30
2000	7	9	10	11	13	16	18	19	21	22	24	25	27	29	31	33
2200	8	9	10	12	14	16	19	20	22	24	25	27	29	31	33	35
2400	8	9	11	13	15	17	20	22	23	25	27	29	31	33	35	37
2600	8	10	11	13	16	18	21	23	24	26	28	30	32	35	37	40
2800	9	10	12	14	16	19	22	24	26	27	30	32	34	36	39	42
3000	9	10	12	14	17	20	23	25	27	29	31	33	35	38	41	44
4000	10	11	14	16	19	22	26	28	31	33	36	39	42	45	48	52
5000	10	12	14	17	20	24	28	31	33	36	39	42	46	50	54	58
6000	10	12	15	17	21	25	30	32	35	38	42	45	49	53	57	62
7000	10	12	15	18	21	25	30	33	36	39	43	46	51	55	60	65
8000	10	12	15	18	21	26	30	33	36	40	43	47	52	56	61	67

APPENDIX A.2

The following pages describe a number of relationships of air temperature, wind speed, and precipitation and the multicorrelation coefficients associated with each relationship for river basins in Alberta. The notations used in these relationships are defined as follows;

T_m is mean of the daily maximum air temperature (°F)
L_A is the latitude (degrees)
L_o is the longitude (degrees)
E is the elevation above sea level (feet)
P_{mp} is the Probable Maximum Precipitation (inches)
A is the watershed area (sq. mi.)
D is the duration of the precipitation (hours)
U_m is the average hourly wind speed (miles per hour)

I. North Saskatchewan River Basin

1. Relationships of Air Temperatures

1.1 $T_m = 130.34 + 0.2503\ L_A - 0.6627\ L_o$ (r=0.591)

1.2 $T_m = 144.87 - 1.2647\ L_A - 0.003169\ L_o - 0.003465\ E$ (r=0.762)

1.3 $\log T_m = 3.2707 + 0.43616 \log L_A - 1.0663 \log L_o$ (r=0.936)

1.4 $\log T_m = 4.0913 - 2.3768 \log L_A + 1.3476 \log L_o$
$- 0.27242 \log E$ (r=0.999)

2. Relationships of Wind speed

2.1 $U_m = 17.365 + 0.8865\ L_A - 0.4679\ L_o$ (r=0.375)

2.2 $U_m = 72.473 - 5.7414\ L_A + 2.4667\ L_o - 0.0140\ E$ (r=0.703)

2.3 $\log U_m = -12.513 + 12.064 \log L_A - 3.5232 \log L_o$ (r=0.691)

2.4 $\log U_m = 0.9254 - 34.005 \log L_A + 36.010 \log L_o$
$- 4.4614 \log E$ (r=0.800)

3. Relationships of 24-hr PMP

3.1 $P_{mp} = -51.265 - 3.7902\ L_A + 2.5287\ L_o - 0.009\ E$ (r=0.944)

3.2 $\log P_{mp} = -20.21 + 3.6685\ L_A + 7.2609\ L_o$ (r=0.793)

3.3 $\log P_{mp} = -11.502 - 26.182 \log L_A + 32.876 \log L_o$
$- 2.8908 \log E$ (r=0.906)

3.4 $P_{mp} = 70.496 - 0.96661\ T_m + 0.51442\ U_m$ (r=0.920)

3.5 $\log P_{mp} = 14.591 - 7.7558 \log T_m + 0.61750 \log U_m$ (r=0.920)

4. Relationships of D-hr PMP

4.1 $P_{mp} = 5.2039 - 7.3106\ L_A + 3.8323\ L_o - 0.01588\ E$
$+ 0.09558\ D - 0.000144\ A$ (r=0.909)

4.2 $\log P_{mp} = -2.372 - 31.584 \log L_A + 33.455 \log L_o$
$- 3.2866 \log E + 0.41885 \log D - 0.071215 \log A$ (r=0.945)

II. South Saskatchewan River Basin

1. Relationships of Air Temperatures

1.1 $T_m = 313.61 + 0.5845\ L_A - 2.425\ L_o$ $(r=0.902)$

1.2 $T_m = 169.8 - 0.8261\ L_A - 0.4081\ L_o - 0.004069\ E$ $(r=0.967)$

1.3 $\log T_m = 9.1855 + 0.4348 \log L_A - 3.9388 \log L_o$ $(r=0.894)$

1.4 $\log T_m = 3.921 \quad 0.6511 \log L_A - 0.1003 \log L_o$
$- 0.2194 \log E$ $(r=0.978)$

2. Relationships of Wind Speed

2.1 $U_m = -221.72 - 1.897\ L_A + 3.0739\ L_o - 0.00462\ E$ $(r=0.949)$

2.2 $\log U_m = -41.372 - 6.3183 \log L_A + 28.088 \log L_o$
$- 1.2456 \log E$ $(r=0.959)$

3. Relationships of D-hr PMP

3.1 $P_{mp} = -77.295 - 0.7653\ L_A + 1.115\ L_o + 0.1373\ D$
$- 0.00041\ A$ $(r=0.914)$

3.2 $P_{mp} = -49.068 - 0.7144\ L_A + 0.8216\ L_o + 0.00076\ E$
$+ 0.1373\ D - 0.00041\ A$ $(r=0.915)$

3.3 $\log P_{mp} = -13.169 - 2.2104 \log L_A + 8.6522 \log L_A$
$- 0.08197 \log E + 0.5029 \log D - 0.0676 \log A$ $(r=0.936)$

3.4 $\log P_{mp} = -11.161 - 2.1137 \log L_A + 7.4547 \log L_o$
$+ 0.5029 \log D - 0.0676 \log A$ $(r=0.935)$

III. Athabasca River Basin

1. Relationships of Air Temperatures

1.1 $T_m = 81.112 + 0.1099\ L_A - 0.1635\ L_o$ (r=0.419)

1.2 $T_m = 99.978 - 0.9638\ L_A + 0.2459\ L_o - 0.0033\ E$ (r=0.733)

1.3 $\log T_m = 2.2064 + 0.0966 \log L_A - 0.262 \log L_o$ (r=0.419)

1.4 $\log T_m = 4.1384 - 1.751 \log L_A + 0.6004 \log L_o - 0.1498 \log E$ (r=0.784)

2. Relationships of Wind Speeds

2.1 $U_m = 87.153 - 0.1793\ L_A - 0.6213\ L_o + 0.00148\ E$ (r=0.570)

2.2 $\log U_m = 49.124 - 26.131 \log L_A + 1.277 \log L_o - 1.616 \log E$ (r=0.702)

3. Relationships of D-hr PMP

3.1 $P_{mp} = 117.57 - 1.0002\ L_A - 0.4849\ L_o + 0.146\ D - 0.00037\ A$ (r=0.960)

3.2 $P_{mp} = 104.69 - 0.5232\ L_A - 0.6245\ L_o + 0.0013\ E + 0.146\ D - 0.00037\ A$ (r=0.961)

3.3 $\log P_{mp} = 19.2 - 4.841 \log L_A - 5.08 \log L_o + 0.597 \log D - 0.0706 \log A$ (r=0.962)

3.4 $\log P_{mp} = 36.72 - 22.365 \log L_A + 3.687 \log L_o - 1.5362 \log E + 0.597 \log D - 0.0706 \log A$ (r=0.968)

IV. Peace River Basins

1. Relationships of Air Temperatures

1.1 $T_m = 62.546 + 0.5792\ L_A - 0.222\ L_o$ (r=0.869)

1.2 $T_m = 63.091 - 0.5347\ L_A + 0.3654\ L_o - 0.0038\ E$ (r=0.950)

1.3 $\log T_m = 1.7907 + 0.478 \log L_A - 0.381 \log l_o$ (r=0.869)

1.4 $\log T_m = 1.778 + 0.0558 \log L_A - 0.0436 \log L_o - 0.039 \log E$ (r=0.889)

2. Relationships of Wind Speeds

(none available because of insufficient wind data)

3. Relationships of D-hr PMP

3.1 $P_{mp} = -251.19 - 0.0134\ L_A + 2.19\ L_o - 0.094\ D - 0.00028\ A$ (r=0.955)

3.2 $P_{mp} = -274.29 + 0.643\ L_A + 2.037\ L_o + 0.0022\ E + 0.094\ D - 0.00028\ A$ (r=0.958)

3.3 $\log P_{mp} = -59.416 + 1.0882 \log L_A + 27.93 \log L_o + 0.508 \log D - 0.0687 \log A$ (r=0.965)

3.4 $\log P_{mp} = -63.818 + 3.8176 \log L_A + 27.310 \log L_o + 0.2773 \log E + 0.508 \log D - 0.0687 \log A$ (r=0.966)

V. Combined Basins in Alberta

(North Saskatchewan, South Saskatchewan, Red Deer, Athabasca, and Peace)

1. Relationships of Air Temperatures

1.1 $T_m = 112.31 - 1.2464\ L_A + 0.3902\ L_o - 0.0089\ E$ (r=0.469)

1.2 $\log T_m = 6.818 + 6.192 \log L_A - 7.631 \log L_o$ (r=0.325)

1.3 $\log T_m = 6.468 + 4.233 \log L_A - 5.391 \log L_o - 0.259 \log E$ (r=0.328)

2. Relationships of Wind Speeds

2.1 $U_m = 38.802 - 1.3324\ L_A + 0.433\ L_o - 0.0018\ E$ (r=0.664)

2.2 $\log U_m = 3.4247 - 6.255 \log L_A + 4.765 \log L_o - 0.3965 \log E$ (r=0.651)

APPENDIX A.3

The following pages contain information calculated and used in the HYMO Model for estimation of PMF. The notations used are defined as follows:

(a) Kellerhals reach number (Kellerhals et al., 1972)
(b) Water loading (inches)
(c) Total intensity (inches per hour)
(d) Drainage area (sq. mi.) (Water Survey of Canada)
(e) Average slope (feet per mile) (Kellerhals et al., 1972)
(f) PMF (cfs)
(g) Instantaneous daily recorded discharge (cfs) (Water Survey of Canada)

Peace River Basin

(a)	(b)	(c)	(d)	(e)	(f)	(g)
9	22.00	2.85	4350.	2.69	508215.	96400.
10	22.00	2.85	4130.	4.96	766062.	37500.
11	22.00	2.85	1810.	6.34	480200.	17800.
8	22.00	2.85	18500.	2.75	1505246.	195000.
3	22.00	2.85	50200.	1.16	1604800.	391000.
4	22.00	2.85	72000.	1.85	3012998.	549000.

Athabasca River Basin

(a)	(b)	(c)	(d)	(e)	(f)	(g)
12	24.76	1.89	1580.	**15.84**	840827.	21800.
13	24.76	1.89	4000.	5.28	888785.	53000.
14	24.76	1.89	7300.	6.34	1597562.	75200.
18	24.76	1.89	373.	28.51	320740.	3870.
19	24.76	1.89	1000.	6.34	347270.	32000.
20	24.76	1.89	2510.	5.28	624102.	80000.
21	24.76	1.89	350.	6.34	149191.	4860.
22	24.76	1.89	662.	17.42	433345.	14100.
23	24.76	1.89	1110.	1.74	150101.	20100.
24	24.76	1.89	1710.	10.56	721111.	19900.
25	24.76	1.89	4550.	1.16	310825.	19400.
116	24.76	1.89	671.	7.39	275957.	3380.
26	24.76	1.89	341.	20.59	268961.	4310.
27	24.76	1.89	124.	10.56	82869.	2340.
28	24.76	1.89	5690.	1.16	366066.	8500.
29	24.76	1.89	430.	3.64	124976.	6270.
30	24.76	1.89	500.	3.06	124803.	8670.
117	24.76	1.89	742.	1.69	108740.	17360.
120	24.76	1.89	6140.	3.06	816025.	7340.
31	24.76	1.89	9380.	2.16	854475.	25200.
32	24.76	1.89	5460.	1.48	429205.	21800.
15	24.76	1.89	29600.	1.53	1523848.	199600.

North Saskatchewan River Basin

(a)	(b)	(c)	(d)	(e)	(f)	(g)
35	27.72	2.48	1980.	13.73	1041845.	43840.
36	27.72	2.48	4220.	13.20	1890563.	145000.
37	27.72	2.48	10500.	1.85	923075.	204500.
39	27.72	2.48	94.	1.21	20468.	2310.
40	27.72	2.48	500.	32.21	501838.	18000.
41	27.72	2.48	1210.	6.34	447946.	39100.
42	27.72	2.48	318.	19.01	269846.	3860.
44	27.72	2.48	2190.	7.92	822365.	24000.
115	27.72	2.48	1310.	8.98	588058.	3170.
45	27.72	2.48	2200.	1.95	304661.	1490.
118	27.72	2.48	990.	2.43	197782.	325.
38	27.72	2.48	21300.	1.00	963260.	120000.

Bow/Nelson River Basin

(a)	(b)	(c)	(d)	(e)	(f)	(g)
113	24.96	2.04	165.	18.48	135152.	4360.

(a)	(b)	(c)	(d)	(e)	(f)	(g)
60	24.96	2.04	858.	0.69	61819.	14100.
61	24.96	2.04	1610.	9.50	647293.	21210.
62	24.96	2.04	1960.	21.12	1153205.	31900.
63	24.96	2.04	2500.	10.56	976264.	21400.
64	24.96	2.04	3010.	9.50	1065615.	53600.
65	24.96	2.04	6000.	6.34	1384634.	44100.
66	24.96	2.04	7610.	4.28	1239312.	89700.
67	24.96	2.04	136.	79.20	142917.	2860.
68	24.96	2.04	54.	100.32	69158.	710.
70	24.96	2.04	276.	35.90	266263.	5060.
71	24.96	2.04	362.	30.62	329457.	362.
72	24.96	2.04	346.	33.79	325536.	13900.
73	24.96	2.04	187.	13.20	128209.	10300.
74	24.96	2.04	306.	40.66	306163.	15200.
77	24.96	2.04	300.	31.15	278040.	10000.
78	24.96	2.04	421.	22.18	327203.	8000.
79	24.96	2.04	906.	8.45	378629.	25100.
81	24.96	2.04	96.	22.70	91043.	2030.
82	24.96	2.04	176.	33.26	177210.	12000.
83	24.96	2.04	232.	31.15	216591.	6900.
84	24.96	2.04	628.	20.06	432848.	21400.
112	24.96	2.04	25600.	1.90	1627605.	75100.
58	24.96	2.04	22500.	2.16	1638390.	151800.
91	24.96	2.04	11000.	2.32	1430983.	68200.

Oldman/Nelson River Basin

85	34.88	2.12	551.	20.06	542510.	16000.
86	34.88	2.12	730.	24.29	745253.	27300.
87	34.88	2.12	1700.	8.45	900451.	26100.
88	34.88	2.12	2230.	8.98	1158739.	78500.
89	34.88	2.12	3450.	6.34	1282467.	67500.
90	34.88	2.12	6630.	4.96	1753966.	149000.
92	34.88	2.12	162.	12.67	154921.	2610.
93	34.88	2.12	268.	16.90	269226.	8000.
94	34.88	2.12	319.	16.90	311788.	18000.
95	34.88	2.12	435.	19.54	429239.	44000.
96	34.88	2.12	57.	35.38	70840.	6090.
97	34.88	2.12	446.	4.22	202083.	10000.
98	34.88	2.12	900.	4.17	343835.	20920.
100	34.88	2.12	121.	44.88	154058.	16400.
101	34.88	2.12	476.	10.03	353055.	11700.
103	34.88	2.12	238.	10.03	195042.	25700.
104	34.88	2.12	674.	13.20	541039.	16500.
106	34.88	2.12	12.	58.08	16830.	1180.
107	34.88	2.12	469.	21.65	475923.	40000.
108	34.88	2.12	1410.	10.56	887738.	16200.
109	34.88	2.12	117.	26.93	140709.	11400.

Milk/Mississippi River Basin

110	34.88	2.12	1040.	3.12	311720.	8730.

(a)	(b)	(c)	(d)	(e)	(f)	(g)
Red Deer River Basin						
48	25.40	1.70	954.	30.10	743482.	23100.
49	25.40	1.70	4480.	6.90	1203303.	68250.
50	25.40	1.70	9580.	2.00	838583.	43000.
55	25.40	1.70	690.	4.60	216936.	7400.
52	25.40	1.70	174.	21.10	143673.	3020.
119	25.40	1.70	291.	4.90	114335.	316.
57	25.40	1.70	1400.	6.34	465673.	2130.
54	25.40	1.70	754.	2.69	160094.	4810.
53	25.40	1.70	924.	11.09	463708.	5310.
51	25.40	1.70	16800.	1.58	1057918.	46200.

APPENDIX A.4

Graphs of HYMO Model results obtained for Alberta river basins. These results include: (1) comparison of PMF normalized discharge with drainage area, (2) comparison of the runoff coefficient (C) with average slope, (3) comparison of the ratio of PMF to maximum recorded discharge with drainage area, and (4) comparison of PMF normalized discharge with average slope.

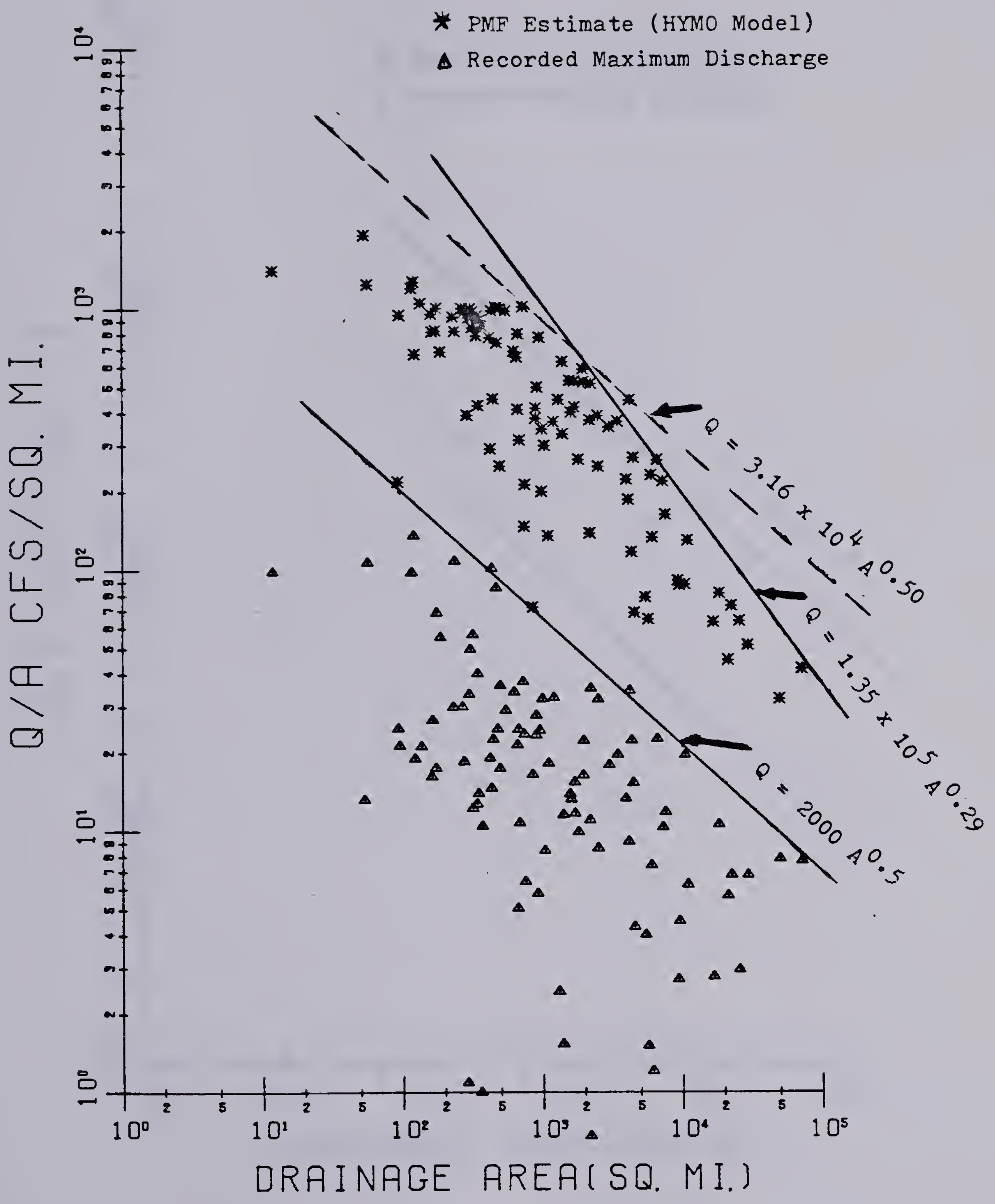

FIGURE A.4.1 Comparison of the PMF Normalized Discharge with Drainage Area for Alberta River basins.

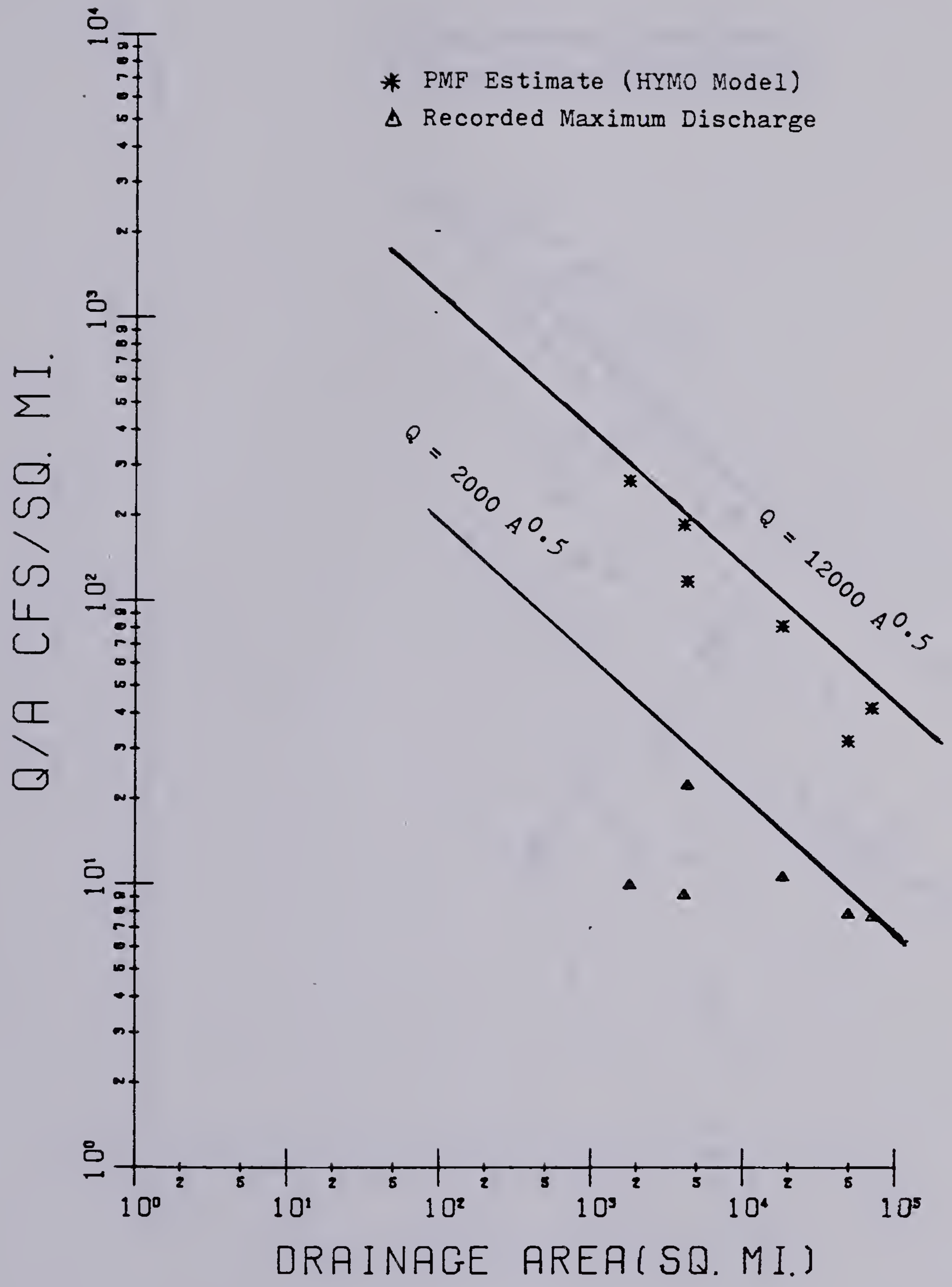

FIGURE A.4.2 Comparison of the PMF Normalized Discharge with Drainage Area for the Peace River Basin.

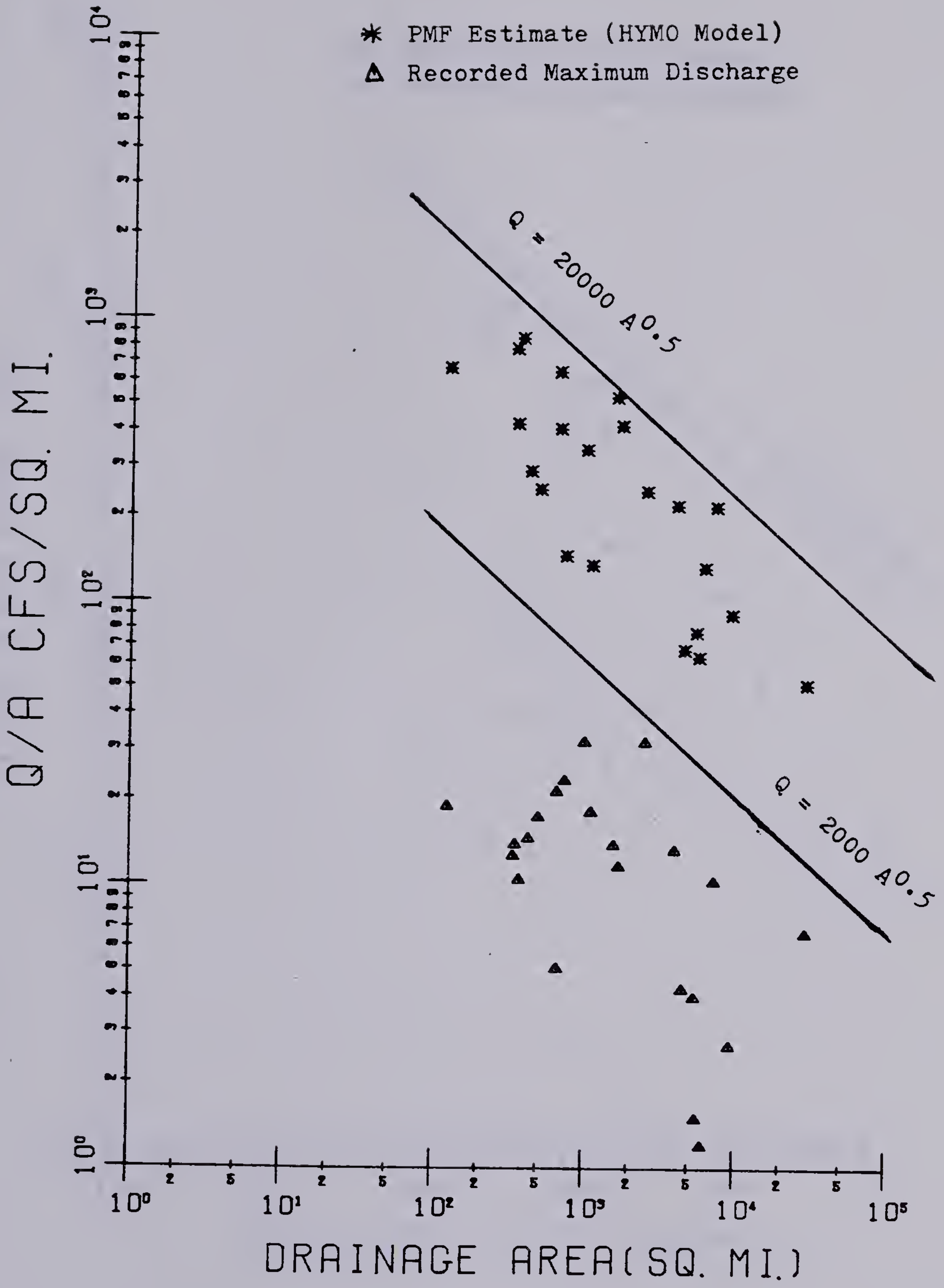

FIGURE A.4.3 Comparison of the PMF Normalized Discharge with Drainage Area for the Athabasca River Basin.

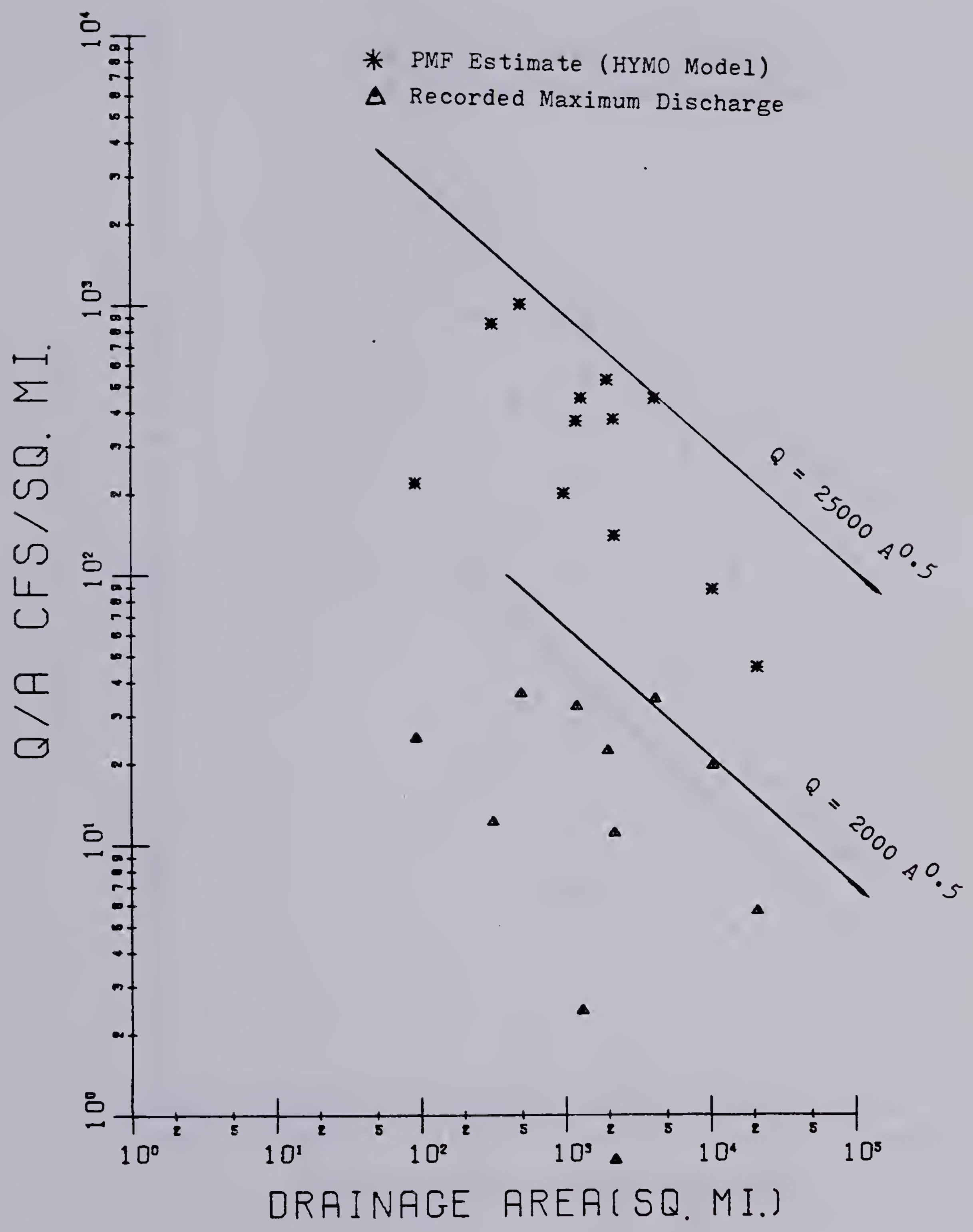

FIGURE A.4.4 Comparison of the PMF Normalized Discharge with Drainage Area for the North Sask. River Basin.

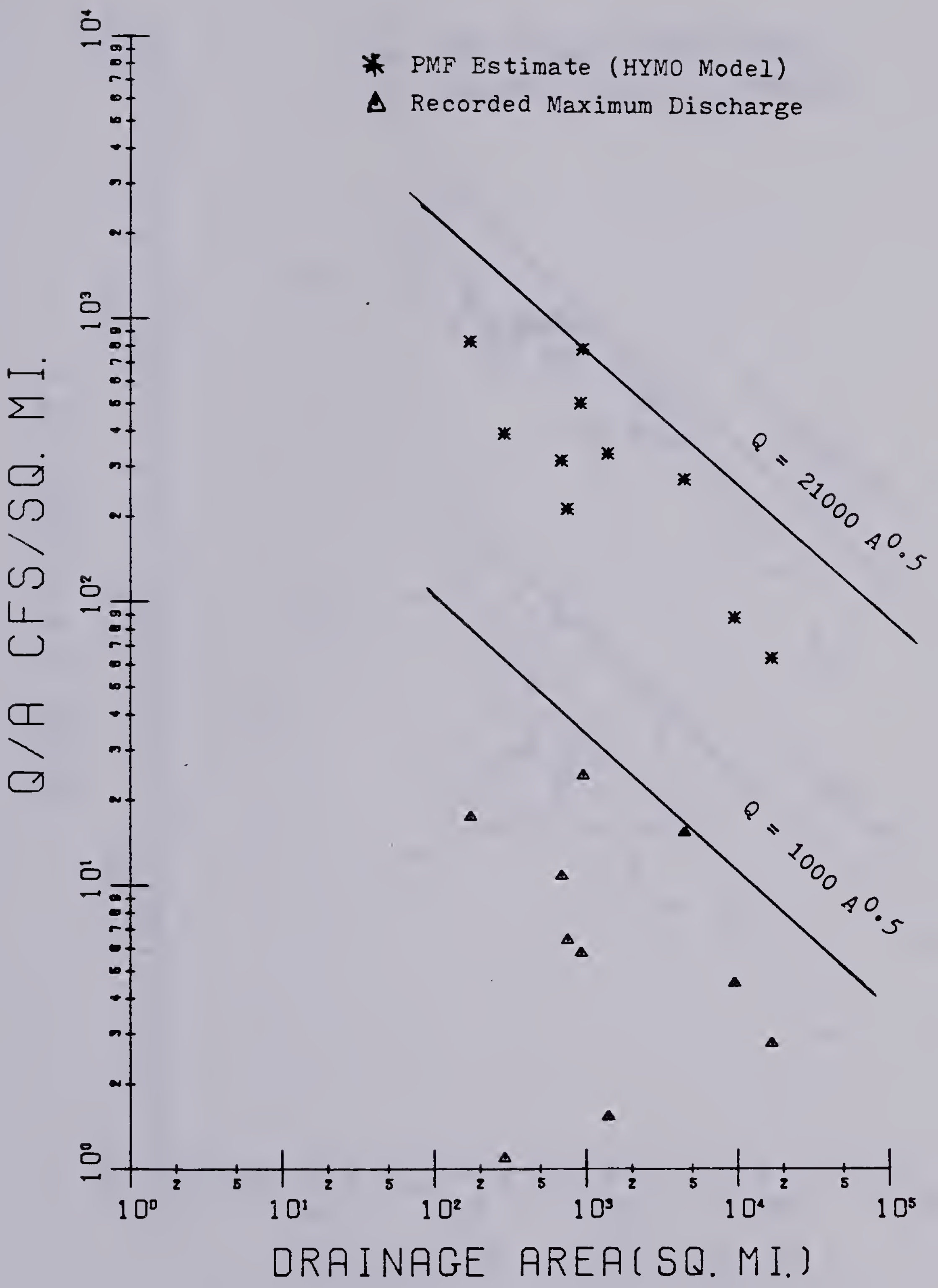

FIGURE A.4.5 Comparison of the PMF Normalized Discharge with Drainage Area for the Red Deer River Basin.

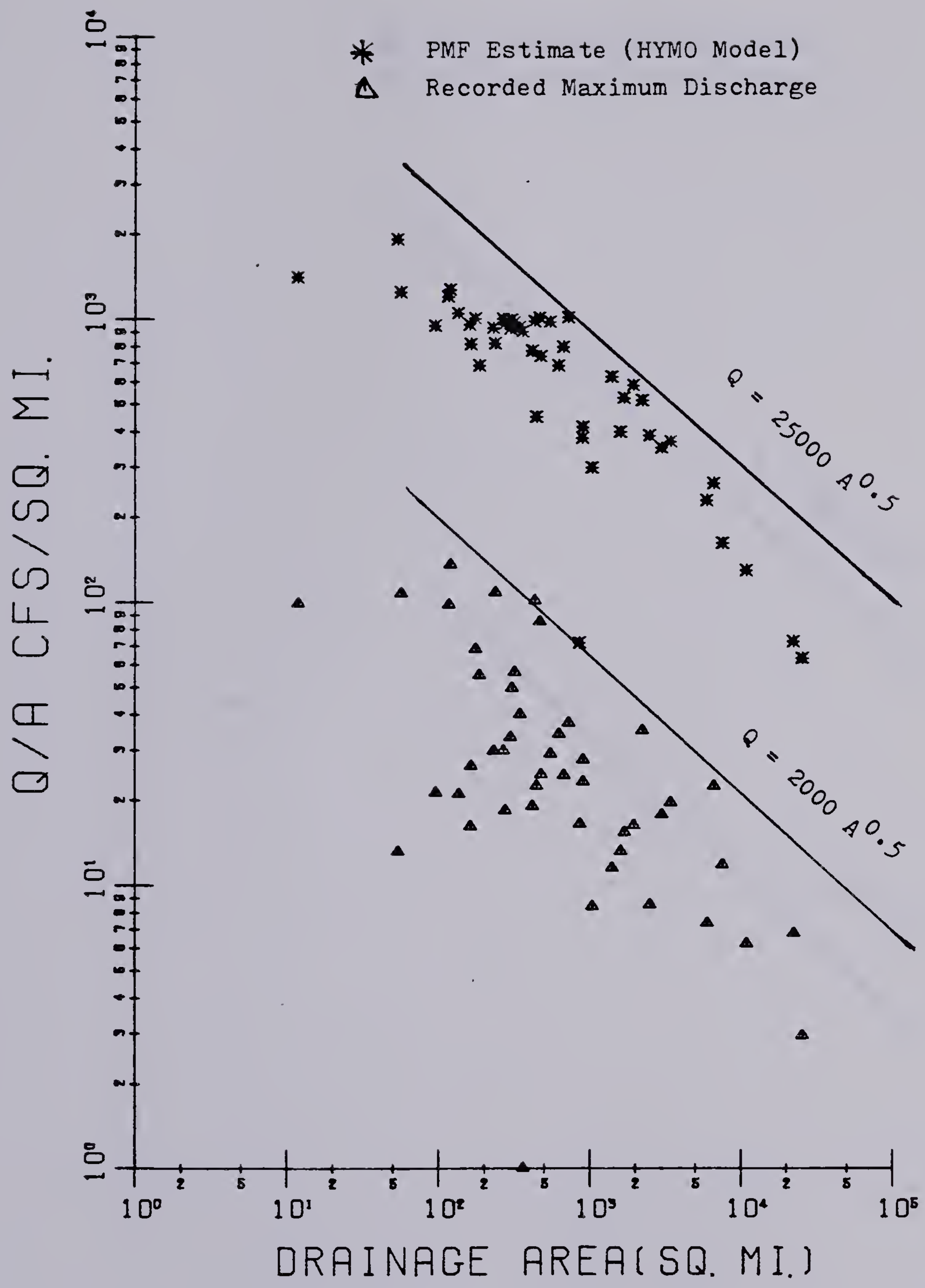

FIGURE A.4.6 Comparison of the PMF Normalized Discharge with Drainage Area for the South Sask. River Basin.

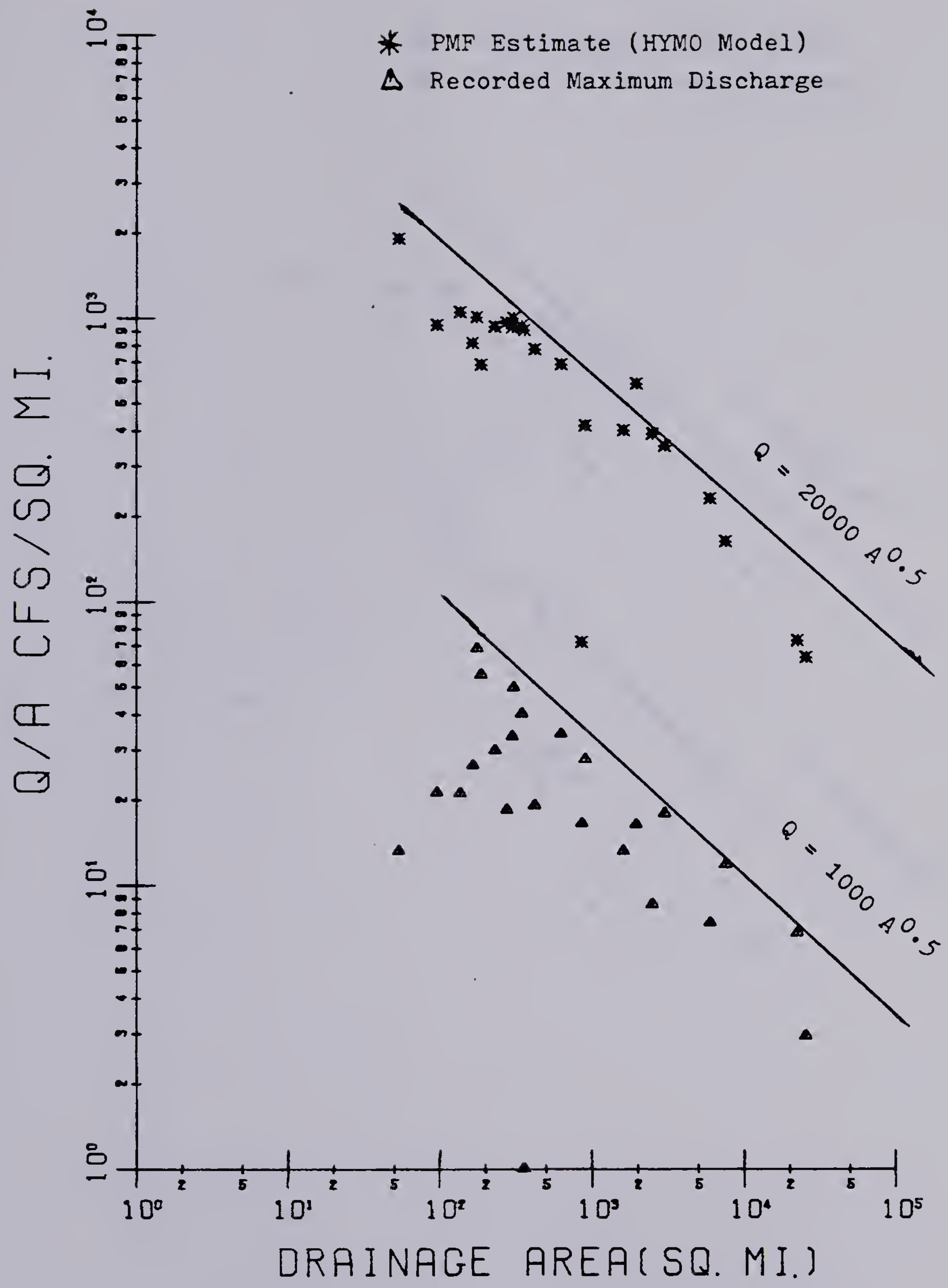

FIGURE A.4.7 Comparison of the PMF Normalized Discharge with Drainage Area for the Bow River Basin.

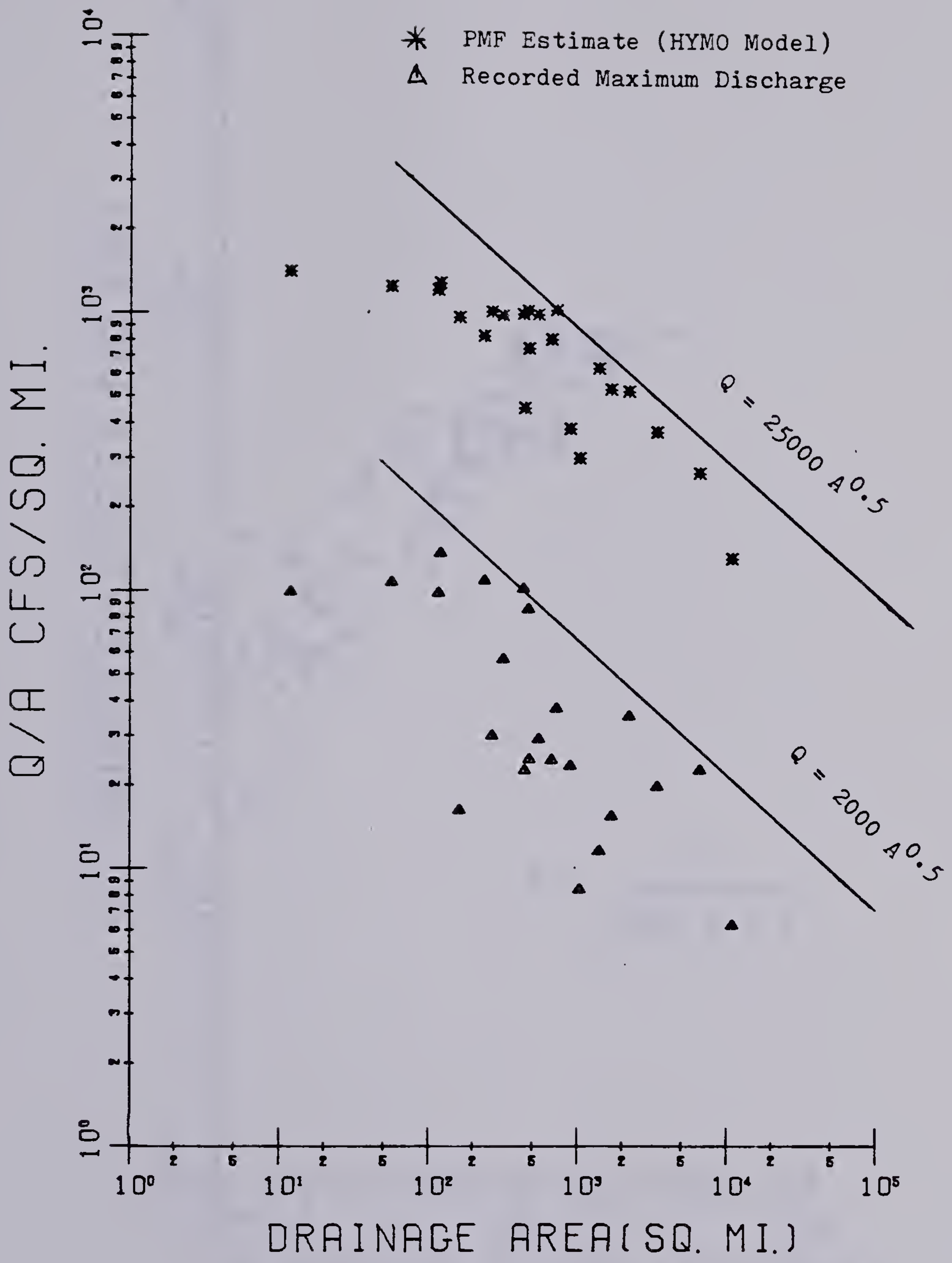

FIGURE A.4.8 Comparison of the PMF Normalized Discharge with Drainage Area for the Oldman River Basin.

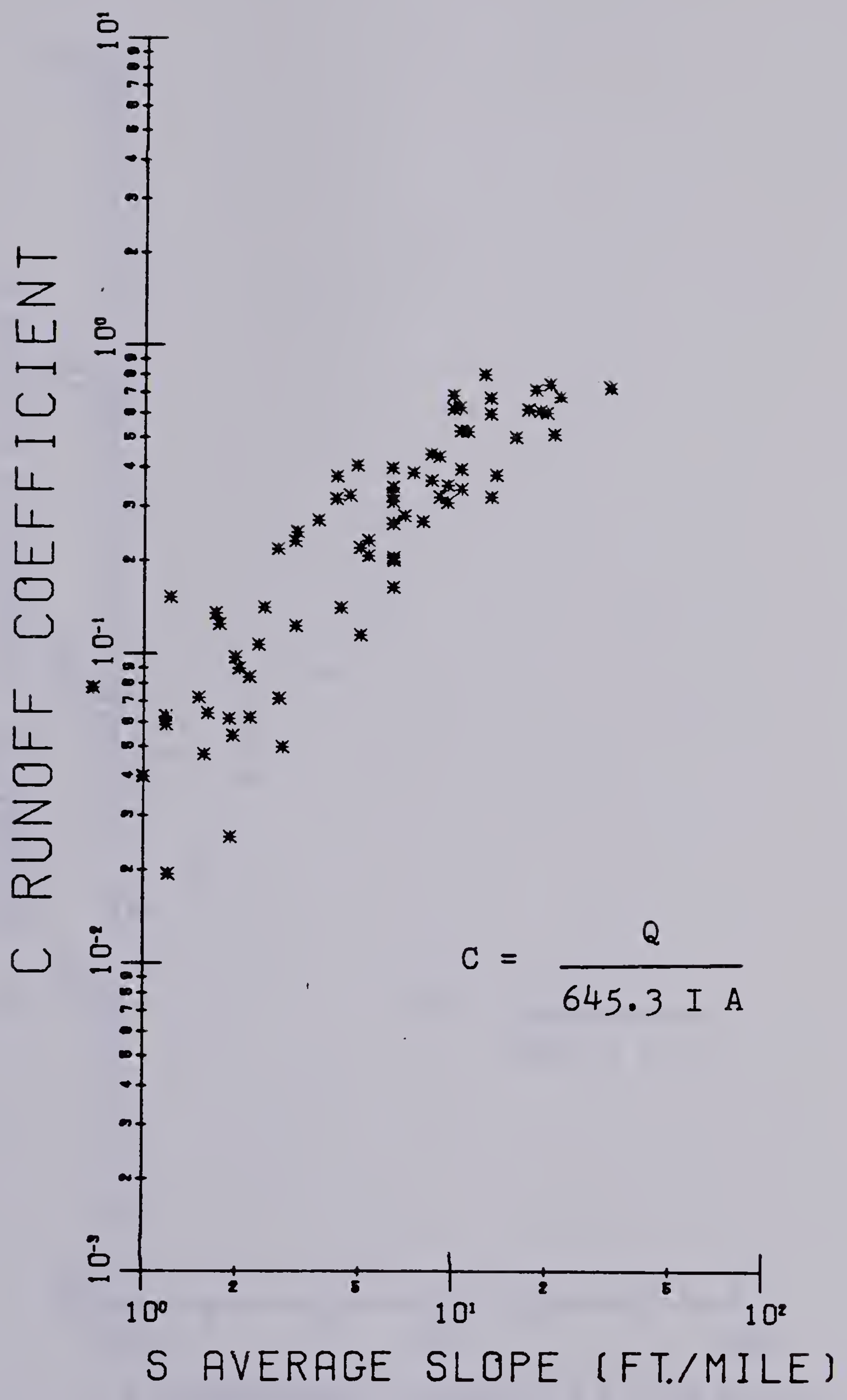

FIGURE A.4.9 Comparison of the Runoff Coefficient with Slope for Alberta River basins.

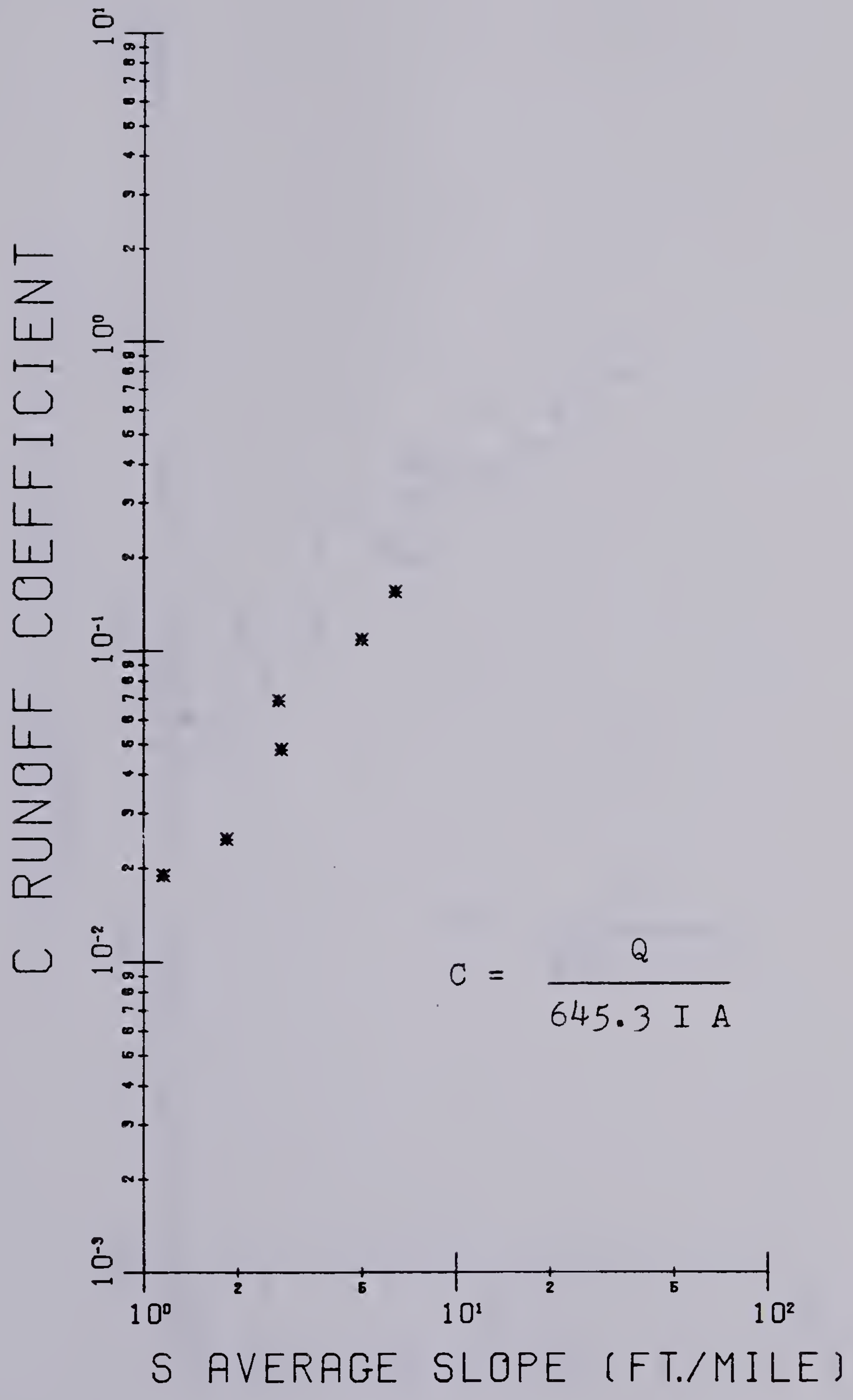

FIGURE A.4.10 Comparison of the Runoff Coefficient with Average Slope for the Peace River Basin.

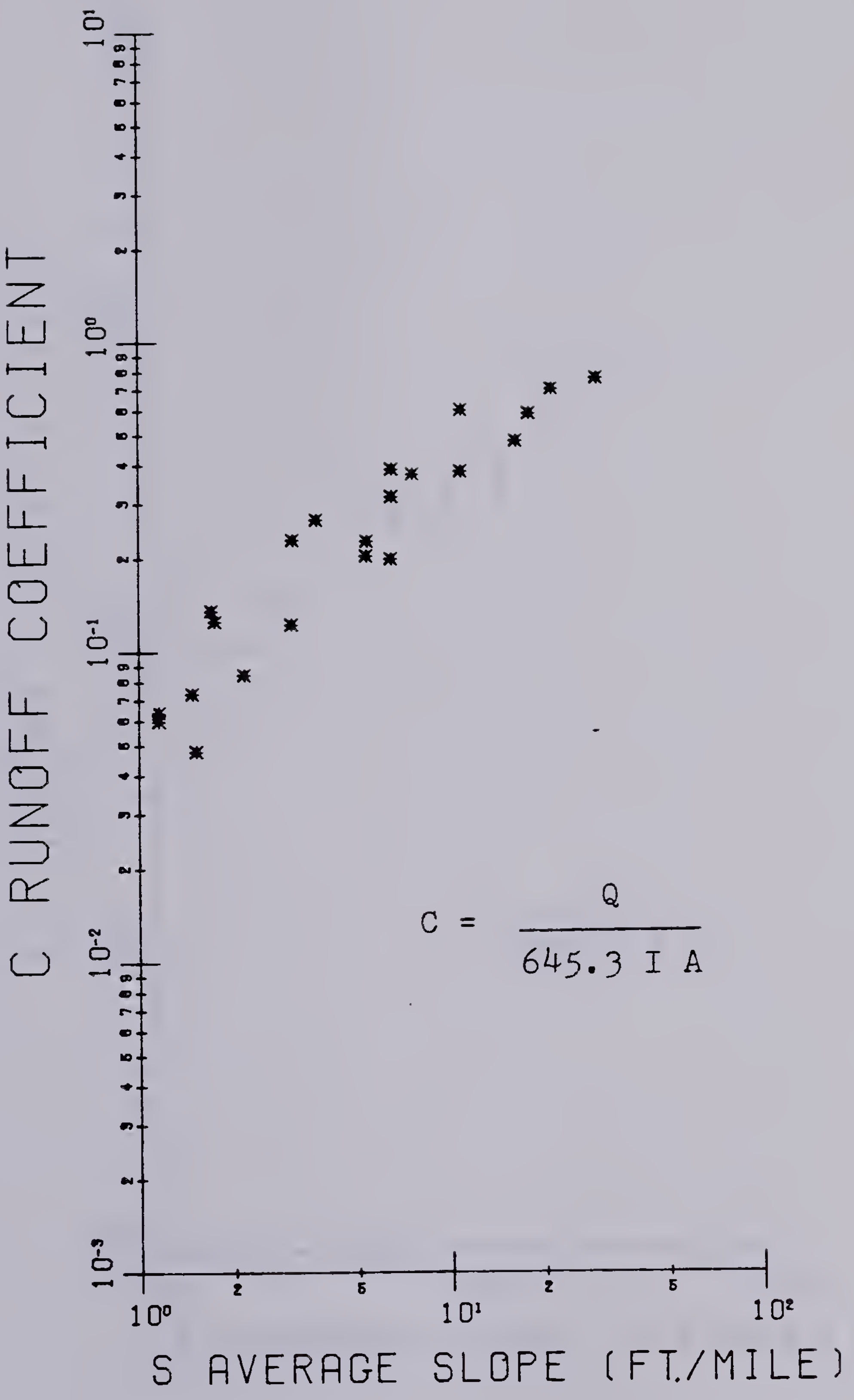

FIGURE A.4.11 Comparison of the Runoff Coefficient with Average Slope for the Athabasca River Basin.

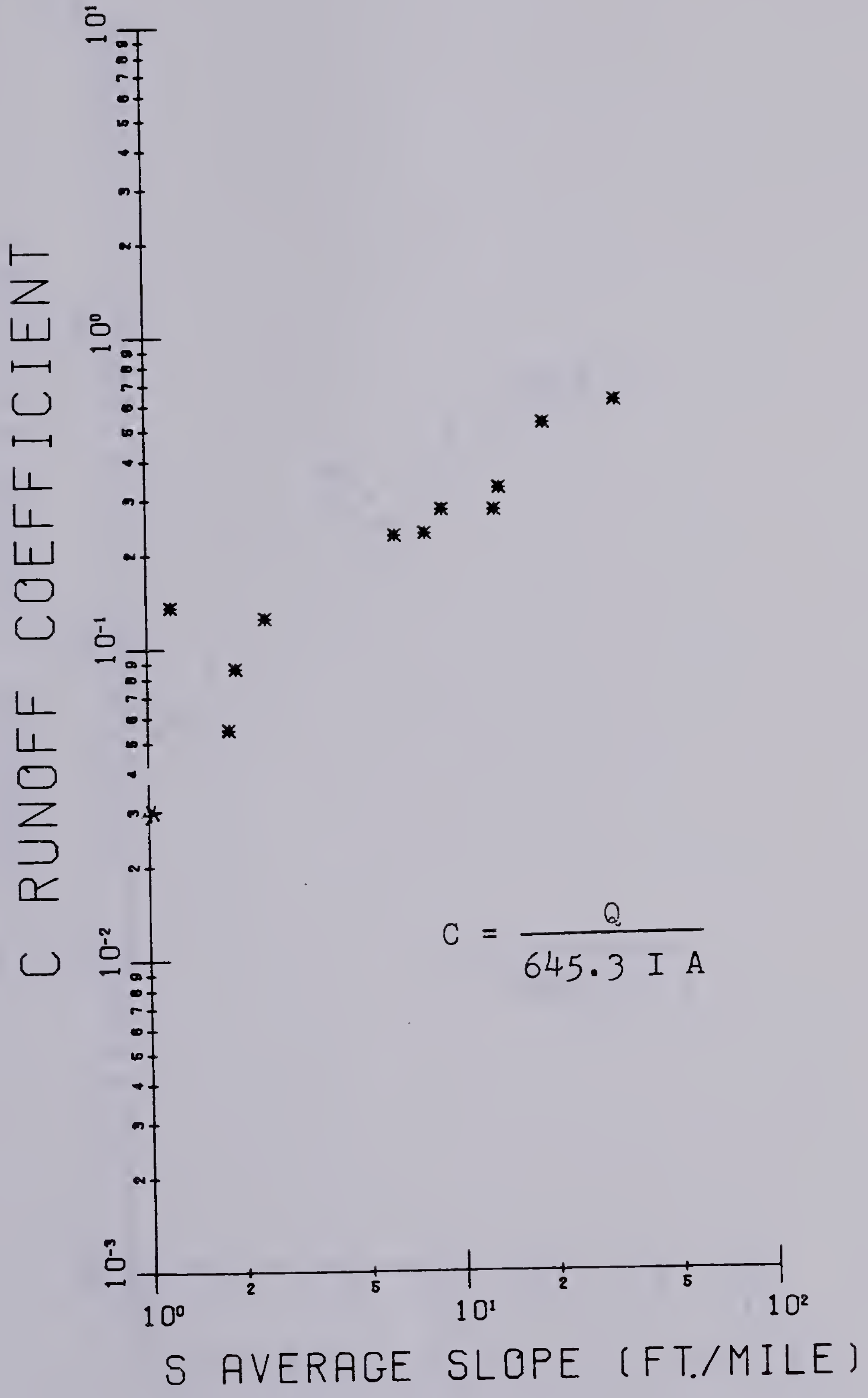

FIGURE A.4.12 Comparison of the Runoff Coefficient with Average Slope for the North Sask. River Basin.

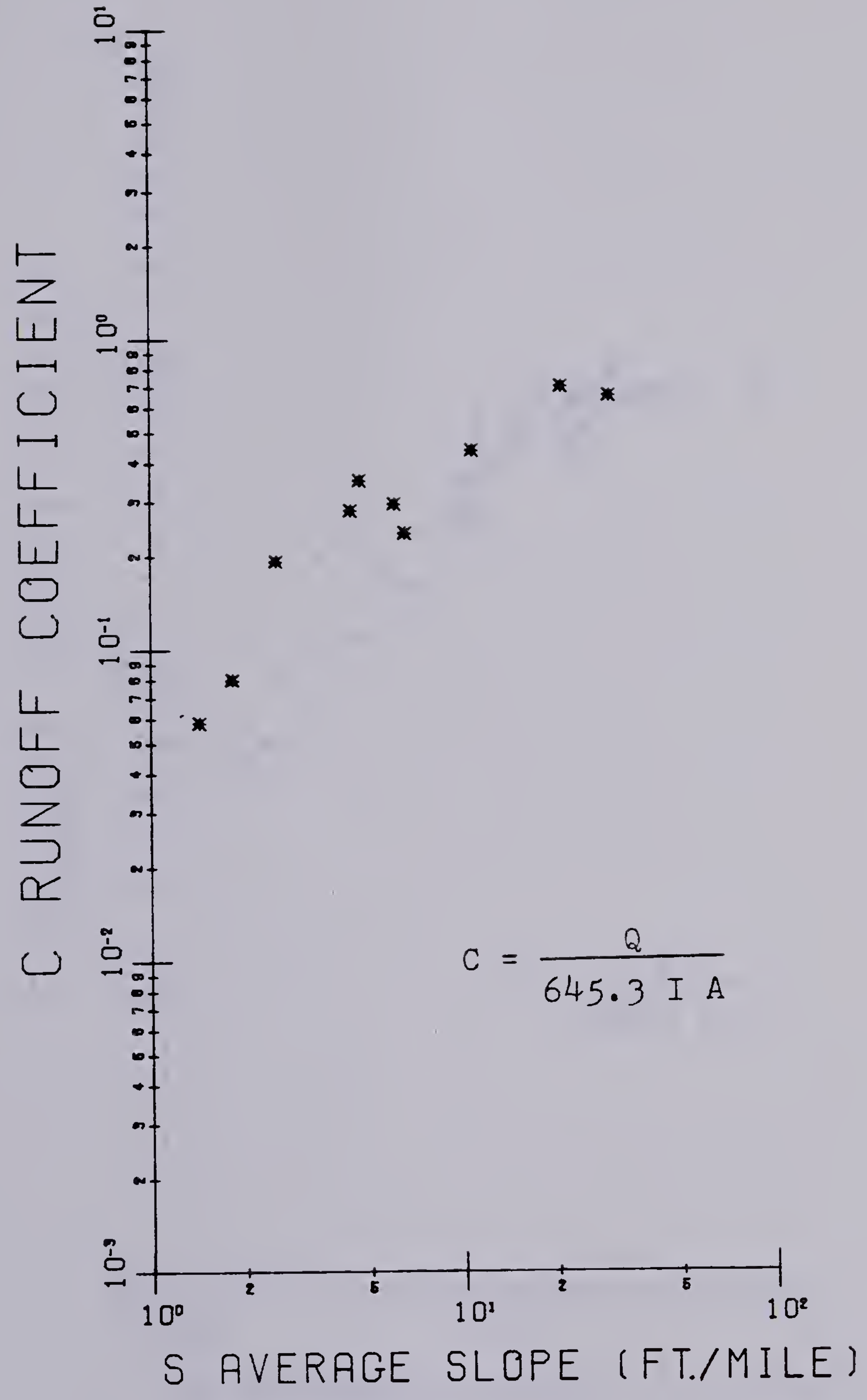

FIGURE A.4.13 Comparison of the Runoff Coefficient with Average Slope for the Red Deer River Basin.

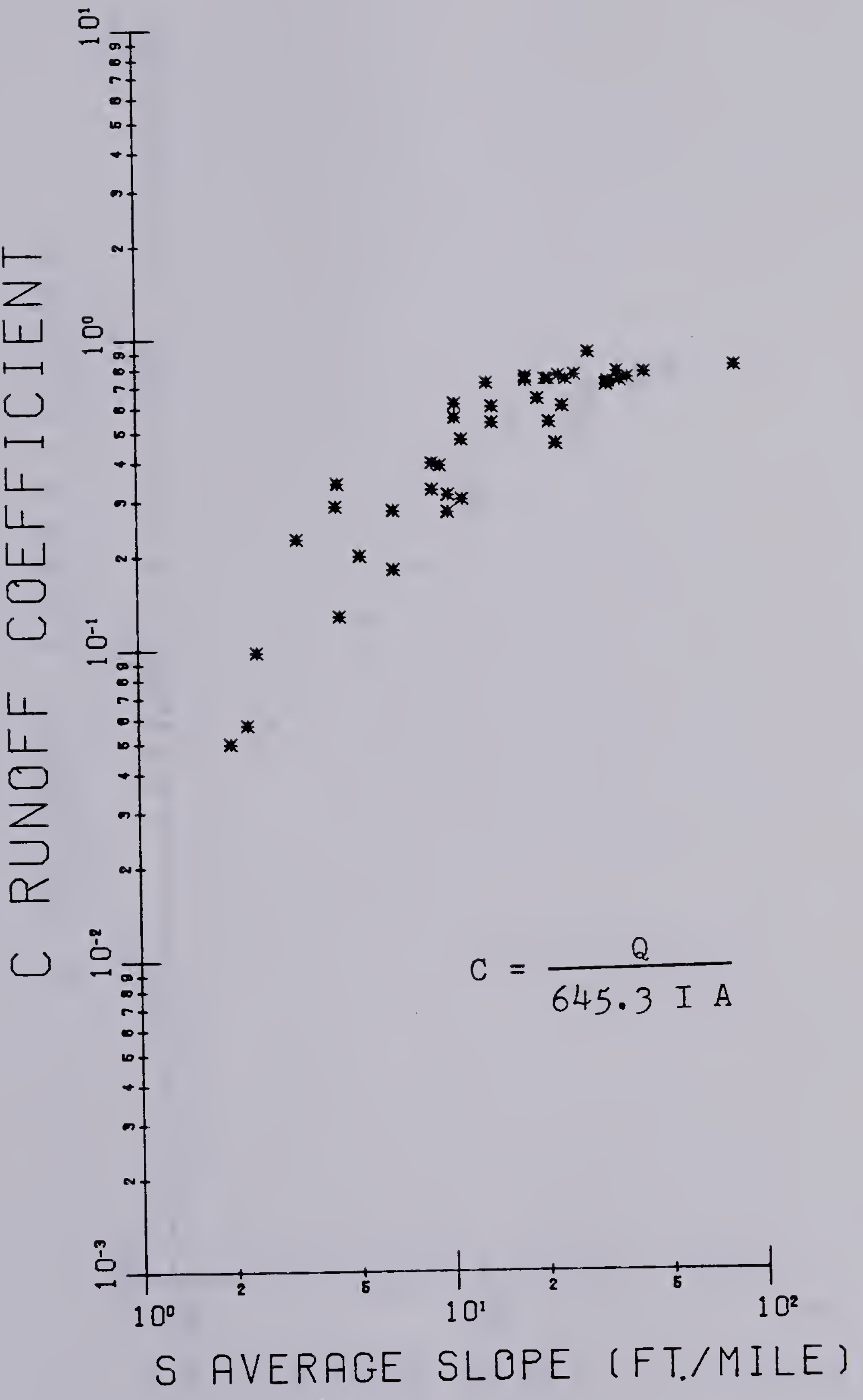

FIGURE A.4.14 Comparison of the Runoff Coefficient with Average Slope for the South Sask. River Basin.

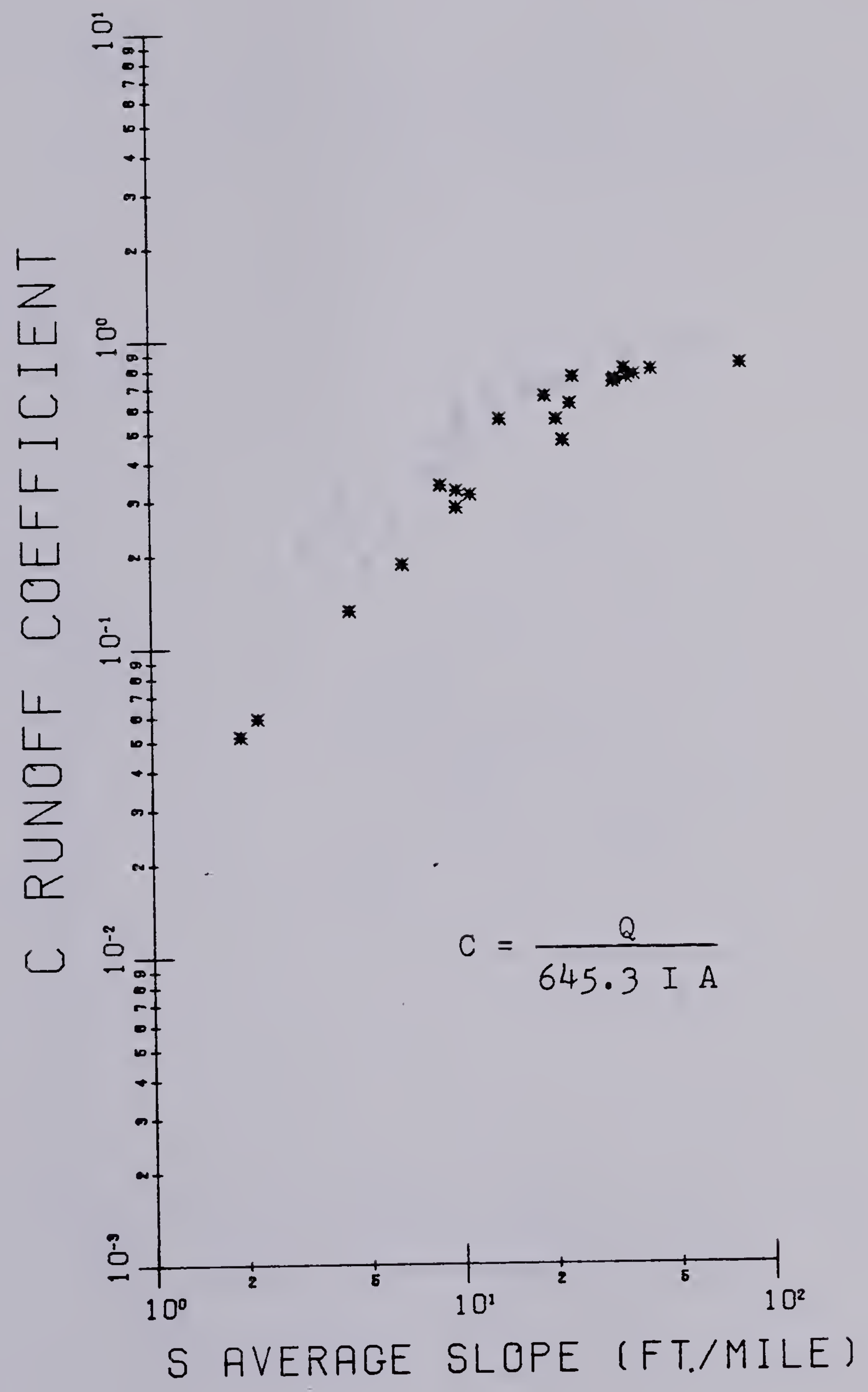

FIGURE A.4.15 Comparison of the Runoff Coefficient with Average Slope for the Bow River Basin.

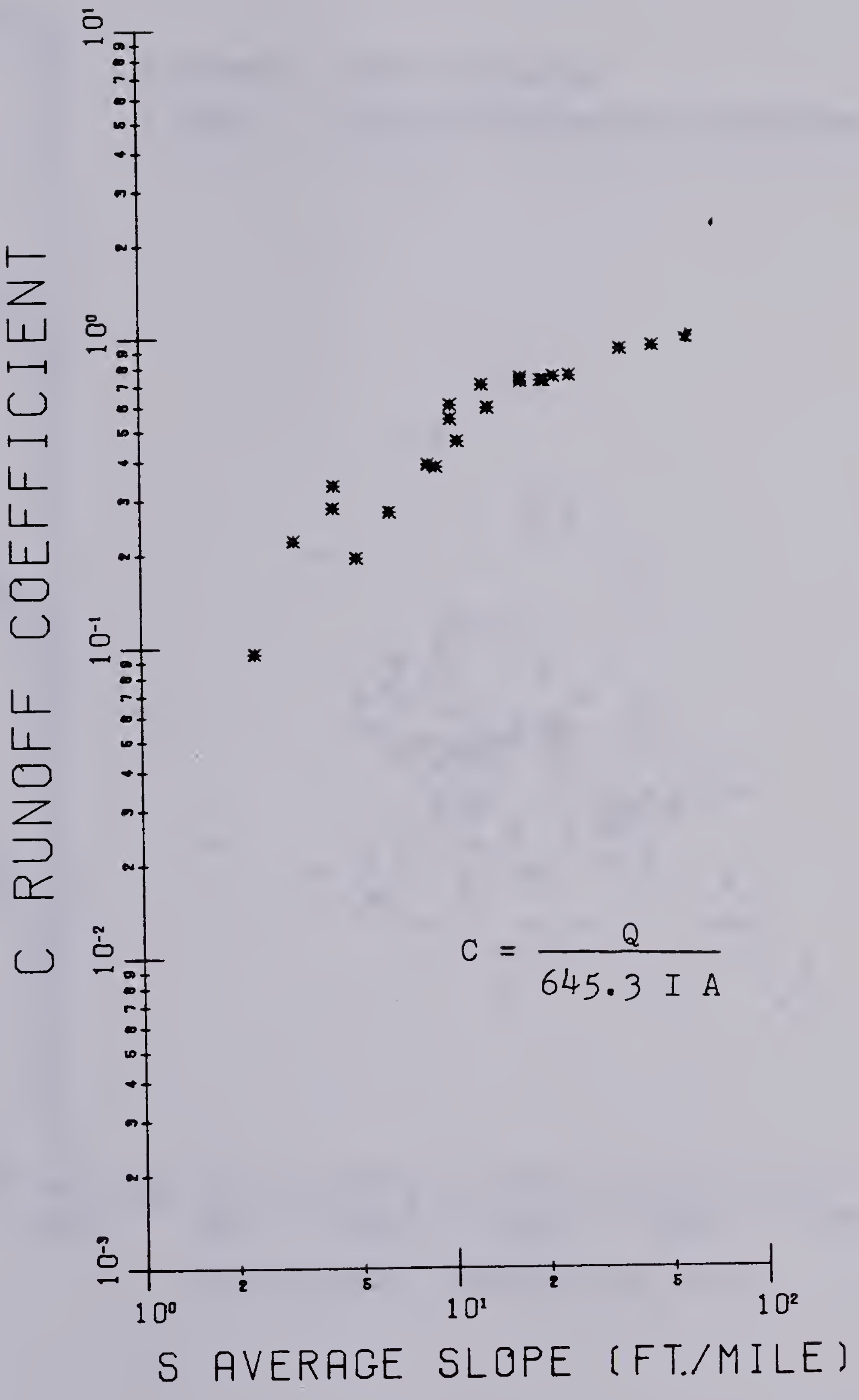

FIGURE A.4.16 Comparison of the Runoff Coefficient with Average Slope for the Oldman River Basin.

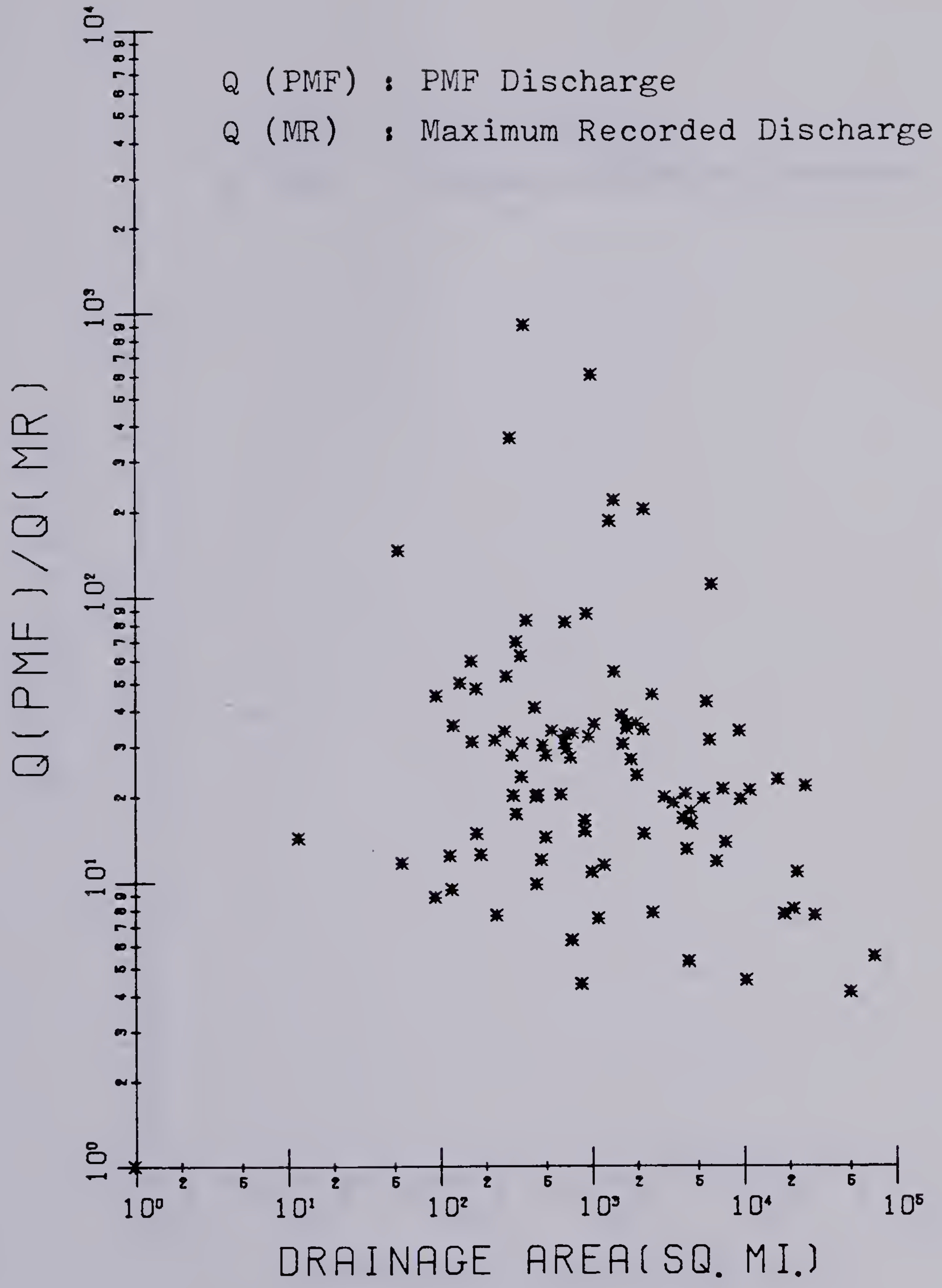

FIGURE A.4.17 Ratio of PMF to Recorded Maximum Discharge with Drainage Area for Alberta River basins.

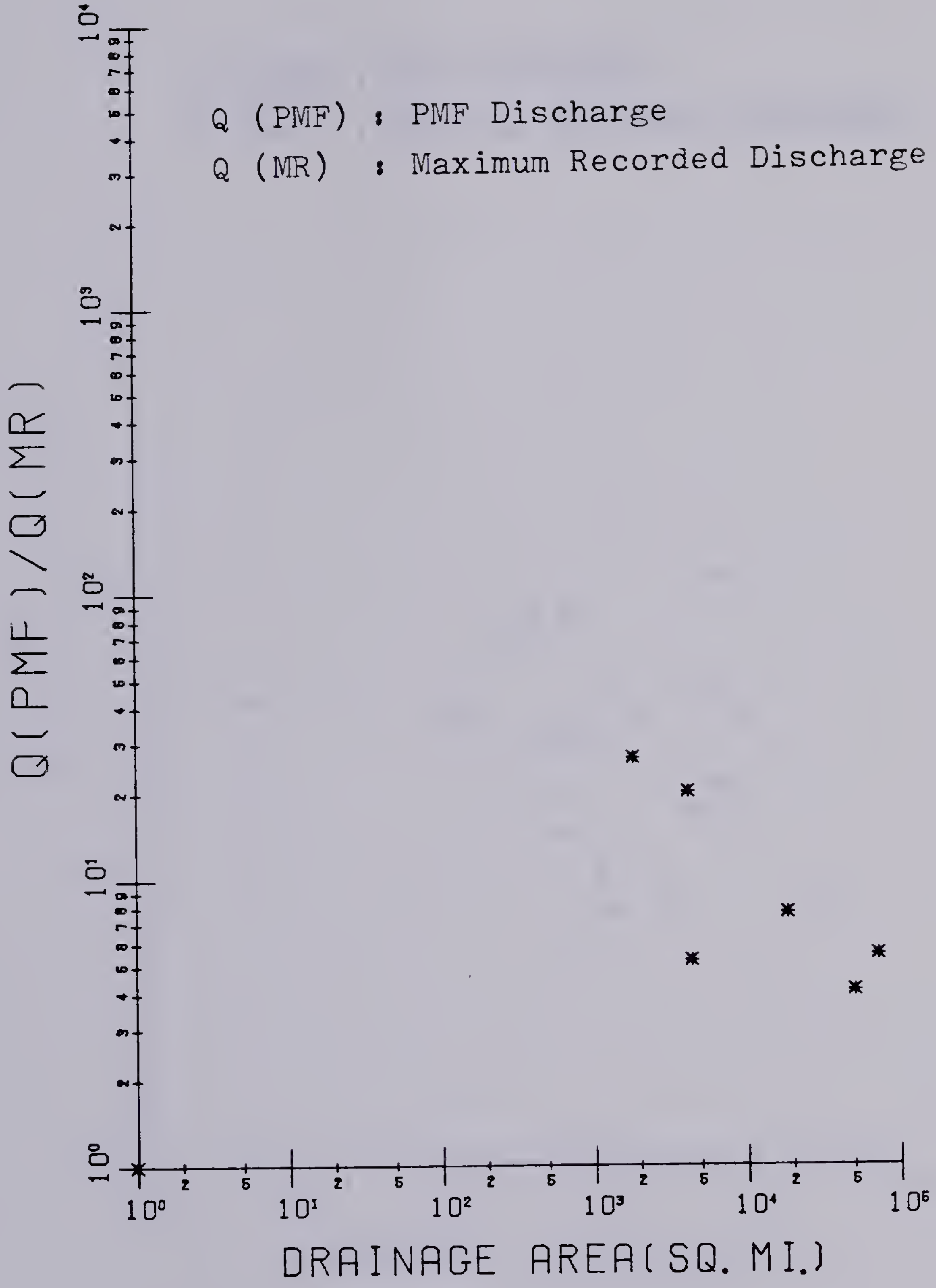

FIGURE A.4.18 Ratio of PMF to Recorded Maximum Discharge with Drainage Area for the Peace River Basin.

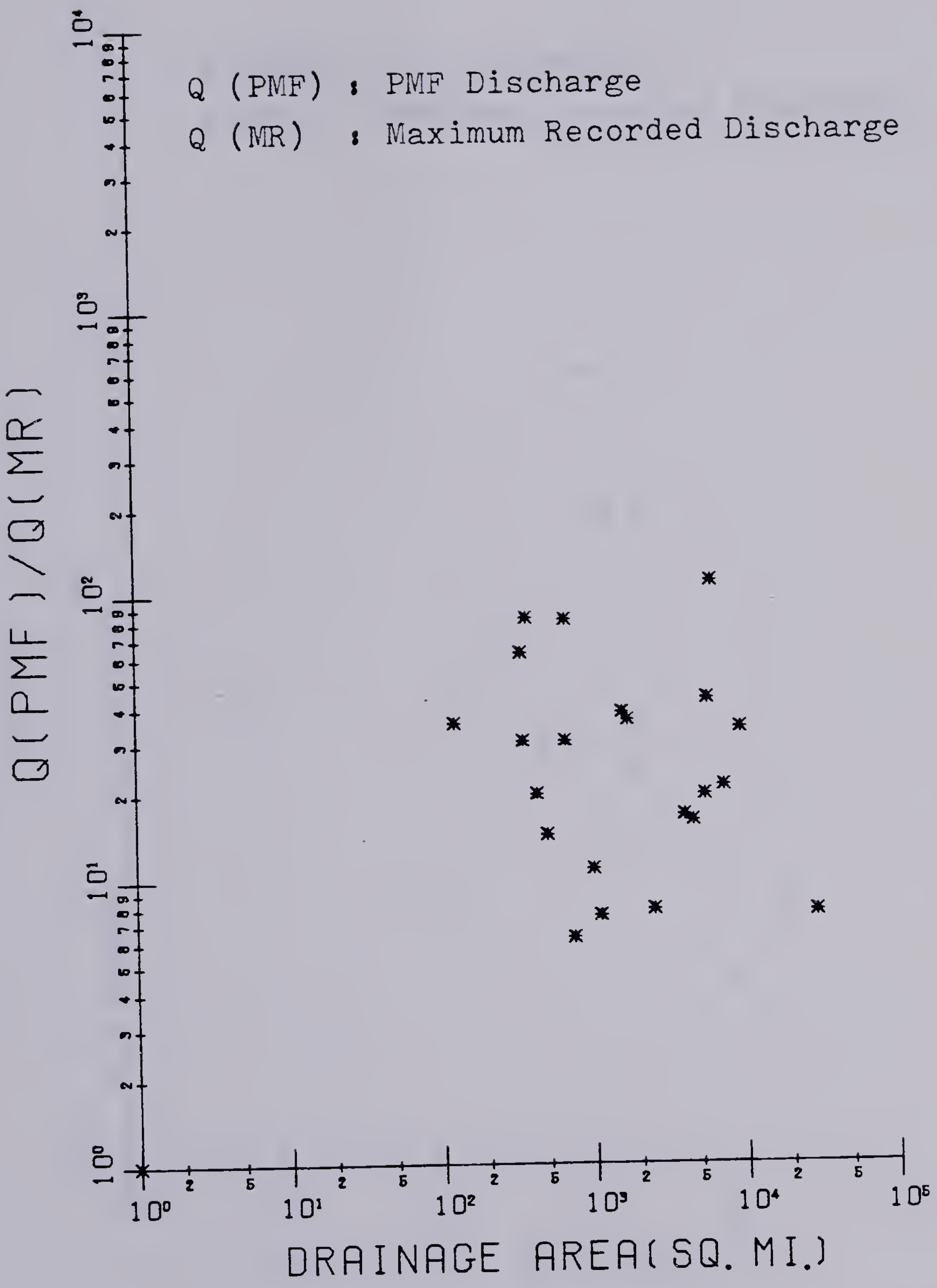

FIGURE A.4.19 Ratio of PMF to Recorded Maximum Discharge with Drainage Area for the Athabasca River Basin.

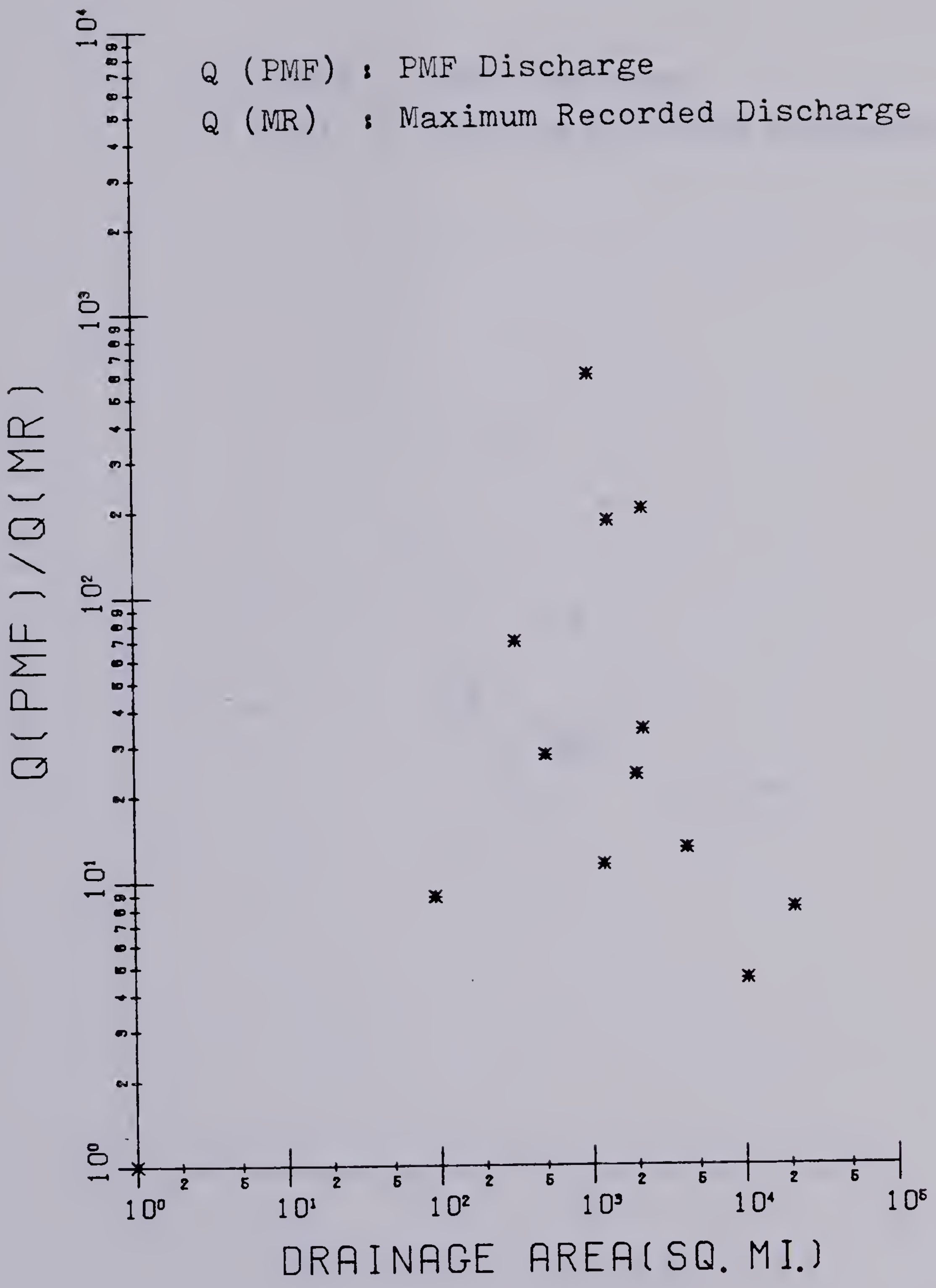

FIGURE A.4.20 Ratio of PMF to Recorded Maximum Discharge with Drainage Area for the North Sask. River Basin.

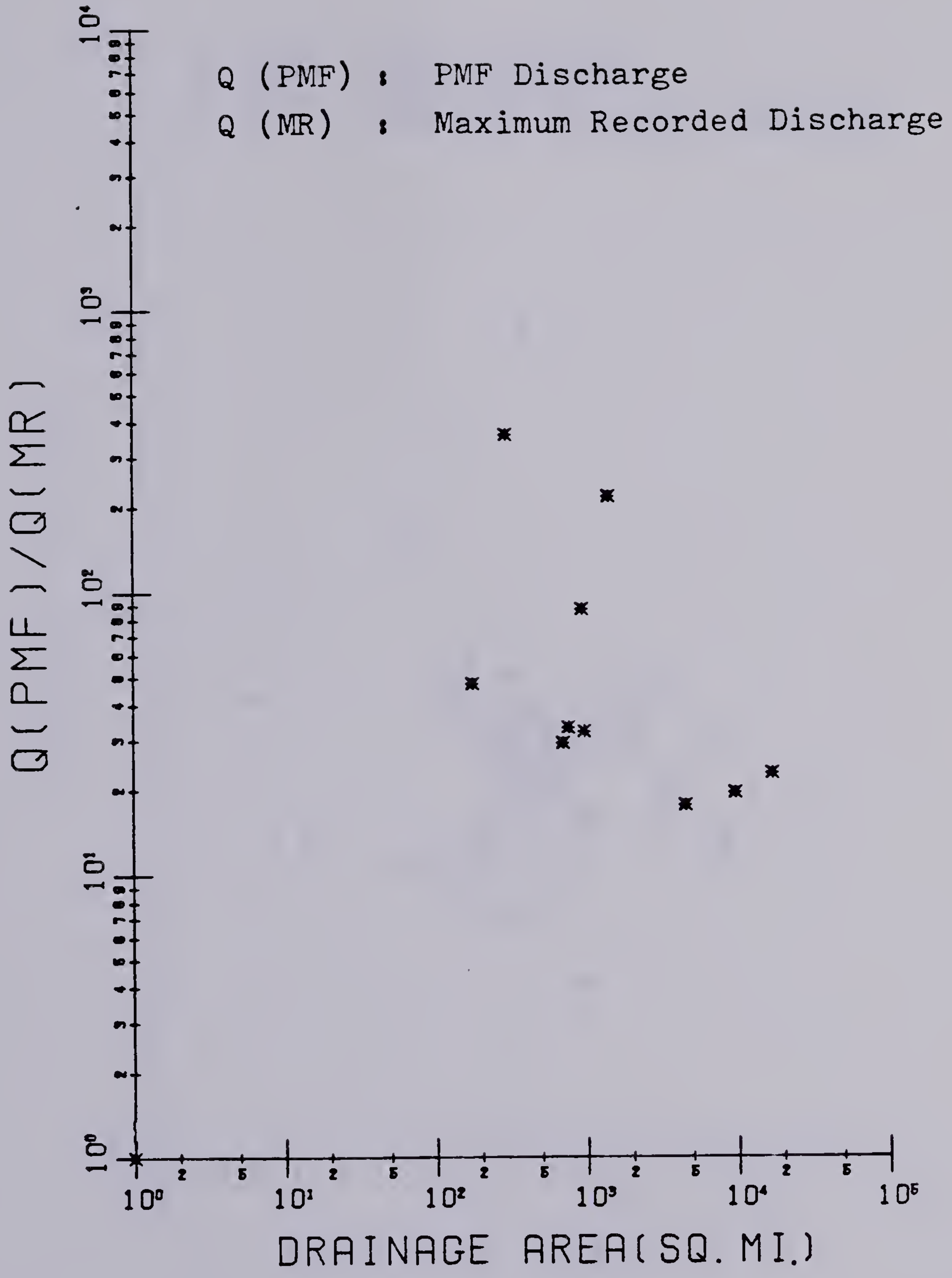

FIGURE A.4.21 Ratio of PMF to Recorded Maximum Discharge with Drainage Area for the Red Deer River Basin.

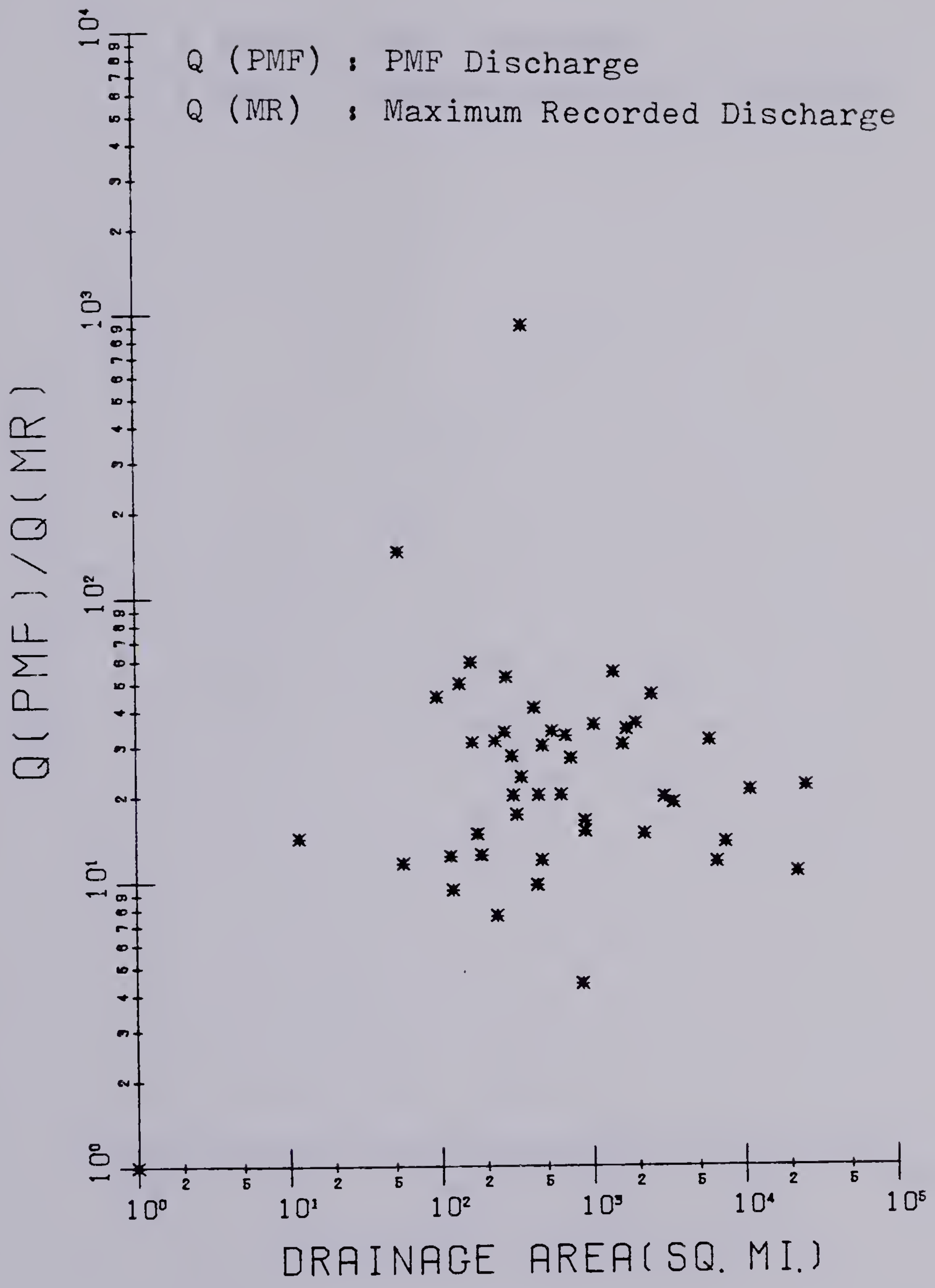

FIGURE A.4.22 Ratio of PMF to Recorded Maximum Discharge with Drainage Area for the South Sask. River Basin.

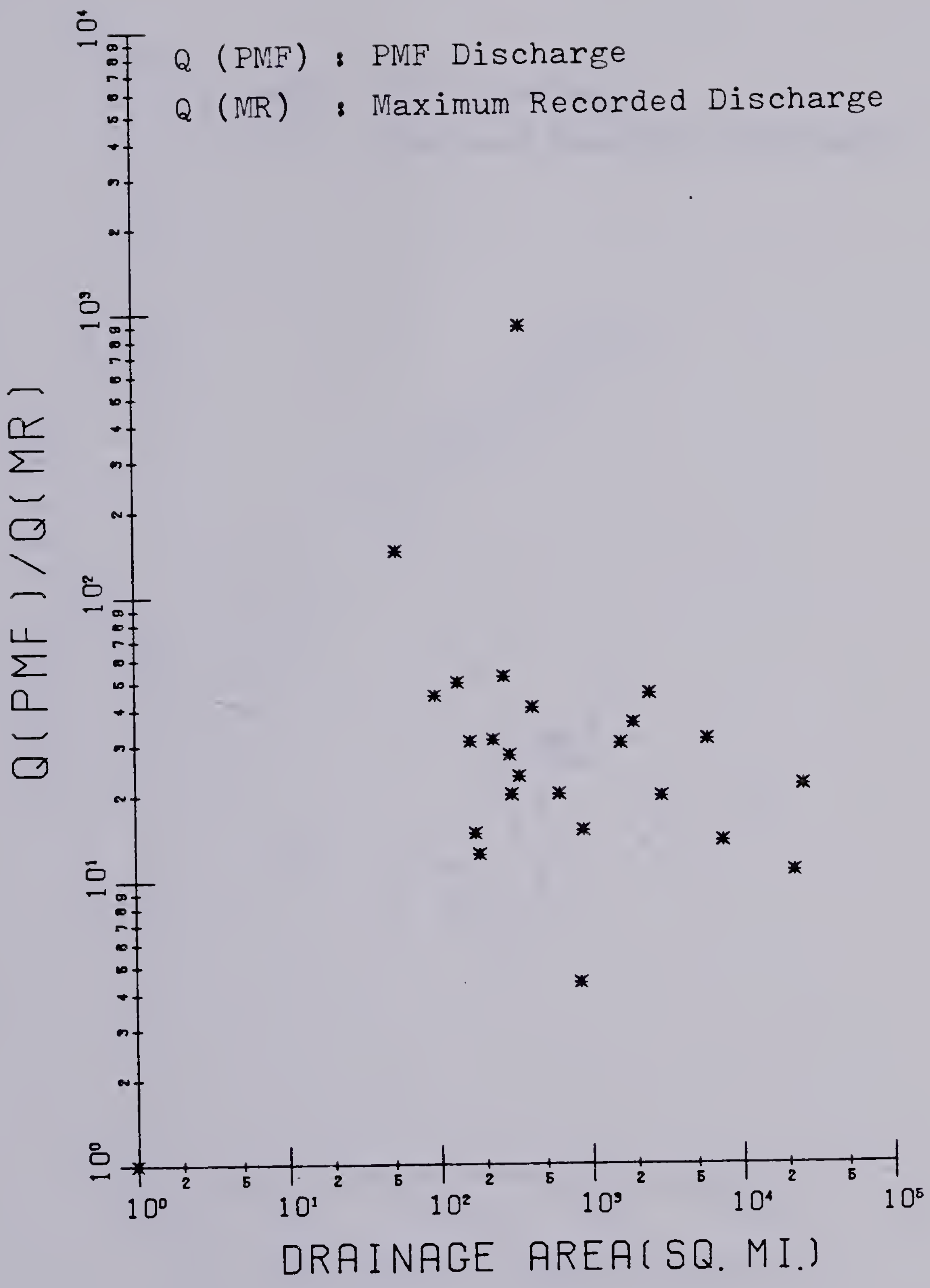

FIGURE A.4.23 Ratio of PMF to Recorded Maximum Discharge with Drainage Area for the Bow River Basin.

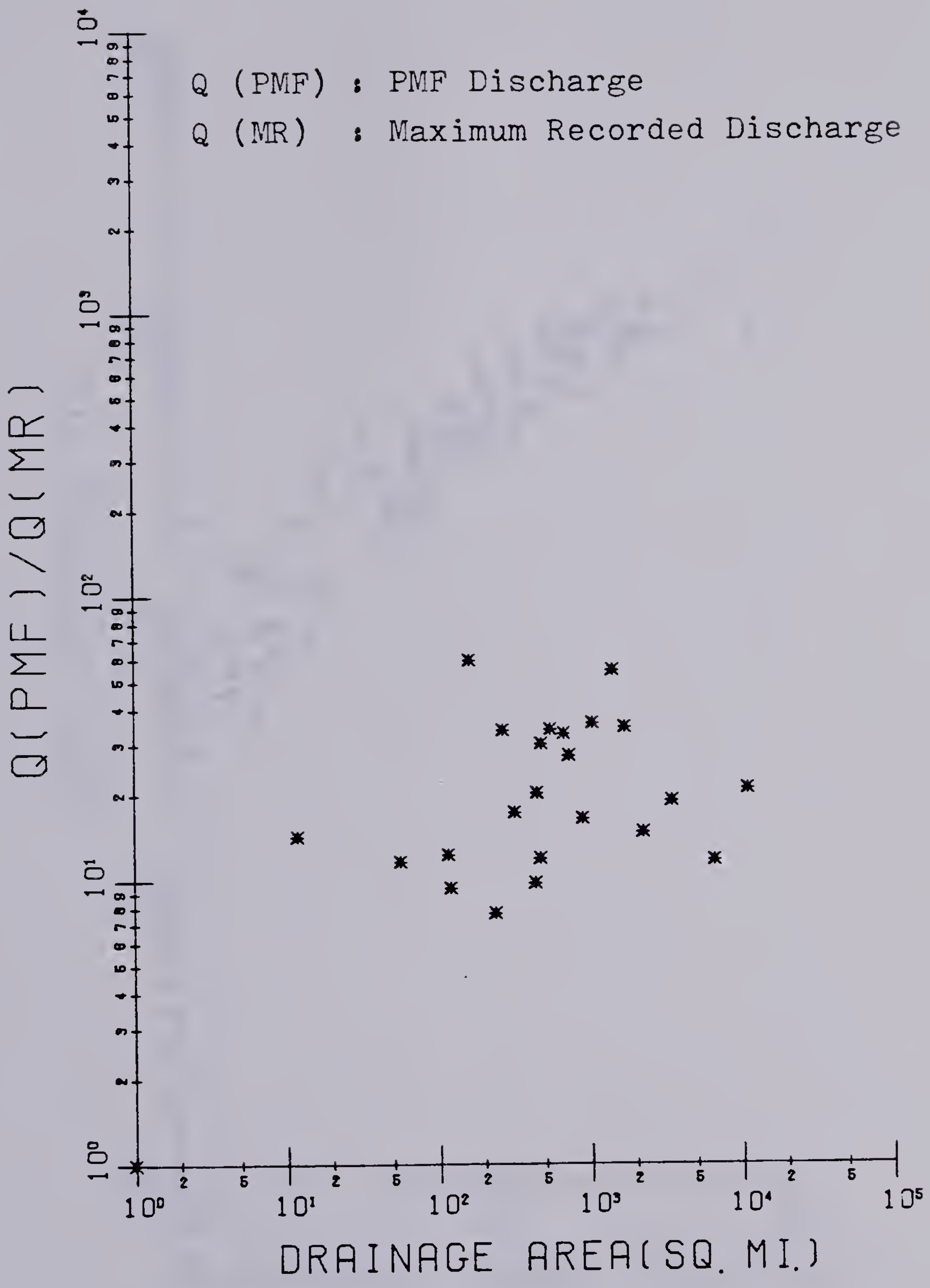

FIGURE A.4.24 Ratio of PMF to Recorded Maximum Discharge with Drainage Area for the Oldman River Basin.

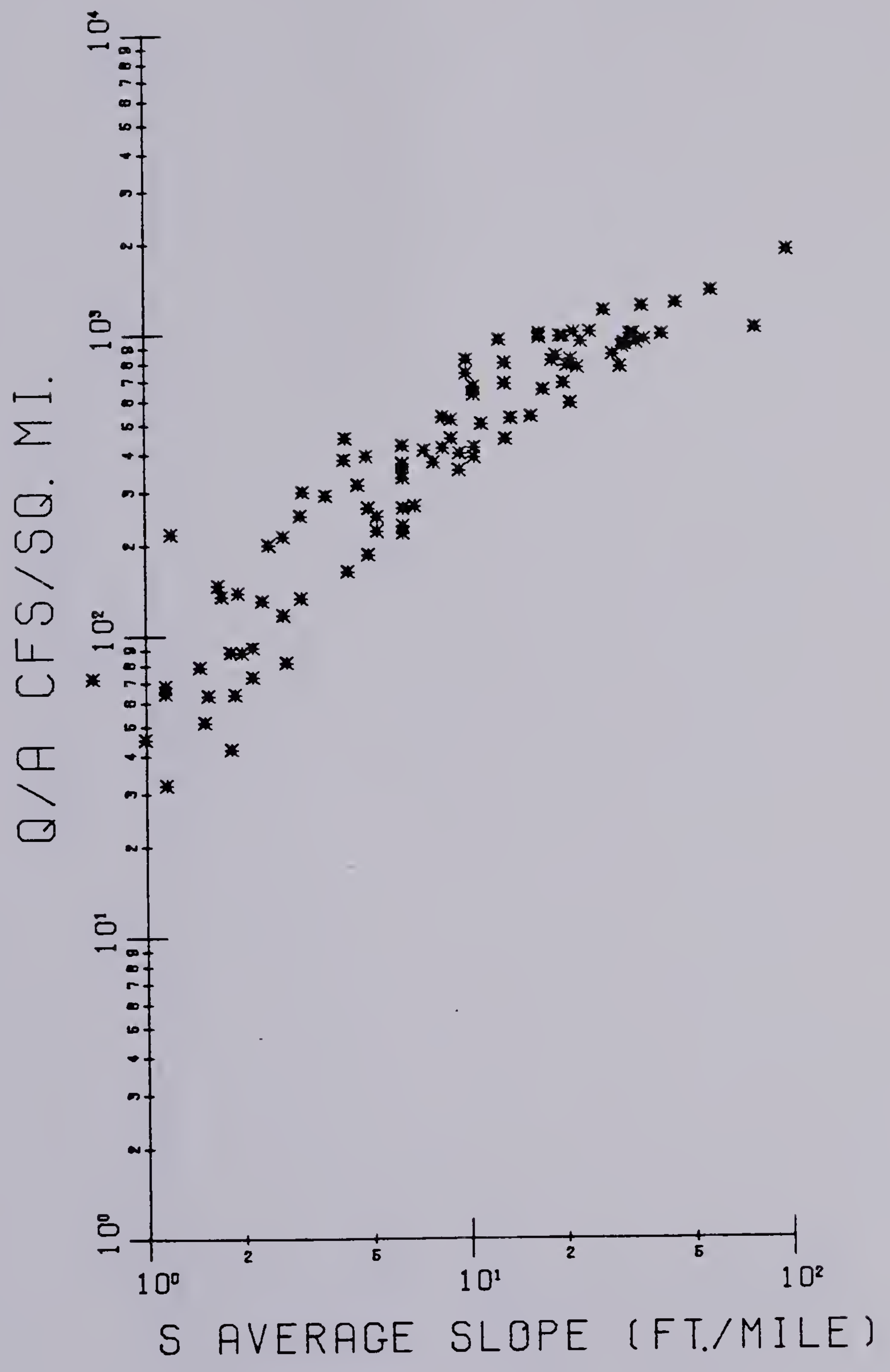

FIGURE A.4.25 Comparison of the PMF Normalized Discharge with Average Slope for Alberta River basins.

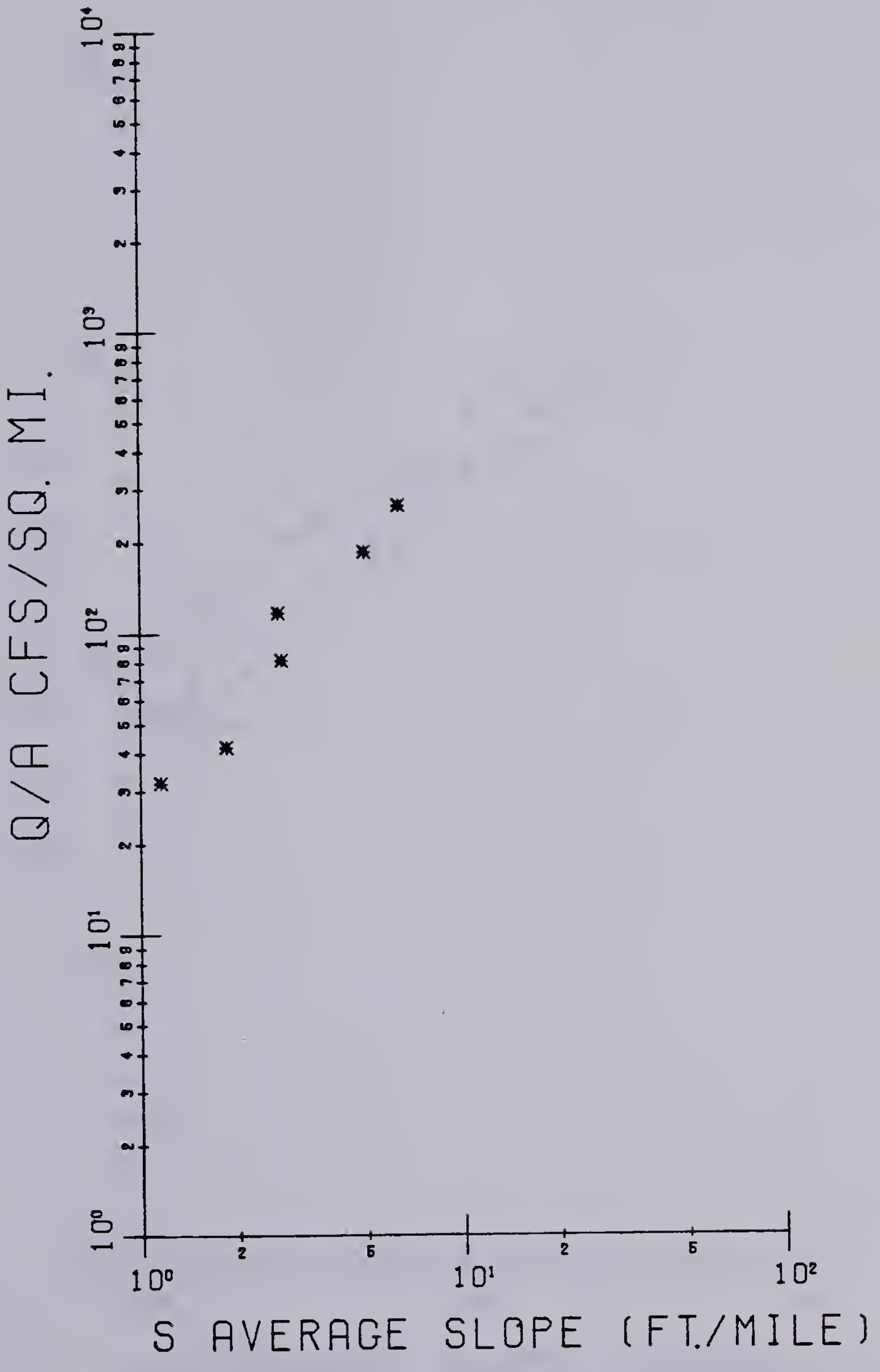

FIGURE A.4.26 Comparison of the PMF Normalized Discharge with Average Slope for the Peace River Basin.

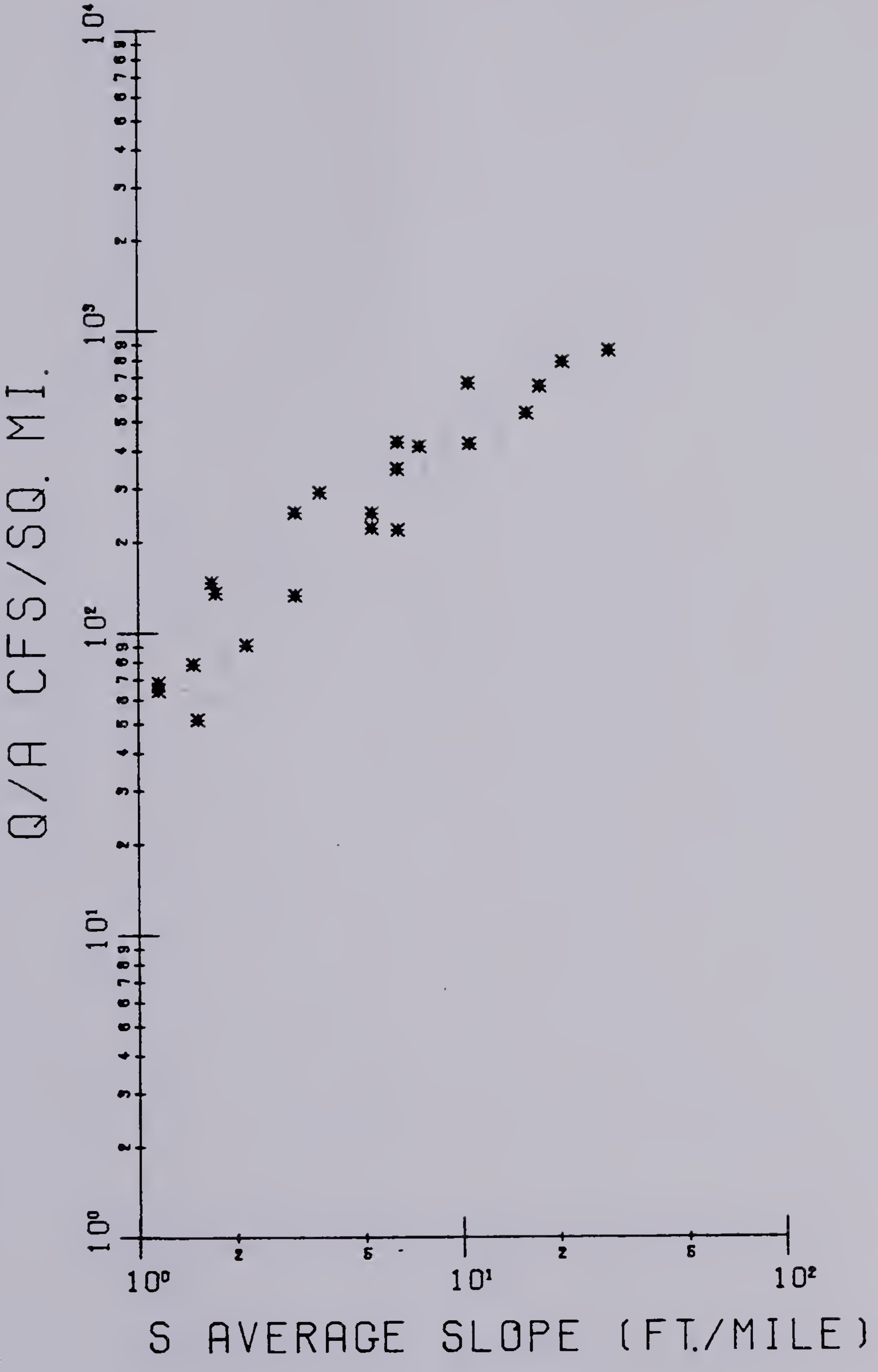

FIGURE A.4.27 Comparison of the PMF Normalized Discharge with Average Slope for the Athabasca River Basin.

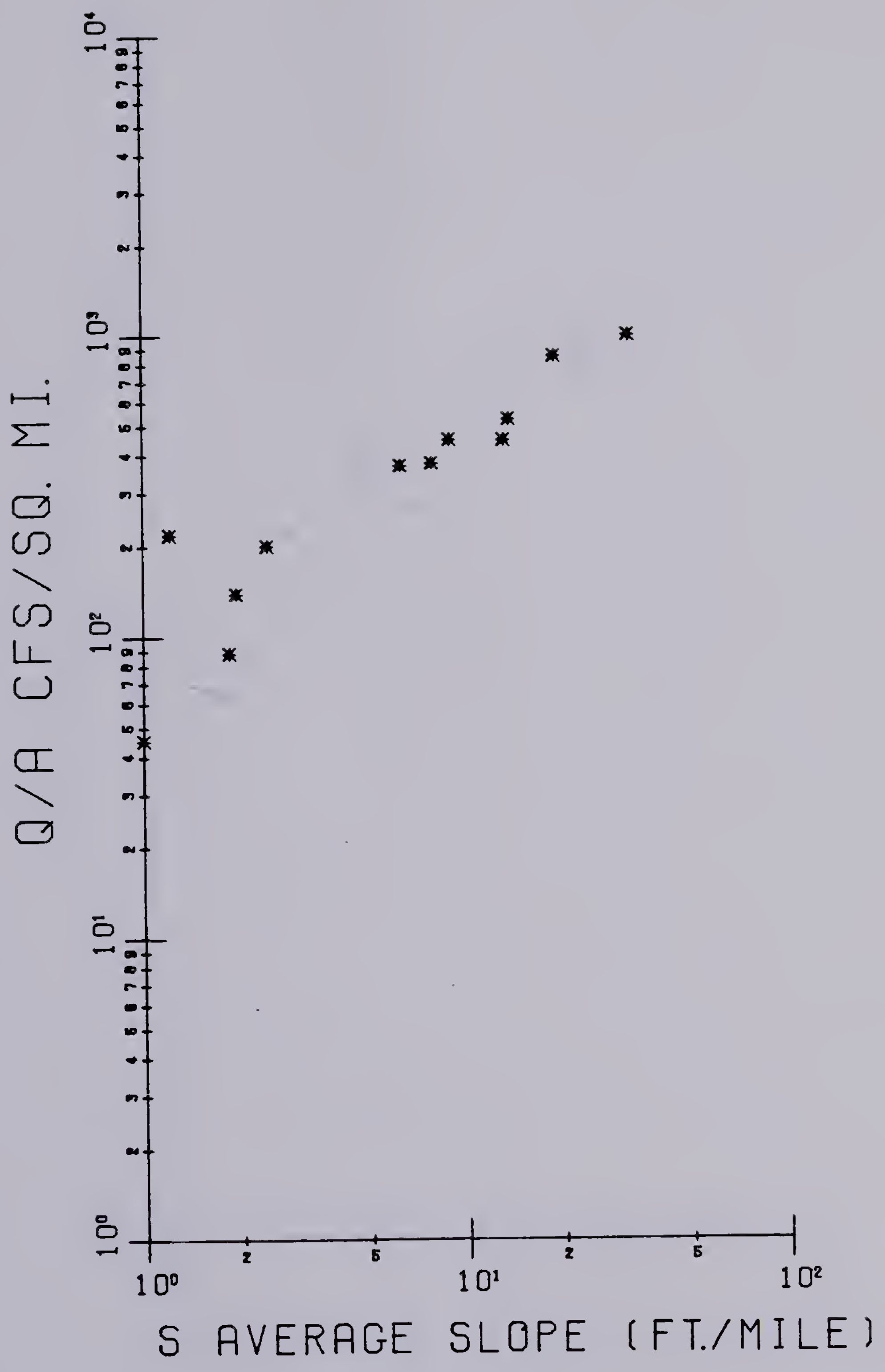

FIGURE A.4.28 Comparison of the PMF Normalized Discharge with Average Slope for the North Sask. River Basin.

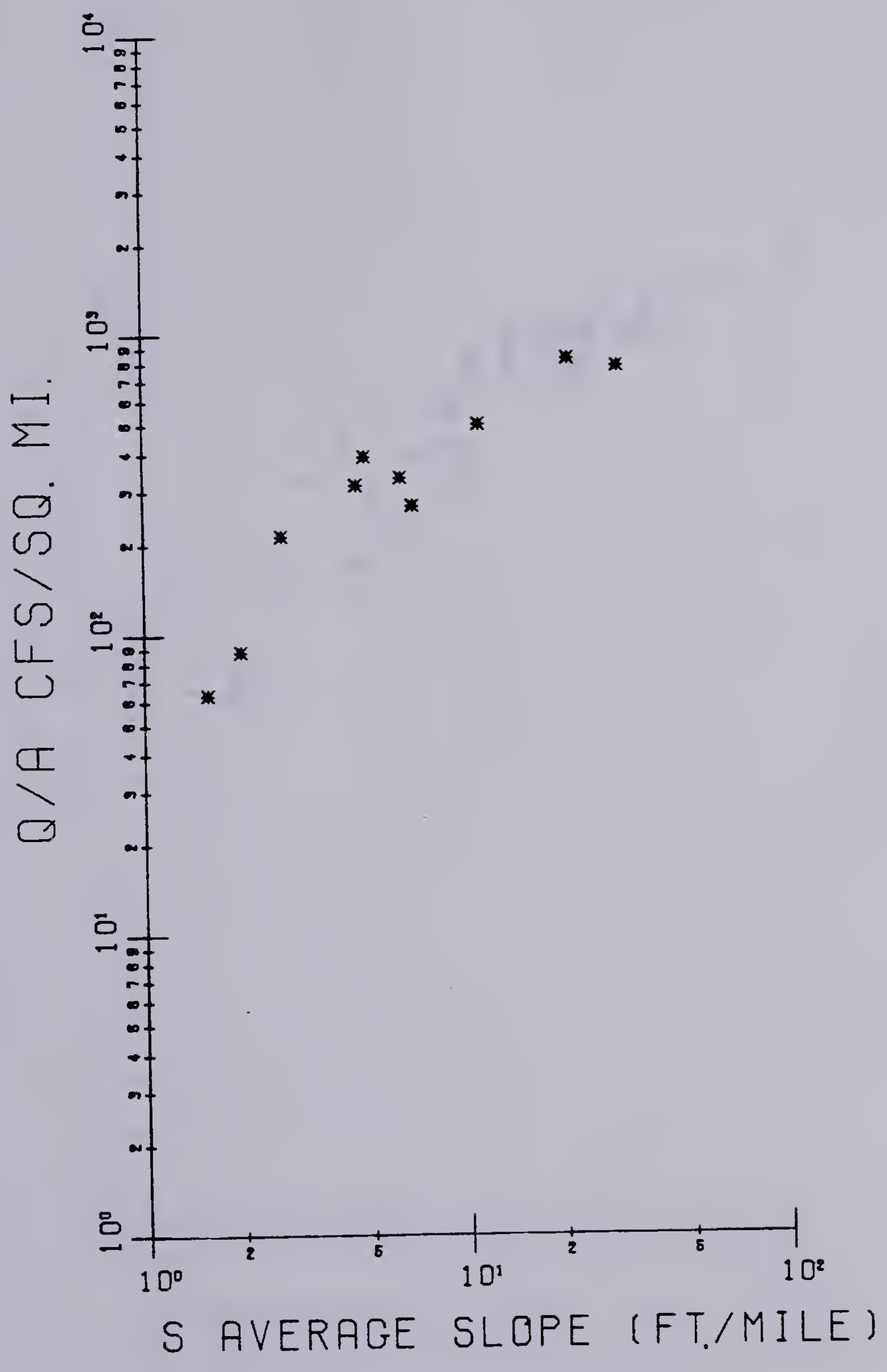

FIGURE A.4.29 Comparison of the PMF Normalized Discharge with Average Slope for the Red Deer River Basin.

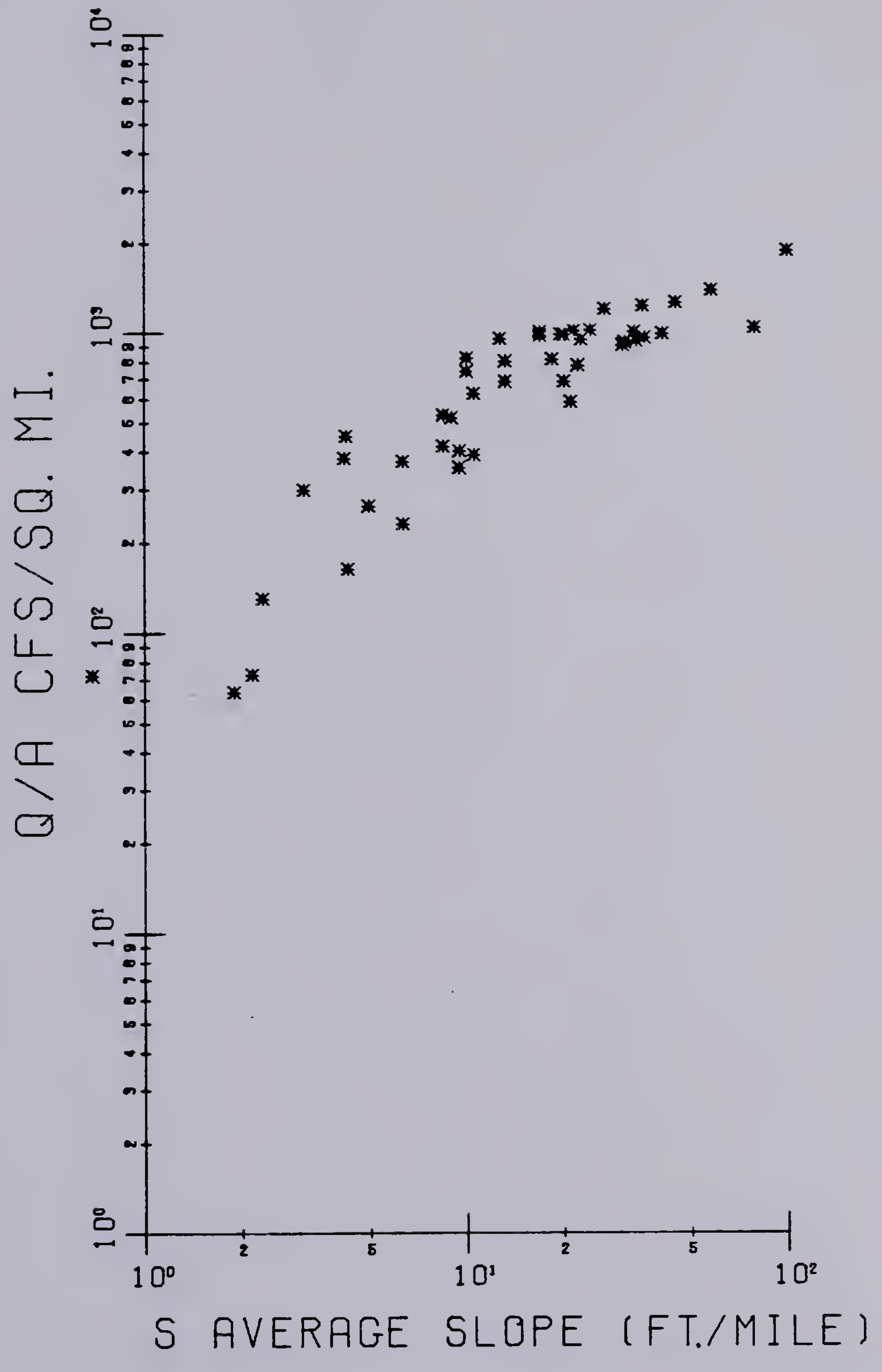

FIGURE A.4.30 Comparison of the PMF Normalized Discharge with Average Slope for the South Sask. River Basin.

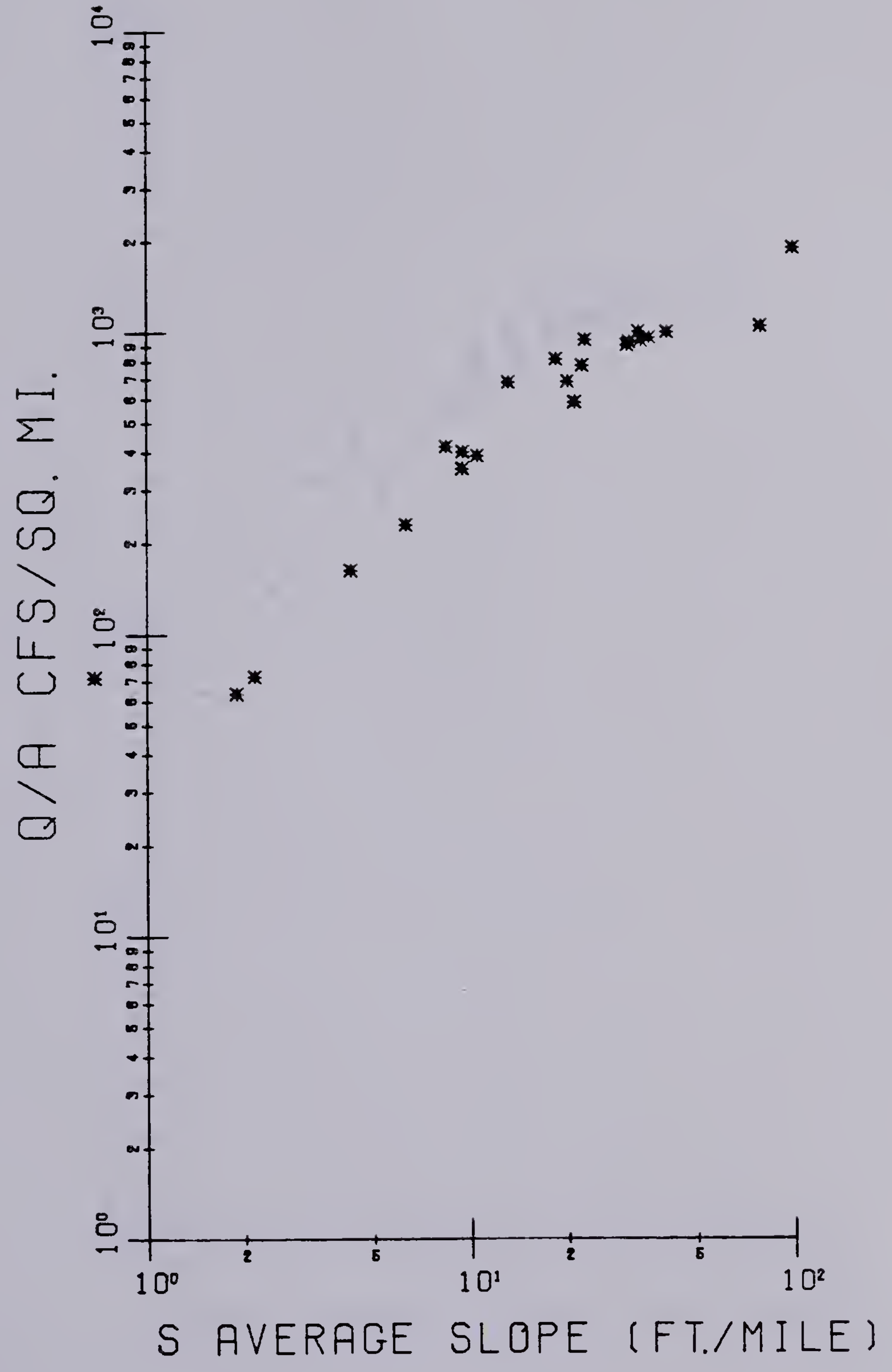

FIGURE A.4.31 Comparison of the PMF Normalized Discharge with Average Slope for the Bow River Basin.

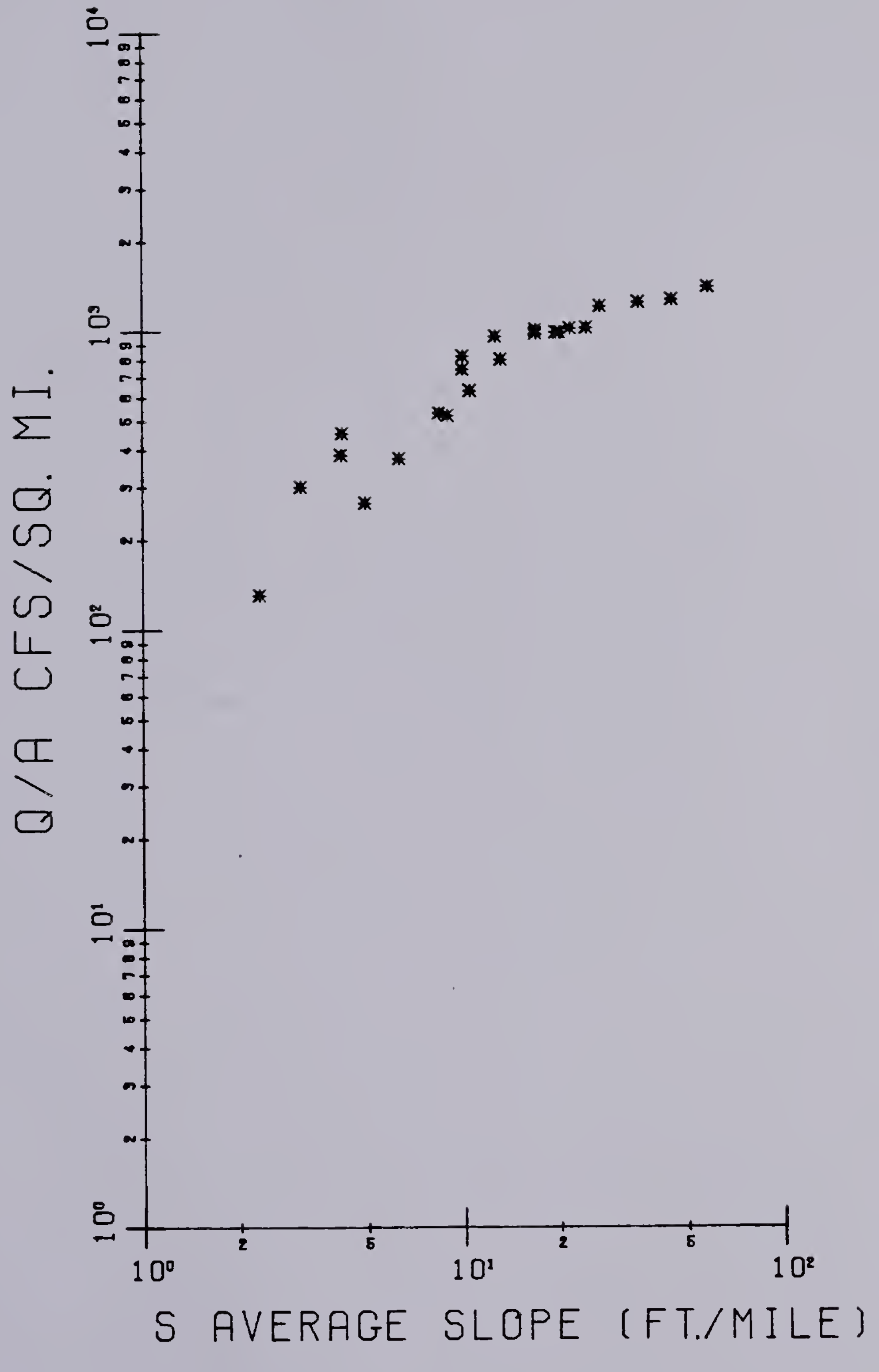

FIGURE A.4.32 Comparison of the PMF Normalized Discharge with Average Slope for the Oldman River Basin.

B30375